IRON EFFLUX AS A MECHANISM OF IRON OVERLOAD RESISTANCE IN *BACILLUS SUBTILIS*

A Dissertation
Presented to the Faculty of the Graduate School
of Cornell University
In Partial Fulfillment of the Requirements for the Degree of
Doctor of Philosophy

by
Valentina Azul Pinochet Barros
May 2020

IRON EFFLUX AS A MECHANISM OF IRON OVERLOAD RESISTANCE IN *BACILLUS SUBTILIS*

Valentina Azul Pinochet Barros, Ph. D.

Cornell University 2020

Iron is an essential element across all domains of life. However, when in excess, this micronutrient is toxic as it can target metalloproteins for mismetallation, and undergo Fenton reactions that generate damaging reactive oxygen species (ROS). Bacteria have developed ways to balance intracellular iron levels and regulate oxidative stress responses. In the model Gram-Positive, non-pathogenic bacterium *Bacillus subtilis*, iron homeostasis and the oxidative stress response is tightly regulated by the Fur family metalloregulators Fur and PerR respectively. Under oxidative stres.s, PerR derepresses a regulon comprised of peroxide detoxifying enzymes and proteins that lower labile iron pools. During periods of iron starvation, Fur derepresses expression of iron importers, allowing the cells to acquire more iron. On the other hand, under high iron levels, iron export has not been reported until recently.

In this work we have expanded our understanding of this newly emerging field through the discovery of the first member of the P_{1B}-family of ATPase transporters to be involved in ferrous iron efflux, PfeT. This *B. subtilis*

Fe^{2+} efflux pump is part of the P_{1B4}-class of ATPases, which in the past has been attributed to cobalt export. This doctoral thesis centers on the identification and characterization of PfeT as an Fe^{2+} exporter which is essential to the cell under iron overload conditions (Chapter 3). From this, we go on to elucidate the complex transcriptional regulation of the *pfeT* gene. Not only do we show direct transcriptional activation by Fur for the first time in Gram-positives, but expand this model to the *Listeria monocytogenes* Fe^{2+} efflux ortholog, *frvA* (Chapter 4). Finally, the recent discovery of cation diffusion facilitator (CDF) Mn^{2+} exporters MneP and MneS provides further insight into Fe^{2+} efflux (Chapter 5). We redefine these transporters as Mn^{2+}/Fe^{2+} efflux pumps, highlighting metal cross-talk in *B. subtilis* and its impact on oxidative stress.

BIOGRAPHICAL SKETCH

Azul Pinochet-Barros was born in Palma de Mallorca in the Balearic Islands, Spain. She was raised between Mexico City (Mexico) and Madrid (Spain). Azul graduated *summa cum laude* from Suffolk University in Boston (MA) with a B.S. in both Biology & Philosophy, and a minor in Chemistry. During her time there she worked in Dr. Melanie Berkmen's Lab where she studied the *Bacillus subtilis* conjugation element ICE*Bs1*.

In 2013, Azul joined the Microbiology doctoral program at Cornell University, where she joined the John D. Helmann research group. There, she worked on bacterial metal ion homeostasis in the Gram-positive model organism *Bacillus subtilis*. Her thesis specifically focuses on iron homeostasis and the genetic pathways through which *B. subtilis* is able to survive iron overload conditions. Her body of work here centers on iron efflux systems and how these confer iron resistance. Additionally, her research also looks into how manganese and oxidative stress relate to iron homeostasis.

During her time at Cornell she has also been actively involved in the sci-art field through her science photography. This has led her to develop a variety of science and science education art projects in collaboration with other Departments across campus including: Cornell Microbiology at Wing Hall, the Robert Frederick Smith School of Chemical and Biomolecular Engineering, and the Fuertes Observatory. Her work has been published in established

photography journals (MUSÉE & Shots) and won awards in international competitions (TIFA, The Photophore, and IPA). Azul also promotes science and sci-art communication through her position as Co-Editor and Head of the Astrobiology Section of the international annual science and art magazine, PLASMA.

After completion of her Ph.D. degree, she will stay in the Helmann laboratory as a postdoctoral associate to finish up remaining projects as she looks for post-doctoral opportunities.

For Chancho, Lorcit, and Stefit.
My three pillars of strength.

ACKNOWLEDGMENTS

"*Physics tells us that all things attract each other gravitationally, from pulsars to planets to petunias, even if those forces are sometimes too small to notice in everyday life. But if you look closely at the trajectories that your life has taken you may notice the results of similar gravitational effects from the people you have known. Sometimes people around us cause massive swings in direction and speed that can propel us on toward new and undiscovered territory and experiences.*"

- Jim Bell, The Interstellar Age, 2015.

No one achieves anything on their own. This doctoral journey would never have been possible without the unconditional love, support, and guidance of so many people. To all of them I am eternally grateful.

I first want to thank my principal advisor, Prof. John D. Helmann. He has been an incredible teacher over the course of my Ph.D. His knowledge, enthusiasm, positive attitude and grit are contagious. Leading by example, his curiosity and determination to get to the root of a question has boosted my passion for science and research even further (something I did not think possible). Not only am I grateful for his mentorship in critical thinking, theory, scientific communication and writing, and so much more, but for his support in my scientific and artistic pursuits. Finally, his sense of humor is also greatly appreciated. I still remember when I first started out in his Lab measuring zone of inhibition plates when he walked up to me and said “So, you in THE zone?”. Thank you John.

I want to thank my committee members Prof. Joseph Peters and Prof.

Linda Nicholson. Their positive and constructive feedback has made this experience much easier to navigate.

I'm very lucky and grateful to have had the most wonderful lab mates during my time here. Vaidehi Patel (my bench mate), Heng Zhao (my free food radar), Ankita Sachla and Xiaojuan Huang (both sparks of cheer), Pete Chandragsu (the pensive walker), Daniel Rojas-Tapias (the singer), and Hualiang Pi (always lovely). I'm especially thankful to Ahmed Gaballa, who not only helped me through the experimental details and technicalities of benchwork, but who always seemed to bring the Egyptian sunshine with him to lab. I also want to give a very special thank you to my remarkable undergraduate student Srinand Paruthiyil who was not only a delight to work with, but who helped me grow as a mentor. Also a very warm thank you to Brian Wendel, Yesha Patel, Caroline Steingard, Bixi He, and Jessica Willdigg.

My friends here at Cornell have also been instrumental to my success here. Without them I simply don't see how I would've made it through. All of them have made me feel like I have a family away from my own. If I thank each and every one of you individually it will take up the whole thesis so I'll just say: thank you Irma Fernandez, Andrea Acevedo, Porter Hall, Rob Swanda, Myfanwy Adams, Julio Sanchez, Josephine Gonzales, Oriana Teran, Mariela Nunez Santos, Arash Latifkar, and Steve Halaby. I also want to thank two of my long-time and dear friends Bunty Ramchandani and Charles Altuzarra, for always cheering me on, in spite of the distance.

Last, but not least, I want to thank my family. The unconditional love and support from my mum, dad, and sister have meant everything to me. I would not be where I am today without them. Through the highs and lows, they have been my rock on which to stand and sky on which to gaze. Thank you. I also want to thank my former undergraduate mentors, Prof. Melanie Berkmen and Prof. Celeste Peterson, as well as my high school Biology teacher Ms. Cathy Booth. They all saw, nourished, and guided my curiosity at each stage of my path towards getting my Ph.D. Thank you.

TABLE OF CONTENTS

LIST OF TABLES

LIST OF FIGURES

Chapter 1

An Introduction to Bacterial Iron Homeostasis

"*The nitrogen in our DNA, the calcium in our teeth, the iron in our blood, the carbon in our apple pies were made in the interiors of collapsing stars. We are made of starstuff.*"
- Carl Sagan, Cosmos, 1980

1.1 Life and its iron-ic essentiality – a brief history

Iron (Fe) is an essential element across all domains of life, including bacteria. Although this metal is highly abundant in the Earth's crust, bioavailable iron is scarce. This is due to iron's redox chemistry, wherein soluble ferrous iron (Fe^{2+}) easily reacts with oxygen to produce insoluble ferric iron (Fe^{3+}). The essentiality of this element stems from its requirement in a myriad of cellular processes spanning DNA synthesis, respiration, photosynthesis, central carbon metabolism, and more (1)! To adapt a quote from Charles Darwin's 1859 *Origin of Species*, "from so simple a beginning..." iron can be thought of as a simple requirement for life, from which "…*endless forms most beautiful and most wonderful*", these forms being enzymes spanning an array of physiological functions that sustain the diversity of life we see today. Yet in a Pale Blue Dot of exhuberant life, most of which remains invisible to the naked eye, why would cell physiology be so reliant on such a poorly accessible element?

To answer this question, we need to look back over 2 billion years ago, in the early stages of the evolution of life. During this time, Earth was an

anoxic environment that allowed iron to be maintained in its reduced, soluble Fe^{2+} form (1). This, along with the ability to confer high and low spin states (regardless of the element's oxidation state), make iron a versatile cofactor for a wide range of proteins. Hence, the development of iron-centric biological chemistry was favoured early on.

However, as the Great Oxygenation Event took place, ferrous precipitation into ferric salts imposed severe depletion of this precious micronutrient. Oxidation of bioavailable iron, in turn, gave rise to a second stressor, the generation of reactive oxygen species (ROS) through Fenton reactions. Between iron starvation and the toxicity imposed by ROS, bacteria developed ways in which to survive this new, hostile environment.

It is worth noting that there are exceptions to this iron requirement. The genus of *Lactobacilli* as well as the causative agent of Lyme disease, *Borrelia burgdorferi* (2,3) need little to no iron for growth. Interestingly, these "iron-less" bacteria need high levels of the more stable transition metal manganese (Mn) and are described as "manganese-centric" organisms.

1.2 Metal ion homeostasis, a Nichomachean phenomenon

In Aristotle's "*The Nichomachean Ethics*" he describes the nature of vices (the two sides of the same coin – lack and excess), virtues (the mean between the two extremes), and their significance in the discussion of ethics:

> *"…and again it (virtue) is a mean because the vices respectively fall short of or exceed what is right in both passions and actions, while virtue both finds and chooses that which is intermediate. Hence in respect of its substance and the definition which states its essence virtue is a mean..."*
>
> *- Book II Nichomachean Ethics, Aristotle (350 B.C.)*

Aristotle's examination of morality is nicely analgous to the physiological balance that cells seek to maintain under extreme conditions of micronutrient deficiency and excess. A vice, whether it stems from lack or excess, is toxic and highlights the importance of balance (the mean, virtue)[1]. Each virtue comes with its own set of vices (e.g., cowardice and rashness are the deficiency and excess of courage respectively). In this same manner, the mechanisms of metal deficiency and excess vary depending on the metal cation.

Optimal metal ion levels depend on the requirement of that element by any given organism. Nonetheless, metal balance must be maintained to establish proper protein metallation. The stability with which each metal binds to protein varies as per the Irving-Williams series (4). Copper (Cu^{+}) and zinc (Zn^{2+}) bind more tightly compared to those with lower affinities like magnesium and calcium (Fig. 1.1). Depletion of a low affinity cation or excess of a tighter binding metal therefore primes the cell for enzyme mismetallation, pathway

[1] It is fitting (and even poetic) that this view should come from a philosopher believed to be the first to question and address problems in biology in a systematic manner.

shutdown, and eventually cell death (5-10). Moreover, the redox chemistry of copper and iron makes these metalloproteins more susceptible to oxidation and subsequent mismetallation (11-14).

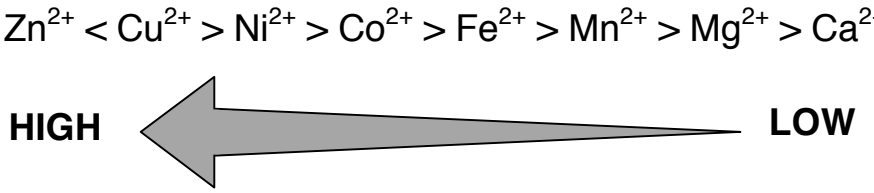

FIG. 1.1) Irving-Williams series
Universal order of the relative stabilities of essential bivalent cations found in the first transition row of the Periodic Table. This order appears to hold true independent of the kind of ligand involved or the number of ligands present. It is often explained by the trends in ionic radius, second ionization energies, and crystal field stabilization energies.

Bacteria have evolved metalloregulators to control intracellular metal levels through gene response control (7,15). By sensing intracellular metal changes, these regulators activate or repress expression of metal transporters (importers and efflux pumps) chaperones, and mobilization (storage and sequestration) proteins to restore metal balance (7). In addition to this, expression of alternative pathways and metalloproteins are activated under conditions where certain metals are limiting (16).

1.3 Iron related stress responses in bacteria

Maintaining an iron dependent physiology is challenging. A lack of iron leads to cellular shutdown, as enzymatic function cannot be sustained (17,18). Similarly, excess iron has deleterious effects of its own by either catalyzing

toxic Fenton reactions or through enzyme mismetallation and pathway blockage (11,13,14,19,20). Here we focus on the transcriptional responses that the non-pathogenic, Gram-positive model organism *Bacillus subtilis* uses to adapt and survive to these iron "vices".

1.3.1 Iron starvation – the vice of depletion

The sole iron metalloregulator in *B. sutilis* is the homodimeric, DNA-binding Fur protein. Fur senses free iron levels in the cell through its metal sensing site. Upon binding, holo-Fur undergoes a conformational change that allows it to bind to specific Fur DNA boxes in the genome. Under conditions of metal sufficiency, Fur remains in its holo-form such that it actively represses the Fur regulon. As iron levels drop, apo-Fur can no longer bind to DNA and gene derepression ensues.

The Fur regulon is comprised of approximately 60 genes, encompassing iron uptake systems and siderophore biosynthesis pathways, amongst other iron acquisition and mobilization systems (21,22). We now know that expression of these genes in response to iron limitation occurs as a "graded response", rather than as an "on-and-off" mechanism (23). Past examination of the Fur regulon derepression under artificial iron starvation induction showed three main waves of expression.[2]

[2] In *B. subtilis*, Zur regulon derepression in response to zinc limitation also occurs in this general manner (24.Shin, J.H. and Helmann, J.D. (2016) Molecular logic of the Zur-regulated zinc deprivation response in Bacillus subtilis. *Nat Commun*, **7**, 12612.)

Briefly, early derepression genes include those encoding uptake systems for petrobactin (FpbNOPQ), elemental iron (EfeUOB), and ferric citrate (FecCDEF). Mid-derepression genes include the bacillibactin biosynthetic pathway (DhbACEBF), siderophore uptake systems FeuABC (which imports bacillibactin and enterobactin) and FhuBCGD (for hydroxamate uptake), and iron-independent flavodoxins YkuN and YkuP which may functionally replace iron-utilizing (4Fe-4S) ferrodoxins. Finally, the late response genes include those responsible for the control of the iron-sparing response, which helps decrease the requirement of dispensable iron-utilizing enzymes. Namely, the small RNA FsrA and its chaperone proteins FbpA, FbpB, and FbpC act together to bind mRNA targets to inhibit translation of these proteins, thus reallocating the scarce iron towards essential pathways (25,26). This late response is also seen in *Escherichia coli*, where the FsrA homolg RhyB functions in a similar manner (27-29), and in *Mycobacterium tuberculosis* (30).

Our knowledge of the mechanisms of bacterial iron starvation is instrumental to better understanding host-pathogen interactions. It is well established that during infection, the host imposes drastic metal imbalances which the infecting agent tries to fend off. This micronutrient tug of war is known as nutritional immunity (31).

Generally, when the pathogen has been engulfed by the macrophage within its phagocytic vacuole, the host imports metals high in the Irving-

Williams series like Zn^{2+} and copper Cu^{+} to impose metal toxicity on the bacterium (32). Copper is imported via the CTR1 transporter (also known as SLC31A1) into the cell, after which it is exported into the phagosome via ATP7A Cu^{+} transporters (33). Zinc is taken up by the cell through family Zn^{2+} transporters (34). Once in the cytosol, small metal-containing vesicles form and fuse with the phagocytic vacuole, delivering toxic Zn^{2+} levels to the infecting agent (35).

The host also imposes manganese (Mn^{2+}) and Fe^{2+} starvation. During the early stages of infection, bacterial acquisition of Fe^{2+} is limited by the production of the antimicrobial metal chelator calprotectin (which also chelates Mn^{2+} and Zn^{2+}) (36,37). Host-imposed iron limitation also occurs in the bloodstream by erythrocyte retention of iron bound to haem (haemobglobin) and by ferritin and transferrin (31). Once in the phagosome, iron export by ferroportin (38,39) and the natural resistance-associated macrophage protein 1 (NRAMP1) transporter (40) imposes further microbial iron limitation.

1.3.2 Oxidative stress – the oxic vice of iron

Although essential, iron is toxic when in excess. Iron toxicity derives from (i) its redox instability, which leads to the propagation of ROS through Fenton chemistry, and (ii) increased chance of metalloprotein mismetallation.

Normally, bacteria produce endogenous ROS like superoxide (O_2^-) and hydrogen peroxide (H_2O_2) as a by-product of metabolic reactions. Studies in *E.*

coli have helped determine the source of this intracellular ROS production. Initially thought to originate from the oxidation of respiratory flavoproteins (41,42), *in vitro* studies have shown that most ROS production originates from the autoxidation of non-respiratory flavoproteins such as glutamate synthase and lipoamide dehydrogenase (43,44). Upshifts in the production of exogenous O_2^- and H_2O_2 has many sources (oxidation of sulphur and reduced metals at the oxic/anoxic interface, photochemical formation of oxidants by chromophores, and direct excretion by other competing bacteria and immune cells), but is generally the result of changes in the environment (45).

In order to survive exposure to these toxic species, the cell employs enzymes like superoxide dismutases (SOD) to scavenge O_2^-, and alkyl-hydroperoxidase reductases (Ahp) and catalases (Kat) to detoxify H_2O_2. In *E. coli*, these enzymes are under direct or indirect transcriptional control of the tetrameric DNA-binding LysR family redox-sensing regulator OxyR (46,47).

Upon exposure to H_2O_2, each OxyR protomer will form intramolecular disulfide bonds that allow the oxidized protein to interact with RNA polymerase (RNAP) to trigger activation of the OxyR regulon, including *ahpC* and *katG*. In addition to this, OxyR also activates expression of mini-ferritin Dps, a dodecameric iron sequestering protein that removes free intracellular iron under conditions of oxidative stress (48). This prevents the exacerbation of oxidative damage through Fenton reactions. To further counteract oxidative stress, OxyR also directly controls expression of the Mn^{2+} importer MntH (49-

51). This sudden intake of Mn^{2+} helps provide iron-utilizing enzymes an alternative, non-redox sensitive functional cofactor, thus helping to maintain activity during oxidative stress (45). Finally, OxyR directly regulates expression of Mn-SOD and indirectly (via RyhB) of Fe-SOD (27,52).

By contrast, the main oxidative stress regulator in *B. subtilis* is PerR, a member of the Fur family of metalloregulators. Briefly, PerR is a homodimeric DNA binding protein with a distinct metal sensing site that binds either Fe^{2+} (PerR:Fe) or Mn^{2+} (PerR:Mn) to repress regulon transcription (53,54). PerR:Fe exposure to H_2O_2 triggers a metal catalyzed oxidation (MCO) event at the metal sensing site (55). This protein oxidation event, catalyzed by the conversion of Fe^{2+} to Fe^{3+}, inactivates PerR and leads to the derepression of the regulon.

Unlike *E. coli*, the *B. subtilis* oxidative response does not influence Mn^{2+} homeostasis, which is regulated by the DtxR family metalloregulator MntR (8,56). Under Mn^{2+} replete conditions, MntR binds to Mn^{2+} (MntR:Mn) to repress expression of *mntH* and *mntABCD*, the two Mn^{2+} import-encoding genes (57). By contrast, during Mn^{2+} overload, MntR:Mn also directly activates expression of the cation diffusion facilitator (CDF) Mn^{2+} efflux pump genes *mneP* and *mneS* (58). Although in *B. subtilis* there is no regulon overlap between MntR and PerR, work in *Streptococcus oligofermentans* suggests that MntR can sense H_2O_2 through Cys11 and Cys156 disulfide formation, leading to the derepression of *mntA* (59). Whether this is also the case in *B.*

subtilis is unknown, but current transcriptional data does not show increased expression of *mntH* or *mntA* in the presence of H_2O_2 (60).

The *B. subtilis* PerR regulon is comprised of two types of genes, (i) those that encode proteins that can directly detoxify H_2O_2, and (ii) those that impact iron homeostasis in order to alleviate oxidative stress. The former includes genes like *katA* (catalase), *ahpCF* (alkyl hydroperoxide reductase), and *hemAXCDBL* (the KatA heme cofactor biosynthetic pathway) (54). PerR regulated genes that impact iron homeostasis include *mrgA* (a Dps-like mini-ferritin that sequesters iron from the cytosol in the presence of oxidant) (53,61), *fur* (the main iron metalloregulator in *B. subtilis,* which represses transcription of high affinity iron importers), and the recently defined P_{1B4}-type ATPase ferrous iron efflux pump *pfeT* (20).

1.3.3 Iron overload – the ferrous vice of iron

Iron excess can cause oxygen-independent toxicity, possibly through protein mismetallation and subsequent blockage of essential cellular pathways. In principle, protein mismetallation caused by a rise in intracellular iron can be alleviated through supplementation of the targeted metal. In *B. subtilis*, iron toxicity is alleviated by adding Mn^{2+} to the high iron growth media (20). Possible targets of Fe^{2+} mismetallation, therefore, could be Mn^{2+}-dependent enzymes.

Ribonucleotide reductase (RNR) is an essential enzyme required for the

reduction of ribonucleotides (rNTPs) to deoxyribonucleotides (dNTPs), the precursors needed for DNA synthesis. Although highly conserved, there are different RNR classes and subclasses, each of which uses a different metal cofactor to catalyze the reaction (62). It is not uncommon for bacteria to have more than one class of RNR, as the different metal requirements helps maintain essential dNTP synthesis under various growth conditions.

E. coli, for example, has three: a class III NrdDG (4Fe-4S), a class Ia NrdAB (di-iron), and a class Ib NrdEF (di-manganese). The main, housekeeping RNR that functions during aerobic growth is NrdA. When *E. coli* transitions into an anoxic environment, it requires class III NrdDG for survival, which uses S-adenosylmethionine (SAM) to generate an oxygen sensitive glycyl radical (63). Moreover, during aerobic growth, the cell might experience conditions that cannot sustain NrdAB function, such as iron starvation or oxidative stress. These changes in the environment cause *E. coli* to switch to its Mn^{2+}-utilizing NrdEF (18,64).

Surprisingly, *B. subtilis* only has a single RNR, a class 1b NrdEF. Previous *in vitro* studies have shown that although Mn^{2+} is the native metal cofactor, iron can sometimes bind to the enzyme, albeit lowering its catalytic activity (65). Given that *B. subtilis* has no alternative RNR, it is possible that NrdEF might be mismetallated under conditions of iron overload, causing either complete functional shut-down or a lowering of catalytic activity beyond the threshold needed to sustain cell growth. Conversely, it is possible that *B.*

subtilis RNR might be cambialistic and function well enough under both metallation states

Another possible target of iron mismetallation could be phosphoglycerate mutase (PGM), an essential glycolytic Mn^{2+}-utilizing enzyme (66-68). Unless cells are supplemented with upstream and downstream glycolytic products (glucose and malate respectively), a *pgm* null strain is lethal (69). It is therefore possible to surmise that PGM mismetallation might render the protein inactive and lead to cell death.

Studies in *Rhodopseudomonas palustris* suggest that there is cross-talk between iron and copper toxicy (70). In this work, they show that *R. palustris* is more sensitive to both Cu^{+} and Fe^{2+} rather than to each metal separately. The cause of this synergistic effect could be in part due to the ability of Fe^{2+} to reduce Cu^{2+} into more damaging Cu^{+} (71,72), as well as for its ability to dysregulate copper homeostasis (70). However, it remains to be seen how prevalent these synergistic effects are across bacteria.

Iron toxicity can also come in the form of unregulated intracellular mineralization of Fe^{2+}, particularly for anoxygenic phototrophic bacteria that couple Fe^{2+} oxidation (as an electron source) with light energy to fixate carbon (73,74). The excessive production of Fe^{3+} mineral oxides can quench essential negatively charged molecules like phosphates and organic compounds (75,76). More generally, this *in vivo* mineralization restricts the functional physical space of the cell. These phototrophic anaerobic iron-oxidizing

bacteria, like *Rhodobacter* sp., therefore employ iron-oxidizing enzymes at the membrane (77-79). This ideal positioning favors the incorporation of mineralized iron into secreted products like exopolysaccharide (80,81), thus spatially removing the mineral byproduct of their essential metabolism.

Another mechanism of spatial protection from excess iron has been reported in *Pseudomonas aeruginosa.* Here, cells grown in iron overload conditions secrete an electrostatic protective layer made of spermidine (82). This physical barrier prevents entry of excess iron into the cell, protecting it from iron mismetallation and Fenton reactions.

An important, yet poorly understood, facet of iron overload resistance is the cellular handling of mismetallated proteins. What is their fate? *E. coli* and *Shewanella oneidensis* studies indicate that under iron overload conditions, mismetallated proteins are targeted by ClpXP protease (83). Moreover, they also show that deletion of the ClpX or ClpP makes cells more iron sensitive. However, further work is needed to understand this mechanism of Fe-mismetallated protein recognition and degradation (19).

Activating pathways that lower free labile iron also help confer resistance. One such mechanism is iron sequestration through the use of ferritins, bacterioferritins, and Dps-like proteins. These are 24-meric (and in the case of the latter, dodecameric) nanocages that take up Fe^{2+} from the cytosol through a ferroxidation step to store it in the cavity center as Fe^{3+} (84). The first two are primarily involved in iron storage when cells undergo periods

of iron starvation, as has been shown in *E. coli* (FtnA), *Campylobacter jejuni* (Cft), *Helicobacter pylori* (Pfr), and other systems (85-87). However, these same studies have also shown that strains lacking their respective ferritins become more iron sensitive, suggesting that they might also play a role in iron resistance. In contrast, Dps-like proteins are primarily involved in iron sequestration during oxidative stress to prevent Fenton reactions. *B. subtilis* contains two such proteins: Dps, which is controlled by the SigB general stress response factor (88), and the PerR regulated MrgA (61). How the iron is later released remains unknown.

Finally, a long under-appreciated mechanism of bacterial iron resistance that also functions by lowering intracellular iron levels is efflux. Until recently, bacterial iron efflux pumps have remained elusive, yet they seem to play an important role in iron detoxification (89). In the following section we explore this iron resistance pathway in more depth.

1.4 Bacterial iron efflux

Iron efflux was first appreciated in mammals with the discovery of ferroportin (90-93). Genetic Xenopus oocyte studies (91,92) as well as transcriptional regulation studies in macrophages and intestinal tissue (92,94,95) all support ferroportin's role in iron efflux. Analysis from clinical patients carrying ferroportin mutations exhibit macrophage iron overload that, if left untreated, can lead to iron induced organ damage (96,97). Development of autosomal

dominant hemochromatosis, commonly referred to as the “ferroportin disease” (98), and the apparent essentiality of this efflux system in early stage embryonic development (99) highlights the importance of iron efflux in mammals.

In light of the understanding of bacterial iron toxicity and the relevance that iron efflux plays in eukaryotes, it seems like iron export should be an integral part of bacterial iron homeostasis. However, this area of research has proved challenging partly because many of these transporters were functionally mis-annotated due to their obscure regulation, unclear transportation substrate/s, and relatively undefined physiological role.

Early studies in *Wautersia metallidurans* CH34 (100) and *E. coli* (101) identified FieF as a CDF transporter with the ability to efflux Fe^{2+} and Zn^{2+} (and in the case of *W. metallidurans* CH34, possibly also pump out Co^{2+}, Cd^{2+}, and Ni^{2+}). Metal transport in CDF pumps is proton-coupled and further work to understand this process has focused attention on the Zn^{2+} efflux properties of FieF (102-104). CDF iron efflux pumps have since been identified in other organisms like *Pseudomonas aeruginosa* (AitP) and *Shewanella oneidensis* MR-1 (FeoE) (105,106). It is therefore not surprising (but still fascinating) to see that magnetotactic bacteria like *Magnetospirillum gryphiswaldense* use FieF-like transporter MamBM for iron delivery and biomineralization in magnetosome maturation (107-109). Finally, as of most recently, the two main

Mn^{2+} efflux pumps in *B. subtilis* (CDF exporters MneP and MneS) can also efflux Fe^{2+}.

In *E. coli*, other proteins have also been proposed to be involved in iron efflux. The ABC transporter FetAB provides resistance to oxidative stress through iron effux (110). Another protein, YaaA, also decreases sensitivity to peroxide stress by lowering of free labile iron levels in the cytosol (111). However, protein sequence analysis revealed a lack of transmembrane domains, suggesting YaaA's putative role in iron trafficking.

Typically, genes involved in iron homeostasis tend to be regulated by iron-sensing (e.g., Fur or Irr), oxidative stress responsive transcription factors (e.g., PerR or OxyR), or stress response sigma factors. However, whilst *yaaA* is under OxyR transcriptional regulation, *fetAB* appears to be under the sole control of the housekeeping *E. coli* sigma factor σ^{70}.

Iron efflux pumps have also been idenitfied within the major facilitator superfamily (MFS) of transporters. The *mdtABCD baeSR* operon in the Gram-negative enteric pathogen *Salmonella typhimurium* encodes, amongst other things, the iron and citrate efflux transporter IceT (formerly known as MdtD). This transporter is proposed to efflux both iron-bound and unbound citrate (112,113). Null mutant strains are iron sensitive and *iceT* expression lowers intracellular iron levels. Although *iceT* is not upregulated by high iron or H_2O_2 exposure, disruption of iron homeostasis in a *fur* null mutant does induce operon expression. What their precise role in pathogenesis is remains to be

determined. Bioinformatic analysis indicates a high prevalence of IceT homologs within the Enterobacteriaceae, suggesting that MFS iron exporters might be more common than previously thought (112).

The membrane bound ferritin A (MbfA) class of transporters, which are part of the erythrin-vacuolar iron transport (Er-VIT1) ferritin-like superfamily are another class of recently defined iron efflux pumps. Structurally, MbfA has an N-terminal ferritin-like domain and a C-terminal membrane-embedded vacuolar iron transporter domain (VIT1). This has made it hard to distinguish its function between iron sequestration and efflux. Work done in *Agrobacterium tumefaciens* has shown that MbfA helps lower intracellular labile iron, thus conferring resistance to high iron (under low pH) and H_2O_2 (114,115). Similar phenotypes have been observed in *Bradyrhizobium japonicum* MbfA (116). In both cases, *mbfA* expression is controlled by Irr and induced by high iron and H_2O_2. Moreover, the *B. japonicum* study showed that MbfA requires the ferritin-like domain for transporter dimerization that thus help assemble the functional channel through which iron export takes place (116).

Finally, a large family of ion transporters that has seen its metal specificity expanded to include Fe^{2+} is the P-type ATPases (89). Efflux in P-type ATPases generally occurs through specific substrate binding to a metal binding domain. This triggers ATP hydrolysis, which in turn drives transport of the metal ion through the transmbrane domain and into the outer mileu. This

large family is comprised of five main subgroups, each of which specializes in the transport of different ligands (117).

In the P_1 subgroup, which mainly transports K^+ and transition metal ions, special attention has been recently drawn to the P_{1B4} subclass. For a long time, P_{1B4}-type ATPases were thought to be solely involved in Co^{2+} export (118), until the discovery of *B. subtilis* PfeT (20).

Through the identification of conserved PerR DNA binding sites and observed gene derepression in the presence of H_2O_2, *pfeT* had been identified as a member of the PerR regulon (54,119). First named as "*ykvW*", not much was known about its function, other than the fact that it encoded a P_1-ATPase. Further work went on to propose that YkvW was a peroxide-induced zinc importer and was thus renamed as a ZosA (zinc uptake under oxidative stress) (119). However, zinc import was never shown directly. The incongruity of this P_{1B4}-type ATPase acting as a zinc importer stemmed from the fact that the only subclass shown to transport zinc is the P_{IB2} type, which differs in structure (118). Moreover, later transcriptional work revealed two Fur operator sites within *zosA*'s promoter region, in addition to its PerR binding site (119,120), further suggesting a role in iron efflux. Since this study, various iron efflux P_{1B4}-ATPase orthologs have been found in pathogens like *Streptococcus pyogenes* (PmtA), *Streptococcus suis* (PmtA), *Listeria monocytogenes* (FrvA) and *Mycobacterium tuberculosis* (CtpD), all of which (except *S. suis* PmtA and maybe *S. pyogenes* PmtA) are virulence factors

(121-125).

1.5 Thesis overview

Chapter 2 is an in-depth overview of the role of iron dependent Fur family metalloregulators Fur and PerR. This chapter uses the *B. subtilis* homologs as a basis for understanding the role of these proteins across bacteria. We go over the genetic regulation that they impose as well the structural details that allow these proteins to function in iron homeostasis and oxidative stress.

Chapter 3 recounts the redefinition of ZosA as the iron efflux P_{1B4}-type ATPase, PfeT (a peroxide induced ferrous efflux transporter). Here we focus on the physiological, genetic, and biochemical characterizations of this transporter to show its role in Fe^{2+} export.

Having already shown the function of PfeT as an Fe^{2+} efflux pump, Chapter 4 focuses on the transcriptional regulation of the *pfeT* gene. Here, we tease apart the complex *pfeT* promoter architecture to better define the roles of PerR and Fur. Through *in vivo* and *in vitro* studies we clarify the role of Fur and PerR in the regulation of *pfeT* by confirming PerR repression and showing direct Fur activation. Moreover, we extend this mechanism of transcription to be applicable to the *L. monocytogenes* ortholog, *frvA*.

Chapter 5 expands on the subject of iron efflux in *B. subtilis* by showing that the two main CDF Mn^{2+} exporters MneP and MneS are also involved in iron efflux. MneP is the major contributor to Mn^{2+} overload relief, whilst MneS

plays a secondary role. However, these roles are reversed for Fe^{2+} efflux. We further expand our understanding of the MntR regulon by showing how dysregulation of Mn^{2+} homeostasis makes cells more susceptible to H_2O_2.

1.6 References

1. Anbar, A.D. (2008) Oceans. Elements and evolution. *Science*, **322**, 1481-1483.
2. Archibald, F. (1986) Manganese: its acquisition by and function in the lactic acid bacteria. *Crit Rev Microbiol*, **13**, 63-109.
3. Posey, J.E. and Gherardini, F.C. (2000) Lack of a role for iron in the Lyme disease pathogen. *Science*, **288**, 1651-1653.
4. P., I.H.a.W.J.R. (1953) The Stability of Transition-metal Complexes. *Journal of the Chemical Society*, 3192–3210.
5. Aguirre, J.D. and Culotta, V.C. (2012) Battles with iron: manganese in oxidative stress protection. *J Biol Chem*, **287**, 13541-13548.
6. Barwinska-Sendra, A. and Waldron, K.J. (2017) The Role of Intermetal Competition and Mis-Metalation in Metal Toxicity. *Adv Microb Physiol*, **70**, 315-379.
7. Chandrangsu, P., Rensing, C. and Helmann, J.D. (2017) Metal homeostasis and resistance in bacteria. *Nat Rev Microbiol*, **15**, 338-350.

8. Helmann, J.D. (2014) Specificity of metal sensing: iron and manganese homeostasis in *Bacillus subtilis*. *J Biol Chem*, **289**, 28112-28120.

9. Johnson, M.D., Kehl-Fie, T.E. and Rosch, J.W. (2015) Copper intoxication inhibits aerobic nucleotide synthesis in *Streptococcus pneumoniae*. *Metallomics*, **7**, 786-794.

10. Naranuntarat, A., Jensen, L.T., Pazicni, S., Penner-Hahn, J.E. and Culotta, V.C. (2009) The interaction of mitochondrial iron with manganese superoxide dismutase. *J Biol Chem*, **284**, 22633-22640.

11. Anjem, A. and Imlay, J.A. (2012) Mononuclear iron enzymes are primary targets of hydrogen peroxide stress. *J Biol Chem*, **287**, 15544-15556.

12. Gu, M. and Imlay, J.A. (2013) Superoxide poisons mononuclear iron enzymes by causing mismetallation. *Mol Microbiol*, **89**, 123-134.

13. Imlay, J.A. (2014) The mismetallation of enzymes during oxidative stress. *J Biol Chem*, **289**, 28121-28128.

14. Sobota, J.M., Gu, M. and Imlay, J.A. (2014) Intracellular hydrogen peroxide and superoxide poison 3-deoxy-D-arabinoheptulosonate 7-phosphate synthase, the first committed enzyme in the aromatic biosynthetic pathway of *Escherichia coli*. *J Bacteriol*, **196**, 1980-1991.

15. Lee, J.W. and Helmann, J.D. (2007) Functional specialization within the Fur family of metalloregulators. *Biometals*, **20**, 485-499.

16. Merchant, S.S. and Helmann, J.D. (2012) Elemental economy: microbial strategies for optimizing growth in the face of nutrient limitation. *Adv Microb Physiol*, **60**, 91-210.

17. Faulkner, M.J., Ma, Z., Fuangthong, M. and Helmann, J.D. (2012) Derepression of the *Bacillus subtilis* PerR peroxide stress response leads to iron deficiency. *J Bacteriol*, **194**, 1226-1235.

18. Martin, J.E. and Imlay, J.A. (2011) The alternative aerobic ribonucleotide reductase of *Escherichia coli*, NrdEF, is a manganese-dependent enzyme that enables cell replication during periods of iron starvation. *Mol Microbiol*, **80**, 319-334.

19. Bennett, B.D. and Gralnick, J.A. (2019) Mechanisms of toxicity by and resistance to ferrous iron in anaerobic systems. *Free Radic Biol Med*, **140**, 167-171.

20. Guan, G., Pinochet-Barros, A., Gaballa, A., Patel, S.J., Arguello, J.M. and Helmann, J.D. (2015) PfeT, a P_{1B4}-type ATPase, effluxes ferrous iron and protects *Bacillus subtilis* against iron intoxication. *Mol Microbiol*, **98**, 787-803.

21. Baichoo, N., Wang, T., Ye, R. and Helmann, J.D. (2002) Global analysis of the *Bacillus subtilis* Fur regulon and the iron starvation stimulon. *Mol Microbiol*, **45**, 1613-1629.

22. Ollinger, J., Song, K.B., Antelmann, H., Hecker, M. and Helmann, J.D. (2006) Role of the Fur regulon in iron transport in *Bacillus subtilis*. *J Bacteriol*, **188**, 3664-3673.

23. Pi, H. and Helmann, J.D. (2017) Sequential induction of Fur-regulated genes in response to iron limitation in *Bacillus subtilis*. *Proc Natl Acad Sci U S A*, **114**, 12785-12790.

24. Shin, J.H. and Helmann, J.D. (2016) Molecular logic of the Zur-regulated zinc deprivation response in *Bacillus subtilis*. *Nat Commun*, **7**, 12612.

25. Gaballa, A., Antelmann, H., Aguilar, C., Khakh, S.K., Song, K.B., Smaldone, G.T. and Helmann, J.D. (2008) The *Bacillus subtilis* iron-sparing response is mediated by a Fur-regulated small RNA and three small, basic proteins. *Proc Natl Acad Sci U S A*, **105**, 11927-11932.

26. Smaldone, G.T., Antelmann, H., Gaballa, A. and Helmann, J.D. (2012) The FsrA sRNA and FbpB protein mediate the iron-dependent induction of the *Bacillus subtilis lutABC* iron-sulfur-containing oxidases. *J Bacteriol*, **194**, 2586-2593.

27. Masse, E. and Gottesman, S. (2002) A small RNA regulates the expression of genes involved in iron metabolism in *Escherichia coli*. *Proc Natl Acad Sci U S A*, **99**, 4620-4625.

28. Masse, E., Salvail, H., Desnoyers, G. and Arguin, M. (2007) Small RNAs controlling iron metabolism. *Curr Opin Microbiol*, **10**, 140-145.

29. Masse, E., Vanderpool, C.K. and Gottesman, S. (2005) Effect of RyhB small RNA on global iron use in *Escherichia coli*. *J Bacteriol*, **187**, 6962-6971.

30. Gerrick, E.R., Barbier, T., Chase, M.R., Xu, R., Francois, J., Lin, V.H., Szucs, M.J., Rock, J.M., Ahmad, R., Tjaden, B. *et al.* (2018) Small RNA profiling in *Mycobacterium tuberculosis* identifies MrsI as necessary for an anticipatory iron sparing response. *Proc Natl Acad Sci U S A*, **115**, 6464-6469.

31. Hood, M.I. and Skaar, E.P. (2012) Nutritional immunity: transition metals at the pathogen-host interface. *Nat Rev Microbiol*, **10**, 525-537.

32. Djoko, K.Y., Ong, C.L., Walker, M.J. and McEwan, A.G. (2015) The Role of Copper and Zinc Toxicity in Innate Immune Defense against Bacterial Pathogens. *J Biol Chem*, **290**, 18954-18961.

33. White, C., Lee, J., Kambe, T., Fritsche, K. and Petris, M.J. (2009) A role for the ATP7A copper-transporting ATPase in macrophage bactericidal activity. *J Biol Chem*, **284**, 33949-33956.

34. Stafford, S.L., Bokil, N.J., Achard, M.E., Kapetanovic, R., Schembri, M.A., McEwan, A.G. and Sweet, M.J. (2013) Metal ions in macrophage antimicrobial pathways: emerging roles for zinc and copper. *Biosci Rep*, **33**.

35. Kapetanovic, R., Bokil, N.J., Achard, M.E., Ong, C.L., Peters, K.M., Stocks, C.J., Phan, M.D., Monteleone, M., Schroder, K., Irvine, K.M. *et*

al. (2016) *Salmonella* employs multiple mechanisms to subvert the TLR-inducible zinc-mediated antimicrobial response of human macrophages. *FASEB J*, **30**, 1901-1912.

36. Nakashige, T.G., Zhang, B., Krebs, C. and Nolan, E.M. (2015) Human calprotectin is an iron-sequestering host-defense protein. *Nat Chem Biol*, **11**, 765-771.

37. Zygiel, E.M. and Nolan, E.M. (2019) Exploring Iron Withholding by the Innate Immune Protein Human Calprotectin. *Acc Chem Res*, **52**, 2301-2308.

38. Forbes, J.R. and Gros, P. (2003) Iron, manganese, and cobalt transport by Nramp1 (Slc11a1) and Nramp2 (Slc11a2) expressed at the plasma membrane. *Blood*, **102**, 1884-1892.

39. Knutson, M.D., Oukka, M., Koss, L.M., Aydemir, F. and Wessling-Resnick, M. (2005) Iron release from macrophages after erythrophagocytosis is up-regulated by ferroportin 1 overexpression and down-regulated by hepcidin. *Proc Natl Acad Sci U S A*, **102**, 1324-1328.

40. Gunshin, H., Mackenzie, B., Berger, U.V., Gunshin, Y., Romero, M.F., Boron, W.F., Nussberger, S., Gollan, J.L. and Hediger, M.A. (1997) Cloning and characterization of a mammalian proton-coupled metal-ion transporter. *Nature*, **388**, 482-488.

41. Kussmaul, L. and Hirst, J. (2006) The mechanism of superoxide production by NADH:ubiquinone oxidoreductase (complex I) from bovine heart mitochondria. *Proc Natl Acad Sci U S A*, **103**, 7607-7612.

42. Messner, K.R. and Imlay, J.A. (1999) The identification of primary sites of superoxide and hydrogen peroxide formation in the aerobic respiratory chain and sulfite reductase complex of *Escherichia coli*. *J Biol Chem*, **274**, 10119-10128.

43. Korshunov, S. and Imlay, J.A. (2010) Two sources of endogenous hydrogen peroxide in *Escherichia coli*. *Mol Microbiol*, **75**, 1389-1401.

44. Seaver, L.C. and Imlay, J.A. (2004) Are respiratory enzymes the primary sources of intracellular hydrogen peroxide? *J Biol Chem*, **279**, 48742-48750.

45. Imlay, J.A. (2013) The molecular mechanisms and physiological consequences of oxidative stress: lessons from a model bacterium. *Nat Rev Microbiol*, **11**, 443-454.

46. Aslund, F., Zheng, M., Beckwith, J. and Storz, G. (1999) Regulation of the OxyR transcription factor by hydrogen peroxide and the cellular thiol-disulfide status. *Proc Natl Acad Sci U S A*, **96**, 6161-6165.

47. Choi, H., Kim, S., Mukhopadhyay, P., Cho, S., Woo, J., Storz, G. and Ryu, S.E. (2001) Structural basis of the redox switch in the OxyR transcription factor. *Cell*, **105**, 103-113.

48. Almiron, M., Link, A.J., Furlong, D. and Kolter, R. (1992) A novel DNA-binding protein with regulatory and protective roles in starved *Escherichia coli*. *Genes Dev*, **6**, 2646-2654.

49. Anjem, A., Varghese, S. and Imlay, J.A. (2009) Manganese import is a key element of the OxyR response to hydrogen peroxide in *Escherichia coli*. *Mol Microbiol*, **72**, 844-858.

50. Kehres, D.G., Janakiraman, A., Slauch, J.M. and Maguire, M.E. (2002) Regulation of *Salmonella enterica* serovar Typhimurium *mntH* transcription by H_2O_2, Fe^{2+}, and Mn^{2+}. *J Bacteriol*, **184**, 3151-3158.

51. Kehres, D.G., Zaharik, M.L., Finlay, B.B. and Maguire, M.E. (2000) The NRAMP proteins of *Salmonella typhimurium* and *Escherichia coli* are selective manganese transporters involved in the response to reactive oxygen. *Mol Microbiol*, **36**, 1085-1100.

52. Tardat, B. and Touati, D. (1991) Two global regulators repress the anaerobic expression of MnSOD in *Escherichia coli*::Fur (ferric uptake regulation) and Arc (aerobic respiration control). *Mol Microbiol*, **5**, 455-465.

53. Chen, L., Keramati, L. and Helmann, J.D. (1995) Coordinate regulation of *Bacillus subtilis* peroxide stress genes by hydrogen peroxide and metal ions. *Proc Natl Acad Sci U S A*, **92**, 8190-8194.

54. Herbig, A.F. and Helmann, J.D. (2001) Roles of metal ions and hydrogen peroxide in modulating the interaction of the *Bacillus subtilis*

PerR peroxide regulon repressor with operator DNA. *Mol Microbiol*, **41**, 849-859.

55. Lee, J.W. and Helmann, J.D. (2006) The PerR transcription factor senses H_2O_2 by metal-catalysed histidine oxidation. *Nature*, **440**, 363-367.

56. Guedon, E. and Helmann, J.D. (2003) Origins of metal ion selectivity in the DtxR/MntR family of metalloregulators. *Mol Microbiol*, **48**, 495-506.

57. Que, Q. and Helmann, J.D. (2000) Manganese homeostasis in *Bacillus subtilis* is regulated by MntR, a bifunctional regulator related to the diphtheria toxin repressor family of proteins. *Mol Microbiol*, **35**, 1454-1468.

58. Huang, X., Shin, J.H., Pinochet-Barros, A., Su, T.T. and Helmann, J.D. (2017) *Bacillus subtilis* MntR coordinates the transcriptional regulation of manganese uptake and efflux systems. *Mol Microbiol*, **103**, 253-268.

59. Chen, Z., Wang, X., Yang, F., Hu, Q., Tong, H. and Dong, X. (2017) Molecular Insights into Hydrogen Peroxide-sensing Mechanism of the Metalloregulator MntR in Controlling Bacterial Resistance to Oxidative Stresses. *J Biol Chem*, **292**, 5519-5531.

60. Helmann, J.D., Wu, M.F., Gaballa, A., Kobel, P.A., Morshedi, M.M., Fawcett, P. and Paddon, C. (2003) The global transcriptional response of *Bacillus subtilis* to peroxide stress is coordinated by three transcription factors. *J Bacteriol*, **185**, 243-253.

61. Chen, L. and Helmann, J.D. (1995) *Bacillus subtilis* MrgA is a Dps(PexB) homologue: evidence for metalloregulation of an oxidative-stress gene. *Mol Microbiol*, **18**, 295-300.

62. Torrents, E. (2014) Ribonucleotide reductases: essential enzymes for bacterial life. *Front Cell Infect Microbiol*, **4**, 52.

63. Garriga, X., Eliasson, R., Torrents, E., Jordan, A., Barbe, J., Gibert, I. and Reichard, P. (1996) *nrdD* and *nrdG* genes are essential for strict anaerobic growth of *Escherichia coli*. *Biochem Biophys Res Commun*, **229**, 189-192.

64. Monje-Casas, F., Jurado, J., Prieto-Alamo, M.J., Holmgren, A. and Pueyo, C. (2001) Expression analysis of the *nrdHIEF* operon from *Escherichia coli*. Conditions that trigger the transcript level *in vivo*. *J Biol Chem*, **276**, 18031-18037.

65. Zhang, Y. and Stubbe, J. (2011) *Bacillus subtilis* class Ib ribonucleotide reductase is a dimanganese(III)-tyrosyl radical enzyme. *Biochemistry*, **50**, 5615-5623.

66. Chander, M., Setlow, B. and Setlow, P. (1998) The enzymatic activity of phosphoglycerate mutase from gram-positive endospore-forming bacteria requires Mn^{2+} and is pH sensitive. *Can J Microbiol*, **44**, 759-767.

67. Vasantha, N. and Freese, E. (1979) The role of manganese in growth and sporulation of *Bacillus subtilis*. *J Gen Microbiol*, **112**, 329-336.

68. Watabe, K. and Freese, E. (1979) Purification and properties of the manganese-dependent phosphoglycerate mutase of *Bacillus subtilis*. *J Bacteriol*, **137**, 773-778.

69. Commichau, F.M., Pietack, N. and Stulke, J. (2013) Essential genes in *Bacillus subtilis*: a re-evaluation after ten years. *Mol Biosyst*, **9**, 1068-1075.

70. Bird, L.J., Coleman, M.L. and Newman, D.K. (2013) Iron and copper act synergistically to delay anaerobic growth of bacteria. *Appl Environ Microbiol*, **79**, 3619-3627.

71. Mathews, S., Kumar, R. and Solioz, M. (2015) Copper Reduction and Contact Killing of Bacteria by Iron Surfaces. *Appl Environ Microbiol*, **81**, 6399-6403.

72. Matocha, C.J., Karathanasis, A.D., Rakshit, S. and Wagner, K.M. (2005) Reduction of copper(II) by iron(II). *J Environ Qual*, **34**, 1539-1546.

73. Ehrenreich, A. and Widdel, F. (1994) Anaerobic oxidation of ferrous iron by purple bacteria, a new type of phototrophic metabolism. *Appl Environ Microbiol*, **60**, 4517-4526.

74. Friedrich Widdel, S.S., Silke Heisingt, Armin Ehrenreich, Bernhard Assmus & Bernhard Schinkt. (1993) Ferrous iron oxidation by anoxygenic phototrophic bacateria. *Nature*, **362**, 834-836.

75. Gu, B., Schmitt, J., Chen, Z., Liang, L. and McCarthy, J.F. (1994) Adsorption and desorption of natural organic matter on iron oxide: mechanisms and models. *Environ Sci Technol*, **28**, 38-46.

76. Rentz, J.A., Turner, I.P. and Ullman, J.L. (2009) Removal of phosphorus from solution using biogenic iron oxides. *Water Res*, **43**, 2029-2035.

77. Croal, L.R., Jiao, Y. and Newman, D.K. (2007) The fox operon from *Rhodobacter* strain SW2 promotes phototrophic Fe(II) oxidation in *Rhodobacter capsulatus* SB1003. *J Bacteriol*, **189**, 1774-1782.

78. Jiao, Y. and Newman, D.K. (2007) The *pio* operon is essential for phototrophic Fe(II) oxidation in *Rhodopseudomonas palustris* TIE-1. *J Bacteriol*, **189**, 1765-1773.

79. Miot, J., Benzerara, K., Obst, M., Kappler, A., Hegler, F., Schadler, S., Bouchez, C., Guyot, F. and Morin, G. (2009) Extracellular iron biomineralization by photoautotrophic iron-oxidizing bacteria. *Appl Environ Microbiol*, **75**, 5586-5591.

80. Chan, C.S., De Stasio, G., Welch, S.A., Girasole, M., Frazer, B.H., Nesterova, M.V., Fakra, S. and Banfield, J.F. (2004) Microbial polysaccharides template assembly of nanocrystal fibers. *Science*, **303**, 1656-1658.

81. Wu, W., Swanner, E.D., Hao, L., Zeitvogel, F., Obst, M., Pan, Y. and Kappler, A. (2014) Characterization of the physiology and cell-mineral

interactions of the marine anoxygenic phototrophic Fe(II) oxidizer *Rhodovulum iodosum* - implications for Precambrian Fe(II) oxidation. *FEMS Microbiol Ecol*, **88**, 503-515.

82. Kreamer, N.N., Costa, F. and Newman, D.K. (2015) The ferrous iron-responsive BqsRS two-component system activates genes that promote cationic stress tolerance. *MBio*, **6**, e02549.

83. Bennett, B.D., Redford, K.E. and Gralnick, J.A. (2018) Survival of Anaerobic Fe^{2+} Stress Requires the ClpXP Protease. *J Bacteriol*, **200**.

84. Honarmand Ebrahimi, K., Hagedoorn, P.L. and Hagen, W.R. (2015) Unity in the biochemistry of the iron-storage proteins ferritin and bacterioferritin. *Chem Rev*, **115**, 295-326.

85. Abdul-Tehrani, H., Hudson, A.J., Chang, Y.S., Timms, A.R., Hawkins, C., Williams, J.M., Harrison, P.M., Guest, J.R. and Andrews, S.C. (1999) Ferritin mutants of *Escherichia coli* are iron deficient and growth impaired, and *fur* mutants are iron deficient. *J Bacteriol*, **181**, 1415-1428.

86. Bereswill, S., Waidner, U., Odenbreit, S., Lichte, F., Fassbinder, F., Bode, G. and Kist, M. (1998) Structural, functional and mutational analysis of the *pfr* gene encoding a ferritin from *Helicobacter pylori*. *Microbiology*, **144 (Pt 9)**, 2505-2516.

87. Wai, S.N., Nakayama, K., Umene, K., Moriya, T. and Amako, K. (1996) Construction of a ferritin-deficient mutant of *Campylobacter jejuni*:

contribution of ferritin to iron storage and protection against oxidative stress. *Mol Microbiol*, **20**, 1127-1134.

88. Antelmann, H., Engelmann, S., Schmid, R., Sorokin, A., Lapidus, A. and Hecker, M. (1997) Expression of a stress- and starvation-induced *dps*/*pexB*-homologous gene is controlled by the alternative sigma factor sigmaB in *Bacillus subtilis*. *J Bacteriol*, **179**, 7251-7256.

89. Pi, H. and Helmann, J.D. (2017) Ferrous iron efflux systems in bacteria. *Metallomics*, **9**, 840-851.

90. Abboud, S. and Haile, D.J. (2000) A novel mammalian iron-regulated protein involved in intracellular iron metabolism. *J Biol Chem*, **275**, 19906-19912.

91. Donovan, A., Brownlie, A., Zhou, Y., Shepard, J., Pratt, S.J., Moynihan, J., Paw, B.H., Drejer, A., Barut, B., Zapata, A. *et al.* (2000) Positional cloning of zebrafish ferroportin1 identifies a conserved vertebrate iron exporter. *Nature*, **403**, 776-781.

92. McKie, A.T., Marciani, P., Rolfs, A., Brennan, K., Wehr, K., Barrow, D., Miret, S., Bomford, A., Peters, T.J., Farzaneh, F. *et al.* (2000) A novel duodenal iron-regulated transporter, IREG1, implicated in the basolateral transfer of iron to the circulation. *Mol Cell*, **5**, 299-309.

93. Ward, D.M. and Kaplan, J. (2012) Ferroportin-mediated iron transport: expression and regulation. *Biochim Biophys Acta*, **1823**, 1426-1433.

94. Knutson, M.D., Vafa, M.R., Haile, D.J. and Wessling-Resnick, M. (2003) Iron loading and erythrophagocytosis increase ferroportin 1 (FPN1) expression in J774 macrophages. *Blood*, **102**, 4191-4197.

95. Liu, X.B., Hill, P. and Haile, D.J. (2002) Role of the ferroportin iron-responsive element in iron and nitric oxide dependent gene regulation. *Blood Cells Mol Dis*, **29**, 315-326.

96. Montosi, G., Donovan, A., Totaro, A., Garuti, C., Pignatti, E., Cassanelli, S., Trenor, C.C., Gasparini, P., Andrews, N.C. and Pietrangelo, A. (2001) Autosomal-dominant hemochromatosis is associated with a mutation in the ferroportin (SLC11A3) gene. *J Clin Invest*, **108**, 619-623.

97. Njajou, O.T., Vaessen, N., Joosse, M., Berghuis, B., van Dongen, J.W., Breuning, M.H., Snijders, P.J., Rutten, W.P., Sandkuijl, L.A., Oostra, B.A. *et al.* (2001) A mutation in SLC11A3 is associated with autosomal dominant hemochromatosis. *Nat Genet*, **28**, 213-214.

98. Pietrangelo, A. (2004) The ferroportin disease. *Blood Cells Mol Dis*, **32**, 131-138.

99. Donovan, A., Lima, C.A., Pinkus, J.L., Pinkus, G.S., Zon, L.I., Robine, S. and Andrews, N.C. (2005) The iron exporter ferroportin/Slc40a1 is essential for iron homeostasis. *Cell Metab*, **1**, 191-200.

100. Munkelt, D., Grass, G. and Nies, D.H. (2004) The chromosomally encoded cation diffusion facilitator proteins DmeF and FieF from

Wautersia metallidurans CH34 are transporters of broad metal specificity. *J Bacteriol*, **186**, 8036-8043.

101. Grass, G., Otto, M., Fricke, B., Haney, C.J., Rensing, C., Nies, D.H. and Munkelt, D. (2005) FieF (YiiP) from *Escherichia coli* mediates decreased cellular accumulation of iron and relieves iron stress. *Arch Microbiol*, **183**, 9-18.

102. Gupta, S., Chai, J., Cheng, J., D'Mello, R., Chance, M.R. and Fu, D. (2014) Visualizing the kinetic power stroke that drives proton-coupled zinc(II) transport. *Nature*, **512**, 101-104.

103. Lu, M., Chai, J. and Fu, D. (2009) Structural basis for autoregulation of the zinc transporter YiiP. *Nat Struct Mol Biol*, **16**, 1063-1067.

104. Lu, M. and Fu, D. (2007) Structure of the zinc transporter YiiP. *Science*, **317**, 1746-1748.

105. Bennett, B.D., Brutinel, E.D. and Gralnick, J.A. (2015) A Ferrous Iron Exporter Mediates Iron Resistance in *Shewanella oneidensis* MR-1. *Appl Environ Microbiol*, **81**, 7938-7944.

106. Salusso, A. and Raimunda, D. (2017) Defining the Roles of the Cation Diffusion Facilitators in Fe^{2+}/Zn^{2+} Homeostasis and Establishment of Their Participation in Virulence in *Pseudomonas aeruginosa*. *Front Cell Infect Microbiol*, **7**, 84.

107. Nies, D.H. (2011) How iron is transported into magnetosomes. *Mol Microbiol*, **82**, 792-796.

108. Uebe, R., Junge, K., Henn, V., Poxleitner, G., Katzmann, E., Plitzko, J.M., Zarivach, R., Kasama, T., Wanner, G., Posfai, M. *et al.* (2011) The cation diffusion facilitator proteins MamB and MamM of *Magnetospirillum gryphiswaldense* have distinct and complex functions, and are involved in magnetite biomineralization and magnetosome membrane assembly. *Mol Microbiol*, **82**, 818-835.

109. Uebe, R., Keren-Khadmy, N., Zeytuni, N., Katzmann, E., Navon, Y., Davidov, G., Bitton, R., Plitzko, J.M., Schuler, D. and Zarivach, R. (2018) The dual role of MamB in magnetosome membrane assembly and magnetite biomineralization. *Mol Microbiol*, **107**, 542-557.

110. Nicolaou, S.A., Fast, A.G., Nakamaru-Ogiso, E. and Papoutsakis, E.T. (2013) Overexpression of *fetA* (*ybbL*) and *fetB* (*ybbM*), Encoding an Iron Exporter, Enhances Resistance to Oxidative Stress in *Escherichia coli*. *Appl Environ Microbiol*, **79**, 7210-7219.

111. Liu, Y., Bauer, S.C. and Imlay, J.A. (2011) The YaaA protein of the *Escherichia coli* OxyR regulon lessens hydrogen peroxide toxicity by diminishing the amount of intracellular unincorporated iron. *J Bacteriol*, **193**, 2186-2196.

112. Frawley, E.R., Crouch, M.L., Bingham-Ramos, L.K., Robbins, H.F., Wang, W., Wright, G.D. and Fang, F.C. (2013) Iron and citrate export by a major facilitator superfamily pump regulates metabolism and stress

resistance in *Salmonella* Typhimurium. *Proc Natl Acad Sci U S A*, **110**, 12054-12059.

113. Frawley, E.R. and Fang, F.C. (2014) The ins and outs of bacterial iron metabolism. *Mol Microbiol*, **93**, 609-616.

114. Bhubhanil, S., Chamsing, J., Sittipo, P., Chaoprasid, P., Sukchawalit, R. and Mongkolsuk, S. (2014) Roles of *Agrobacterium tumefaciens* membrane-bound ferritin (MbfA) in iron transport and resistance to iron under acidic conditions. *Microbiology*, **160**, 863-871.

115. Ruangkiattikul, N., Bhubhanil, S., Chamsing, J., Niamyim, P., Sukchawalit, R. and Mongkolsuk, S. (2012) *Agrobacterium tumefaciens* membrane-bound ferritin plays a role in protection against hydrogen peroxide toxicity and is negatively regulated by the iron response regulator. *FEMS Microbiol Lett*, **329**, 87-92.

116. Sankari, S. and O'Brian, M.R. (2014) A bacterial iron exporter for maintenance of iron homeostasis. *J Biol Chem*, **289**, 16498-16507.

117. Chan, H., Babayan, V., Blyumin, E., Gandhi, C., Hak, K., Harake, D., Kumar, K., Lee, P., Li, T.T., Liu, H.Y. *et al.* (2010) The p-type ATPase superfamily. *J Mol Microbiol Biotechnol*, **19**, 5-104.

118. Arguello, J.M. (2003) Identification of ion-selectivity determinants in heavy-metal transport P_{1B}-type ATPases. *J Membr Biol*, **195**, 93-108.

119. Gaballa, A. and Helmann, J.D. (2002) A peroxide-induced zinc uptake system plays an important role in protection against oxidative stress in *Bacillus subtilis*. *Mol Microbiol*, **45**, 997-1005.

120. Fuangthong, M. and Helmann, J.D. (2003) Recognition of DNA by three ferric uptake regulator (Fur) homologs in *Bacillus subtilis*. *J Bacteriol*, **185**, 6348-6357.

121. Patel, S.J., Lewis, B.E., Long, J.E., Nambi, S., Sassetti, C.M., Stemmler, T.L. and Arguello, J.M. (2016) Fine-tuning of Substrate Affinity Leads to Alternative Roles of *Mycobacterium tuberculosis* Fe^{2+}-ATPases. *J Biol Chem*, **291**, 11529-11539.

122. Pi, H., Patel, S.J., Arguello, J.M. and Helmann, J.D. (2016) The *Listeria monocytogenes* Fur-regulated virulence protein FrvA is an Fe(II) efflux P_{1B4}-type ATPase. *Mol Microbiol*, **100**, 1066-1079.

123. Turner, A.G., Ong, C.Y., Djoko, K.Y., West, N.P., Davies, M.R., McEwan, A.G. and Walker, M.J. (2017) The PerR-Regulated P_{1B-4}-Type ATPase (PmtA) Acts as a Ferrous Iron Efflux Pump in *Streptococcus pyogenes*. *Infect Immun*, **85**.

124. VanderWal, A.R., Makthal, N., Pinochet-Barros, A., Helmann, J.D., Olsen, R.J. and Kumaraswami, M. (2017) Iron Efflux by PmtA Is Critical for Oxidative Stress Resistance and Contributes Significantly to Group A *Streptococcus* Virulence. *Infect Immun*, **85**.

125. Zheng, C., Jia, M., Gao, M., Lu, T., Li, L. and Zhou, P. (2019) PmtA functions as a ferrous iron and cobalt efflux pump in *Streptococcus suis*. *Emerg Microbes Infect*, **8**, 1254-1264.

Chapter 2

Redox Sensing by Fe^{2+} in Bacterial Fur Family Metalloregulators[3]

> "*Living and non-living entities are strikingly different, yet somehow the precise manner in which these two material forms relate to one another has remained provocatively out of reach. Life's evident design, in particular, stands out, a source of endless speculation… Due to the remarkable advances in molecular biology over the past six decades we have discovered that nature's design capabilities can be immeasurably greater.*"
>
> *- Addy Pross, What is Life? How Chemistry Becomes Biology, 2012.*

2.1 Abstract

***Significance*:** Iron is required for growth and is often redox active under cytosolic conditions. As a result of its facile redox chemistry, iron homeostasis is intricately involved with oxidative stress. Bacterial adaptation to iron limitation and oxidative stress often involves ferric uptake regulator (Fur) proteins: a diverse set of divalent cation-dependent, DNA-binding proteins that vary widely in both metal selectivity and sensitivity to metal-catalyzed oxidation.

***Recent Advances*:** Bacteria contain two Fur family metalloregulators that use ferrous iron (Fe^{2+}) as their cofactor, Fur and PerR. Fur functions to regulate

[3] This chapter is adapted from review article: Pinochet-Barros A. & Helmann J. D. Antioxidants and Redox Signaling 2018 Dec 20;29(18):1858-1871.

iron homeostasis in response to changes in intracellular levels of Fe^{2+}. PerR also binds Fe^{2+}, which enables metal-catalyzed protein oxidation as a mechanism for sensing hydrogen peroxide (H_2O_2).

***Critical Issues*:** To effectively regulate iron homeostasis, Fur has an Fe^{2+} affinity tuned to monitor the labile iron pool of the cell and may be under selective pressure to minimize iron oxidation, which would otherwise lead to an inappropriate increase in iron uptake under oxidative stress conditions. Conversely, Fe^{2+} is bound more tightly to PerR but exhibits high H_2O_2 reactivity, which enables a rapid induction of peroxide stress genes.

***Future Directions*:** The features that determine the disparate reactivity of these proteins with oxidants are still poorly understood. A controlled, comparative analysis of the affinities of Fur/PerR proteins for their metal cofactors and their rate of reactivity with H_2O_2, combined with structure/function analyses, will be needed to define the molecular mechanisms that have facilitated this divergence of function between these two paralogous regulators.

2.2 Iron's double-edged sword

Iron is an essential element across all domains of life. It is used as a cofactor by enzymes involved in a wide array of metabolic processes spanning central metabolism, respiration, photosynthesis, nitrogen fixation, and DNA synthesis and repair (6). Bacteria are no exception to this, as is evident by

their use of three major classes of iron-requiring proteins: (1) mono- and di-nuclear iron enzymes, (2) iron/sulfur cluster enzymes, and (3) heme proteins. These three classes of iron-utilizing enzymes permeate many aspects of bacterial metabolism. This need for iron in bacteria is ancient and dates from the earliest stages in the evolution of life >2 billion years ago. During this time, the Earth was an anoxic environment, which allowed iron to be maintained in its reduced, soluble ferrous (Fe^{2+}) form (5). Iron was therefore highly bioavailable and found use as a cofactor for stabilizing proteins as ‘‘iron rivets’’ (39), for electron transfer reactions, and as a Lewis acid catalyst. However, as photosynthetic organisms became more prevalent, the gradual oxygenation of the Earth’s atmosphere imposed a transition from anaerobic to aerobic conditions. This shifted the redox state of iron into its oxidized, weakly soluble ferric (Fe^{3+}) form and led to the geologic deposition of massive amounts of iron in banded iron formations (5). These environmental changes imposed two new physiological challenges on early microbial life: iron starvation and oxidative stress.

The restriction on microbial growth that resulted from the depletion of dissolved iron from the ancient oceans persists to this day (97). As a result, bacteria evolved systems for iron homeostasis, which are often regulated by ferric uptake regulator (Fur) proteins (74). Iron homeostasis involves three distinct mechanisms (Fig. 2.1). First, bacteria synthesize high-affinity iron chelators (siderophores), their cognate uptake systems, and other transporters

for iron import (6). Second, Fur often controls an ‘‘iron-sparing’’ response in which a Fur-regulated small RNA serves to inhibit the translation of nonessential iron requiring enzymes (82). Third, cells may replace iron-containing proteins with alternative, iron-independent proteins (87). For example, under iron limitation, many bacteria express flavodoxins as a substitute for iron-utilizing ferredoxins and manganese superoxide dismutase (MnSOD) in place of FeSOD (87). Collectively, these responses provide the cell with a viable iron economy despite the scarcity of the growth-limiting micronutrient.

The second chemical consequence of the rise of diatomic oxygen in the atmosphere was an increase in reactive oxygen species (ROS) such as hydrogen peroxide (H_2O_2) and superoxide radicals (O_2^-). ROS are naturally generated in the environment in a variety of photosynthetic reactions and as metabolic by-products of flavoprotein autoxidation (62, 84). ROS can exert toxicity in several distinct ways, but one common theme is the oxidative inactivation of iron-containing enzymes, including both iron/sulfur-containing dehydratases and mononuclear iron enzymes (63). H_2O_2 reacts with ferrous iron through Fenton chemistry, and the resulting highly reactive hydroxyl radical can impair metabolism through DNA and protein damage, which can inevitably lead to cell death (63).

$$Fe^{2+} + H_2O_2 \rightarrow [FeO]^{2+} + H_2O$$

$$[FeO]^{2+} + H^+ \rightarrow Fe^{3+} HO^{\bullet}$$

Similarly, superoxide inactivates iron-containing enzymes by oxidation of their required cofactors. In the case of mononuclear iron enzymes, oxidation and loss of iron have been shown to lead to mismetallation by zinc (Zn^{2+}), which binds with higher avidity than iron (64). This has been observed in *Escherichia coli*, where ribulose-5-phosphate 3-epimerase and 3-deoxy-$_D$-arabinoheptulosonate 7-phosphate synthase become mismetallated by Zn^{2+} on exposure to ROS, causing enzyme inactivation and subsequent blockage of specific metabolic pathways (64, 104, 105).

Aerobic bacteria are reliant on detoxification mechanisms to help counter the deleterious effects of ROS, by either directly detoxifying oxidants such as H_2O_2 or by decreasing intracellular labile iron to mitigate the effects of Fenton chemistry (61, 63, 77). H_2O_2 is removed enzymatically by catalase and alkyl hydroperoxide reductase (99), whereas superoxide is removed by SOD (63). Quantitative modeling in *E. coli* suggests that iron/sulfur-containing dehydratases and mononuclear iron enzymes are likely to be oxidized and repaired on a time scale of minutes under aerobic growth, even in cells ROS requires the induction of defensive enzymes to an even higher titer (63). In *E. coli*, having a normal complement of defensive enzymes (63, 104, 105). Any further increase in the induction of pathways for defense against ROS is controlled by the OxyR and SoxRS systems (63). Whereas OxyR senses H_2O_2 by disulfide bond formation, many other bacteria rely on a chemically distinct sensing mechanism involving metal-catalyzed oxidation of a regulator protein.

The prototype for this class of regulators is the *Bacillus subtilis* PerR protein, a paralog of Fur (73).

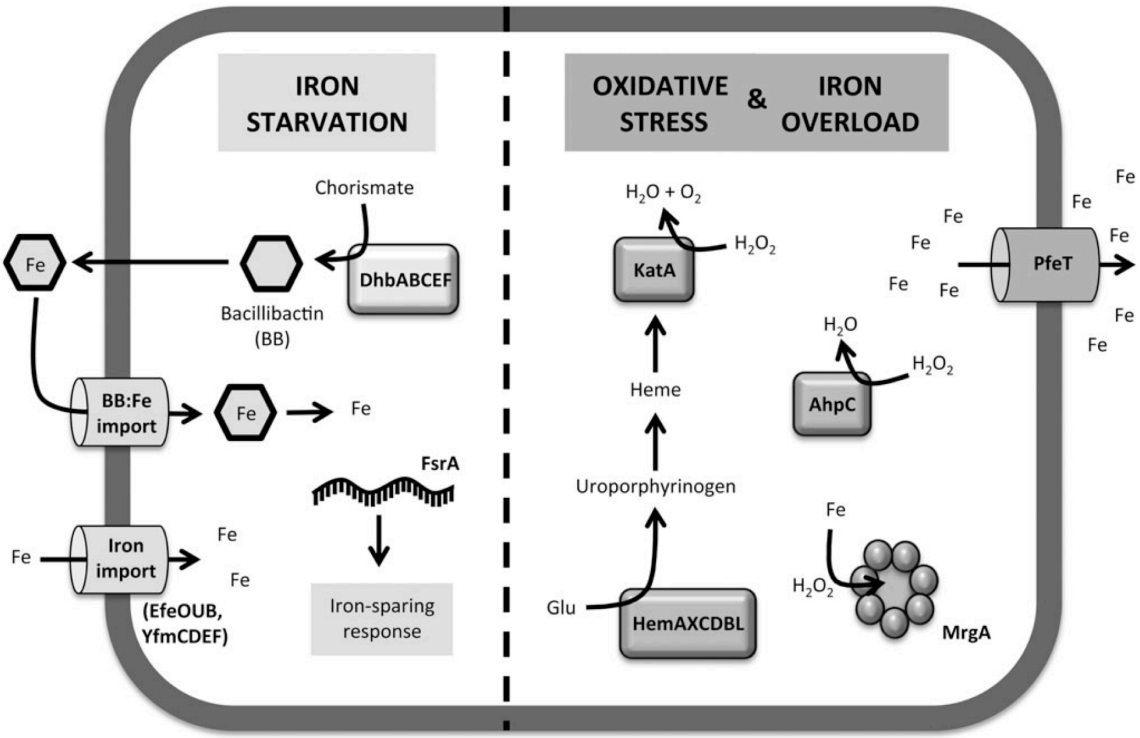

FIG. 2.1) Iron-related stress responses in *Bacillus subtilis*.

Schematic summary of the response mechanisms in *B. subtilis* to different types of iron-related stresses. When cells are subjected to iron starvation, cells express genes involved in iron acquisition, which encode iron importers and siderophore biosynthesis enzymes. Cells also express the small RNA FsrA, which targets posttranscriptional inhibition of low-priority iron requiring enzymes, thus implementing the iron sparing response. Under conditions of oxidative stress, cells induce expression of peroxide detoxifying enzymes (KatA and AhpC) and their cofactors (HemAXCDBL), as well as enzymes that have an impact on cellular iron levels, such as the iron sequestration ferritin-like protein (MrgA) and the P_{1B4}-type ATPase iron efflux pump PfeT. Note that under iron overload conditions, PfeT and (to a lesser extent) MrgA also confer resistance to excess iron. AhpC, alkyl hydroperoxide reductase; KatA, catalase.

The facile redox chemistry of ferrous iron requires that bacteria tightly

regulate iron homeostasis and maintain an efficient mechanism to sense and respond to ROS such as H_2O_2. Defenses against both iron limitation and ROS are important in the physiology of many pathogens. During infection, the host restricts bacterial growth by sequestration of essential metal ions, including iron, and innate immune cells kill bacteria using ROS and reactive nitrogen species (RNS) (36).

This review will focus on the role of Fur family metalloregulators in coordinating these two interacting adaptive responses. A special emphasis will be placed on the biochemistry and genetics of two Fur family proteins in the gram-positive soil bacterium *B. subtilis*, which will be designated as Fur_{Bs} and $PerR_{Bs}$. Comparison of the reactivity of these proteins and their orthologs with ROS and RNS reveals a wide range of sensitivity, and recent results have begun to shed light on how this reactivity may be tuned by changes in protein structure.

2.3 Fur family metalloregulators

The ferric uptake regulator (Fur) protein was first characterized in *E. coli* (Fur_{Ec}) where it functions as an iron-responsive repressor. Initial genetic studies revealed that *E. coli fur* null mutants produced very high levels of siderophores (51, 53). Subsequent biochemical characterization demonstrated that Fur_{Ec} is a dimeric, helix-turn-helix (HTH) containing DNA-binding protein that binds Fe^{2+} as corepressor (10, 11, 26). These observations, together with

subsequent studies (89), led to a general model in which Fur_{Ec} directly senses Fe^{2+} levels in the cell to maintain iron homeostasis.

Fur family metalloregulators are ubiquitous in bacteria and are commonly identified through the conserved $HHHXHX_2CX_2C$ motif positioned at the hinge region between the metal-sensing C-terminus and the DNA-binding domain (40, 74). Although Fur proteins are most closely associated with iron homeostasis, it is now appreciated that the Fur family includes many proteins with distinct metal selectivities. Variations in the metal-binding sites have enabled the evolution of Fur family members that are activated by a diverse set of metals. For example, the Fur family includes sensors of zinc (Zur), manganese (Mur), and nickel (Nur) (3, 53, 74). In addition, a subset of the iron-utilizing Fur family proteins functions physiologically as sensors of intracellular H_2O_2 (PerR) (73, 74).

Given the broad metal-sensing scope of these regulators, it is not surprising that bacteria may possess multiple Fur homologs. For example, *B. subtilis* has three Fur family paralogs: a Zn^{2+}-sensing Zur (45), an Fe^{2+}-sensing Fur, and a peroxide-sensing PerR (16, 91). Interestingly, *B. subtilis* does not sense Mn^{2+} via a Fur family protein, but rather through MntR, a member of the diphtheria toxin regulator (DtxR) family (59, 96). Furthermore, it was recently reported that *Bacillus licheniformis* not only has Fur and Zur but also contains three PerR paralogs (68).

Paralogous Fur family members may evolve distinct metal selectivity by

changes in the chemical nature and geometry of the metal-coordinating ligands at the metal-sensing sites (74). Furthermore, each sensor must have an affinity appropriate for detecting fluctuations in the intracellular buffered pool of free metal ions, as reviewed in detail elsewhere (49, 112, 113). However, Fur family regulators can bind to non-cognate metals either as agonists or antagonists. The binding of noncognate metals to metalloregulatory proteins (mismetallation) can have deleterious consequences for regulators, just as it can for enzymes. For example, in *E. coli* and related proteobacteria, high levels of Mn^{2+} are toxic and mutations that inactivate Fur often arise conferring resistance to these elevated manganese levels (52). This suggests that mismetallation of Fur with Mn^{2+} may inappropriately repress Fe^{2+} uptake. Similarly, in *B. subtilis*, a modest increase in Fur_{Bs} expression (in a *perR* null mutant) leads to mismetallation with Mn^{2+} and results in iron starvation (38, 78), and mismetallation of $PerR_{Bs}$ with Zn^{2+} can lead to dysregulation of the PerR regulon resulting in heme intoxication (20).

Structural studies have provided insight into how Fur family proteins sense metals and, in the case of PerR, respond to oxidants (73, 74, 79, 95), as well as into how they interact with DNA (32, 47). In general, Fur family proteins are homodimeric, and DNA-binding proteins comprised two main domains. The amino-terminal domain contains HTH motif and binds to DNA. The C-terminal domain is required for metal sensing and mediates

dimerization. This metal-sensing domain typically contains two to three metal-

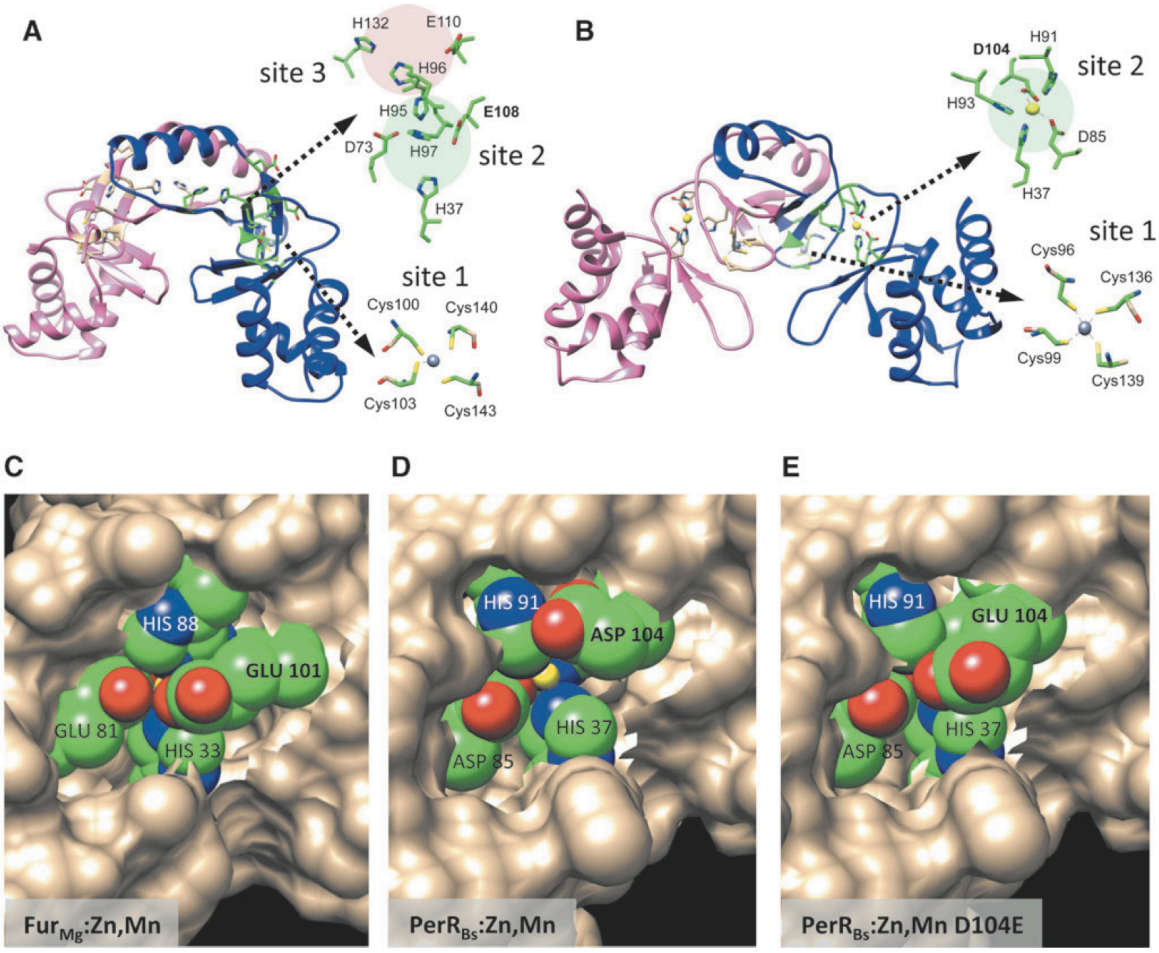

FIG. 2.2) Fur and PerR structures.

(A) Fur$_{Bs}$ structural homology model based on the *Streptomyces coelicolor* Zur structure (PDB: 3mwm; sequence identity: 33.3%) (102). This Fur$_{Bs}$ model shows the predicted homodimer in its holo-form. Close-up views of its three conserved metal-binding sites are provided in stick form. Site 1 is a Cys-rich pocket that binds a structural Zn^{2+} atom to provide protein stability to the dimer. Sites 2 and 3 comprise the iron-sensing site (shown without metal atoms), where site 2 seems to play a primary role in triggering the conformational changes required for DNA binding [figure adapted from (78)]. **(B)** PerR$_{Bs}$ crystal structure bound with Mn^{2+}. A close-up of the metal-sensing site (site 2) and the structural site (site 1) is depicted in stick form (PDB code: 3F8N). **(C)** Crystal structure of Fur$_{Mg}$:Zn,Mn (PDB code: 4RAZ) showing a close-up of binding site 1, which is analogous to site 2 in Fur$_{Bs}$ and in PerR$_{Bs}$. Mn^{2+} is not easily accessible. **(D)** Crystal structure of PerR$_{Bs}$:Zn,Mn (PDB code: 3F8N) showing a close-up of binding site 2. Mn^{2+} is easily accessible. **(E)** Crystal structure of PerR$_{Bs}$:Zn,Mn showing a close-up of binding site 2 with conserved Asp104 residue mutated into a Glu. Mn^{2+} is completely occluded (Mn^{2+} = yellow; nitrogen atom = blue; oxygen atom = red; carbon atom = green).

binding sites (Fig. 2.2A). The first (site 1) is a structural metal-binding site comprising four cysteine residues that interact with a single Zn^{2+} atom (Cys_4:Zn). This site is required for protein folding and dimerization for many Fur family proteins (4, 25, 72, 111, 115). However, some Fur homologs lack a structural zinc site. Such is the case for *Pseudomonas aeruginosa* Fur (Fur_{Pa}), which only has one of the four conserved Cys residues, making the site functionally dispensable *in vivo*, and *Pseudomonas putida*, which lacks all four conserved Cys residues (76). The metal-sensing site in most Fur family proteins (site 2) is located in the C-terminal metal-binding domain and often bridges to the DNA-binding domain, thereby providing a mechanism for allosteric activation of DNA binding (40, 66). This is the key site for iron sensing by Fur and for peroxide sensing by PerR (73, 78). In some Fur proteins, including Fur_{Bs}, there is also a third metal-binding site (site 3) of poorly defined function (33, 78).

2.4 Iron utilizing Fur family regulators in *B. subtilis*: Fur_{Bs} and $PerR_{Bs}$

B. subtilis has two Fur regulators that bind to iron: Fur_{Bs} and $PerR_{Bs}$. Although these two proteins are closely related and bind to the same divalent cation, their functions are quite distinct. This is evident from the set of genes they control (13, 37, 56, 91). Fur_{Bs} controls a large regulon that comprises ~40 genes involved in iron homeostasis, consistent with its role as the primary sensor of iron limitation (13). $PerR_{Bs}$ is involved in controlling expression of

genes that help combat H_2O_2 stress, including genes that encode iron efflux and storage functions (21, 37, 48). Characterization of *B. subtilis* Fur and PerR illustrates an important feature of Fur family regulators: it is quite difficult to unambiguously assign function solely from inspection of protein sequence. Often, functional assignments can be best inferred by considering the set of genes regulated by each protein.

2.4.1 The Fur_{Bs} regulon

The Fur_{Bs} regulon can be divided into two main groups: iron acquisition genes and genes involved in the iron-sparing response. In the former, one subset is involved in siderophore biosynthesis. Fur_{Bs} regulates the *dhb* operon, which encodes proteins involved in the synthesis of bacillibactin (BB) (13, 15, 46, 85). The second subset encodes ABC transporters involved in ferric siderophore uptake with specificity for BB and enterobactin (*feuABC*), ferrichrome (*fhuBCDG*), and schizokinen/arthrobactin (*yfiZY*/*yfhA*) (94). In addition, Fur_{Bs} regulates ferric citrate uptake (*yfmCDEF*) and elemental iron uptake (*efeOUB*) (Fig. 2.1) (13, 88, 94). Second, Fur controls expression of a small RNA (FsrA) and three RNA chaperones (FbpA, FbpB, and FbpC). When derepressed, FsrA targets specific genes that code for selected iron enzymes, inhibiting their translation and thus effectively carrying out the iron-sparing response, which efficiently prioritizes iron utilization in the cell (Fig. 2.1) (44, 103). This system is functionally analogous to the similar iron-sparing

response of *E. coli* mediated by the Fur-controlled small RNA RyhB (81–83).

Fur recognizes genes within its regulon by binding to specific DNA operator sites (Fur boxes) located within the promoter region of its target genes. Originally, the Fur box was defined as a 19 bp inverted repeat (35), but subsequent studies demonstrated that a minimal-binding site is a heptameric inverted repeat motif (7-1-7): the 19 bp consensus corresponds to two, overlapping 7-1-7 motifs (12). The binding of Fur to these two overlapping binding sites has been visualized in crystals of *Magnetospirillum gryphiswaldense* Fur (Fur_{Mg}) metallated with Mn^{2+} and bound to a Fur box DNA sequence (32). Remarkably, all three Fur paralogs in *B. subtilis* recognize very similar inverted repeat motifs, but there is minimal overlap in their target genes (42). Specific recognition takes place, in part, through a conserved arginine (Arg) residue located at position 61 (R61) of the Fur_{Bs} DNA-binding domain (18). This residue recognizes the conserved guanine (G) and cytosine (C) bases located within the 7-1-7 motif (TGATAAT-N-ATTATCA), which are precisely the bases that distinguish Fur-binding sites from typical PerR-binding sites (42).

When *B. subtilis* cells experience iron depletion, the Fur regulon is derepressed. In the laboratory, iron depletion can be generated by treating cells with dipyridyl, an intracellular iron chelator, thus affecting the labile iron pool (13). As free iron levels drop in the cell, iron is no longer bound to Fur. The resultant conformational change leads to dissociation from DNA, thus

allowing RNA polymerase to bind to the previously occluded promoter regions and initiate transcription. These Fur-regulated genes are thereby regulated directly by Fur binding, as confirmed by DNaseI footprinting (13). Some Fur family regulators may retain regulatory activity in the apo-form and bind to sites distinct from those bound by the metallated holo-protein. This type of more complex regulation has been described for Fur from both *Campylobacter jejuni* (17) and *Helicobacter pylori* (1).

Regulon derepression can take place in one of two general ways. As iron levels fall, all members of the regulon may be derepressed simultaneously, or instead as a stepwise (graded) response where different subsets of genes are derepressed according to the level of stress the cell is experiencing. For example, the *B. subtilis* Zur regulon is derepressed in three distinct stages as bioavailable zinc levels decline (101). A similar effect is observed in the *Streptomyces coelicolor* Zur (102).

Fur regulons may also respond to gradual iron depletion by the sequential derepression of various adaptive mechanisms, but the details are still emerging. The mechanisms underlying this sequential response are also not yet well understood, but may be related to variations in the architecture of the Fur-binding sites. For example, at some sites, Fur may function as a single dimeric protein and bind an isolated 7-1-7 motif (12). At other sites, Fur may bind to the classic 19 bp consensus as two, opposed dimers (binding on opposite faces of the DNA helix) (32, 47). Finally, Fur is known to have a

propensity to bind to extended regions of DNA, and this cooperativity may be facilitated by protein/protein interactions (19, 29, 31, 41, 71). Differences in both the number and affinity of Fur-binding sites presumably help tune both the magnitude of the induction and the responsiveness of each target operon to the level of iron depletion.

2.4.2 Structural insights into Fe^{2+} sensing by Fur

The activity of Fur_{Bs} is regulated by its specific interaction with Fe^{2+}. As noted above, Fur_{Bs} is representative of those Fur family members with a structural Zn^{2+} site and two additional metal-binding sites (Fig. 2.2A). Purification of Fur_{Bs} in the presence of metal chelators yields the stable, dimeric apo-protein containing only the structural Zn^{2+} ion (Fur_{Bs}:Zn) (78). Addition of Fe^{2+} (or other divalent cations) activates DNA binding with a stoichiometry of two Fe^{2+} atoms per monomer. The site 2 metal-sensing site is required for iron sensing. In addition, Fur_{Bs} contains a third site (site 3) near the dimerization interface. *In vitro*, Fe^{2+} first binds to site 3, followed by subsequent binding of the metal to site 2 (78). Although both site 2 and site 3 are required for DNA binding, site 2 is the major iron-sensing site; binding to site 3 has a relatively modest effect (~7-fold) on DNA-binding affinity compared to that achieved by binding to site 2 (~150-fold) (78).

The precise mechanism by which these two metal-sensing sites interact to trigger the conformational changes that activate DNA binding by Fur

remains unclear (74, 78). It is possible that the sequential binding of Fe^{2+} to site 3 and then site 2 helps to fine-tune the expression of genes within the Fur regulon, or to help Fur_{Bs} avoid inappropriate activation by mismetallation. For example, sensing of Mn^{2+} by the DtxR family protein MntR involves the sequential loading of Mn^{2+} into two neighboring sites in each monomer, which is thought to provide a mechanism to increase the selectivity of metal responsiveness (86). Alternatively, site 3 may play a largely structural role in stabilizing the dimeric repressor. Indeed, it has not even been established whether or not Fe^{2+} is the metal that occupies site 3 *in vivo*.

Under normal physiological conditions, Fur binds specifically to Fe^{2+}, and other divalent metal ions do not elicit repression of the Fur regulon. The concentration of free iron required to trigger DNA binding by Fur_{Bs} is defined by the K_d for Fe^{2+} binding (~1 μM) *in vitro*, which thereby provides an estimate of the buffered concentration of free Fe^{2+} in the cell. A nearly identical affinity (~1.2 μM) has been measured for Fur_{Ec} (89).

However, *in vitro* studies reveal that Fur_{Bs} can also be activated by Mn^{2+}, although with a lower binding affinity (K_d of ~24 μM) (78). Typically, the cellular concentration of free Mn^{2+} is maintained at a level too low to mismetallate Fur_{Bs}. Mn^{2+} levels are regulated by MntR, which both represses uptake and activates efflux of Mn^{2+} and has an Mn^{2+} affinity (K_d ~6 μM) several fold higher than that of Fur_{Bs} (K_d ~24 μM). Interestingly, under conditions where Fur_{Bs} is overexpressed (as is the case in a *perR* null strain),

Fur_{Bs} is now constitutively activated by physiological levels of intracellular Mn^{2+} (78). In addition, Fur_{Bs} has also been shown to exhibit some cross talk with Cd^{2+} or Zn^{2+} in the presence of sufficiently high concentrations of these metals (90), but it is unknown if this is mediated by direct binding of these cations to Fur_{Bs} or indirectly. The high selectivity of Fur_{Bs} for Fe^{2+} *in vivo* is remarkable in light of the many genetic studies suggesting that mismetallation of Fur by Mn^{2+} leads to dysregulation of the Fur regulon in many proteobacteria, including *E. coli* and *Salmonella enterica* (52, 60).

2.4.3 The PerR regulon

$PerR_{Bs}$ was originally identified as a Fur family protein required for the adaptation of *B. subtilis* to H_2O_2 stress (16, 119). The $PerR_{Bs}$ regulon comprised two groups of genes: (1) those involved in the direct detoxification of ROS and (2) those that contribute to iron homeostasis. The former group consists of *katA* (vegetative catalase) and *ahpCF* (alkyl hydroperoxide reductase), both of which encode enzymes involved in the direct detoxification of hydrogen peroxide (H_2O_2) (16, 22, 37, 63). The heme biosynthesis operon (*hemAXCDBL*) also falls under this category, since induction of heme biosynthesis supports the activity of the abundantly expressed, heme-dependent catalase KatA (38) (Fig. 2.1). The second group of PerR-regulated genes encodes a Dps-like miniferritin involved in iron sequestration (MrgA) (21, 23) and a P_{1B4}-type ATPase involved in ferrous iron efflux (PfeT) (Fig. 2.1)

(48). Finally, PerR also controls *fur* and autoregulates its own expression (41, 54). The observation that $PerR_{Bs}$ specifically regulates H_2O_2 detoxification and iron sequestration (MrgA), efflux (PfeT), and import (indirectly through Fur) is consistent with a primary role in minimizing the damage elicited by iron-catalyzed Fenton chemistry.

Early genetic studies revealed that *B. subtilis* peroxide stress genes were regulated by both metal ions and by H_2O_2, and this regulation required the same cis-acting operator site and the same trans-acting factor (22). This coordinate regulation is explained by the role of $PerR_{Bs}$ as a metal-dependent repressor (strongly activated by either Fe^{2+} or Mn^{2+}). Like other Fur family proteins, $PerR_{Bs}$ contains a structural Zn^{2+} (site 1) and metal-sensing site 2 (Fig. 2.2B). $PerR_{Bs}$ is highly sensitive to H_2O_2 inactivation when in its Fe^{2+}-cofactored form (designated PerR:Zn,Fe). In response to H_2O_2 stress, the *mrgA*, *katA*, and *pfeT* genes are all highly induced (55) (Fig.2.3). The *ahpC* and *hemA* promoters are also modestly induced by H_2O_2, and $PerR_{Bs}$ also exhibits a weak (twofold to threefold) repression of *fur* and *perR* (43) (Fig. 2.3). Operator sites for PerR-regulated genes (Per boxes) are very similar to those for Fur (42). They both align as 7-1-7 motifs and have a high sequence similarity with the exception of thymine (T) and adenine (A) at the -6 and +6 positions, respectively, of the two heptamers (TTATAAT-ATTATAA). These two bases are typically a G and a C in Fur boxes. These conserved bases are recognized by an asparagine (Asn) residue in position 61 of $PerR_{Bs}$ (18). A

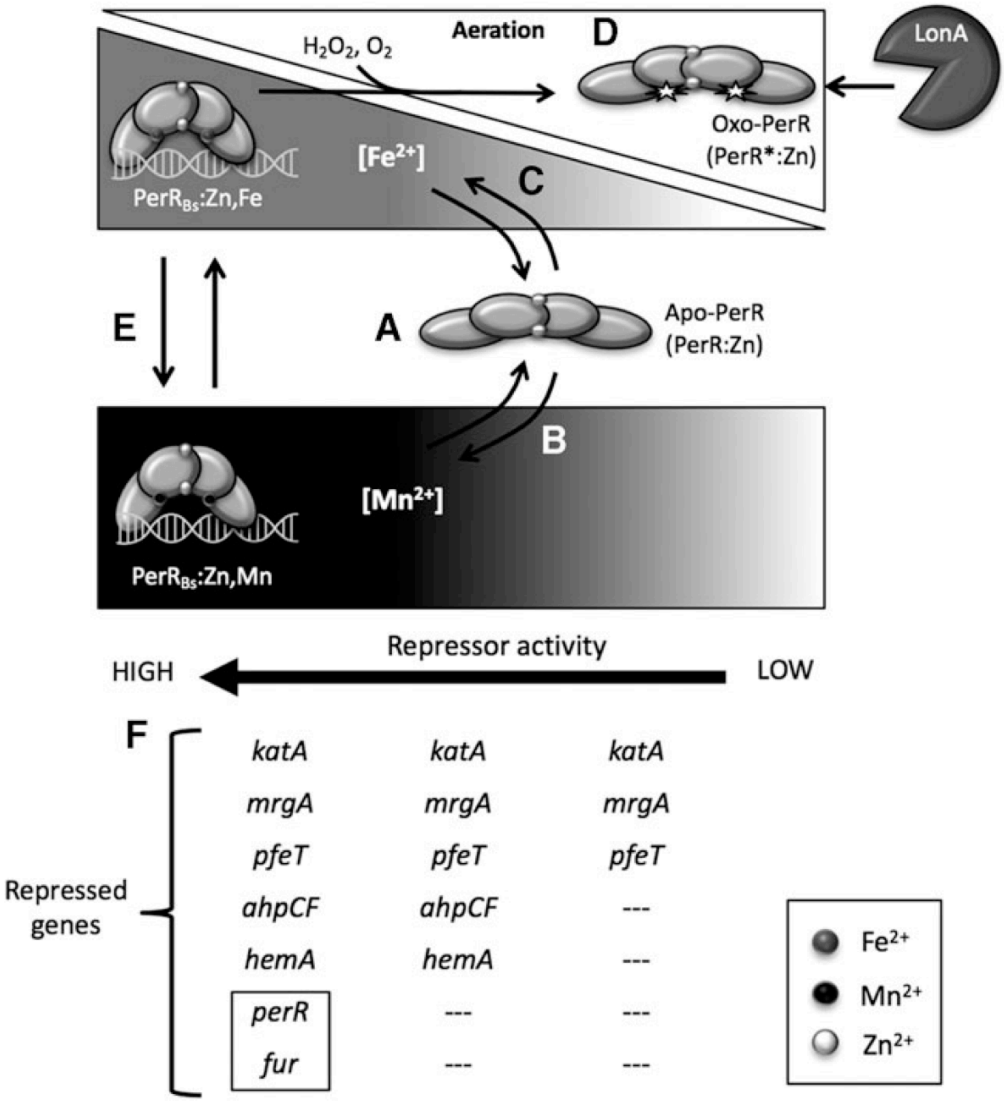

FIG. 2.3) Mechanism of gene regulation by $PerR_{Bs}$.

(A) Apo-PerR (PerR:Zn) lacks a metal cofactor at its metal-sensing site. This causes PerR to adopt a conformation that prevents it from binding to its DNA operator sites. As a result, no gene repression takes place. **(B)** As Mn^{2+} concentrations increase, apo-PerR becomes metallated, triggering a conformational change in PerR:Zn,Mn allowing it to bind its specific operator sites and repress PerR-regulated genes. Note that PerR:Zn,Mn is insensitive to oxidizing agents. **(C)** As Fe^{2+} concentrations increase, apo-PerR becomes metallated by iron. PerR:Zn,Fe binds to PerR operator sites and repress genes in the PerR regulon. However, during aerobic growth or in the presence of ROS, the ability of PerR:Zn,Fe to act as a repressor is limited by protein oxidation. **(D)** Oxidation of PerR exposes a conserved signature residue sequence recognized by LonA. Thus, oxo-PerR is targeted for degradation by the protease, preventing accumulation of

inactive protein. **(E)** Metallated PerR can reversibly bind to Mn^{2+} or Fe^{2+} as metal concentrations in the cell vary. **(F)** Overview of the ability of PerR to repress various genes as a function of metal availability. In the presence of iron, under aerobic conditions, inactivation of PerR prevents accumulation of high levels of active repressor. As a result, metallated PerR:Zn,Fe is most efficient at repression of genes postulated to have high-affinity operator sites (*katA*, *mrgA*, *pfeT*). PerR:Zn,Mn, which is not susceptible to oxidation, can accumulate to a high effective level and strongly represses genes the entire PerR regulon, including those genes postulated to have the lowest affinity operator sites (*perR*, *fur*) (as highlighted by box). ROS, reactive oxygen species.

similar inverted repeat pattern is also observed in Zur boxes, additionally requiring a three base pair extension on both sides of the minimal operator (42). Although these operator sites are very similar, there is little if any overlap of regulators across operator sites.

2.4.4 Structural insights into H_2O_2 sensing by PerR

Much like Fur_{Bs}, $PerR_{Bs}$ is a dimeric DNA-binding protein with two distinct functional domains: a DNA-binding domain and a sensing domain. $PerR_{Bs}$ binds two metal ions per monomer (72, 73, 78, 79, 108), instead of three as noted for Fur_{Bs} (78) (Fig. 2.2A&B). The first is a structural Zn^{2+} atom necessary for structural integrity and protein dimerization. This Zn^{2+} is bound tightly to $PerR_{Bs}$ in a cysteine pocket (Cys_4:Zn) and remains intact even with high concentrations of peroxides. Indeed, this Zn^{2+} is often retained in the protein structure even during denaturing sodium dodecyl sulfate/ polyacrylamide gel electrophoresis (SDS-PAGE) (72). The binding of a second metal to the metal-sensing site 2 leads to activation of DNA binding. In cells,

PerR can be metallated by either Fe^{2+} or Mn^{2+} simply by altering the availability of metals in the growth medium (43, 56). In most iron-rich media, $PerR_{Bs}$ is bound with Fe^{2+} and, in this state, is responsive to H_2O_2 (56). However, addition of excess Mn^{2+} can shift PerR into the Mn^{2+}-activated form (PerR:Zn,Mn) and in this state, peroxide stress genes are tightly repressed (Fig. 2.3).

Typically, peroxide sensing is mediated by redox active cysteines, in sensors such as OxyR in *E. coli* (116) and OhrR in *B. subtilis* (75, 106). These are metal-independent peroxide sensors that detect ROS via the oxidation and subsequent formation of reversible disulfide bonds (8, 14, 34, 107). This contrasts with $PerR_{Bs}$, which senses H_2O_2 by metal-catalyzed oxidation through site 2 (73). Binding of H_2O_2 to Fe^{2+} in PerR:Zn,Fe is proposed to generate a localized hydroxyl radical that modifies one of two His residues (H37 or H91) in site 2 to 2-oxo-histidine (Fig. 2.4) (73, 98, 109). Recently, an alternative mechanism has also been suggested in which the initial bound H_2O_2 undergoes heterolytic cleavage releasing water and generating an Fe(IV) oxo intermediate (100). His oxidation may also occur on direct reaction of PerR:Zn,Fe with O_2, and the presence of O_2 also stimulates the modification by H_2O_2 (Fig. 2.4) (100). Interestingly, these two oxidizing agents appear to use distinct modification pathways: reaction with H_2O_2 targets H37 and H91 at about equal rates, whereas reaction with O_2 selectively leads to H37 modification (100) (Fig. 2.4).

Regardless of the precise pathway, oxidized PerR loses its iron cofactor and the resulting conformational changes trigger its release from DNA and exposes specific signature residues targeted by the LonA protease (Fig. 2.3) (2). Thus, after regulon derepression occurs, oxidized $PerR_{Bs}$ is degraded thereby preventing the accumulation of nonfunctional protein (2). Oxidation of $PerR_{Bs}$ also leads to derepression of the autoregulated *perR* gene, which presumably helps re-establish repression once the newly synthesized PerR:Zn,Fe protein is no longer consumed by reaction with H_2O_2. Transcriptomic studies demonstrate that derepression of the PerR regulon in response to H_2O_2 is transient and repression is rapidly reestablished (55). This is likely important since constitutive derepression of the PerR regulon, such as seen in a *perR* null mutant, imposes a very high iron demand on the cell due to the high levels of catalase that are produced (38, 78). This iron deficiency imposed in a *perR* null mutant is also observed in *B. licheniformis*, where overexpression of *fur*, rather than *katA*, is the main reason why cells cannot grow in media not supplemented with iron (70).

2.4.5 Metal-dependent changes in $PerR_{Bs}$ repressor activity

In addition to Fe^{2+}, $PerR_{Bs}$ also binds Mn^{2+} to generate PerR:Zn,Mn. This form of PerR also represses the PerR regulon but is peroxide insensitive and fails to derepress the PerR regulon in response to H_2O_2 (43, 73). The reason why $PerR_{Bs}$ binds to both Fe^{2+} and Mn^{2+} is not well understood: in *B. subtilis* the

PerR regulon does not control any manganese related genes. In contrast, *E. coli* OxyR, which also senses H_2O_2, directly activates the expression of the NRAMP family manganese importer MntH in response to H_2O_2 stress (7, 37, 80). This is not the case in *B. subtilis*, where manganese homeostasis is maintained independently of $PerR_{Bs}$, via MntR (59). The repression of the $PerR_{Bs}$ regulon by Mn^{2+} may have resulted as a corollary of comparatively high affinity of PerR for Fe^{2+}: $PerR_{Bs}$ binds Fe^{2+} tighter than Fur_{Bs} (79), and this may have also led to a high Mn^{2+} affinity. This high Fe^{2+} affinity ensures that the peroxide stress response is not induced by mild iron depletion, which would be maladaptive and impose a high iron demand through the increased synthesis of heme and catalase and the expression of proteins mediating iron sequestration (MrgA) and efflux (PfeT). Hence, PerR may have sacrificed metal selectivity to help increase its specificity to respond to H_2O_2 stress rather than fluctuations in metal availability.

The binding of either Fe^{2+} or Mn^{2+} may additionally allow PerR to function as a ratiomeric sensor of the relative iron and manganese levels. For example, when the level of Mn^{2+} is much higher than Fe^{2+} in the cell, the threat posed by H_2O_2 may be significantly reduced, thereby justifying a reduced induction of PerR regulon genes. Furthermore, there is suggestive evidence that the PerR:Zn,Fe and PerR:Zn,Mn forms of the repressor may differentially affect some genes (43) (Fig. 2.3). For example, in resuspension experiments, either Mn^{2+} or Fe^{2+} enabled repression of some PerR regulated genes (*katA*,

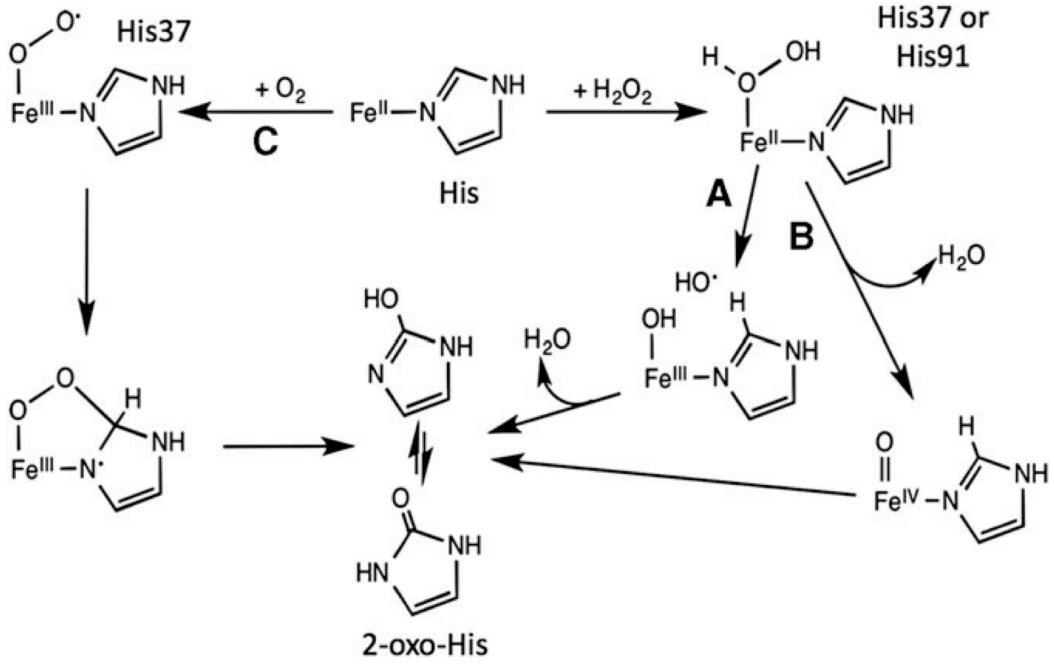

FIG. 2.4) Metal-Catalyzed Oxidation of PerR.

Formation of 2-oxo-histidine of $PerR_{Bs}$:Zn,Fe site 2 via three putative pathways. His37 or His91 can both become oxidized when exposed to H_2O_2. This can lead to either **(A)** the generation of a hydroxyl radical via oxidation of Fe^{2+} into Fe^{3+} as a result of the homolytic cleavage of the O-O of the peroxido intermediate or **(B)** the production of a high valent Fe^{4+} ion (especially under pH ~7.0) caused by the heterolytic cleavage of that same bond. Conversely, **(C)** in the presence of O_2, His37 is specifically targeted, resulting in a superoxo-Fe^{3+} intermediate. Subsequent bond formation and O-O bond cleavage of the end derivative leads to the final production of 2-oxo-His [figure adapted from (100)].

ahpCF, *mrgA*), whereas only Mn^{2+} elicited repression at the *pfeT*, *perR*, and *fur* promoters. The basis for this Mn^{2+} selectivity is presently unknown, but two models have been suggested. First, PerR:Zn,Fe and PerR:Zn,Mn may be qualitatively different: they may have slightly different conformations that affect their DNA-binding selectivity. Second, the difference may be primarily quantitative: the much more stable PerR:Zn,Mn form may accumulate in cells to a higher active concentration allowing interaction with weaker operators

within the PerR regulon (Fig. 2.3). Regardless of the mechanism, these observations are relevant when we consider below PerR orthologs that were reported to be specific for Mn^{2+} as a corepressor.

2.4.6 Structural differences that tune H_2O_2 sensitivity (it is the little things that count)

Despite the overall structural similarity between Fur_{Bs} and $PerR_{Bs}$, they differ greatly in their sensitivity to H_2O_2. $PerR_{Bs}$ is highly sensitive to H_2O_2 with a second-order rate constant for protein oxidation of $\sim 10^5$ M^{-1} s^{-1} when associated with iron (73). This is comparable to the reported sensitivity of OxyR, which responds to submicromolar levels of intracellular H_2O_2 (9). As a result, isolation of unoxidized PerR:Zn is technically challenging and is best achieved by purification from cells grown with high Mn^{2+} (or in medium amended with iron chelators) to prevent *in vivo* oxidation, lysis, and purification in the presence of EDTA to remove any Fe^{2+} from the protein, and exclusion of thiol reducing agents (which can facilitate reduction of Fe^{3+} to Fe^{2+}) (73, 100). The high sensitivity of $PerR_{Bs}$ to H_2O_2 inactivation is appropriate for its role in regulating detoxification functions.

In contrast with PerR, Fur proteins are generally less sensitive to H_2O_2 inactivation, which is likely adaptive since the derepression of iron uptake functions in response to elevated H_2O_2 levels would likely be deleterious to the cell. Compared to $PerR_{Bs}$, Fur_{Bs} is relatively easy to purify in an active state,

although care is needed to prevent the adventitious binding of metals to the sensing site(s) (15). As discussed in more detail below, Fur proteins from a variety of organisms can be activated *in vitro* by addition of Fe^{2+} as a corepressor, even in aerobic buffers.

Recent results have begun to provide insights into how $PerR_{Bs}$ and Fur_{Bs} display such different sensitivities to H_2O_2. Both $PerR_{Bs}$ and Fur_{Bs} have a histidine-rich binding pocket (site 2) that coordinates Fe^{2+} (15, 54, 74). However, an aspartate (Asp) residue in $PerR_{Bs}$ (position 104) replaces a glutamate (Glu) in Fur_{Bs} (position 108) as the Fe^{2+} ligand (95). Mutational studies demonstrate that the $PerR_{Bs}$ D104E and Fur_{Bs} E108D mutants still bind Mn^{2+} with near-normal affinities. However, the sensitivity of each protein to MCO of the neighboring histidine ligands (H37 and H91 in PerR and the equivalent residues in Fur) was significantly reduced. This was assessed using electrospray ionization mass spectrometry analysis to monitor His oxidation in proteins overexpressed and purified from aerobically growing *E. coli*, which generally maintains steady-state levels of H_2O_2 in the range of 50 nM. Under these conditions, ~63% of the recovered PerR was oxidized, with a much lower value noted for Fur (4%). Significantly, oxidation of the $PerR_{Bs}$ D104E mutant was substantially reduced (to 3%) whereas that for Fur_{Bs} E108D was somewhat increased (to 14%) (95). These results were corroborated by *in vitro* analyses of protein oxidation by H_2O_2.

These mutational studies support a model in which the H_2O_2 reactivity

of the bound Fe^{2+} can be quantitatively modulated by single amino acid changes in site 2 that affect coordination geometry. Structural studies of PerR:Zn,Mn revealed a penta-coordinate site 2 with three His and two Asp residues (32, 66). Assuming Fe^{2+} binds similarly to Mn^{2+}, this leaves a sixth coordination site available for interaction with incoming H_2O_2. Structural modeling supports the notion that substitution of the PerR Asp104 ligand with the longer Glu side chain allows formation of a weak bidentate interaction between Glu and Fe^{2+} that occludes access of H_2O_2 and thereby minimizes protein oxidation (95) (Fig. 2.2C–E). The resultant Fe^{2+}-binding site can be considered to have a ‘‘5 + 1’’ coordination mode as proposed previously for Fur based on Mössbauer and X-ray absorption spectroscopy (65). Recent structural studies of *M. gryphiswaldense* Fur indicate that Mn^{2+} (bound as an iron surrogate) is indeed hexacoordinate in this protein, with three His and two Glu ligands (32).

Collectively, these results support a simple model in which PerR proteins bind Fe^{2+} with five ligands and one open coordination site that can interact with H_2O_2, whereas Fur proteins use six ligands and the interaction of H_2O_2 with Fe^{2+} is sterically impeded. It would be revealing to determine if these same types of steric access effects influence the reactivity of bound Fe^{2+} with other molecules. In addition to H_2O_2, PerR can also be inactivated by O_2 (100) and nitric oxide (NO) inactivates Fur_{Ec} by direct nitrosylation of the bound Fe^{2+} (27, 28). Transcriptomic studies indicate that NO, as well as

sodium nitroprusside, also inactivates both $PerR_{Bs}$ and Fur_{Bs} under both aerobic and anaerobic conditions (92). Finally, it has been shown *in vitro* that Fe^{2+} bound to Fur can be oxidized by $K_3Fe(CN)_6$ (89). It would be interesting to test the ability of these various redox agents to interact with $PerR_{Bs}$ and Fur_{Bs} and the corresponding mutants affecting the Fe^{2+} ligands. However, it is likely that it will ultimately be necessary to account for second coordination sphere effects and allosteric coupling to fully understand metal selectivity and peroxide reactivity, as noted in biophysical studies of other metalloregulators (49).

2.5 PerR and Fur orthologs across species: key directions for further work

The revelation that varying a single amino acid in the Fe^{2+} coordination sphere of Fur/PerR type proteins can modulate H_2O_2 sensitivity (Fig. 2.2) is an important first step in understanding how these regulators have evolved distinct physiological roles. As evident from the literature, it is likely that there is a wide variation in H_2O_2 sensitivity among Fur and PerR orthologs in other organisms, and we are yet to tackle the complex problem of understanding how this variation has emerged. Certainly, variations in protein structure and the metal coordination environment are important factors, but the most relevant data relate to H_2O_2 sensitivity *in vivo*, and variations in the cellular environment are also likely important in interpreting the observed differences.

As noted above, it is clear from numerous studies that Fur and PerR proteins can function with either Fe^{2+} or Mn^{2+} as corepressors. However, these two forms cannot be considered as equivalent. This is important when considering *in vitro* studies that often use Mn^{2+} as a cofactor to activate DNA binding, even for Fur proteins that function physiologically to sense Fe^{2+}. With these caveats in mind, we here review recent insights into the effects of H_2O_2 and other oxidants on Fur and PerR function across a variety of bacteria, and identify some key questions to guide future research.

2.5.1 PerR orthologs with varying susceptibility to oxidation

PerR orthologs have been identified in a wide range of bacteria and seem to exhibit significant variation in their sensitivity to oxidation. However, comparative sensitivities are difficult to derive, given the differences in experimental parameters cited across the literature, including differences in media and treatment protocols for each organism tested. For example, the facultative anaerobe *Staphylococcus aureus* regulates peroxide stress using a PerR ortholog designated $PerR_{Sa}$ (67% identical to $PerR_{Bs}$). Initial reports indicated that $PerR_{Sa}$ repressed its target genes (e.g., *katA*, *ahpCF*, *mrgA*) only in the presence of Mn^{2+} (24, 58, 67). Indeed, in Fe^{2+}-amended medium, the expression of *katA* was as high as in a *perR* null mutant. Although these studies led to the suggestion that $PerR_{Sa}$ is functionally distinct, and is specialized to use Mn^{2+} as corepressor, this seems unlikely since this form

(PerR:Zn,Mn) would not be able to respond to peroxide using the mechanism established for $PerR_{Bs}$ (Fig. 2.4).

An alternative explanation is that under the aerobic growth conditions used, $PerR_{Sa}$ is oxidized by endogenously generated H_2O_2 and only the Mn^{2+} form is able to accumulate to levels needed to effect repression. Support for this model is provided by recent *in vivo* and *in vitro* studies that allow a direct comparison of $PerR_{Sa}$ and $PerR_{Bs}$ (67). These studies reveal that the apparent lack of Fe^{2+}-dependent repressor activity for $PerR_{Sa}$ reflects a hypersensitivity to protein oxidation under aerobic culture conditions: Fe^{2+} is an effective corepressor under microaerobic conditions and the cell is poised to respond to increased oxygen availability and the resultant production of ROS (67). Biochemical studies also indicate that $PerR_{Sa}$ maintains its ability to bind to both Fe^{2+} and Mn^{2+}, and that $PerR_{Sa}$:Zn,Fe is more sensitive to H_2O_2 than either $PerR_{Bs}$ or *B. licheniformis* PerR ($PerR_{Bl}$) (67, 69). This increased sensitivity likely confers this facultative anaerobic pathogen with the necessary fine-tuning to detect lower levels of peroxides.

PerR orthologs from other facultative aerobes and strict anaerobes may have similarly increased sensitivity to oxidation and may thereby function for survival under aerobic conditions (aerotolerance). Such is the case for *Clostridium acetobutylicum* PerR ($PerR_{Ca}$), which controls genes important for survival in the presence of H_2O_2 or when exposed to air (57). The sulfate reducing, obligate anaerobe *Desulfovibrio vulgaris* Hildenborough also may

contain a highly sensitive PerR (114). In this organism, cells exposed to air for 30min were more tolerant to subsequent challenge with H_2O_2. Similarly, PerR in the microaerophilic food pathogen *C. jejuni* is important for adaptation to aerobic conditions (50).

It is presently unclear whether PerR functions during the transition from anaerobic to aerobic conditions by sensing endogenously produced H_2O_2 or whether O_2 itself suffices (100). Indeed, recent results indicate that O_2 can modify $PerR_{Bs}$ directly (100). Since this modification proceeds by a chemically distinct pathway (Fig. 2.4) and at least with $PerR_{Bs}$ leads to a notable increase in the ratio of His37 to His91 oxidation (100), it may be possible to determine whether O_2 is the true signal for PerR orthologs that function to sense the transition from anaerobic to aerobic growth conditions.

2.5.2 Fur orthologs with varying sensitivity to oxidation

Fur orthologs have also been identified from many different bacteria, and subject to the same caveats noted above, they seem to display a wide variation in their sensitivity to oxidation. Insights into the relative susceptibility to oxidation can be obtained by comparisons of the susceptibility of Fur proteins to inactivation *in vitro* and *in vivo*, although in both cases detailed side-by-side comparisons have generally not been done, and few studies have directly addressed the issue of sensitivity to ROS.

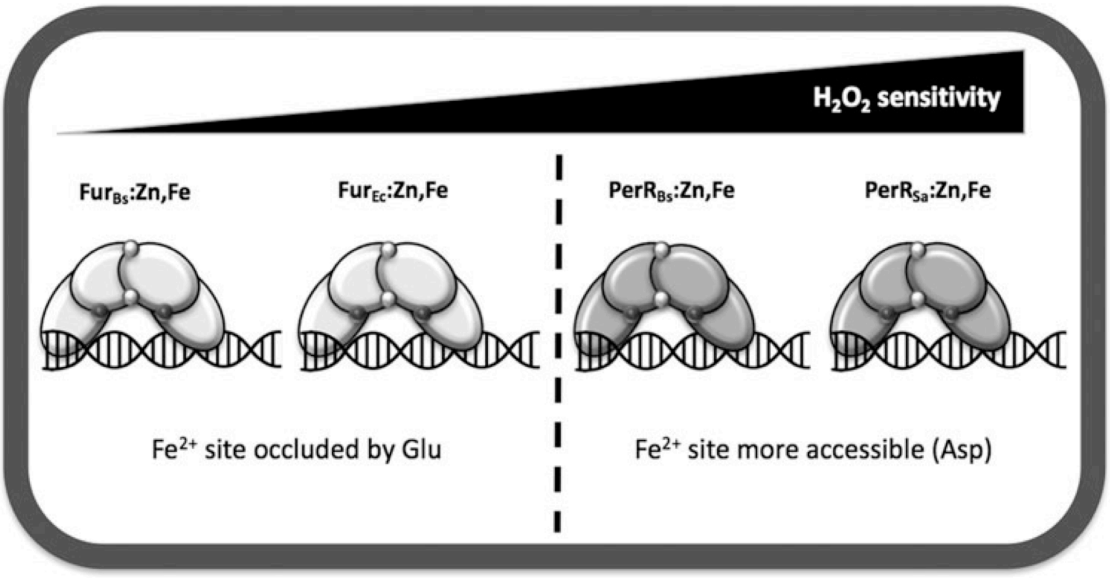

FIG. 2.5) Different iron-binding Fur family regulators display different sensitivities to H_2O_2.

Variation in H_2O_2 sensitivity among Fur family metalloregulators. The key difference seems to lie in the structural variations between Fur and PerR at the metal-sensing site. However, other differences also likely affect H_2O_2 sensitivity. $PerR_{Sa}$:Zn,Fe is more sensitive to oxidation by H_2O_2 than $PerR_{Bs}$:Zn,Fe, and Fur_{Ec} seems to be more sensitive to peroxides than Fur_{Bs}, although the basis for these differences has not been completely defined.

The vast majority of biochemical studies of Fur proteins have as their major goal the demonstration that Fur acts directly at a specific target promoter region, and for this purpose it is common to metallate Fur with the more redox stable Mn^{2+} rather than the more relevant Fe^{2+} cofactor. Nevertheless, there are several reports of activation of DNA binding by Fe^{2+} *in vitro* (1, 15). This contrasts with $PerR_{Bs}$, which is rapidly inactivated if Fe^{2+} is added to air-saturated buffer (73). Indeed, the original demonstration that Fur_{Ec} functions as a direct sensor of Fe^{2+} was obtained by addition of Fe^{2+} to a coupled *in vitro* transcription/translation reaction (10) and subsequent DNA

footprinting studies demonstrating activation of Fur binding by Fe^{2+} (30). Similarly, *H. pylori* Fur was active *in vitro* when reconstituted with Fe^{2+} as monitored by DNAse I footprinting (1, 31). Since DNA-binding activity was monitored aerobically in these studies, this suggests that the iron metallated form of Fur proteins is often relatively stable, even in air-saturated buffers. In one of the few side-by-side comparisons to date, incubation of anaerobically reconstituted Fur_{Bs} with bound Fe^{2+} with a single molar equivalent (50 μM) of H_2O_2 led to a modest level of protein oxidation (23%), but notably less than that see for $PerR_{Bs}$ under identical conditions (66%) (95).

We can also glean insights into the reactivity of Fur proteins to ROS from the large number of transcriptome and proteome studies of cellular responses to redox stress. For example, treatment of *B. subtilis* with either a low (8 μM) or high (58 μM) dose of H_2O_2 strongly induces the PerR regulon, but had only a modest effect, and only at the higher concentration, on Fur-repressed genes (55). However, a second study did find substantial derepression of the Fur regulon in cells treated with 58 μM H_2O_2 as well as by superoxide stress (93). Early studies also indicated that the *E. coli* Fur regulon was relatively insensitive to H_2O_2. Treatment of cells growing in rich medium with 1 mM H_2O_2 for 10min strongly induced the OxyR-mediated stress response, but did not derepress the Fur regulon (118). In contrast with this result, an *E. coli* strain (*hpx*$^-$) lacking all three major peroxide detoxification enzymes (*katG*, *katE*, and *ahpCF*) was found to derepress the Fur regulon in

minimal medium. In this strain, endogenously generated H_2O_2 accumulates to levels between 500 nM and 1 μM, suggesting that this level is sufficient for oxidative inactivation of Fur (110). The authors further show that this derepression is not observed in rich medium due to the OxyR-dependent upregulation of Fur synthesis, which increases Fur levels from ~5000 to 10,000 molecules per cell (117). The nature of the oxidative inactivation of Fur_{Ec} is unclear and could result from oxidation and loss of the bound Fe^{2+} corepressor, with or without accompanying protein oxidation. It has been noted, however, that oxidation of Fur_{Ec} bound with Fe^{2+} to the Fe^{3+} bound state did not appreciably decrease DNA binding (89), supportive of a model in which MCO is required for protein inactivation.

2.6 Conclusions and perspectives

Iron sensing and oxidative stress are intricately intertwined. The major physiological effects from ROS often involve the inactivation of iron-dependent enzymes. We have here reviewed how *B. subtilis* used two functionally distinct members of the Fur family of metalloregulators, Fur_{Bs} and $PerR_{Bs}$, to coordinate the adaptive responses to iron limitation and peroxide stress, respectively. These proteins provide an attractive model system to begin to understand how protein structural changes can modulate both the metal selectivity and the sensitivity to H_2O_2 and other oxidants in this family of regulators. Fur and PerR proteins are widespread among bacteria, yet

available evidence suggests that they vary markedly in their sensitivity to redox active compounds. These proteins seem to occupy a continuum of reactivity from highly sensitive (PerR proteins from facultative aerobes and anaerobes) to relatively nonreactive (some Fur proteins) (Fig. 2.5). Unfortunately, controlled side-by-side comparisons of redox reactivity are rare. PerR proteins are typically inactivated by a wide variety of redox stresses (O_2, H_2O_2, HOCl, NO), and a subset of these agents, although sometimes only at much higher levels, may also affect Fur activity. Recent studies are beginning to shed light on some of the key differences in the metal-sensing sites that modulate redox sensitivity, but it is clear that much work remains to be done.

2.7 References

1. Agriesti F, Roncarati D, Musiani F, Del Campo C, Iurlaro M, Sparla F, Ciurli S, Danielli A, and Scarlato V. FeON- FeOFF: the *Helicobacter pylori* Fur regulator commutates iron-responsive transcription by discriminative readout of opposed DNA grooves. Nucleic Acids Res 42: 3138–3151, 2014.
2. Ahn BE and Baker TA. Oxidization without substrate unfolding triggers proteolysis of the peroxide-sensor, PerR. Proc Natl Acad Sci U S A 113: E23–E31, 2016.
3. Ahn BE, Cha J, Lee EJ, Han AR, Thompson CJ, and Roe JH. Nur, a nickel-responsive regulator of the Fur family, regulates superoxide

dismutases and nickel transport in *Streptomyces coelicolor*. Mol Microbiol 59: 1848–1858, 2006.

4. Althaus EW, Outten CE, Olson KE, Cao H, and O'Halloran TV. The ferric uptake regulation (Fur) repressor is a zinc metalloprotein. Biochemistry 38: 6559–6569, 1999.

5. Anbar AD. Elements and evolution. Science 322: 1481– 1483, 2008.

6. Andrews SC, Robinson AK, and Rodriguez-Quinones F. Bacterial iron homeostasis. FEMS Microbiol Rev 27: 215– 237, 2003.

7. Anjem A, Varghese S, and Imlay JA. Manganese import is a key element of the OxyR response to hydrogen peroxide in *Escherichia coli*. Mol Microbiol 72: 844–858, 2009.

8. Antelmann H and Helmann JD. Thiol-based redox switches and gene regulation. Antioxid Redox Signal 14: 1049–1063, 2011.

9. Aslund F, Zheng M, Beckwith J, and Storz G. Regulation of the OxyR transcription factor by hydrogen peroxide and the cellular thiol-disulfide status. Proc Natl Acad Sci U S A 96: 6161–6165, 1999.

10. Bagg A and Neilands JB. Ferric uptake regulation protein acts as a repressor, employing iron (II) as a cofactor to bind the operator of an iron transport operon in *Escherichia coli*. Biochemistry 26: 5471–5477, 1987.

11. Bagg A and Neilands JB. Molecular mechanism of regulation of siderophore-mediated iron assimilation. Microbiol Rev 51: 509–518,

1987.

12. Baichoo N and Helmann JD. Recognition of DNA by Fur: a reinterpretation of the Fur box consensus sequence. J Bacteriol 184: 5826–5832, 2002.

13. Baichoo N, Wang T, Ye R, and Helmann JD. Global analysis of the *Bacillus subtilis* Fur regulon and the iron starvation stimulon. Mol Microbiol 45: 1613–1629, 2002.

14. Barford D. The role of cysteine residues as redox-sensitive regulatory switches. Curr Opin Struct Biol 14: 679–686, 2004.

15. Bsat N and Helmann JD. Interaction of *Bacillus subtilis* Fur (ferric uptake repressor) with the *dhb* operator *in vitro* and *in vivo*. J Bacteriol 181: 4299–4307, 1999.

16. Bsat N, Herbig A, Casillas-Martinez L, Setlow P, and Helmann JD. *Bacillus subtilis* contains multiple Fur homologues: identification of the iron uptake (Fur) and peroxide regulon (PerR) repressors. Mol Microbiol 29: 189–198, 1998.

17. Butcher J, Sarvan S, Brunzelle JS, Couture JF, and Stintzi A. Structure and regulon of *Campylobacter jejuni* ferric uptake regulator Fur define apo-Fur regulation. Proc Natl Acad Sci U S A 109: 10047–10052, 2012.

18. Caux-Thang C, Parent A, Sethu R, Maiga A, Blondin G, Latour JM, and Duarte V. Single asparagine to arginine mutation allows PerR to switch from PerR box to Fur box. ACS Chem Biol 10: 682–686, 2015.

19. Chai S, Welch TJ, and Crosa JH. Characterization of the interaction between Fur and the iron transport promoter of the virulence plasmid in *Vibrio anguillarum*. J Biol Chem 273: 33841–33847, 1998.

20. Chandrangsu P and Helmann JD. Intracellular Zn(II) intoxication leads to dysregulation of the PerR regulon resulting in heme toxicity in *Bacillus subtilis*. PLoS Genet 12: e1006515, 2016.

21. Chen L and Helmann JD. *Bacillus subtilis* MrgA is a Dps(PexB) homologue: evidence for metalloregulation of an oxidative-stress gene. Mol Microbiol 18: 295–300, 1995.

22. Chen L, Keramati L, and Helmann JD. Coordinate regulation *of Bacillus subtilis* peroxide stress genes by hydrogen peroxide and metal ions. Proc Natl Acad Sci U S A 92: 8190–8194, 1995.

23. Chiancone E and Ceci P. The multifaceted capacity of Dps proteins to combat bacterial stress conditions: detoxification of iron and hydrogen peroxide and DNA binding. Biochim Biophys Acta 1800: 798–805, 2010.

24. Cosgrove K, Coutts G, Jonsson IM, Tarkowski A, Kokai- Kun JF, Mond JJ, and Foster SJ. Catalase (KatA) and alkyl hydroperoxide reductase (AhpC) have compensatory roles in peroxide stress resistance and are required for survival, persistence, and nasal colonization in *Staphylococcus aureus*. J Bacteriol 189: 1025–1035, 2007.

25. Coy M, Doyle C, Besser J, and Neilands JB. Site-directed mutagenesis

of the ferric uptake regulation gene of *Escherichia coli*. Biometals 7: 292–298, 1994.

26. Coy M and Neilands JB. Structural dynamics and functional domains of the Fur protein. Biochemistry 30: 8201– 8210, 1991.

27. D'Autreaux B, Horner O, Oddou JL, Jeandey C, Gambarelli S, Berthomieu C, Latour JM, and Michaud-Soret I. Spectroscopic description of the two nitrosyl-iron complexes responsible for fur inhibition by nitric oxide. J Am Chem Soc 126: 6005–6016, 2004.

28. D'Autreaux B, Touati D, Bersch B, Latour JM, and Michaud-Soret I. Direct inhibition by nitric oxide of the transcriptional ferric uptake regulation protein via nitrosylation of the iron. Proc Natl Acad Sci U S A 99: 16619–16624, 2002.

29. de Lorenzo V, Giovannini F, Herrero M, and Neilands JB. Metal ion regulation of gene expression. Fur repressor-operator interaction at the promoter region of the aerobactin system of pColV-K30. J Mol Biol 203: 875–884, 1988.

30. de Lorenzo V, Wee S, Herrero M, and Neilands JB. Operator sequences of the aerobactin operon of plasmid ColV-K30 binding the ferric uptake regulation (Fur) repressor. J Bacteriol 169: 2624–2630, 1987.

31. Delany I, Spohn G, Rappuoli R, and Scarlato V. The Fur repressor controls transcription of iron-activated and repressed genes in

Helicobacter pylori. Mol Microbiol 42: 1297–1309, 2001.

32. Deng Z, Wang Q, Liu Z, Zhang M, Machado AC, Chiu TP, Feng C, Zhang Q, Yu L, Qi L, Zheng J, Wang X, Huo X, QiX, LiX,WuW,RohsR,LiY,and Chen Z. Mechanistic insights into metal ion activation and operator recognition by the ferric uptake regulator. Nat Commun 6: 7642, 2015.

33. Dian C, Vitale S, Leonard GA, Bahlawane C, Fauquant C, Leduc D, Muller C, de Reuse H, Michaud-Soret I, and Terradot L. The structure of the *Helicobacter pylori* ferric uptake regulator Fur reveals three functional metal binding sites. Mol Microbiol 79: 1260–1275, 2011.

34. Duarte V and Latour JM. PerR vs OhrR: selective peroxide sensing *in Bacillus subtilis*. Mol Biosyst 6: 316–323, 2010.

35. Escolar L, Perez-Martin J, and de Lorenzo V. Opening the iron box: transcriptional metalloregulation by the Fur protein. J Bacteriol 181: 6223–6229, 1999.

36. Fang FC. Antimicrobial reactive oxygen and nitrogen species: concepts and controversies. Nat Rev Microbiol 2: 820–832, 2004.

37. Faulkner MJ and Helmann JD. Peroxide stress elicits adaptive changes in bacterial metal ion homeostasis. Antioxid Redox Signal 15: 175–189, 2011.

38. Faulkner MJ, Ma Z, Fuangthong M, and Helmann JD. Derepression of the *Bacillus subtilis* PerR peroxide stress response leads to iron

deficiency. J Bacteriol 194: 1226–1235, 2012.

39. Ferrer M, Golyshina OV, Beloqui A, Golyshin PN, and Timmis KN. The cellular machinery of *Ferroplasma acidiphilum* is iron-protein-dominated. Nature 445: 91–94, 2007.

40. Fillat MF. The FUR (ferric uptake regulator) superfamily: diversity and versatility of key transcriptional regulators. Arch Biochem Biophys 546: 41–52, 2014.

41. Frechon D and Le Cam E. Fur (ferric uptake regulation) protein interaction with target DNA: comparison of gel retardation, footprinting and electron microscopy analyses. Biochem Biophys Res Commun 201: 346–355, 1994.

42. Fuangthong M and Helmann JD. Recognition of DNA by three ferric uptake regulator (Fur) homologs in *Bacillus subtilis*. J Bacteriol 185: 6348–6357, 2003.

43. Fuangthong M, Herbig AF, Bsat N, and Helmann JD. Regulation of the *Bacillus subtilis fur* and *perR* genes by PerR: not all members of the PerR regulon are peroxide inducible. J Bacteriol 184: 3276–3286, 2002.

44. Gaballa A, Antelmann H, Aguilar C, Khakh SK, Song KB, Smaldone GT, and Helmann JD. The *Bacillus subtilis* iron-sparing response is mediated by a Fur-regulated small RNA and three small, basic proteins. Proc Natl Acad Sci U S A 105: 11927–11932, 2008.

45. Gaballa A and Helmann JD. Identification of a zinc specific

metalloregulatory protein, Zur, controlling zinc transport operons in *Bacillus subtilis*. J Bacteriol 180:5815–5821, 1998.46.

46. Gaballa A, MacLellan S, and Helmann JD. Transcription activation by the siderophore sensor Btr is mediated by ligand-dependent stimulation of promoter clearance. Nucleic Acids Res 40: 3585–3595, 2012.

47. Gilston BA, Wang S, Marcus MD, Canalizo-Hernandez MA, Swindell EP, Xue Y, Mondragon A, and O'Halloran TV. Structural and mechanistic basis of zinc regulation across the *E. coli* Zur regulon. PLoS Biol 12: e1001987, 2014.

48. Guan G, Pinochet-Barros A, Gaballa A, Patel SJ, Arguello JM, and Helmann JD. PfeT, a P_{1B4}-type ATPase, effluxes ferrous iron and protects *Bacillus subtilis* against iron intoxication. Mol Microbiol 98: 787–803, 2015.

49. Guerra AJ and Giedroc DP. Metal site occupancy and allosteric switching in bacterial metal sensor proteins. Arch Biochem Biophys 519: 210–222, 2012.

50. Handley RA, Mulholland F, Reuter M, Ramachandran VK, Musk H, Clissold L, Le Brun NE, and van Vliet AH. PerR controls oxidative stress defence and aerotolerance but not motility-associated phenotypes of *Campylobacter jejuni*. Microbiology 161: 1524–1536, 2015.

51. Hantke K. Regulation of ferric iron transport in *Escherichia coli* K12:

isolation of a constitutive mutant. Mol Gen Genet 182: 288–292, 1981.

52. Hantke K. Selection procedure for deregulated iron transport mutants (*fur*) in *Escherichia coli* K 12: *fur* not only affects iron metabolism. Mol Gen Genet 210: 135–139, 1987.

53. Hantke K. Iron and metal regulation in bacteria. Curr Opin Microbiol 4: 172–177, 2001.

54. Helmann JD. Specificity of metal sensing: iron and manganese homeostasis in *Bacillus subtilis*. J Biol Chem 289: 28112–28120, 2014.

55. Helmann JD, Wu MF, Gaballa A, Kobel PA, Morshedi MM, Fawcett P, and Paddon C. The global transcriptional response of *Bacillus subtilis* to peroxide stress is coordinated by three transcription factors. J Bacteriol 185: 243– 253, 2003.

56. Herbig AF and Helmann JD. Roles of metal ions and hydrogen peroxide in modulating the interaction of the *Bacillus subtilis* PerR peroxide regulon repressor with operator DNA. Mol Microbiol 41: 849–859, 2001.

57. Hillmann F, Fischer RJ, Saint-Prix F, Girbal L, and Bahl H. PerR acts as a switch for oxygen tolerance in the strict anaerobe *Clostridium acetobutylicum*. Mol Microbiol 68: 848–860, 2008.

58. Horsburgh MJ, Clements MO, Crossley H, Ingham E, and Foster SJ. PerR controls oxidative stress resistance and iron storage proteins and is required for virulence in *Staphylococcus aureus*. Infect Immun 69: 3744–3754, 2001.

59. Huang X, Shin JH, Pinochet-Barros A, Su TT, and Helmann JD. *Bacillus subtilis* MntR coordinates the transcriptional regulation of manganese uptake and efflux systems. Mol Microbiol 103: 253–268, 2017.

60. Ikeda JS, Janakiraman A, Kehres DG, Maguire ME, and Slauch JM. Transcriptional regulation of *sitABCD* of *Salmonella enterica* serovar Typhimurium by MntR and Fur. J Bacteriol 187: 912–922, 2005.

61. Ilari A, Ceci P, Ferrari D, Rossi GL, and Chiancone E. Iron incorporation into *Escherichia coli* Dps gives rise to a ferritin-like microcrystalline core. J Biol Chem 277: 37619–37623, 2002.

62. Imlay JA. Pathways of oxidative damage. Annu Rev Microbiol 57: 395–418, 2003.

63. Imlay JA. The molecular mechanisms and physiological consequences of oxidative stress: lessons from a model bacterium. Nat Rev Microbiol 11: 443–454, 2013.

64. Imlay JA. The mismetallation of enzymes during oxidative stress. J Biol Chem 289: 28121–28128, 2014.

65. Jacquamet L, Dole F, Jeandey C, Oddou JL, Perret E, Le Pape L, Aberdam D, Hazemann JL, Michaud-Soret I, and Latour JM. First spectroscopic characterization of FeII- Fur, the physiological active form of the Fur protein. J Am Chem Soc 122: 394–395, 2000.

66. Jacquamet L, Traore DA, Ferrer JL, Proux O, Testemale D, Hazemann

JL, Nazarenko E, El Ghazouani A, Caux-Thang C, Duarte V, and Latour JM. Structural characterization of the active form of PerR: insights into the metal-induced activation of PerR and Fur proteins for DNA binding. Mol Microbiol 73: 20–31, 2009.

67. Ji CJ, Kim JH, Won YB, Lee YE, Choi TW, Ju SY, Youn H, Helmann JD, and Lee JW. *Staphylococcus aureus* PerR is a hypersensitive hydrogen peroxide sensor using iron-mediated histidine oxidation. J Biol Chem 290: 20374– 20386, 2015.

68. Kim JH, Ji CJ, Ju SY, Yang YM, Ryu SH, Kwon Y, Won YB, Lee YE, Youn H, and Lee JW. *Bacillus licheniformis* contains two more PerR-like proteins in addition to PerR, Fur, and Zur Orthologues. PLoS One 11: e0155539, 2016.

69. Kim JH, Won YB, Ji CJ, Yang YM, Ryu SH, Ju SY, Kwon Y, Lee YE, and Lee JW. The difference in *in vivo* sensitivity between *Bacillus licheniformis* PerR and *Bacillus subtilis* PerR is due to the different cellular environments. Biochem Biophys Res Commun 484: 125–131, 2017.

70. Kim JH, Yang YM, Ji CJ, Ryu SH, Won YB, Ju SY, Kwon Y, Lee YE, Youn H, and Lee JW. The inability of *Bacillus licheniformis perR* mutant to grow is mainly due to the lack of PerR-mediated *fur* repression. J Microbiol 55: 457–463, 2017.

71. Le Cam E, Frechon D, Barray M, Fourcade A, and Delain E.

Observation of binding and polymerization of Fur repressor onto operator-containing DNA with electron and atomic force microscopes. Proc Natl Acad Sci U S A 91: 11816–11820, 1994.

72. Lee JW and Helmann JD. Biochemical characterization of the structural Zn^{2+} site in the *Bacillus subtilis* peroxide sensor PerR. J Biol Chem 281: 23567–23578, 2006.

73. Lee JW and Helmann JD. The PerR transcription factor senses H_2O_2 by metal-catalysed histidine oxidation. Nature 440: 363–367, 2006.

74. Lee JW and Helmann JD. Functional specialization within the Fur family of metalloregulators. Biometals 20: 485– 499, 2007.

75. Lee JW, Soonsanga S, and Helmann JD. A complex thiolate switch regulates the *Bacillus subtilis* organic peroxide sensor OhrR. Proc Natl Acad Sci U S A 104: 8743–8748, 2007.

76. Lewin AC, Doughty PA, Flegg L, Moore GR, and Spiro S. The ferric uptake regulator of *Pseudomonas aeruginosa* has no essential cysteine residues and does not contain a structural zinc ion. Microbiology 148: 2449–2456, 2002.

77. Liu Y, Bauer SC, and Imlay JA. The YaaA protein of the *Escherichia coli* OxyR regulon lessens hydrogen peroxide toxicity by diminishing the amount of intracellular unincorporated iron. J Bacteriol 193: 2186–2196, 2011.

78. Ma Z, Faulkner MJ, and Helmann JD. Origins of specificity and cross-

talk in metal ion sensing by *Bacillus subtilis* Fur. Mol Microbiol 86: 1144–1155, 2012.

79. Ma Z, Lee JW, and Helmann JD. Identification of altered function alleles that affect *Bacillus subtilis* PerR metal ion selectivity. Nucleic Acids Res 39: 5036–5044, 2011.

80. Martin JE, Waters LS, Storz G, and Imlay JA. The *Escherichia coli* small protein MntS and exporter MntP optimize the intracellular concentration of manganese. PLoS Genet 11: e1004977, 2015.

81. Masse E and Gottesman S. A small RNA regulates the expression of genes involved in iron metabolism in *Escherichia coli*. Proc Natl Acad Sci U S A 99: 4620–4625, 2002.

82. Masse E, Salvail H, Desnoyers G, and Arguin M. Small RNAs controlling iron metabolism. Curr Opin Microbiol 10: 140–145, 2007.

83. Masse E, Vanderpool CK, and Gottesman S. Effect of RyhB small RNA on global iron use in *Escherichia coli*. J Bacteriol 187: 6962–6971, 2005.

84. Massey V. Activation of molecular oxygen by flavins and flavoproteins. J Biol Chem 269: 22459–22462, 1994.85.

85. May JJ, Wendrich TM, and Marahiel MA. The *dhb* operon of *Bacillus subtilis* encodes the biosynthetic template for the catecholic siderophore 2,3-dihydroxybenzoate- glycine-threonine trimeric ester bacillibactin. J Biol Chem 276: 7209–7217, 2001.

86. McGuire AM, Cuthbert BJ, Ma Z, Grauer-Gray KD, Brunjes Brophy M, Spear KA, Soonsanga S, Kliegman JI, Griner SL, Helmann JD, and Glasfeld A. Roles of the A and C sites in the manganese-specific activation of MntR. Biochemistry 52: 701–713, 2013.

87. Merchant SS and Helmann JD. Elemental economy: microbial strategies for optimizing growth in the face of nutrient limitation. Adv Microb Physiol 60: 91–210, 2012.

88. Miethke M, Monteferrante CG, Marahiel MA, and van Dijl JM. The *Bacillus subtilis* EfeUOB transporter is essential for high-affinity acquisition of ferrous and ferric iron. Biochim Biophys Acta 1833: 2267–2278, 2013.

89. Mills SA and Marletta MA. Metal binding characteristics and role of iron oxidation in the ferric uptake regulator from *Escherichia coli*. Biochemistry 44: 13553–13559, 2005.

90. Moore CM, Gaballa A, Hui M, Ye RW, and Helmann JD. Genetic and physiological responses of *Bacillus subtilis* to metal ion stress. Mol Microbiol 57: 27–40, 2005.

91. Moore CM and Helmann JD. Metal ion homeostasis in *Bacillus subtilis*. Curr Opin Microbiol 8: 188–195, 2005.

92. Moore CM, Nakano MM, Wang T, Ye RW, and Helmann JD. Response of *Bacillus subtilis* to nitric oxide and the nitrosating agent sodium nitroprusside. J Bacteriol 186:4655–4664, 2004.

93. Mostertz J, Scharf C, Hecker M, and Homuth G. Transcriptome and proteome analysis of *Bacillus subtilis* gene expression in response to superoxide and peroxide stress. Microbiology 150: 497–512, 2004.

94. Ollinger J, Song KB, Antelmann H, Hecker M, and Helmann JD. Role of the Fur regulon in iron transport in *Bacillus subtilis*. J Bacteriol 188: 3664–3673, 2006.

95. Parent A, Caux-Thang C, Signor L, Clemancey M, Sethu R, Blondin G, Maldivi P, Duarte V, and Latour JM. Single glutamate to aspartate mutation makes ferric uptake regulator (Fur) as sensitive to H_2O_2 as peroxide resistance regulator (PerR). Angew Chem Int Ed Engl 52: 10339– 10343, 2013.

96. Que Q and Helmann JD. Manganese homeostasis in *Bacillus subtilis* is regulated by MntR, a bifunctional regulator related to the diphtheria toxin repressor family of proteins. Mol Microbiol 35: 1454–1468, 2000.

97. Schoffman H, Lis H, Shaked Y, and Keren N. Iron-Nutrient Interactions within Phytoplankton. Front Plant Sci 7: 1223, 2016.

98. Schoneich C. Mechanisms of metal-catalyzed oxidation of histidine to 2-oxo-histidine in peptides and proteins. J Pharm Biomed Anal 21: 1093–1097, 2000.

99. Seaver LC and Imlay JA. Alkyl hydroperoxide reductase is the primary scavenger of endogenous hydrogen peroxide in *Escherichia coli*. J Bacteriol 183: 7173–7181, 2001.

100. Sethu R, Goure E, Signor L, Caux-Thang C, Clemancey M, Duarte V, and Latour JM. Reaction of PerR with molecular oxygen may assist H_2O_2 sensing in anaerobes. ACS Chem Biol 11: 1438–1444, 2016.

101. Shin JH and Helmann JD. Molecular logic of the Zur-regulated zinc deprivation response in *Bacillus subtilis*. Nat Commun 7: 12612, 2016.

102. Shin JH, Jung HJ, An YJ, Cho YB, Cha SS, and Roe JH. Graded expression of zinc-responsive genes through two regulatory zinc-binding sites in Zur. Proc Natl Acad Sci U S A 108: 5045–5050, 2011.

103. Smaldone GT, Antelmann H, Gaballa A, and Helmann JD. The FsrA sRNA and FbpB protein mediate the iron-dependent induction of the *Bacillus subtilis lutABC* iron-sulfur-containing oxidases. J Bacteriol 194: 2586–2593, 2012.

104. Sobota JM, Gu M, and Imlay JA. Intracellular hydrogen peroxide and superoxide poison 3-deoxy-D-arabinoheptulosonate 7-phosphate synthase, the first committed enzyme in the aromatic biosynthetic pathway of *Escherichia coli*. J Bacteriol 196: 1980–1991, 2014.

105. Sobota JM and Imlay JA. Iron enzyme ribulose-5-phosphate 3-epimerase in *Escherichia coli* is rapidly damaged by hydrogen peroxide but can be protected by manganese. Proc Natl Acad Sci U S A 108: 5402–5407, 2011.

106. Soonsanga S, Lee JW, and Helmann JD. Oxidant-dependent switching between reversible and sacrificial oxidation pathways for *Bacillus*

subtilis OhrR. Mol Mi- crobiol 68: 978–986, 2008.

107. Toledano MB, Delaunay A, Monceau L, and Tacnet F. Microbial H_2O_2 sensors as archetypical redox signaling modules. Trends Biochem Sci 29: 351–357, 2004.

108. Traore DA, El Ghazouani A, Ilango S, Dupuy J, Jacquamet L, Ferrer JL, Caux-Thang C, Duarte V, and Latour JM. Crystal structure of the apo-PerR-Zn protein from *Bacillus subtilis*. Mol Microbiol 61: 1211–1219, 2006.

109. Traore DA, El Ghazouani A, Jacquamet L, Borel F, Ferrer JL, Lascoux D, Ravanat JL, Jaquinod M, Blondin G, Caux-Thang C, Duarte V, and Latour JM. Structural and functional characterization of 2-oxo-histidine in oxidized PerR protein. Nat Chem Biol 5: 53–59, 2009.

110. Varghese S, Wu A, Park S, Imlay KR, and Imlay JA. Submicromolar hydrogen peroxide disrupts the ability of Fur protein to control free-iron levels in *Escherichia coli*. Mol Microbiol 64: 822–830, 2007.

111. Vitale S, Fauquant C, Lascoux D, Schauer K, Saint-Pierre C, and Michaud-Soret I. A ZnS_4 structural zinc site in the *Helicobacter pylori* ferric uptake regulator. Biochemistry 48: 5582–5591, 2009.

112. Waldron KJ and Robinson NJ. How do bacterial cells ensure that metalloproteins get the correct metal? Nat Rev Microbiol 7: 25–35, 2009.

113. Waldron KJ, Rutherford JC, Ford D, and Robinson NJ. Metalloproteins

and metal sensing. Nature 460: 823–830, 2009.

114. Wildschut JD, Caffrey SM, Voordouw JK, and Voordouw G. Oxygen exposure increases resistance of *Desulfovibrio vulgaris* Hildenborough to killing by hydrogen peroxide. Antonie Van Leeuwenhoek 101: 303–311, 2012.

115. Zheleznova EE, Crosa JH, and Brennan RG. Characterization of the DNA- and metal-binding properties of *Vibrio anguillarum* Fur reveals conservation of a structural Zn^{2+} ion. J Bacteriol 182: 6264–6267, 2000.

116. Zheng M, Aslund F, and Storz G. Activation of the OxyR transcription factor by reversible disulfide bond formation. Science 279: 1718–1721, 1998.

117. Zheng M, Doan B, Schneider TD, and Storz G. OxyR and SoxRS regulation of fur. J Bacteriol 181: 4639–4643, 1999.

118. Zheng M, Wang X, Templeton LJ, Smulski DR, LaRossa RA, and Storz G. DNA microarray-mediated transcriptional profiling of the *Escherichia coli* response to hydrogen peroxide. J Bacteriol 183: 4562–4570, 2001.

119. Zuber P. Management of oxidative stress in *Bacillus*. Annu Rev Microbiol 63: 575–597, 2009.

Chapter 3

PfeT, a P_{1B4}-Type ATPase, Effluxes Ferrous Iron and Protects *Bacillus subtilis* Against Iron Intoxication[4]

> "*And another set of discoveries, the microscopic organisms (descried by Hooke and Leeuwenhoek) inhabiting the air, the surface of a pond, and human bodies, also made it easy to imagine life in distant or invisible places. From this point of view, most early scientists could no more conceive of an empty cosmos than early poets and painters could picture an empty landscape.*"
>
> *- Lawrence Lipking, What Galileo Saw: Imagining the Scientific Revolution, 2014.*

3.1 Abstract

Iron is an essential element for nearly all cells and limited iron availability often restricts growth. However, excess iron can also be deleterious, particularly when cells expressing high affinity iron uptake systems transition to iron rich environments. *Bacillus subtilis* expresses numerous iron importers, but iron efflux has not been reported. Here, we describe the *B. subtilis* PfeT protein (formerly YkvW/ZosA) as a P_{1B4}- type ATPase in the PerR regulon that serves as an Fe^{2+} efflux pump and protects cells against iron intoxication. Iron and manganese homeostasis in *B. subtilis*

[4] This chapter is adapted from Guan G., Pinochet-Barros A., Gaballa A., Patel S. J., Argüello J. M., & Helmann J. D. Molecular Microbiology 2015 Nov ;98(4):787-803. Experiments were performed with equal contribution by Guan G. and Pinochet-Barros A. Metal dependent ATPase assays were carried out by Patel S. J. in the Argüello Lab. Gaballa A. performed the cobalt sensitivity assay and Fur regulon bioscreen experiments.

are closely intertwined: a *pfeT* mutant is iron sensitive, and this sensitivity can be suppressed by low levels of Mn^{2+}. Conversely, a *pfeT* mutant is more resistant to Mn^{2+} overload. *In vitro*, the PfeT ATPase is activated by both Fe^{2+} and Co^{2+}, although only Fe^{2+} efflux is physiologically relevant in wild-type cells, and null mutants accumulate elevated levels of intracellular iron. Genetic studies indicate that PfeT together with the ferric uptake repressor (Fur) cooperate to prevent iron intoxication, with iron sequestration by the MrgA mini-ferritin playing a secondary role. Protection against iron toxicity may also be a key role for related P_{1B4}-type ATPases previously implicated in bacterial pathogenesis.

3.2 Introduction

Iron homeostasis is a highly regulated process controlled both by iron availability and by reactive oxygen species such as hydrogen peroxide (H_2O_2). In *Bacillus subtilis*, the ferric uptake repressor (Fur) protein is the primary sensor of intracellular iron levels and directly represses several operons encoding iron import functions (1,2). In addition, Fur also indirectly activates the expression of some abundant iron-containing enzymes under conditions of iron sufficiency (3,4). *B. subtilis* also exhibits a complex adaptive response to peroxide stress that is coordinated by three transcription factors, PerR, OhrR and σ^B (5). Low levels of H_2O_2 inactivate the iron-containing repressor protein PerR leading to the derepression of enzymes for peroxide detoxification as

well as iron storage. Higher levels of H_2O_2 additionally induce the general stress σ^B regulon, whereas the OhrR-regulated *ohrA* gene responds selectively to organic peroxides.

PerR is a member of the Fur family of metalloregulatory proteins and requires a metal cofactor to bind with high affinity to its operator sites (6,7). Both structural and biochemical studies support a model in which PerR functions as a dimer with each monomer containing a structural Zn^{2+} ion and a second, regulatory metal ion (8,9). PerR can be activated to bind DNA by either Fe^{2+} or Mn^{2+}, which lead to the PerR:Zn,Fe and PerR:Zn,Mn forms of the repressor respectively. Importantly, only the PerR:Zn,Fe form responds to H_2O_2 (10). Exposure to H_2O_2 leads to oxidation of the bound Fe^{2+} atom and results in the oxidation of one of two histidine ligands (H37 or H91) that serve to co-ordinate the iron (10,11). The resulting conformational change leads to derepression of the PerR regulon.

PerR functions in the adaptive response to H_2O_2 in which low levels of H_2O_2 induce a regulon including those enzymes (the KatA catalase and AhpCF alkylhydroperoxide reductase) that directly detoxify H_2O_2 (1,12). This response thereby protects cells against challenge with higher doses of H_2O_2 (13,14). In addition to its role as the primary regulator of KatA and AhpCF, PerR also regulates expression of proteins that have direct impacts on cellular iron levels (15,16). These include the MrgA mini-ferritin, Fur, KatA and heme biosynthesis enzymes. MrgA is a dodecameric mini-ferritin that sequesters Fe^{2+} and

simultaneously consumes H_2O_2, by oxidation of Fe^{2+} to form a ferric-hydroxide core inside the spherical protein shell (17,18). Finally, PerR regulates enzymes for heme biosynthesis that are co-induced with the heme-requiring catalase (KatA) and are needed to support high levels of catalase activity.

The impact of the PerR regulon on iron homeostasis is highlighted by the severe growth defects of a *perR* null mutant, which have been ascribed to iron deficiency (16,19). The two main contributors to iron deficiency in the absence of PerR are the very high levels of catalase protein, which creates a high demand for its iron-containing heme cofactor, and increased expression of the Fur repressor. When iron is deficient, Fur is expected to be inactive as a repressor and therefore derepress iron uptake functions. However, in the *perR* mutant the increased Fur protein levels result in Fur acting as a repressor that is now cofactored by the ambient levels of Mn^{2+} in the cell (19). This results in the inappropriate repression of iron uptake, despite iron deficiency.

We previously reported that PerR also regulates ZosA/YkvW (20), a P_{1B4}-type ATPase, here renamed as PfeT. Unlike other PerR regulon members, the *pfeT* regulatory region is notable for the presence of both Fur and PerR boxes, suggesting that this gene may be regulated by both available Fe^{2+} and H_2O_2 (21). In addition, like some other members of the PerR regulon, repression of *pfeT* by PerR is primarily mediated by PerR:Zn,Mn and not PerR:Zn,Fe (22). Based on our prior studies, we proposed that YkvW might function in Zn^{2+} import in response to oxidative stress, and we therefore

renamed the protein as ZosA (20). Indeed, null mutants do display increased growth under zinc excess conditions (as confirmed here). However, whether or not this was due to alterations in Zn^{2+} transport was not clear. Moreover, P_{1B}-type ATPases are most frequently implicated in efflux rather than import, and the few characterized members of the P_{1B4} subfamily of ATPases are implicated in efflux of Co^{2+} (23). We therefore set out to reexamine the role of YkvW/ZosA in metal ion homeostasis in *B. subtilis*. As reported herein, this P_{1B4}-ATPase effluxes ferrous iron and is therefore now renamed as a peroxide-induced ferrous efflux transporter, PfeT.

3.3 Results & discussion

3.3.1 A *pfeT* mutant increases sensitivity to Fe^{2+} and Fe^{3+} salts

Bacillus subtilis PfeT is a member of the P_{1B4}-subfamily of P-type ATPases, which are generally classified as Co^{2+}-efflux pumps (24). Typically, mutations in metal ion efflux systems lead to an increased sensitivity to the transported metal ions. Metal ion sensitivity can be conveniently assayed using a disk diffusion (zone of inhibition) assay, which is a reflection of the maximal permissive concentration (MPC) for growth. Compared with wild-type (WT), the *pfeT* null mutant strain displayed a significantly increased sensitivity to Fe^{2+} and Fe^{3+} (Fig. 3.1A). In contrast, there was no apparent change in sensitivity to Zn^{2+} or Co^{2+}, and a small but significant decrease in sensitivity to Mn^{2+}, as monitored by this assay. The elevated sensitivity to iron salts is

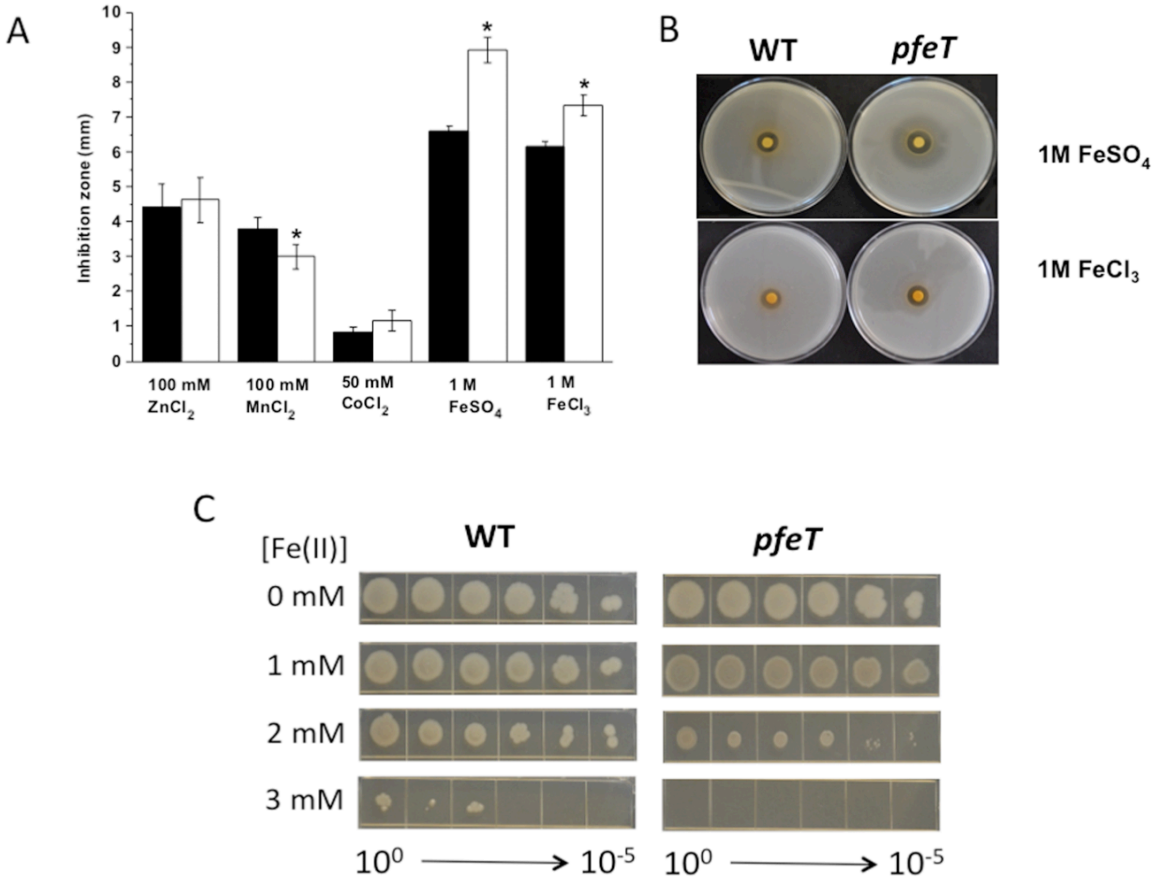

FIG. 3.1) A *pfeT* mutant is sensitive to iron intoxication.

(A) Sensitivity of wild-type (WT; CU1065; black bars) and an isogenic *pfeT* null mutant (HB17802, white bars) to metal ion stress as monitored using a disk diffusion (zone of inhibition) assay. The results are expressed as the diameter of the inhibition zone (mm) minus the diameter of the filter paper disk (6.5 mm). The mean ± SE from at least three biological replicates are reported. Significant differences from WT as determined by two-tailed *t*-test are indicated: *, $P < 0.01$. **(B)** Representative photograph (from at least six replicates) of a disk diffusion assay with WT and *pfeT* mutant cells on LBC plates. The disks were spotted with 10 μl 1 M $FeSO_4$ or 1 M $FeCl_3$ as indicated. **(C)** Efficiency of plating of WT and an isogenic *pfeT* null mutant under Fe^{2+} intoxication conditions as monitored using a spot dilution assay (photo representative of three biological replicates). Mid-logarithmic phase cultures were sequentially diluted by 10-fold and 3 μl spotted on LB medium amended with the indicated concentration of $FeSO_4$. The columns are (left to right), undiluted, 10^{-1}, 10^{-2}, 10^{-3}, 10^{-4} and 10^{-5} fold dilutions.

apparent both as an increased zone of growth inhibition (Fig. 3.1A) and, in the

case of Fe^{2+}, as a large zone of reduced cell density that is often observed after 24–72 h of incubation (Fig. 3.1B). Inspection of cell density over time suggests that this secondary zone is largely a result of increased cell lysis. These results indicate that the *pfeT* null mutant has reduced fitness under conditions of iron excess.

The sensitivity of the *pfeT* null mutant to iron excess is also apparent in an efficiency of plating (EOP) assay in which mid-logarithmic phase cells (OD_{600} ~ 0.4) are serially diluted and spotted on lysogeny broth (LB) medium amended with Fe^{2+} (Fig. 3.1C). Both WT and the *pfeT* null mutant form colonies with high efficiency up to a concentration of 2 mM Fe^{2+}, but the *pfeT* null mutant strain forms very small colonies, indicative of a reduced growth rate, under this condition. With 3 mM Fe^{2+}, the EOP of WT is reduced and the *pfeT* null strain is unable to form colonies.

3.3.2 A *pfeT* mutation increases sensitivity to the Fe^{2+} activated antibiotic streptonigrin

Streptonigrin (SN) is a quinone antibiotic whose activity is correlated with intracellular iron availability (25). In order to compare the levels of intracellular free iron between WT and *pfeT,* the sensitivity to SN was tested by both disk diffusion and growth curve assays. The *pfeT* mutant displayed a significantly increased SN sensitivity on LB plates amended with 100 μM $FeSO_4$. In contrast, only a slight increase in SN sensitivity was noted on LB

plates, and the *pfeT* mutation had no effect on sensitivity on LB plates amended with 2, 2′-dipyridyl (DP), a cell membrane-permeable iron chelator (Fig. 3.2). These results suggest that deletion of *pfeT* led to an increase in intracellular iron levels, particularly in an iron-rich medium. Consistent results were noted in liquid culture growth experiments: the *pfeT* mutant displayed increased SN sensitivity, and this was enhanced in medium amended with $FeSO_4$ (Fig. 3.3).

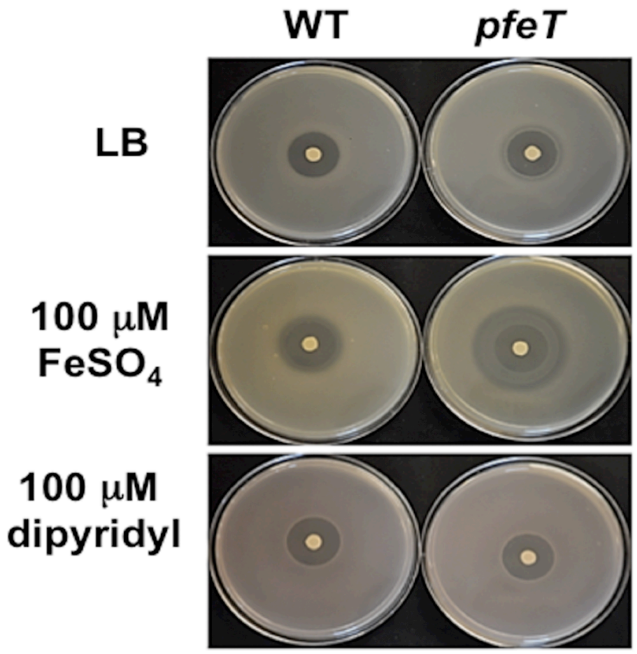

FIG. 3.2) A *pfeT* mutation increases sensitivity to streptonigrin (SN).

Representative photographs (from at least six replicates) of a disk diffusion assay with WT and *pfeT* mutant cells on LB plates containing either no supplement, 100 μM $FeSO_4$ or 100 μM dipyridyl. Each disk was spotted with 5 μl of 5 mg ml^{-1} (25 μg) SN.

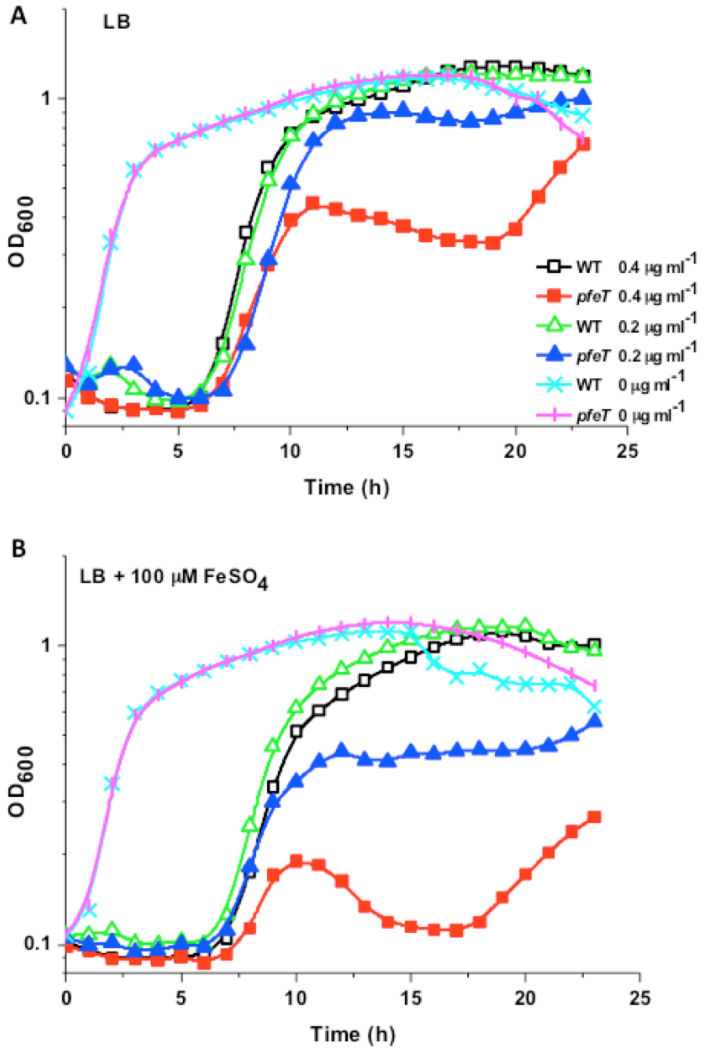

FIG. 3.3) Mutation of *pfeT* increases sensitivity to streptonigrin (SN) in liquid culture.

(A) Effect of SN (at the indicated concentration) on the growth of WT and *pfeT* mutant cells in LB medium. **(B)** Effect of SN on the growth of WT and *pfeT* mutant cells in LB medium amended with 100 μM $FeSO_4$. Growth curves are an average of more than six experiments.

3.3.3 Cells lacking PfeT accumulate elevated levels of intracellular iron

To test directly the effects of PfeT on intracellular metal ion levels, we

challenged cells in LB + 1 g per liter of citrate trisodium dihydrate (LBC) medium with 4 mM $FeSO_4$, and monitored metal ion levels by inductively coupled plasma mass spectrometry (ICP-MS). For this experiment, we used a

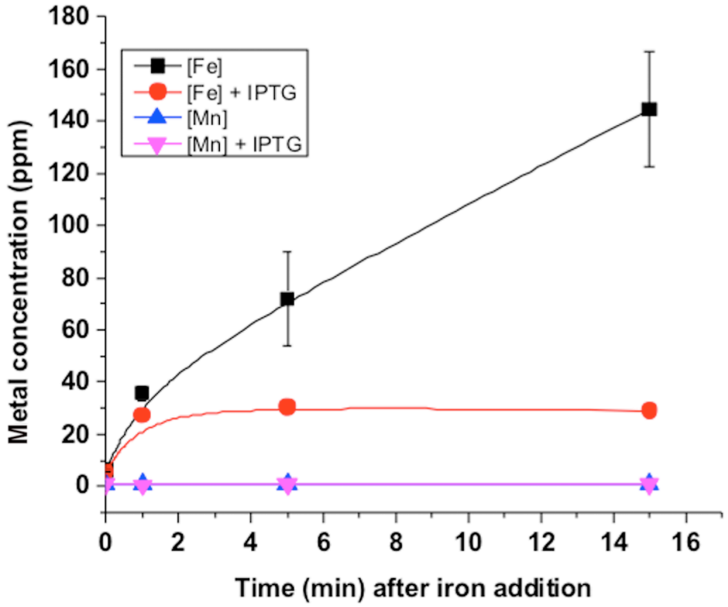

FIG. 3.4) The *pfeT* mutant accumulates high levels of intracellular iron.

Levels of intracellular Fe (mean ± SE of duplicate measurements) were monitored by inductively coupled plasma mass spectrometry (ICP-MS) for the *pfeT* mutant strain complemented with an IPTG-inducible copy of *pfeT* (HB17852; CU1065 *pfeT::spc amyE*::P_{spac}-*pfeT*) before and after addition of4 mM $FeSO_4$ to LBC medium. In uninduced cells (■), Fe accumulates to a high level (~ 144 ppm) within 15 min. In cells grown with IPTG (and therefore expressing PfeT), the accumulation of Fe is much reduced (●). Prior to Fe addition (time 0), the basal level of Fe (~ 5.7 ppm) was ~ 5-fold higher than Mn (~ 1.1 ppm) under these conditions. Over the course of the experiment, levels of Mn (▲, ▼) and Zn (not shown) were largely unchanged with values averaged over the eight measurements (± SD) of 0.81 ± 0.16 ppm and 4.2 ± 0.8 ppm respectively.

pfeT null mutant complemented with an IPTG- inducible copy of the *pfeT* gene. In samples taken between 1 and 15 min after iron addition, there was a large increase in intracellular iron in the absence of IPTG. However, when the same

strain was grown in the presence of 1 mM IPTG, there was relatively little iron accumulation (Fig. 3.4). Note that prior to iron addition, the levels of Mn^{2+} were ~ 5-fold lower than iron under these conditions and were largely unchanged over the course of the experiment.

3.3.4 PfeT is an Fe^{2+} and Co^{2+} activated ATPase

The above results are most simply explained by postulating that PfeT functions physiologically to efflux iron from cells. Since the dominant form of iron in the reducing environment of the cytoplasm is Fe^{2+}, we anticipated that PfeT might function to efflux Fe^{2+}. P-type ATPases couple ATP hydrolysis to metal ion transport. Consequently, monitoring metal ion activated ATPase activity provides a convenient method to survey substrate selectivity (26). The *B. subtilis* PfeT protein was overproduced in *E. coli*, solubilized from the membrane fraction, purified by affinity chromatography, and reconstituted in micellar form as described previously for other P-type ATPases (27,28).

When the ability of various metal ions to activate the PfeT ATPase was surveyed, the highest activity was observed with Fe^{2+}, with lower activity noted for Co^{2+}. No activation was observed with Fe^{3+}, Ni^{2+}, Zn^{2+}, Mn^{2+}, Cu^{2+} or Cu^{1+} (Fig. 3.5A). Fe^{2+} activated the ATPase most strongly, albeit with a relatively low apparent affinity ($K_{1/2}$ for activation 0.52 $\pm$ 0.12 mM). The V_{max} observed with Fe^{2+} was 3.25 $\pm$ 0.21 μmol mg^{-1} h^{-1} (Fig. 3.5B), which compares favorably to the reported values for several other metal activated P-type ATPases. For

example, a 14 μmol mg^{-1} h^{-1} activity was observed in ZntA, the *E. coli* Zn^{2+}-ATPase (29) and P_{1B1}-family Cu^{1+} efflux ATPases have reported values of 3–4 μmol mg^{-1} h^{-1} as measured for *Archaeoglobus fulgidus* CopA when activated by Cu^{1+} (30). In particular, PfeT Co^{2+}-ATPase activity is similar to CtpD and CtpJ, P_{1B4}-family ATPases. These had V_{max} values for Co^{2+} in the range of ~ 0.5–1.5 μmol mg^{-1} h^{-1} (27,28). The maximal ATPase activation of PfeT by Co^{2+} (V_{max} of 0.70 ± 0.07 μmol mg^{-1} h^{-1}) is substantially lower than for Fe^{2+} (0.7 vs. 3.3 μmol mg^{-1} h^{-1}). However, the apparent affinity for Co^{2+} is higher than for Fe^{2+} with a $K_{1/2}$ of 42±16 μM for Co^{2+} vs. 520±120 μM Fe^{2+} (Fig. 3.5B & C).

In our initial survey, we had failed to detect a significant role for PfeT in resistance to Co^{2+} (Fig. 3.1A). We reasoned that the ability of PfeT to efflux Co^{2+} may have been largely masked by the presence of other efflux mechanisms, including the CzcD protein. CzcD is a broad specificity cation diffusion facilitator protein known to be the primary determinant of Co^{2+} resistance in *B. subtilis* (31,32). As expected, deletion of *czcD* significantly increased Co^{2+} sensitivity, but there was no increase in sensitivity when *pfeT* was additionally deleted (Fig. 3.6). However, when PfeT was expressed from an IPTG-inducible promoter in the *czcD* null mutant strain, resistance to Co^{2+} was largely restored. Indeed, increased resistance was noted even in the absence of IPTG induction, likely due to leaky expression from the P_{spac} promoter. This indicates that PfeT can serve as an efflux pump for Co^{2+} *in vivo* but that this activity is unlikely to be significant under physiological conditions

due to (i) the much greater activity of the CzcD transporter and (ii) poor expression of the *pfeT* gene under these conditions. The *pfeT* gene is known to be repressed by PerR (20). Although, PerR-regulated genes are often repressed in response to Mn^{2+} and Fe^{2+}, they can also be repressed by Co^{2+} (33).

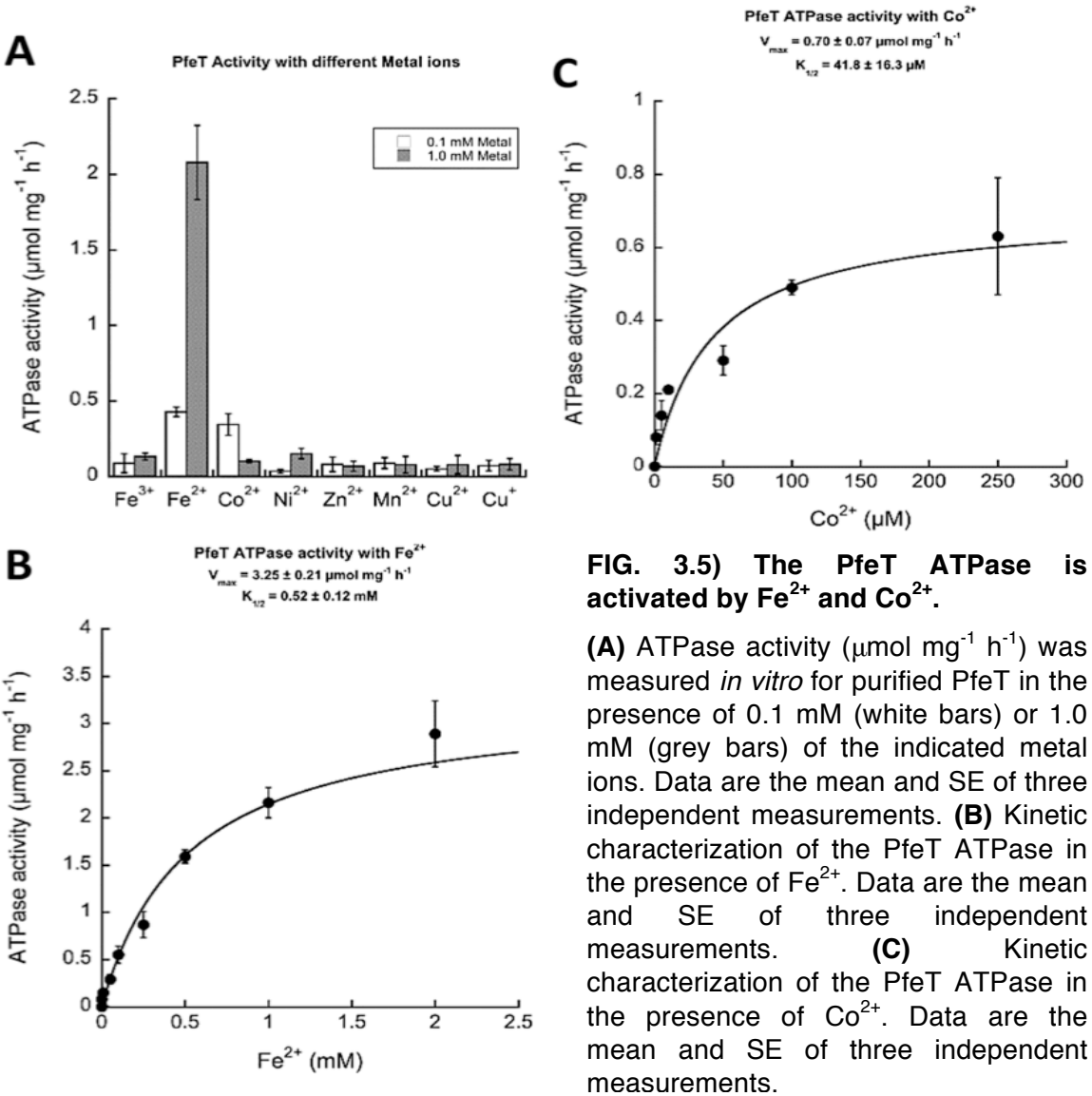

FIG. 3.5) The PfeT ATPase is activated by Fe^{2+} and Co^{2+}.

(A) ATPase activity (µmol mg^{-1} h^{-1}) was measured *in vitro* for purified PfeT in the presence of 0.1 mM (white bars) or 1.0 mM (grey bars) of the indicated metal ions. Data are the mean and SE of three independent measurements. **(B)** Kinetic characterization of the PfeT ATPase in the presence of Fe^{2+}. Data are the mean and SE of three independent measurements. **(C)** Kinetic characterization of the PfeT ATPase in the presence of Co^{2+}. Data are the mean and SE of three independent measurements.

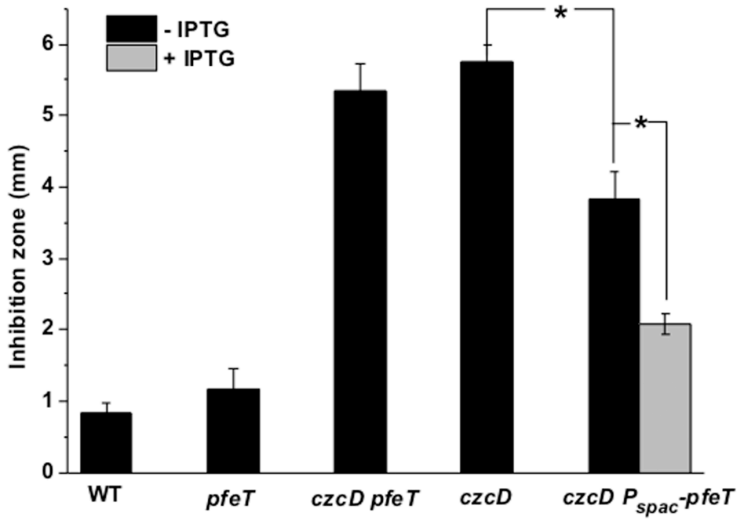

FIG. 3.6) PfeT can confer Co^{2+} resistance if artificially expressed in an efflux defective mutant.

The effect of a *pfeT* mutation on sensitivity to Co^{2+} was monitored using a zone of inhibition assay on LB plates. The WT, *pfeT*, *czcD* and *czcD pfeT* double mutant were plated on LB with a filter disk containing 100 mM $CoCl_2$. In the final columns, the *czcD* mutant strain contained an inducible P_{spac}-*pfeT* construct, and cells were grown on plates with (gray) and without (black) 0.1 mM IPTG. The zone of inhibition was measured as the total diameter of the clearance zone minus the diameter of filter paper disk (6.5 mm). The mean and SE from at least three biological replicates are reported. Significant differences were determined by two-tailed *t*-test.*, $P < 0.01$.

3.3.5 A *pfeT* mutation modestly improves growth under high Zn^{2+} stress

Previously, PfeT was reported to affect Zn^{2+} homeostasis as judged by an increase in cell growth in the presence of excess Zn^{2+} in strains containing a *pfeT* mutation (20). In addition, the *pfeT* mutation was reported to reduce intracellular Zn^{2+} accumulation, consistent with a postulated role in Zn^{2+} import (20). However, Zn^{2+} does not activate the PfeT ATPase (Fig. 3.5A). We therefore re-investigated the effects of the *pfeT* mutation on Zn^{2+} sensitivity,

both in WT and in efflux defective strains, using both disk diffusion (Fig. 3.7A) and growth assays (Fig. 3.7B–F). A *pfeT* null mutation did not lead to a significant change in the MPC for Zn^{2+} (Fig. 3.1A), and similar results were seen in strains defective for either or both Zn^{2+} efflux systems (*pfeT cadA*, *pfeT czcD* and *pfeT cadA czcD*; Fig. 3.7A). However, the *pfeT* mutant did grow better under high Zn^{2+} stress conditions in liquid medium. This effect was most notable when comparing a *perR* null strain, in which *pfeT* is expressed constitutively, against a *perR pfeT* double mutant (Fig. 3.7B). However, effects were also noted in the WT (Fig. 3.7C) and *cadA* mutant backgrounds (Fig. 3.7D). The exception is a *cadA czcD* double mutant (defective for Zn^{2+} efflux) (Fig. 3.7E & F), which displayed a greatly increased Zn^{2+} sensitivity (Fig. 3.7A) (34).

We conclude that mutation of *pfeT* does influence Zn^{2+} tolerance (20), but in light of the results reported herein this is likely an indirect effect of alterations in intracellular Fe^{2+} levels. The molecular basis of Zn^{2+} toxicity in bacteria is poorly understood, but under conditions of oxidative stress Zn^{2+} may competitively inhibit binding of Fe^{2+} to mononuclear enzymes and reduce their activity (35,36). We can therefore speculate that elevated cytosolic iron, as a consequence of the *pfeT* mutation, may help prevent enzyme mismetallation by Zn^{2+}. This mechanism may suffice to partially suppress Zn^{2+} toxicity in cells that are also competent for Zn^{2+} efflux but may be insufficient in efflux defective cells.

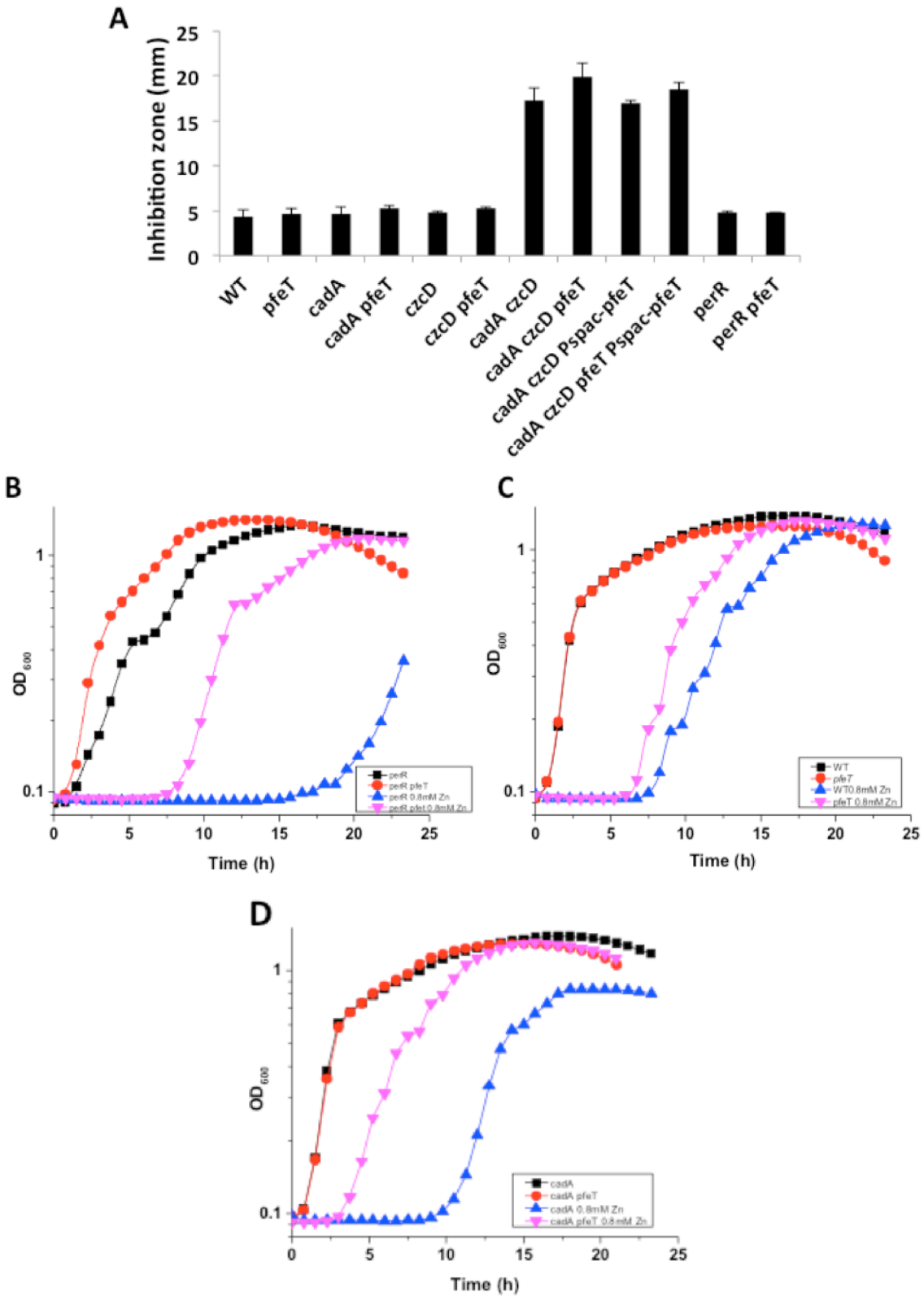
A
Inhibition zone (mm)
25
20
15
10
5
0
WT
pfeT
cadA
cadA pfeT
czcD
czcD pfeT
cadA czcD
cadA czcD pfeT
cadA czcD Pspac-pfeT
cadA czcD pfeT Pspac-pfeT
perR
perR pfeT
B
OD600
1
0.1
0
5
10
15
20
25
Time (h)
perR
perR pfeT
perR 0.8mM Zn
perR pfeT 0.8mM Zn
C
OD600
1
0.1
0
5
10
15
20
25
Time (h)
WT
pfeT
WT0.8mM Zn
pfeT 0.8mM Zn
D
OD600
1
0.1
0
5
10
15
20
25
Time (h)
cadA
cadA pfeT
cadA 0.8mM Zn
cadA pfeT 0.8mM Zn

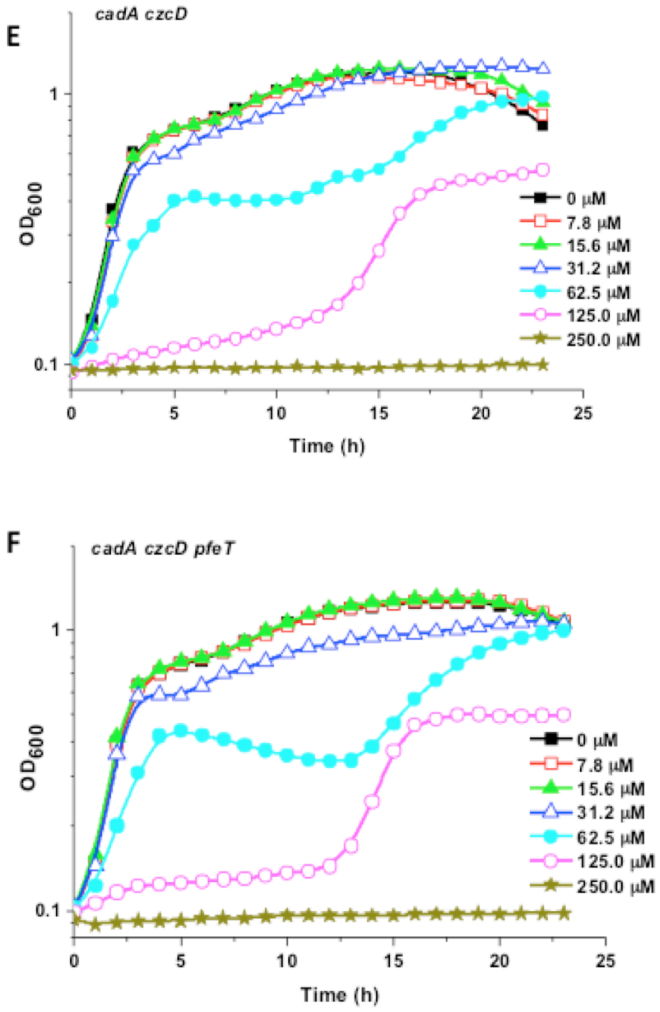

FIG. 3.7) Mutation of *pfeT* enhances Zn^{2+} tolerance.

(A) Presence of absence of PfeT does not affect Zn^{2+} sensitivity as measured in a disk diffusion assay. Disk diffusion assays were used to monitor the relative maximum permissive concentrations (MPC) for WT and mutant strains using LB medium and a filter disk spotted with 10 µl of 100 mM $ZnCl_2$. Thezone of inhibition is expressed as the total diameter of the clearance zone minus the diameter of filter paper disk (6.5 mm). The mean and SE from at least three biological replicates are reported. No significant differences ($p < 0.01$) were noted between any pairs of strains (with and without *pfeT*) as determined by two-tailed *t* test. The *cadA czcD* double mutant is much more sensitive to Zn^{2+} than WT, consistent with previous results (Ma *et al.,* 2014). **(B)** Growth curve assays comparing a *perR* mutant and *perR pfeT* double mutant in the absence or presence of 0.8 mM $ZnCl_2$. In the presence of 0.8 mM Zn^{2+} the *perR pfeT* double mutant has a much shorter lag phase than the *perR* single mutant, presumably because the *pfeT* mutation leads to anincrease in intracellular iron availability. Thisleads to the hypothesis that increased intracellular iron availability helps protect against Zn^{2+} toxicity. **(C)** Growth curve assays comparing WT and a *pfeT* mutant in the absen-

ce or presence of 0.8 mM Zn^{2+}. The *pfeT* mutant has a modest growth advantage (relative to WT) under Zn^{2+} stress conditions. Note that the *perR* mutant (B) grows more slowly than wild-type (C) in LB medium alone. This is consistent with prior results indicating that *perR* is iron-limited in LB medium (Faulkner *et al.,* 2012). **(D)** Growth curve assays comparing a *cadA* mutant and a *cadA pfeT* double mutant in the absence or presence of 0.8 mM Zn^{2+}. Again, the strain carrying the *pfeT* mutation has a growth advantage under these Zn^{2+} stress conditions. **(E)** and **(F)** Growth curve assays comparing Zn^{2+} sensitivity of the *cadA czcD* double mutant (E) to the *cadA czcD pfeT* triple mutant (F) in LB medium and Zn^{2+} added at the concentrations indicated. In this comparison, PfeT has no discernable effect on the Zn^{2+} tolerance for these two very sensitive strains.

3.3.6 PfeT reduces Fe^{2+} dependent cell killing and facilitates adaptation to Fe^{2+} excess

To further characterize the effects of *pfeT* on iron intoxication, we sought to develop a robust and reproducible growth assay using a Bioscreen growth analyzer. To reduce the precipitation of insoluble ferric hydroxides (which can interfere with optical density measurements of the Bioscreen growth analyzer), we amended LB medium (with a basal level of ~ 8–10 μM Fe; (2)) with 1 g per liter of citrate trisodium dihydrate (3.4 mM). This is the same concentration of citrate used in metal-limiting minimal medium in previous studies of iron physiology (2,4,33,37) and was shown previously to allow increased iron availability (as judged by repression of the Fur regulon) when added to M9 medium (4). In this medium (designated LBC), cells tolerate high levels of $FeSO_4$ (up to 3 mM), but when the Fe^{2+} concentration surpasses that of citrate, iron toxicity results and WT cells only resume growth after a long lag phase (Fig. 3.8A). In this medium, *pfeT* mutant cells are unable to grow in the presence of 4 mM $FeSO_4$ (Fig. 3.8B).

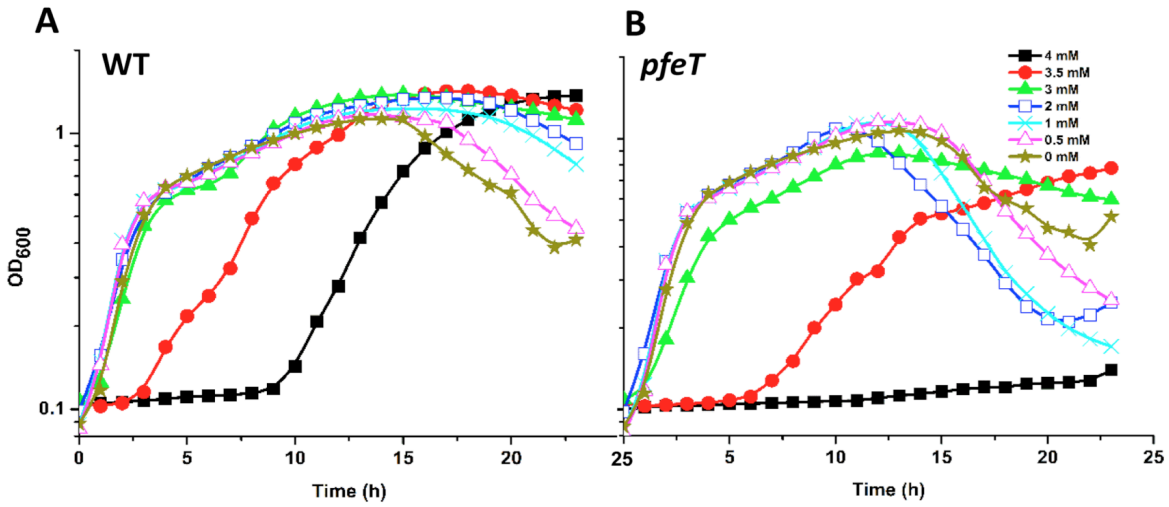

FIG. 3.8) Role of PfeT under iron intoxication conditions by monitoring cell growth in liquid culture.

(A) Iron concentration dependence of growth inhibition for WT in LBC medium amended with various concentrations of $FeSO_4$ (added from a 100 mM stock prepared in 0.1 N HCl). **(B)** Iron concentration of growth inhibition for the *pfeT* mutant in LBC medium amended with $FeSO_4$. Growth inhibition is most apparent with 3.5 mM Fe^{2+} (●) and 4 mM Fe^{2+} (■). Growth curves are an average of four cultures monitored in parallel (technical replicates), and the results are representative of experiments performed at least three times.

The long lag phase in this assay is due, in part, to a significant loss of viability upon dilution of mid-logarithmic phase (OD_{600} ~ 0.4) cells into the LBC + 4 mM Fe^{2+} medium. To estimate the extent of killing under these conditions, we estimated the concentration of viable cells by spot dilution onto LB medium prior to and 30 and 60 min after amendment with 4 mM Fe^{2+} (Fig. 3.9). We estimate that the viable cells counts for WT decrease by ~ 10^4 to 10^5-fold under these conditions, and there is an even larger decrease for the *pfeT* null mutant. Significantly, cells in which *pfeT* was induced from an IPTG-inducible promoter prior to Fe^{2+} shock are able to survive this treatment with relatively little loss of viability.

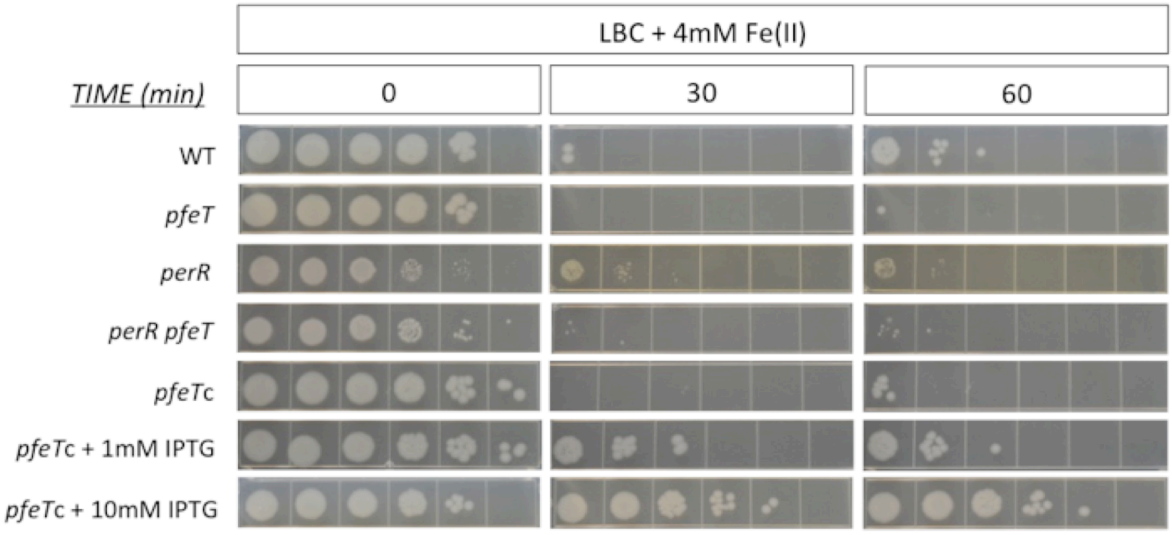

FIG 3.9) High level expression of PfeT prevents cell killing by Fe^{2+} intoxication.

Cells were grown in 5 ml LBC medium with 0, 1, or 10 mM IPTG as indicated. The WT, *pfeT*, *perR*, *perR pfeT*, and *pfeT* complemented strains (*pfeTc*) were shocked by addition of $FeSO_4$ to a final concentration of 4 mM Fe^{2+} (200 µl from a 100 mM stock in 0.1 N HCl) when cells reached an OD_{600} ~0.4. 1 ml samples were taken before shock (0 min) and 30 min and 60 min after shock, washed by centrifugation (2 min at 13,000rpm) and a gentle resusupension in 1 mL LB, and serially diluted in LB pre-warmed to 37°C. 3 µl of cells were spotted in each quadrant on 30 mL LB plates and left to dry before incubating at 37°C overnight (note that for the strains carrying a *perR* null mutation the plates were incubated for an additional 4-6 h to better visualize the small colonies). The columns are (left to right), undiluted, 10^{-1}, 10^{-2}, 10^{-3}, 10^{-4}, and 10^{-5} fold dilutions of the washed cells.

To monitor cell recovery after Fe^{2+} shock under conditions directly comparable with the Bioscreen experiments, we diluted cells 100-fold into LBC medium with and without 4 mM Fe^{2+} and monitored viable cell counts over time. As expected from the Bioscreen results (Fig. 3.8) and the cell killing assay (Fig. 3.9), there was a large decrease in viable cell counts after dilution into the Fe^{2+}-amended medium with cell density recovering after 9 h (Fig. 3.10). No recovery was seen for the *pfeT* null mutant up to 15 h. In contrast, a *perR* null strain (constitutively expressing *pfeT*) experienced comparatively

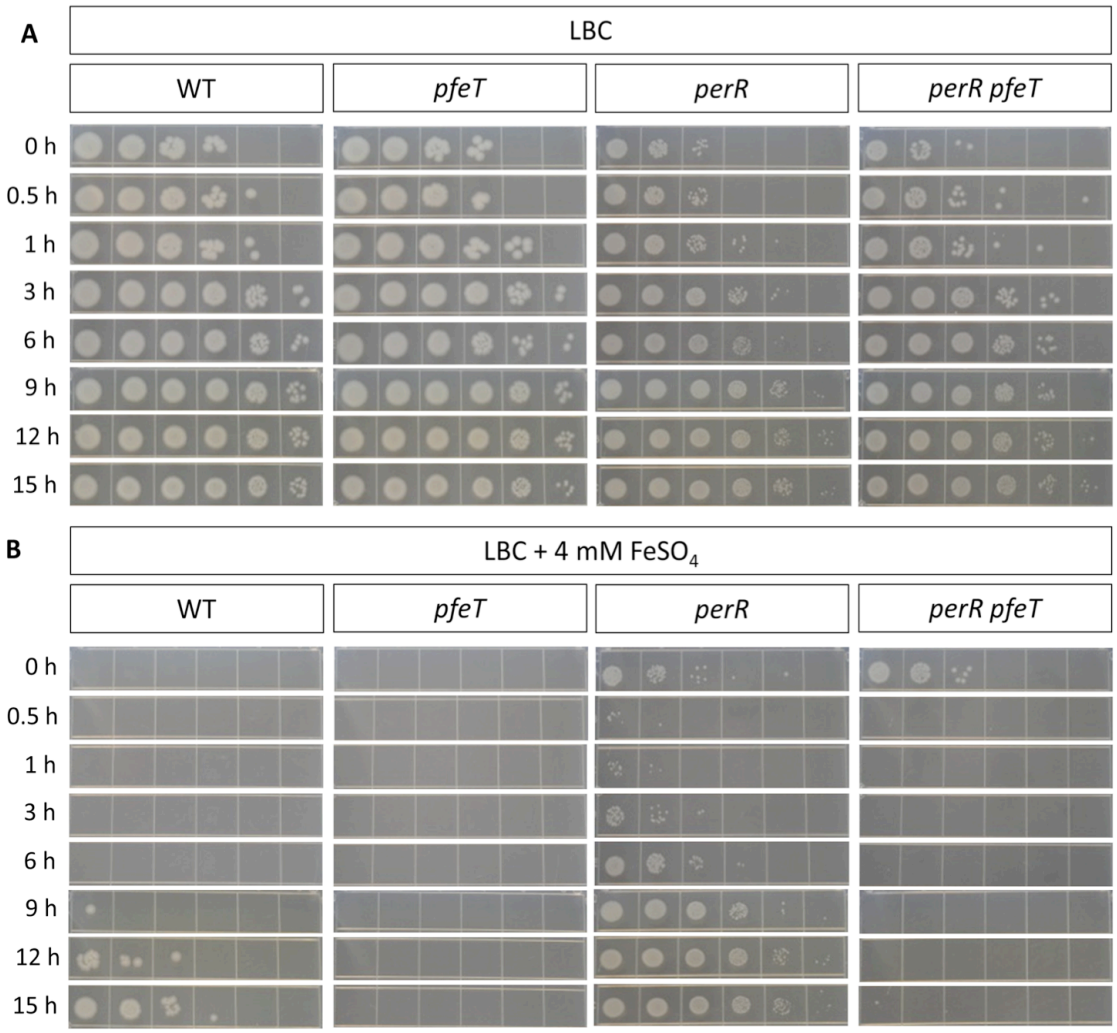

FIG. 3.10) Role of PfeT under iron intoxication conditions: cell viability and growth in liquid culture.

To determine whether the long lag phase observed under Fe^{2+} intoxication was due to cell stasis or cell killing, mid-logarithmic phase cultures were diluted 100-fold into either LBC **(A)** or LBC + 4 mM Fe^{2+} **(B)** and samples were taken as a function of time (time 0 is immediately after dilution). Cell viability (colony-forming units) was estimated using a spot dilution assay with washed cells (spots represent undiluted on the left to 10^{-5} on the right in 10-fold decrements). Photos are representative of three biological replicates. Under these conditions, only the *perR* null mutant strain recovers rapidly (an ~ 3 h lag relative to the unstressed cells) and this recovery requires PfeT.

little cell killing (~ 100-fold) and resumed growth immediately. The ability of the *perR* strain to survive Fe^{2+} intoxication was dependent on PfeT: the *perR pfeT*

double mutant was unable to adapt and failed to resume growth within 15 h (Fig. 3.10B). We suggest that the resumption of growth under these conditions of Fe^{2+} intoxication requires efflux of Fe^{2+} from the cytosol, rather than modification of the growth medium by the cells. In cultures inoculated with both WT and *pfeT* mutant cells, only the WT cells are recovered after out-growth (data not shown).

3.3.7 Sensitivity of cells to Fe^{2+} intoxication is pH dependent

In a series of further experiments (see Fig. 3.11–3.13), we systematically investigated the effects of variations in $FeSO_4$, citrate and pH on cell growth as monitored using the Bioscreen assay. In LB medium amended with 4 mM $FeSO_4$ neither WT nor the *pfeT* null mutant are able to grow in the absence of citrate (Fig. 3.11). With citrate amended at 1 g l^{-1}, WT resumes growth after an extended (~ 10 h) lag, whereas the *pfeT* null mutant is unable to grow (consistent with Figs 3.8 and 3.10).

One key finding from these studies is that iron intoxication is highly sensitive to pH: the observed toxicity (Figs 3.8 and 3.10) is due to both the high iron concentration (added from a 100 mM $FeSO_4$ stock in 0.1 N HCl) and a reduction of the pH of the growth medium to ~5.7 upon addition of $FeSO_4$ to 4 mM. We serendipitously observed that if Fe^{2+} is added from a 1 M stock (and therefore less HCl is added), there is comparatively little growth inhibition (Fig. 3.12) motivated studies to define the pH dependence of iron intoxication.

In LBC medium amended with 4 mM $FeSO_4$ and buffered using 60 mM 2-(N-morpholino) ethanesulfonic acid (MES; pKa 6.1), iron intoxication increases substantially as the pH is reduced below 7, and the effect of PfeT is most notable when the pH is less than 6.5 (Fig. 3.14A & B). Indeed, when the pH is 5.7, growth is largely dependent on PfeT. Presumably, the increased solubility of Fe^{2+} at low pH, and perhaps increased uptake, increase Fe^{2+} intoxication. Indeed, in LB medium buffered to pH 5.7, PfeT contributes significantly to Fe^{2+} tolerance even in the absence of citrate (Fig. 3.13).

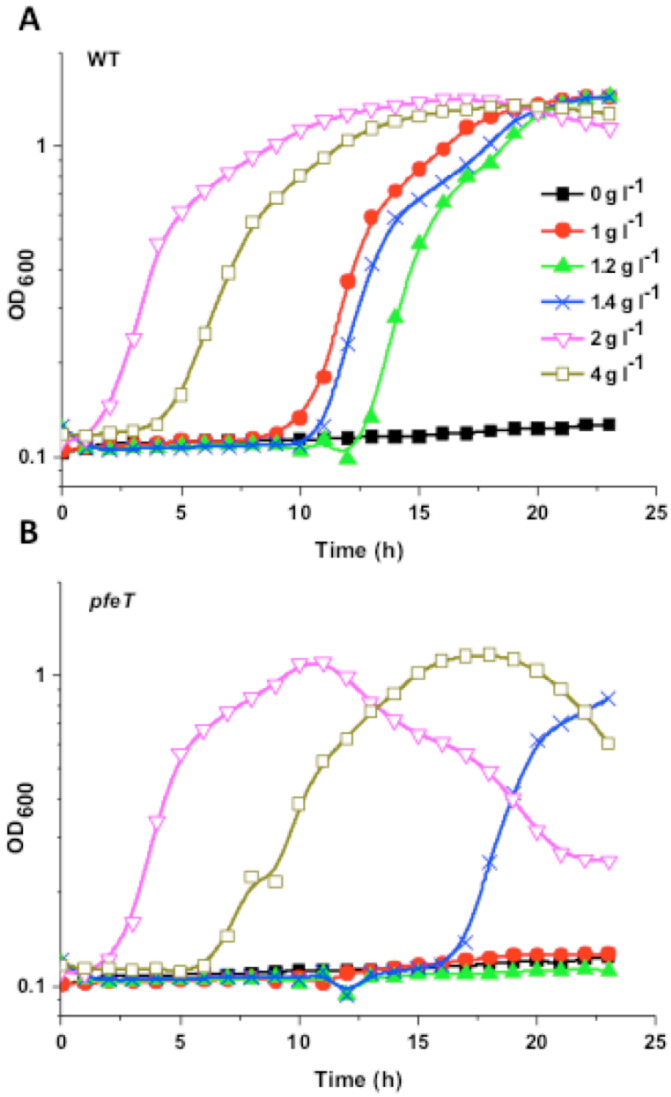

FIG. 3.11) Effects of citrate on the iron sensitivity of the WT and *pfeT* mutant strain in LB medium amended with 4 mM $FeSO_4$.

WT and *pfeT* mutant cells were grown in LB medium with 4 mM $FeSO_4$ (added from a 100 mM stock prepared in 0.1 N HCl) and citrate trisodium dihydrate was added to the final concentrations indicated. Neither WT nor *pfeT* mutant can grow in 4 mM $FeSO_4$ alone. With 1 g l^{-1} citrate trisodium dihydrate the WT can grow (albeit with a long lag phase), but *pfeT* cannot. Growth was restored for both strains at citrate levels of 1.4 g l^{-1} with optimal growth at 2 g l^{-1}. Note also that the *pfeT* mutant displays an increased tendency to lyse in stationary phase compared with the wild-type under iron intoxication conditions, consistent with the inference that lysis contributes to the secondary inhibition zone noted in Fig. 3.1B.

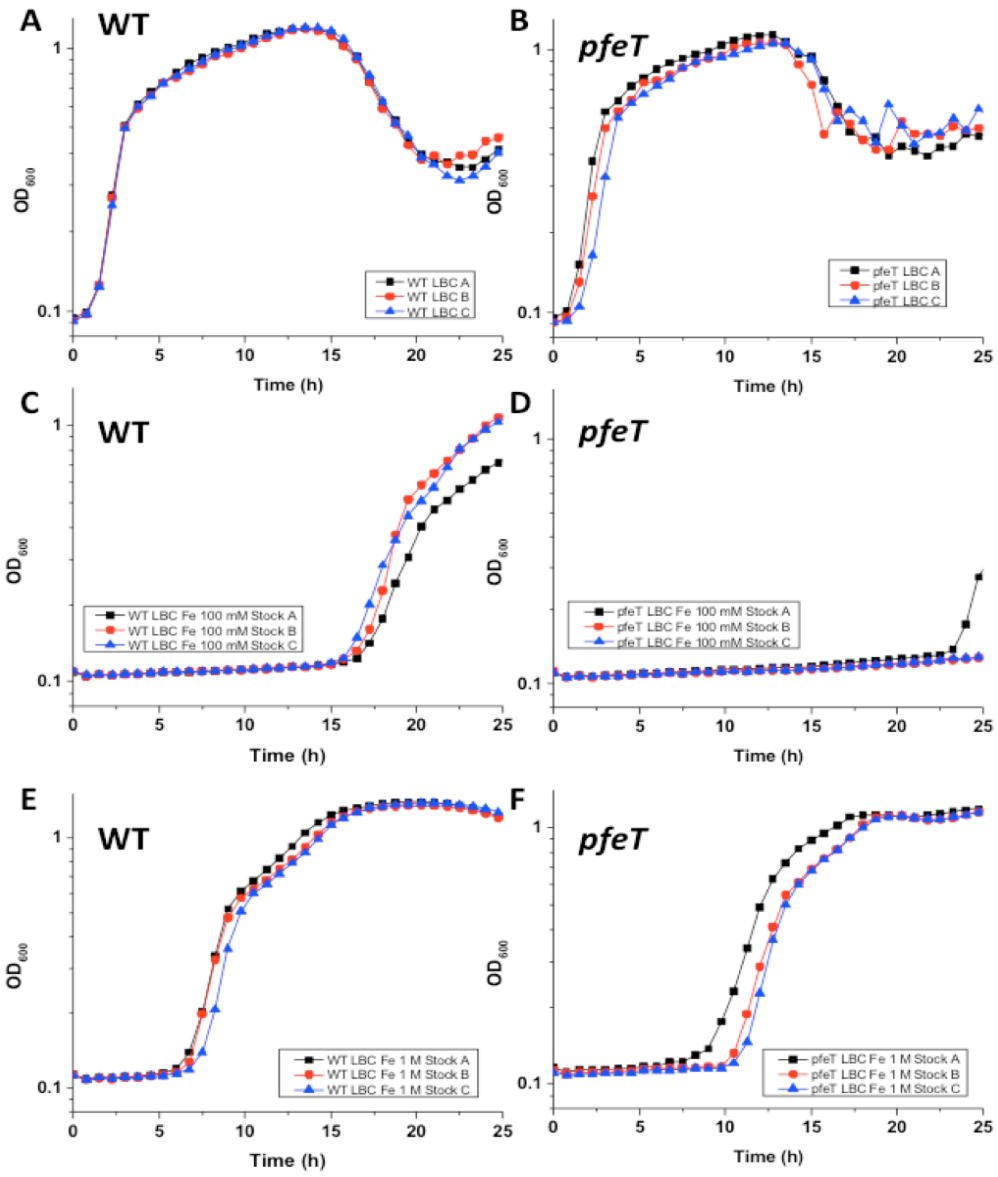

FIG. 3.12) Effects of pH (due to different $FeSO_4$ stock solutions) on iron intoxication.

In the course of reproducing the PfeT dependence of growth in LBC medium with 4 mM $FeSO_4$, we serendipitously noted that this phenotype was dependent on the concentration of the $FeSO_4$ stock solution. **(A)** & **(B)** In the absence of added Fe^{2+}, both the WT and *pfeT* mutant grow at similar rates in LBC medium (biological triplicates grown in parallel are shown). **(C)** & **(D)** When 4 mM $FeSO_4$ is added from a stock prepared in 0.1 N HCl (final medium pH ~5.7) the WT strain grows after an extended lag, but the *pfeT* null mutant grows little if at all in the first 24 hours. **(E)** & **(F)**. In contrast, when Fe^{2+} is added from a 1 M stock solution in 0.1 N HCl (final medium pH of 6.6), both the WT and the *pfeT* mutant can grow, although the *pfeT* mutant has a longer lag phase (~10 h) than the WT (~7 h).

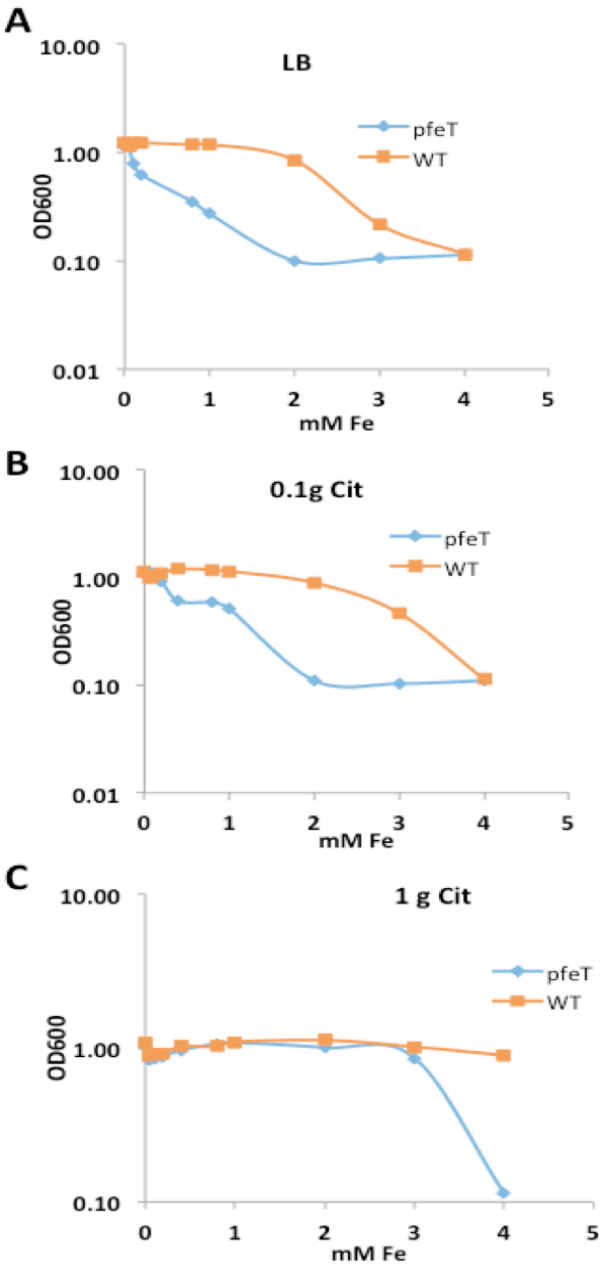

FIG. 3.13) Citrate effects on growth inhibition of WT and *pfeT* by iron in LB medium (pH 5.7).

Growth of the WT and *pfeT* null mutants was compared as a function of added $FeSO_4$. The OD_{600} is shown as measured by Bioscreen 12 h after inoculation with a 100:1 dilution from logarithmically growing (OD_{600} = 0.4) cultures and is plotted vs. added Fe^{2+} for each growth condition. **(A)** When LB is buffered to pH 5.7 (60 mM MES), the *pfeT* mutant is much more sensitive to Fe^{2+} than WT. **(B)** A similar pattern of growth inhibition is seen in LB (buffered to pH 5.7) amended with 0.1 g l^{-1} of citrate. **(C)** In LBC medium (LB with 1 g l^{-1} citrate; buffered to pH 5.7) the toxic effects of iron are minimal until the iron concentration is in excess of the citrate concentration (3.4 mM).

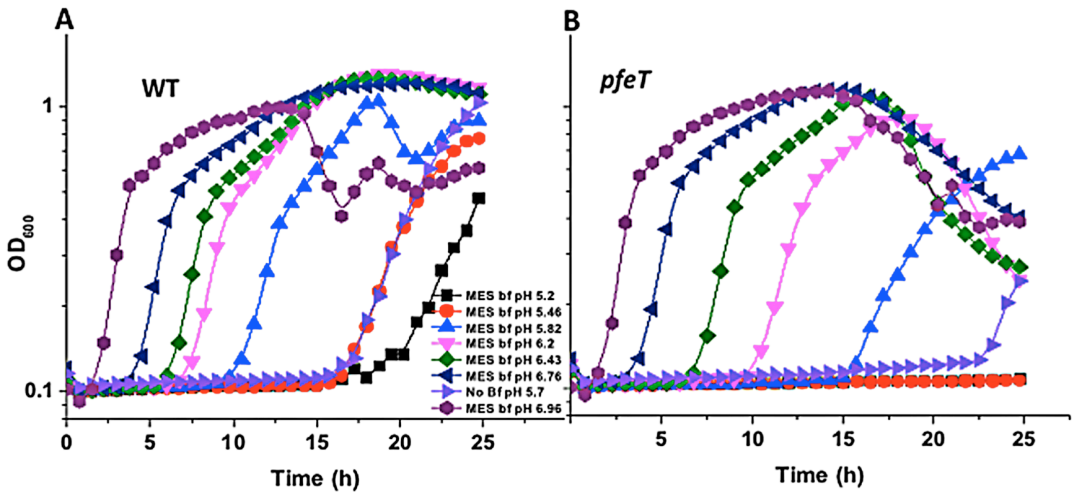

FIG. 3.14) Iron intoxication of the *pfeT* null strain is exacerbated at low pH.

(A) pH dependence of growth inhibition for WT in LBC medium amended with 4 mM $FeSO_4$ (added from a 100 mM stock prepared in 0.1 N HCl). LBC medium was either unbuffered (No Bf; ▶) leading to a final pH of 5.7, or buffered with 60 mM MES to final pHs ranging from 5.2 (■, longest lag) to ~ 7 (●, shortest lag). **(B)** pH dependence of growth inhibition for the *pfeT* mutant in LBC medium (as for panel A).

3.3.8 Mn^{2+} suppresses Fe^{2+} intoxication.

As noted above (Fig. 3.8), the *pfeT* null mutant cannot grow under conditions of Fe^{2+} intoxication (4 mM $FeSO_4$ in LBC medium) whereas WT grows but only after an extended lag phase. The molecular origins of the growth inhibition are not yet understood but presumably reflect high intracellular levels of Fe^{2+} that interfere with essential cell processes. One likely target of Fe^{2+} toxicity is interference with the proper metallation of enzymes requiring other metals as cofactors (35,38). In general, Fe^{2+} and Mn^{2+} are both maintained at homeostatic levels of ~ 10^{-5} to 10^{-4} M in the cytoplasm, as judged by the metal-binding affinity of their cognate uptake regulators (Fur and MntR), and both ions compete for metallation of many

mononuclear metalloenzymes (39). Thus, we hypothesized that inhibition of one or more Mn^{2+}-dependent enzymes could contribute to Fe^{2+} toxicity. Consistent with this notion, supplementation of LBC medium with as little as 2.5 μM Mn^{2+} enabled growth of the *pfeT* mutant strain with a lag phase only slightly longer than for WT under comparable conditions, and both the WT and the *pfeT* mutant strains responded to elevated Mn^{2+} with a substantial reduction in growth lag (Fig. 3.15A & B).

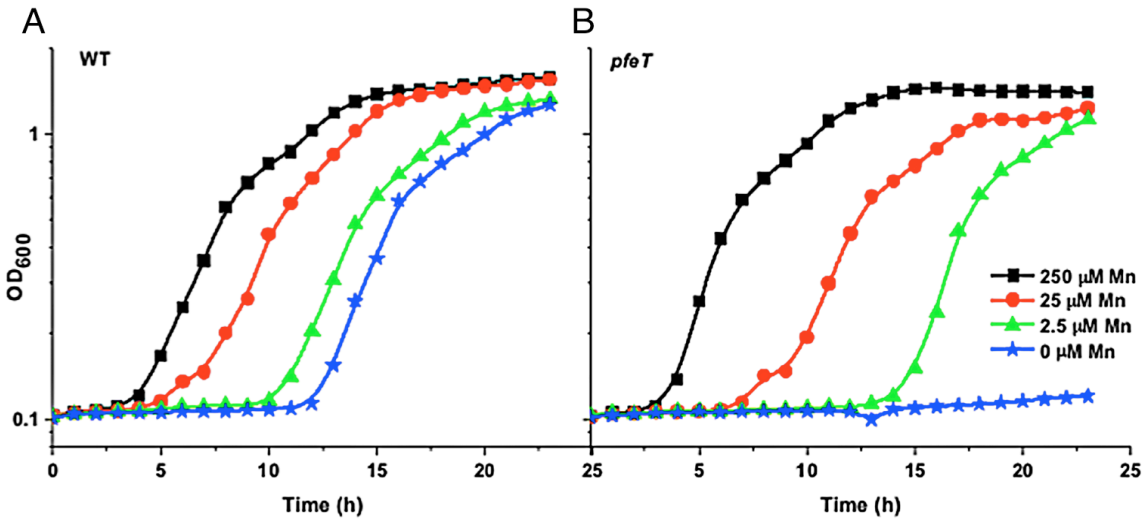

FIG. 3.15) Iron intoxication of the *pfeT* null strain is abrogated by Mn^{2+}.

(A) WT cells were grown in LBC medium with 4 mM $FeSO_4$ with additional Mn^{2+} added. **(B)** *pfeT* mutant cells were grown in LBC medium with 4 mM $FeSO_4$ and Mn^{2+} added at the concentrations indicated (as for panel A). Growth curves are an average of four cultures monitored in parallel (technical replicates), and the results are representative of experiments performed at least three times.

3.3.9 A *pfeT* null mutant is more resistant to Mn^{2+} intoxication

In our initial survey of metal sensitivity (Fig. 3.1A), we noted that a *pfeT* null mutant was slightly more resistant to $MnCl_2$ as measured in a disk diffusion

assay. Consistent with this observation, in LB medium supplemented with 2 mM $MnCl_2$ WT is unable to grow, while the *pfeT* null mutant does grow, albeit with a lag phase of ~8 h. Similarly, the lag phase for growth in LB supplemented with 1 mM $MnCl_2$ is reduced ~2-fold in a *pfeT* mutant strain (Fig. 3.16A&B). As demonstrated previously, an *mntR* mutant strain constitutively expresses both the MntH and the MntABC Mn^{2+} uptake systems and is highly sensitive to Mn^{2+} intoxication (40). In an *mntR* mutant background, deletion of the gene encoding PfeT also improves fitness (Fig. 3.16C & D). These phenotypes suggest that deletion of *pfeT* protects against Mn^{2+} intoxication, presumably by leading to an elevation of intracellular Fe^{2+} levels even in LB medium lacking iron supplementation. This is consistent with the increased SN sensitivity observed in unsupplemented LB medium (Fig. 3.2 and Fig. 3.3A). Furthermore, this supports a model in which Mn^{2+} intoxication results from the competitive inhibition of one or more Fe^{2+}-dependent processes or enzymes in the cell. Indeed, recent results in *E. coli* have identified ferrochelatase as a target of Mn^{2+} toxicity in that organism (41).

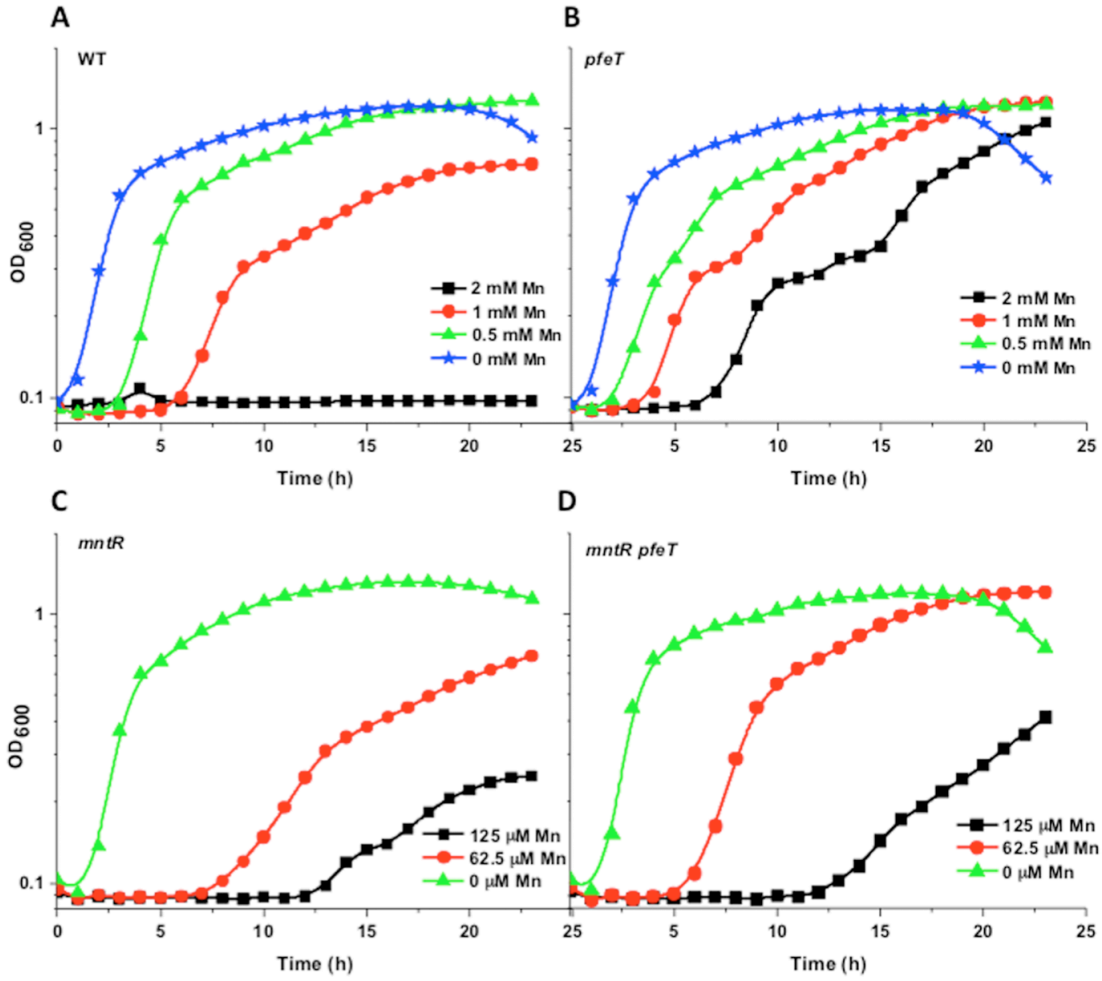

FIG. 3.16) Deletion of *pfeT* increases resistance to Mn^{2+} intoxication.

(A) & **(B)** Comparison of growth of WT (A) and a *pfeT* null mutant (B) in LB medium amended with additional Mn^{2+}. Growth curves are an average of at least six cultures. **(C)** & **(D)** Comparison of an *mntR* mutant (C) and an *mntR pfeT* double mutant (D) in the presence of additional Mn^{2+}. Growth curves are an average of at least six cultures.

3.3.10 PerR regulated genes critical for protection against Fe^{2+} intoxication

To determine if other PerR regulon members also play a role in resistance to Fe^{2+} intoxication, we analyzed the epistatic interactions between

perR, *pfeT* and other PerR regulon members (Fig. 3.17). As expected, under conditions of Fe^{2+} intoxication (LBC medium with 4 mM $FeSO_4$), WT grows (albeit after a long lag), the *pfeT* mutant is unable to grow, and this defect is complemented by ectopic expression of *pfeT*. Note that in this experiment, IPTG was not included in the preculture, so the induction of *pfeT* occurs concomitant with exposure to high Fe^{2+} and this eventually enables adaptation of the surviving cells and outgrowth of the culture. This is comparable with what happens in the WT strain, where *pfeT* expression is also induced by high Fe^{2+} conditions (data not shown).

Remarkably, the *perR* null mutant grows very well under these conditions with only a ~ 1 h lag (Fig. 3.17A). We conclude that derepression of the PerR regulon greatly enhances resistance to Fe^{2+} intoxication, consistent with the results observed by spot dilution (Fig. 3.10B). The resistance of the *perR* null mutant to Fe^{2+} intoxication is due almost entirely to derepression of PfeT as evidenced by comparison of the *perR* null strain and the *perR pfeT* double mutant (Figs 3.17A and 7B). We infer that the relatively high level of survival and rapid adaptation of the *perR* mutant strain is likely due to the presence of comparatively high levels of PfeT in the precultures. This is consistent with the observation that induction of PfeT from an IPTG-inducible promoter prior to challenge also greatly reduces cell killing (Fig. 3.9).

In addition to PfeT, derepression of other members of the PerR regulon also provides some advantage to cells experiencing Fe^{2+} intoxication. The lag

phase of the *perR* null mutant (~ 1 h) is increased in strains additionally containing mutations in *mrgA* (~ 1.5 h), *katA* (~ 3 h) or both *katA* and *ahpCF* (~ 6 h), but in all cases, these strains still grow better than WT (~ 10 h). These results indicate that PfeT plays the primary role in protection against Fe^{2+} intoxication, whereas other PerR regulon members play a secondary role. This is further apparent from comparison of the *pfeT* strain (unable to grow) and the *pfeT perR* double mutant (growth after a lag of > 13 h). This rescue of the *pfeT* growth defect is lost in the *perR pfeT mrgA* triple mutant (Fig. 3.17A) and in the *perR pfeT katA ahpCF* quadruple mutant (Fig. 3.17B). In the absence of the PfeT efflux ATPase, the MrgA mini-ferritin (Dps family protein) presumably contributes to fitness by virtue of its ability to sequester iron.

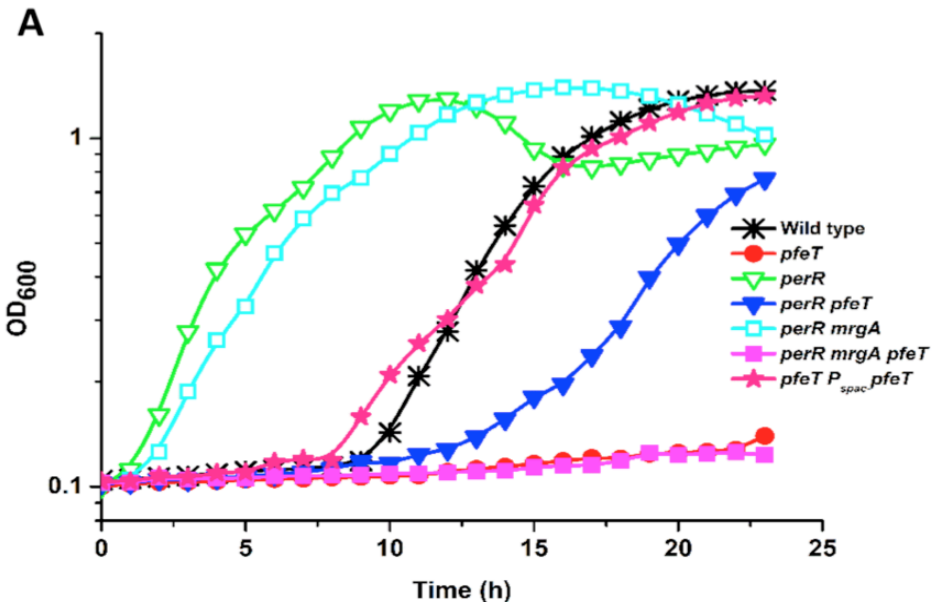

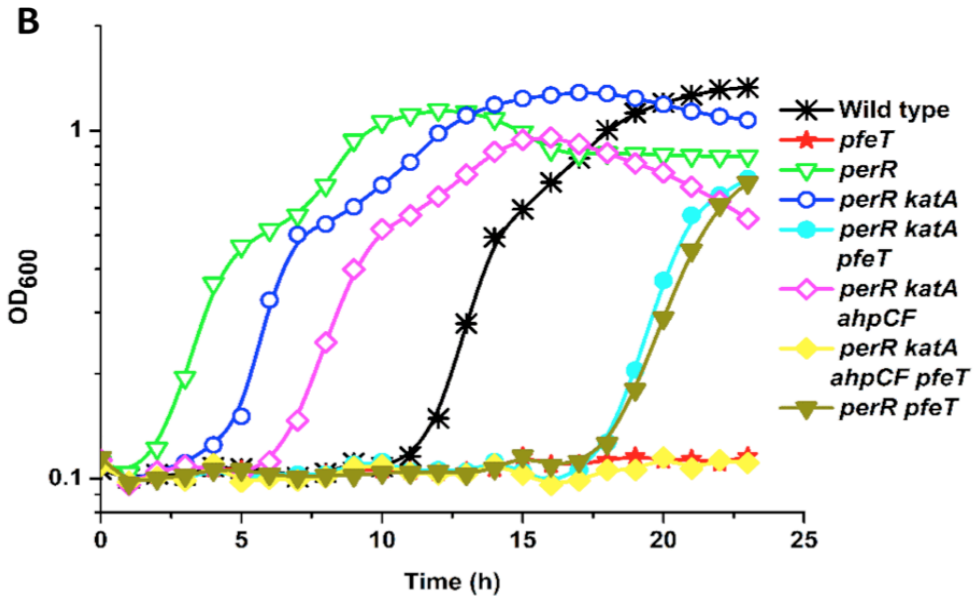

FIG. 3.17) Multiple PerR-regulated genes contribute to growth under iron intoxication.

(A) Strains were grown in LBC containing 4 mM $FeSO_4$. The *perR* null mutant is highly resistant to iron intoxication due primarily to PfeT, and secondarily to MrgA. Growth curves are an average of at least four cultures, and the results shown are representative of at least three biological replicates. **(B)** PerR-regulated genes involved in H_2O_2 detoxification play a comparatively minor role in resistance to iron intoxication. Strains were grown in LBC containing 4 mM $FeSO_4$.The increased fitness of the *perR* mutant (relative to WT) is not eliminated even in strains lacking both catalase (*katA*) and alkyl hydroperoxide reductase (*ahpCF*). Growth curves are an average of three cultures.

3.3.11 PerR regulated genes critical for protection against H_2O_2 stress

The PerR regulon is widely appreciated for its role in inducible resistance to H_2O_2 (14,15). We considered the possibility that adding high concentrations of Fe^{2+} to aerobic LBC medium might lead to the generation of reactive oxygen species (ROS) (42) and that Fe^{2+} intoxication might simply be a manifestation of stress imposed by ROS. However, direct measurements of H_2O_2 levels in our LBC medium with and without amendment with 4 mM $FeSO_4$

failed to reveal a significant increase; under all measured conditions, the ambient levels of H_2O_2 were in the range of 2–3 μM, consistent with prior measurements of aerobic LB medium (43). Under these conditions, excess Fe^{2+} likely catalyzes the decomposition of H_2O_2 (Fenton reaction) with formation of hydroxyl radicals, which are quenched by the organic-rich LBC medium.

Bacterial killing by elevated levels of H_2O_2 is exacerbated by an increase in intracellular labile iron pools (44). We therefore anticipated that PfeT, which is known to be induced by H_2O_2 (5,20,45), might be an important resistance determinant for H_2O_2. To determine if PfeT plays a significant role in H_2O_2 resistance, we measured sensitivity using a disk diffusion assay in a series of mutant strains lacking PfeT or other members of the PerR regulon, as well as the σ^B-regulated Dps protein that functions, like MrgA, as an Fe-sequestration protein (Fig. 3.18). The results indicate that PfeT plays a comparatively minor role in H_2O_2 resistance, with small effects noted only in the *dps* null mutant and the *katA ahpCF mrgA* triple mutant backgrounds. The data further highlight the importance of PerR-regulated genes in inducible H_2O_2 resistance and demonstrate, as previously reported (20), that catalase is the primary determinant for resistance to high levels of H_2O_2. Together, these results indicate that Fe^{2+} intoxication and H_2O_2 intoxication, although physiologically linked, are distinct stresses with different proteins playing the most central roles in adaptation. Indeed, PfeT can efficiently protect cells

against Fe^{2+} intoxication even in cells lacking the major H_2O_2 detoxification enzymes, KatA and AhpCF (Fig. 3.17B; e.g. compare *perR katA ahpCF* versus *perR katA ahpCF pfeT*).

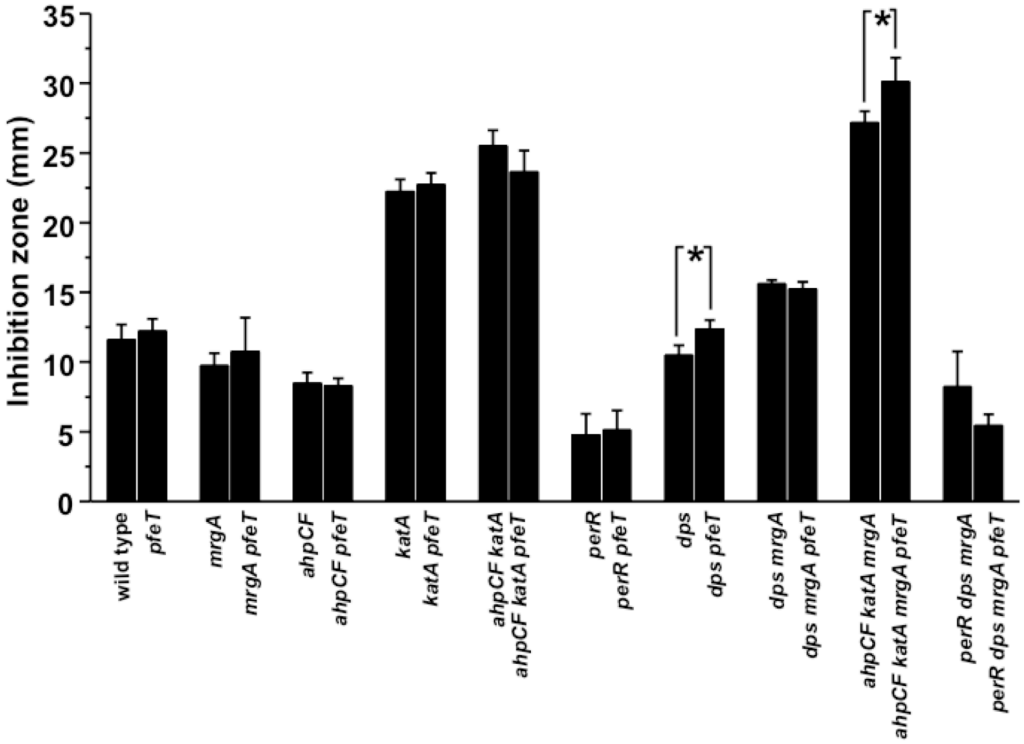

FIG. 3.18) Disk diffusion assay of WT and mutant strains with 0.48 M H_2O_2.

The zone of inhibition is expressed as the total diameter of the clearance zone minus the diameter of filter paper disk (6.5 mm). The means and SE from at least three biological replicates are reported. Significant differences were determined by two-tailed *t* test.*, $p < 0.01$. These results indicate that catalase (KatA) is the major resistance determinant that protects against high levels of H_2O_2 with AhpCF and MrgA playing second role. In contrast with the results for Fe^{2+} intoxication, PfeT plays a comparatively minor role in H_2O_2 resistance under these conditions.

3.3.12 Genetic interactions between PfeT and the Fur regulon: PfeT and Fur cooperate to prevent Fe intoxication

Next, we investigated the genetic interactions between PfeT, a PerR-regulated iron efflux system, and the Fur-regulated iron uptake systems. As

we anticipated that the *fur* mutation would exacerbate the growth defect of the *pfeT* null mutant, we reduced the level of iron intoxication by using LBC medium amended with 3.5 mM $FeSO_4$ (Fig. 3.8). Whereas WT grows well in this medium, both the *pfeT* and *fur* single mutants grow after an ~ 5 h lag (Fig. 3.19). These effects are additive, with the *pfeT fur* double mutant growing after a lag of over 10 h.

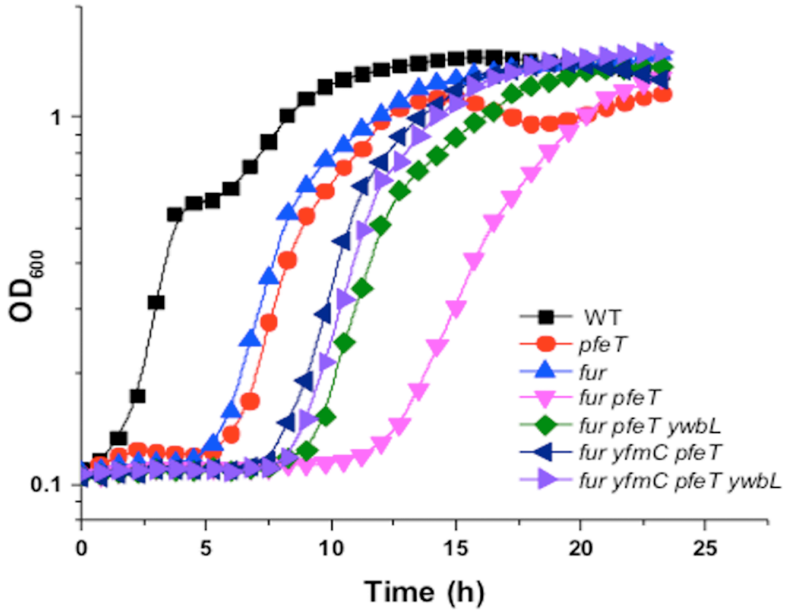

FIG. 3.19) The Fur repressor cooperates with PfeT to prevent Fe intoxication.

WT and mutant strains were grown in LBC amended with 3.5 mM $FeSO_4$, a concentration that is growth inhibitory but still allows growth of the *pfeT* mutant.

To test the hypothesis that the *fur* mutation was acting by derepressing iron uptake functions, we mutated the genes encoding the major iron-citrate uptake system (encoded by the *yfmC* operon) and the elemental iron uptake system (encoded by the *ywbL* operon; also known as *efeU*; (46)), shown

previously to be the major iron uptake pathways in LB medium (16). Note that *B. subtilis* 168 strains do not make a functional bacillibactin siderophore due to the presence of an *sfp*^{0} mutation (47). The growth results indicate that elimination, either individually or in combination, of the iron-citrate and the elemental iron uptake pathways improves growth, but these two systems do not completely account for the effect of the *fur* mutation on iron sensitivity (Fig. 3.19).

The roles of the PerR and Fur regulators in iron homeostasis are also apparent using spot dilution assays (Fig. 3.20). In this assay, the *fur* and *pfeT* null mutants both form very small colonies on LB medium amended with 2 mM $FeSO_4$, whereas the *pfeT fur* double mutant has a low EOP under these conditions, and forms small colonies on plates containing 1 mM $FeSO_4$. These additive effects are consistent with the notion that iron intoxication is most severe in cells that are unable to repress iron uptake, due to the *fur* mutation, and also lack PfeT. In contrast, the *perR* null mutant (but not the *perR pfeT* double mutant) has a high EOP even on plates with 3 mM $FeSO_4$, a condition that restricts the growth of WT.

It is notable that the *perR* null mutant displays a small colony size on the unamended LB medium, and better growth on medium amended with 1 mM $FeSO_4$. This is consistent with prior results demonstrating that this strain is growth-restricted due to iron sequestration by the abundant catalase hemoprotein and repression of iron uptake by the Fur protein which, under

these conditions, is mismetallated by Mn^{2+} (16,19). Although derepression of PfeT, in a *perR* null mutant, increases fitness in high iron (e.g. 3 mM, Fig. 3.20), it does not contribute to the iron limita- tion that characterizes the *perR* mutant strain. As shown previously, both the *perR* and *perR pfeT* mutants are very slow growing on standard LB medium (containing ~ 10 μM iron) (16). In contrast, deletion of either or both of *katA* and *fur* dramatically relieve the iron limitation phenotype (16). We conclude that derepression of PfeT does not

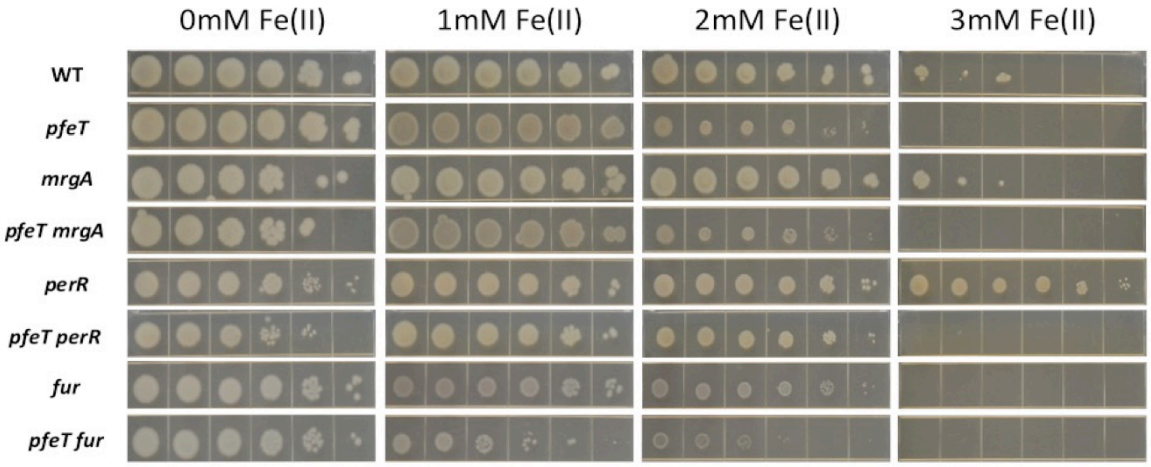

FIG. 3.20) Contributions of the PerR and Fur regulons to growth under iron stress monitored by a spot dilution assay.

Mid-logarithmic phase (OD_{600} ~0.4) cultures of the indicated strains were sequentially diluted by 10-fold (from undiluted to 10^{-5} in each series) and 3 μl were spotted on LB medium amended with the indicated concentration of $FeSO_4$ (added from a 100 mM stock in 0.1N HCl). Note that the WT and *pfeT* results are also shown (rearranged) in Fig. 3.1C.

contribute significantly to iron deprivation, even when it is constitutively expressed in a *perR* null mutant. This is likely due to the relatively low affinity of this efflux pump for its substrate ($K_{1/2}$ ~ 0.52 mM, Fig. 3.5B), Fe^{2+}, which is

calibrated to efficiently pump iron out of the cell under conditions of excess, but is of sufficiently weak affinity so as not to deplete the cytosol of iron.

3.3.13 PfeT homologs are implicated in bacterial virulence

PfeT is the first member of the P_{1B}-type ATPases implicated in iron efflux. Within P_{1B}-type ATPases, it has been possible to predict metal selectivity based on primary amino acid sequence and, in particular, the presence of specific metal-coordinating residues (24). PfeT resides within the P_{1B4} subgroup of transporters that have been generally considered to function as Co^{2+} efflux pumps. Indeed, as shown here, PfeT can be activated by Co^{2+} *in vitro* (Fig. 3.5C) and can confer Co^{2+} resistance when expression is artificially induced (Fig. 3.6). However, this does not appear to be its normal physiological role. Several other P_{1B4} family ATPases have been characterized and representatives of this subfamily have been implicated in virulence for some bacterial pathogens. In *Listeria monocytogenes*, a PfeT homolog (FrvA) was suggested to enhance resistance to heme and shown to be important for virulence in mice (48). In this same study, however, it was also noted that an *frvA* deletion strain had increased sensitivity to $FeSO_4$ in a zone of inhibition assay. PfeT homologs have also been studied in *Mycobacterium* spp. In this case, one homolog (CtpJ) is inducible by and confers resistance to Co^{2+} (27). However, the other homolog, and likely PfeT ortholog, CtpD was induced by redox stress and was shown to be important for survival in the mouse lung and

for virulence (27). We suggest, based on the results herein, that CtpD may function physiologically as an iron exporter, a hypothesis that is currently under investigation.

3.4 Conclusions

Although iron uptake mechanisms have been studied since the 1930s, as recently as 1991 Joe Neilands could write that 'There seems to be no known biological mechanism for the excretion of iron, uptake of the element being regulated at the membrane level in all species studied (49). Iron excretion mechanisms were first appreciated in mammals where ferroportin was identified as a key iron exporter (50). In *E. coli*, the FieF cation diffusion facilitator has been implicated physiologically in iron efflux (51), but most detailed characterization has focused on the ability of this system to transport Zn^{2+} (52,53). In addition, an ABC transporter has been proposed to function in iron efflux (54). In *Salmonella* Typhimurium, a major facilitator superfamily pump designated IceT was shown to efflux iron citrate and contributes to resistance under iron stress conditions (55,56). Finally, MbfA proteins containing both a ferritin like domain and a membrane-localized domain related to CCC1 family eukaryotic vacuolar metal transporters have been shown to efflux iron in *Agrobacterium tumefaciens* (57) and *Bradyrhizobium japonicum* (58). Thus, there is an emerging realization that many bacteria likely have mechanisms to efflux excess iron, analogous to the long-known

mechanisms for resistance to other metals.

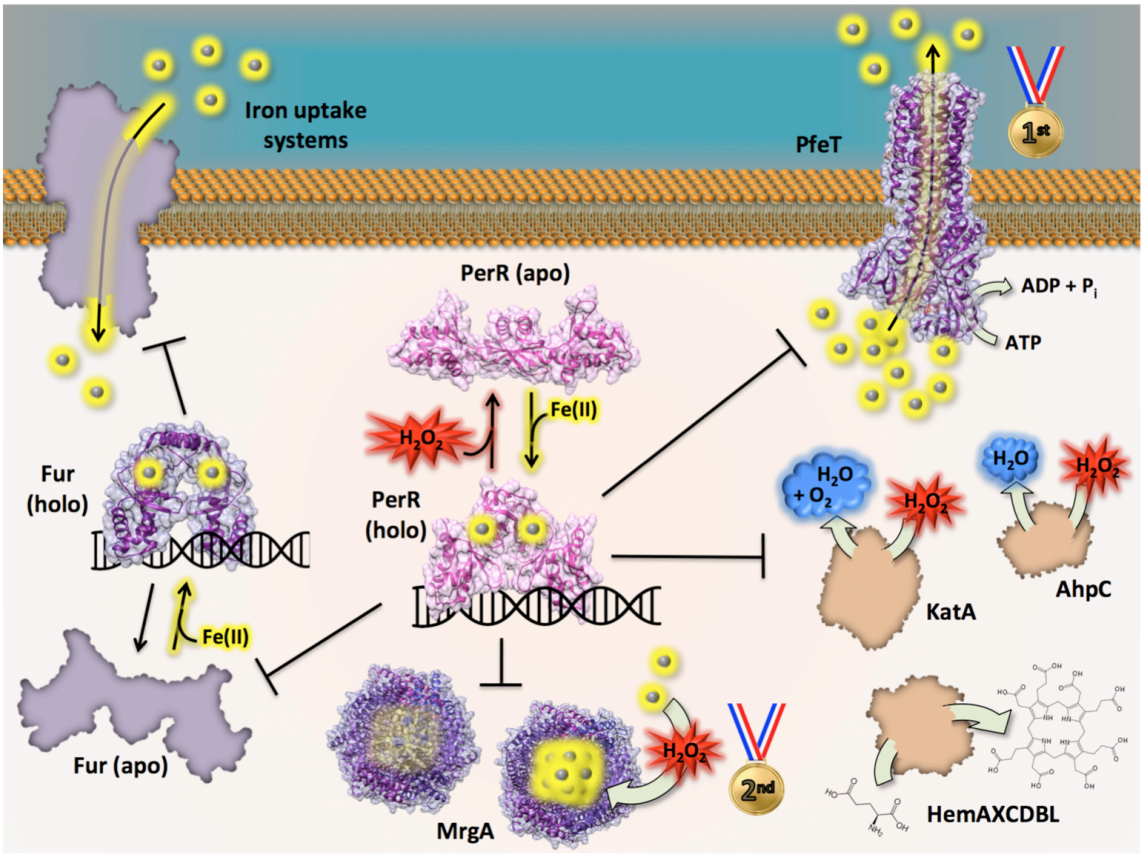

FIG. 3.21) Schematic summary of the contributions of the PerR and Fur regulons to growth under iron intoxication.

The holo-form of PerR (PDB code: 3F8N) is shown with Fe^{2+} (yellow spheres) bound at its metal sensing site (PerR:Zn,Fe). In this form, PerR binds to DNA, repressing its target genes. H_2O_2 oxidizes PerR:Zn,Fe leading to derepression of the PerR regulon. PerR-regulated genes encode proteins whose primary role relates to H_2O_2 detoxification (KatA, AhpCF and heme biosynthesis functions; orange) and those that directly impact iron homeostasis (PfeT and MrgA; purple). PfeT is induced both by H_2O_2 stress and, independently, by high Fe^{2+} (not shown). MrgA (here represented using the structure of the ortholog from *E. coli*, Dps, PDB code: 1DPS) is a dodecameric mini-ferritin that sequesters iron in the presence of H_2O_2. PfeT (here represented by the structure of the *Legionella pneumophila* copper P_{1B}-type ATPase, PDB code: 4BBJ) is a P_{1B4}-type ATPase that pumps out excess intracellular iron, thus protecting the cell from its toxic effects. PerR also regulates the expression of the ferric uptake repressor, Fur, which in its holoform (here modeled on *Streptomyces coelicolor* Zur, PDB code: 3MWM) represses the expression of iron import functions (namely, YwbLMN and YfmCDEF). With respect to Fe^{2+} intoxication, PfeT is the primary resistance determinant (1st place medal), whereas MrgA places a secondary role (2nd place).

The studies described herein demonstrate that *B. subtilis* PfeT can be added to the list of transporters that function physiologically to efflux iron from bacterial cells. Our results demonstrate that Fur, by regulation of iron import, and PfeT, required for iron export, cooperate to allow cells to survive and ultimately grow under iron intoxication conditions (Fig. 3.21). MrgA, a mini-ferritin that sequesters iron, plays a secondary role as revealed in a *perR* null strain that is derepressed for *mrgA* expression. Our results also highlight the complex interactions between iron and manganese homeostasis: increased intracellular iron (in a *pfeT* null strain) leads to greater tolerance to Mn^{2+} and, conversely, even micromolar levels of Mn^{2+} protect cells against the effects of iron intoxication. In ongoing studies, we seek to better understand how iron intoxication perturbs cell physiology and ultimately limits growth.

3.5 Experimental procedures

Bacterial strains and growth conditions

Bacillus subtilis strains used are derivatives of strain CU1065 and are shown in Table 3.1. *E. coli* strain DH5α was used for standard cloning procedures. Bacteria were grown in LB medium (10 g tryptone, 5 g yeast extract and 5 g l^{-1} NaCl) at 37°C with vigorous shaking or on solid LB containing 1.5% Bacto agar with appropriate selection. Where indicated, LBC medium (LB medium amended with 1 g l^{-1} of citrate trisodium dihydrate; 3.4 mM) was used. Ampicillin (*amp*; 100 μg ml^{-1}) was used to select *E. coli* transformants. For *B.*

subtilis, antibiotics used for selection were: spectinomycin (*spc*; 100 μg ml^{-1}), kanamycin (*kan*; 15 μg ml^{-1}), chloramphenicol (*cat*; 10 μg ml^{-1}), tetracycline (*tet*; 5 μg ml^{-1}), neomycin (*neo*;10 μg ml^{-1}), and macrolide lincosoamide-streptogramin B (MLS; contains 1 μg ml^{-1} erythromycin and 25 μg ml^{-1} lincomycin). For iron intoxication experiments, 100 mM $FeSO_4$ stocks (except where indicated) were prepared in 0.1 N HCl, and iron was added to the indicated concentrations. OD_{600} readings were taken on a Spectronic 21 spectrophotometer. H_2O_2 concentrations in the growth medium were determined using the Amplex red/horseradish peroxidase method as described (43).

Strain constructions

Gene deletions were generated by replacing the coding region with an antibiotic resistance cassette using long flanking homology PCR (LFH-PCR) followed by DNA transformation as previously described (59). Chromosomal DNA was used for transformation as described previously (60). The IPTG-inducible constructs were generated using vector pPL82 (61). PCR products were amplified from *B. subtilis* CU1065 chromosomal DNA, digested with endonucleases and cloned into pPL82. pPL82 contains a chloramphenicol resistance cassette, a multiple cloning site downstream of the $P_{spac(hy)}$ promoter, and the *lacI* gene between the up- and downstream fragments of the *amyE* gene. Primer pairs used for PCR amplification are 6170/6171 for

pfeT (Table 3.2). The sequences of the inserts were verified by DNA sequencing (Cornell DNA sequencing facility). Plasmids were linearized by ScaI and used to transform *B. subtilis*, where they integrated into the *amyE* locus.

Measurement of maximal permissive concentrations for growth using disk diffusion assays

Disk diffusion assays were performed as described (62). Briefly, strains were grown to an OD_{600} of 0.4. A 100 μl aliquot of these cultures was mixed with 4 ml of 0.75% LB soft agar (kept at 50°C) and directly poured onto LB plates (containing 15 ml of 1.5% LB agar). The plates were dried for 10 min in a laminar airflow hood. Filter paper disks containing 10 μl of the chemicals to be tested were placed on the top of the agar, and the plates were incubated at 37°C overnight. The overall diameter of the inhibition zones was measured along two orthogonal lines. Plates were imaged using a Chemi DocTM MP Imaging System (Bio-Rad) with white trans illumination. For IPTG-treated cells, IPTG was added to both the soft agar and the plates to a concentration of 0.1 mM. Unless otherwise noted, 10 μl of the following chemicals was used in the disk diffusion assays: 100 mM $ZnCl_2$, 100 mM $MnCl_2$, 10 mM $CdCl_2$, 1 M $FeSO_4$, 1 M $FeCl_3$, 50 mM $CoCl_2$. For SN sensitivity tests, $FeSO_4$ or 2, 2′-dipyridyl (DP) was added to both the soft agar and the plates to a concentration of 0.1 mM, 5 mg ml^{-1} SN solution in dimethyl sulfoxide (DMSO)

was added to the filter paper disks.

Measurement of growth using Bioscreen growth analyzer

Strains were grown to an OD_{600} of 0.4 in LB media. Two microliters of culture was inoculated to 200 μl LB or LBC containing $FeSO_4$ and/or $MnCl_2$ in a Bioscreen 100-well microtiter plate. As Fe^{2+} rapidly oxidizes to Fe^{3+} in aerobic solutions generating insoluble ferric hydroxides, unless oth- erwise noted, 1 g l^{-1} citrate trisodium dihydrate was added to LB media containing $FeSO_4$ (LBC medium). Growth was measured spectrophotometrically (OD_{600}) every 15 min for 24 h using a Bioscreen C incubator (Growth Curves USA, Piscataway, NJ) at 37°C with continuous shaking. For SN susceptibility studies, WT (CU1065) and Δ*pfeT* were grown in LB medium, LB containing 0.1 mM $FeSO_4$ or LB containing 0.1 mM DP.

Measurement of EOP and growth (colony size) by spot dilution

Strains were grown to an OD_{600} of 0.4 in LB media. For Fig. 3.1C and Fig. 3.20, serial 10-fold dilutions were made from the original culture for each strain and 3 μl aliquots were spotted on LB plates containing 0, 1, 2 or 3 mM $FeSO_4$. The plates were incubated at 37°C overnight. In this assay, an inability to grow at the highest dilutions indicates a reduced EOP. When cells can grow, they may grow at a slower rate, as is apparent from those strains and conditions where the EOP is high, but the colony size (as observed at the highest

dilutions) is reduced.

To monitor the extent of cell killing upon exposure to Fe^{2+} intoxication conditions (Fig. 3.9), cells were grown in 5 ml LBC medium with 0, 1 or 10 mM IPTG as indicated. The WT, *pfeT*, *perR*, *perR pfeT* and *pfeT* complemented strains were shocked by addition of $FeSO_4$ to a final concentration of 4 mM Fe^{2+} (from a 100 mM stock in 0.1 N HCl) when cells reached an OD_{600} ~ 0.4. One milliliter samples were taken before shock (0 min) and 30 min and 60 min after shock, washed by centrifugation (2 min at 13 000 r.p.m.) and gentle resuspension in 1 ml LB, and serially diluted in LB pre-warmed to 37°C. Three microliters of cells were spotted in each quadrant on 30 ml LB plates and left to dry before incubating at 37°C overnight. The columns are (left to right), undiluted, 10^{-1}, 10^{-2}, 10^{-3}, 10^{-4} and 10^{-5} fold dilutions of the washed cells.

To monitor cell killing and outgrowth under conditions comparable with the Bioscreen growth analyzer experiments, cells were grown in LB to an OD_{600} of ~ 0.4 and 0.5 ml of culture was inoculated into either 50 ml of LBC or LBC+4 mM Fe^{2+}. One milliliter samples were removed at time 0 (right after inoculation), 0.5, 1, 3, 6, 9, 12 and 15 h. The cells were harvested (5 min at 13 000 r.p.m.) and resuspended in LB. Viable cell counts were estimated by spotting (3 μl) of serial dilutions onto LB plates.

Protein expression and purification

DNA encoding *B. subtilis pfeT* was amplified using genomic DNA as template

and primers that introduced a Tobacco etch virus (TEV) protease site coding sequence at the amplicon 3′ ends. The PCR product was cloned into the pBAD-TOPO/His vector (Invitrogen) that introduces a $(His)_6$-tag at the carboxyl end of the protein. For PfeT-TEV-$(His)_6$ expression, the construct was introduced into *E.coli* LMG194 Δ*copA* cells (63). Cells were grown at 37°C in Terrific broth media (64) supplemented with 0.1% arabinose, 100 μg ml^{-1} ampicillin and 20 μg ml^{-1} kanamycin. Affinity purification of membrane proteins and removal of the $(His)_6$-tag was performed as previously described (27). Solubilized lipid/detergent micellar forms of PfeT proteins were stored at −20°C in buffer C containing 25mM Tris, pH8.0, 50mM NaCl, 0.01% n-dodecyl-β-d- maltopyranoside, 0.01% asolectin and 20% glycerol until use. The $(His)_6$-tag was removed from the PfeT-$(His)_6$ fusion protein by treatment with $(His)_6$-tagged TEV protease (65) at 5:1 PfeT:TEV weight ratio for 1 h at 22°C in buffer C plus 1 mM Tris(2-carboxyethyl)phosphine (TCEP) and 0.5 mM EDTA. TEV-$(His)_6$ was removed by affinity purification with Ni-NTA resin. Protein determinations were performed in accordance to Bradford (66). Protein purity was assessed by Coomassie brilliant blue staining of overloaded SDS-PAGE gels and by immunostaining of Western blots with rabbit anti-$(His)_6$ polyclonal primary antibody (GenScript) and goat anti-rabbit IgG secondary antibody coupled to horseradish peroxidase. Prior to ATPase activity determinations, proteins (1 mg ml^{-1}) were treated with 0.5 mM EDTA and 0.5 mM tetrathiomolybdate for 45 min at room temperature. Chelators were

removed using Ultra-30 Centricon (Millipore) filtration devices.

ATPase assays

These were performed at 37°C in a medium containing 50 mM Tris (pH 7.4), 50 mM NaCl, 3 mM $MgCl_2$, 3 mM ATP, 0.01% asolectin, 0.01% n-dodecyl-β-d-maltopyranoside, 2.5 mM TCEP, 40 μg ml^{-1} purified protein, and freshly prepared transition metal ions at the desired concentrations. Fe^{3+} was added as $FeCl_3$, Cu^{2+} as $CuSO_4$ and in both cases TCEP was not included in the assay media. Cu^{+} was obtained by including TCEP with $CuSO_4$ salt. Fe^{2+} and Zn^{2+} were included in the assay media as the sulfate salts, whereas Co^{2+}, Ni^{2+} and Mn^{2+} were included as their chloride salts. ATPase activity was stopped after 20 min incubation and released P_i determined (67). ATPase activity measured in the absence of transition metals was subtracted from plotted values. Curves of ATPase activity versus metal concentrations were fit to $v = V_{max}$ [metal]/ ([metal] + $K_{1/2}$). The reported standard errors for V_{max} and $K_{1/2}$ are asymptotic standard errors reported by the fitting software KaleidaGraph (Synergy).

Measurements of intracellular metal ion concentrations by ICP-MS

Cells were grown in LBC medium to an OD_{600} of 0.4 with or without 1 mM IPTG and then shocked with 4 mM $FeSO_4$. Four milliliter samples were taken before shock and at several time points after shock. Samples were harvested

and washed twice with phosphate buffered saline (PBS) buffer containing 0.1 M EDTA followed by two chelex-treated PBS buffer only washes. Cells were resuspended in 400 μl of chelex-treated PBS buffer containing 75 mM NaN_3 to induce autolysis (68) and 1% Triton X-100, and incubated at 37°C for 90 min. Samples were centrifuged and a Bradford assay was carried out with 10 μl of the sample. Then, 600 μl of 5% HNO_3 with 0.1% (v/v) Triton X-100 was added to the samples that were boiled at 95°C for 30 min. After centrifuging the samples again, the supernatant was diluted for inductively coupled plasma mass spectrometry (ICP-MS) measurements. All samples were analyzed using a Perkin-Elmer ELAN DRC II ICP-MS, equipped with a Microflow PFA-ST nebulizer. The DRC mode was used with ammonia as the reaction gas. Gallium was added at 50 ppb as an internal standard by an in-line mixing block. The total concentration of ions was calculated relative to the protein content of the sample to determine the mean metal concentration (expressed as ppm by weight).

Table 3.1) Strains and plasmids used in this study

STRAIN	GENOTYPE	REFERENCE
CU1065	W168 *attSP*β *trpC2*	Laboratory stock
HB17802	CU1065 *pfeT*::*spc*	This work
HB17803	CU1065 *mrgA*::*mls pfeT*::*spc*	This work
HB16034	CU1065 *mrgA*::*mls*	This work
HB2621	CU1065 *mntR*::*kan*	(Guedon et al. 2003)
HB17806	CU1065 *mntR*::*kan pfeT*::*spc*	This study
HB11395	CU1065 *cadA*::*kan czcD*::*tet*	(Ma et al. 2014)
HB17808	CU1065 *cadA*::*kan czcD*::*tet pfeT*::*spc*	This study

HB17814	CU1065 *amyE*:: P_{spac}- *pfeT* (*cat*)	This study
HB17818	CU1065 *cadA*::*kan pfeT*::*spc*	This study
HB17819	CU1065 *czcD*::*tet pfeT*::*spc*	This study
HB17821	CU1065 *ahpCF*::*cat*	This study
HB17822	CU1065 *ahpCF*::*cat pfeT*::*spc*	This study
HB16005	CU1065 *katA*::*tet*	This study
HB11393	CU1065 *cadA*::*kan*	(Ma et al. 2014)
HB11394	CU1065 *czcD*::*tet*	(Ma et al. 2014)
HB17829	CU1065 *ahpCF*::*cat katA*::*tet*	This study
HB17830	CU1065 *ahpCF*::*cat katA*::*tet pfeT*::*spc*	This study
HB17831	CU1065 *katA*::*tet pfeT*::*spc*	This study
HB17832	CU1065 *perR*::*tet pfeT*::*spc*	This study
HB17833	CU1065 *cadA*::*kan amyE*:: P_{spac}- *pfeT* (*cat*)	This study
HB9703	CU1065 *perR*::*tet*	(Lee & Helmann. 2006)
HB7360	CU1065 *fur*::*kan*	(Smaldone et al. 2012)
HB16004	CU1065 *dps*::*neo*	This study
HB17842	CU1065 *dps*::*neo mrgA*::*mls*	This study
HB17843	CU1065 *ahpCF*::*cat katA*::*tet mrgA*::*mls*	This study
HB17844	CU1065 *ahpCF*::*cat katA*::*tet mrgA*::*mls pfeT*::*spc*	This study
HB17845	CU1065 *amyE*:: P_{spac}- *pfeT* (*cat*) *cadA*::*kan czcD*::*tet*	This study
HB17846	CU1065 *pfeT*::*spc fur*::*kan*	This study
HB17848	CU1065 *pfeT*::*spc dps*::*neo*	This study
HB17851	CU1065 *pfeT*::*spc dps*::*neo mrgA*::*mls*	This study
HB17852	CU1065 *pfeT*::*spc amyE*::P_{spac}- *pfeT*	This study
HB17853	CU1065 *pfeT*::*spc dps*::*neo mrgA*::*mls perR*::*tet*	This study
HB17854	CU1065 *dps*::*neo mrgA*::*mls perR*::*tet*	This study
HB17855	CU1065 *amyE*:: P_{spac}- *pfeT* (*cat*) *czcD*::*tet*	This study
HB17862	CU1065 *perR*::*tet mrgA*::*mls*	This study
HB17863	CU1065 *perR*::*tet mrgA*::*mls pfeT*::*spc*	This study
HB5612	CU1065 *yfmC*::*mls*	(Ollinger et al. 2006)
HB17867	CU1065 *yfmC*::*mls pfeT*::*spc*	This study
HB17868	CU1065 *fur*::*kan yfmC*::*mls*	This study
HB17869	CU1065 *fur*::*kan yfmC*::*mls pfeT*::*spc*	This study
HB11457	CU1065 *fur*::*kan pfeT*::*spc ywbL*::*cat yfmC*::*mls*	This study
HB11459	CU1065 *fur*::*kan pfeT*::*spc ywbL*::*cat*	This study
HB14110	CU1065 *katA*::*mls*	(Faulkner et al. 2012)
HB17878	CU1065 *katA*::*mls perR*::*tet*	This study
HB17879	CU1065 *katA*::*mls perR*::*tet pfeT*::*spc*	This study
HB17880	CU1065 *perR*::*tet katA*::*mls ahpCF*::*cat*	This study
HB17881	CU1065 *perR*::*tet katA*::*mls ahpCF*::*cat pfeT*::*spc*	This study
HB17882	CU1065 *katA*::*mls ahpCF*::*cat*	This study
HB17883	CU1065 *katA*::*mls ahpCF*::*cat pfeT*::*spc*	This study

HB17884	CU1065 *katA*::*mls pfeT*::*spc*	This study
PLASMID	**DESCRIPTION**	**REFERENCE**
pDG1726	Source for *spc* resistance gene	(Guérout-Fleury et al. 1995)
pGEM-cat	Source for *mls* resistance gene	Laboratory stock
pPL82	Expression of gene under P_{spac} promoter	(Quisel et al. 2001)
pGG101	pPL82-*pfeT*	This study
pBAD	Arabinose-induced expression of protein	Thermo-Fisher

Table 3.2) Primer oligonucleotides

NUMBER	NAME	SEQUENCE
6148	*pfeT*-up-for	TATTAGGGTTGATTGCATGGTT
6149	*pfeT*-up-rev (*spc*)	CGTTACGTTATTAGCGAGCCAGTCCGCGTGCTGTGCCCAGTT
6150	*pfeT*-do-rev (*spc*)	CAATAAACCCTTGCCCTCGCTACGACTTTTTGCAGGCGATGGAAT
6151	*pfeT*-do-for	TTCGTGATCCGCATAGCCAA
6162	*ahpCF*- up-for	CTGCTGATCGCGCCTTATTT
6163	*ahpCF*-up-rev (*cat*)	CTTGATAATAAGGGTAACTATTGCCCCGTTTTTGAATGCTTTTGCTT
6164	*ahpCF*-do-fwd(*cat*)	GGGTAACTAGCCTCGCCGGTCCACGTCTATGGGATCAGGTGCAAC
6165	*ahpCF*-do-rev	AATTTGAACGCGAAGGCTACA
6170	*pfeT-Pspac-HindIII-fwd*	GCGAAGCTTCTCAATTAGAGAGGAGAATTC
6171	*pfeT*-Pspac-BglII-rev	CGCAGATCTGATTAGGCTGCTGGTTTTAT
1293	cat-fwd	CGGCAATAGTTACCCTTATTATCAAG
1294	cat-rev	CCAGCGTGGACCGGCGAGGCTAGTTACCC
1587	spc-fwd	GACTGGCTCGCTAATAACGTAACGTGACTGGCAAGAG
1588	spc-rev	CGTAGCGAGGGCAAGGGTTTATTGTTTTCTAAAATCTG
1449	cat-check rev	GTCTGCTTTCTTCATTAGAATCAATCC
1452	spc-check rev	CGTATGTATTCAAATATATCCTCCTCAC
7599	*pfeT-pBAD-F*	ATGAATGAACAAGTTATCGTTCAACG
7600	*pfeT-pBAD-R*	GGACTGAAAATACAGGTTTTCGCCGCTGCTTTTTAGGAGTCTTAAACCGTTTA

3.6 References

1. Bsat, N., Herbig, A., Casillas-Martinez, L., Setlow, P. and Helmann, J.D. (1998) *Bacillus subtilis* contains multiple Fur homologues: identification

of the iron uptake (Fur) and peroxide regulon (PerR) repressors. *Mol Microbiol*, **29**, 189-198.

2. Ollinger, J., Song, K.B., Antelmann, H., Hecker, M. and Helmann, J.D. (2006) Role of the Fur regulon in iron transport in *Bacillus subtilis*. *J Bacteriol*, **188**, 3664-3673.

3. Smaldone, G.T., Antelmann, H., Gaballa, A. and Helmann, J.D. (2012) The FsrA sRNA and FbpB protein mediate the iron-dependent induction of the *Bacillus subtilis lutABC* iron-sulfur-containing oxidases. *J Bacteriol*, **194**, 2586-2593.

4. Smaldone, G.T., Revelles, O., Gaballa, A., Sauer, U., Antelmann, H. and Helmann, J.D. (2012) A global investigation of the *Bacillus subtilis* iron-sparing response identifies major changes in metabolism. *J Bacteriol*, **194**, 2594-2605.

5. Helmann, J.D., Wu, M.F., Gaballa, A., Kobel, P.A., Morshedi, M.M., Fawcett, P. and Paddon, C. (2003) The global transcriptional response of *Bacillus subtilis* to peroxide stress is coordinated by three transcription factors. *J Bacteriol*, **185**, 243-253.

6. Herbig, A.F. and Helmann, J.D. (2001) Roles of metal ions and hydrogen peroxide in modulating the interaction of the *Bacillus subtilis* PerR peroxide regulon repressor with operator DNA. *Mol Microbiol*, **41**, 849-859.

7. Lee, J.W. and Helmann, J.D. (2007) Functional specialization within the Fur family of metalloregulators. *Biometals*, **20**, 485-499.

8. Lee, J.W. and Helmann, J.D. (2006) Biochemical characterization of the structural Zn^{2+} site in the *Bacillus subtilis* peroxide sensor PerR. *J Biol Chem*, **281**, 23567-23578.

9. Ma, Z., Lee, J.W. and Helmann, J.D. (2011) Identification of altered function alleles that affect *Bacillus subtilis* PerR metal ion selectivity. *Nucleic Acids Res*, **39**, 5036-5044.

10. Lee, J.W. and Helmann, J.D. (2006) The PerR transcription factor senses H_2O_2 by metal-catalysed histidine oxidation. *Nature*, **440**, 363-367.

11. Traore, D.A., El Ghazouani, A., Jacquamet, L., Borel, F., Ferrer, J.L., Lascoux, D., Ravanat, J.L., Jaquinod, M., Blondin, G., Caux-Thang, C. *et al.* (2009) Structural and functional characterization of 2-oxo-histidine in oxidized PerR protein. *Nat Chem Biol*, **5**, 53-59.

12. Chen, L., Keramati, L. and Helmann, J.D. (1995) Coordinate regulation of *Bacillus subtilis* peroxide stress genes by hydrogen peroxide and metal ions. *Proc Natl Acad Sci U S A*, **92**, 8190-8194.

13. Duarte, V. and Latour, J.M. (2010) PerR vs OhrR: selective peroxide sensing in *Bacillus subtilis*. *Mol Biosyst*, **6**, 316-323.

14. Zuber, P. (2009) Management of oxidative stress in *Bacillus*. *Annu Rev Microbiol*, **63**, 575-597.

15. Faulkner, M.J. and Helmann, J.D. (2011) Peroxide stress elicits adaptive changes in bacterial metal ion homeostasis. *Antioxid Redox Signal*, **15**, 175-189.

16. Faulkner, M.J., Ma, Z., Fuangthong, M. and Helmann, J.D. (2012) Derepression of the *Bacillus subtilis* PerR peroxide stress response leads to iron deficiency. *J Bacteriol*, **194**, 1226-1235.

17. Chen, L. and Helmann, J.D. (1995) *Bacillus subtilis* MrgA is a Dps(PexB) homologue: evidence for metalloregulation of an oxidative-stress gene. *Mol Microbiol*, **18**, 295-300.

18. Chiancone, E. and Ceci, P. (2010) The multifaceted capacity of Dps proteins to combat bacterial stress conditions: Detoxification of iron and hydrogen peroxide and DNA binding. *Biochim Biophys Acta*, **1800**, 798-805.

19. Ma, Z., Faulkner, M.J. and Helmann, J.D. (2012) Origins of specificity and cross-talk in metal ion sensing by *Bacillus subtilis* Fur. *Mol Microbiol*, **86**, 1144-1155.

20. Gaballa, A. and Helmann, J.D. (2002) A peroxide-induced zinc uptake system plays an important role in protection against oxidative stress in *Bacillus subtilis*. *Mol Microbiol*, **45**, 997-1005.

21. Fuangthong, M. and Helmann, J.D. (2003) Recognition of DNA by three ferric uptake regulator (Fur) homologs in *Bacillus subtilis*. *J Bacteriol*, **185**, 6348-6357.

22. Fuangthong, M., Herbig, A.F., Bsat, N. and Helmann, J.D. (2002) Regulation of the *Bacillus subtilis fur* and *perR* genes by PerR: not all members of the PerR regulon are peroxide inducible. *J Bacteriol*, **184**, 3276-3286.

23. Arguello, J.M., Gonzalez-Guerrero, M. and Raimunda, D. (2011) Bacterial transition metal P_{1B}-ATPases: transport mechanism and roles in virulence. *Biochemistry*, **50**, 9940-9949.

24. Arguello, J.M. (2003) Identification of ion-selectivity determinants in heavy-metal transport P_{1B}-type ATPases. *J Membr Biol*, **195**, 93-108.

25. Yeowell, H.N. and White, J.R. (1982) Iron requirement in the bactericidal mechanism of streptonigrin. *Antimicrob Agents Chemother*, **22**, 961-968.

26. Arguello, J.M., Eren, E. and Gonzalez-Guerrero, M. (2007) The structure and function of heavy metal transport P_{1B}-ATPases. *Biometals*, **20**, 233-248.

27. Raimunda, D., Long, J.E., Padilla-Benavides, T., Sassetti, C.M. and Arguello, J.M. (2014) Differential roles for the Co^{2+}/Ni^{2+} transporting ATPases, CtpD and CtpJ, in *Mycobacterium tuberculosis* virulence. *Mol Microbiol*, **91**, 185-197.

28. Raimunda, D., Long, J.E., Sassetti, C.M. and Arguello, J.M. (2012) Role in metal homeostasis of CtpD, a Co^{2+} transporting P(1B4)-ATPase of *Mycobacterium smegmatis*. *Mol Microbiol*, **84**, 1139-1149.

29. Mitra, B. and Sharma, R. (2001) The cysteine-rich amino-terminal domain of ZntA, a Pb(II)/Zn(II)/Cd(II)-translocating ATPase from *Escherichia coli*, is not essential for its function. *Biochemistry*, **40**, 7694-7699.

30. Mandal, A.K., Cheung, W.D. and Arguello, J.M. (2002) Characterization of a thermophilic P-type Ag^{+}/Cu^{+}-ATPase from the extremophile *Archaeoglobus fulgidus*. *J Biol Chem*, **277**, 7201-7208.

31. Guffanti, A.A., Wei, Y., Rood, S.V. and Krulwich, T.A. (2002) An antiport mechanism for a member of the cation diffusion facilitator family: divalent cations efflux in exchange for K^{+} and H^{+}. *Mol Microbiol*, **45**, 145-153.

32. Moore, C.M., Gaballa, A., Hui, M., Ye, R.W. and Helmann, J.D. (2005) Genetic and physiological responses of *Bacillus subtilis* to metal ion stress. *Mol Microbiol*, **57**, 27-40.

33. Chen, L., James, L.P. and Helmann, J.D. (1993) Metalloregulation in *Bacillus subtilis*: isolation and characterization of two genes differentially repressed by metal ions. *J Bacteriol*, **175**, 5428-5437.

34. Ma, Z., Chandrangsu, P., Helmann, T.C., Romsang, A., Gaballa, A. and Helmann, J.D. (2014) Bacillithiol is a major buffer of the labile zinc pool in *Bacillus subtilis*. *Mol Microbiol*, **94**, 756-770.

35. Imlay, J.A. (2014) The mismetallation of enzymes during oxidative stress. *J Biol Chem*, **289**, 28121-28128.

36. Sobota, J.M., Gu, M. and Imlay, J.A. (2014) Intracellular hydrogen peroxide and superoxide poison 3-deoxy-D-arabinoheptulosonate 7-phosphate synthase, the first committed enzyme in the aromatic biosynthetic pathway of *Escherichia coli*. *J Bacteriol*, **196**, 1980-1991.

37. Gaballa, A., Antelmann, H., Aguilar, C., Khakh, S.K., Song, K.B., Smaldone, G.T. and Helmann, J.D. (2008) The *Bacillus subtilis* iron-sparing response is mediated by a Fur-regulated small RNA and three small, basic proteins. *Proc Natl Acad Sci U S A*, **105**, 11927-11932.

38. Cotruvo, J.A., Jr. and Stubbe, J. (2012) Metallation and mismetallation of iron and manganese proteins *in vitro* and *in vivo*: the class I ribonucleotide reductases as a case study. *Metallomics*, **4**, 1020-1036.

39. Helmann, J.D. (2014) Specificity of metal sensing: iron and manganese homeostasis in *Bacillus subtilis*. *J Biol Chem*, **289**, 28112-28120.

40. Que, Q. and Helmann, J.D. (2000) Manganese homeostasis in *Bacillus subtilis* is regulated by MntR, a bifunctional regulator related to the diphtheria toxin repressor family of proteins. *Mol Microbiol*, **35**, 1454-1468.

41. Martin, J.E., Waters, L.S., Storz, G. and Imlay, J.A. (2015) The *Escherichia coli* small protein MntS and exporter MntP optimize the intracellular concentration of manganese. *PLoS Genet*, **11**, e1004977.

42. King, D.W., Lounsbury, H.A. and Millero, F.J. (1995) Rates and Mechanism of Fe(II) Oxidation at Nanomolar Total Iron Concentrations. *Environ Sci Technol*, **29**, 818-824.

43. Seaver, L.C. and Imlay, J.A. (2001) Alkyl hydroperoxide reductase is the primary scavenger of endogenous hydrogen peroxide in *Escherichia coli*. *J Bacteriol*, **183**, 7173-7181.

44. Imlay, J.A. (2013) The molecular mechanisms and physiological consequences of oxidative stress: lessons from a model bacterium. *Nat Rev Microbiol*, **11**, 443-454.

45. Mostertz, J., Scharf, C., Hecker, M. and Homuth, G. (2004) Transcriptome and proteome analysis of *Bacillus subtilis* gene expression in response to superoxide and peroxide stress. *Microbiology*, **150**, 497-512.

46. Miethke, M., Monteferrante, C.G., Marahiel, M.A. and van Dijl, J.M. (2013) The *Bacillus subtilis* EfeUOB transporter is essential for high-affinity acquisition of ferrous and ferric iron. *Biochim Biophys Acta*, **1833**, 2267-2278.

47. Quadri, L.E., Weinreb, P.H., Lei, M., Nakano, M.M., Zuber, P. and Walsh, C.T. (1998) Characterization of Sfp, a *Bacillus subtilis* phosphopantetheinyl transferase for peptidyl carrier protein domains in peptide synthetases. *Biochemistry*, **37**, 1585-1595.

48. McLaughlin, H.P., Xiao, Q., Rea, R.B., Pi, H., Casey, P.G., Darby, T., Charbit, A., Sleator, R.D., Joyce, S.A., Cowart, R.E. *et al.* (2012) A putative P-type ATPase required for virulence and resistance to haem toxicity in *Listeria monocytogenes*. *PLoS One*, **7**, e30928.

49. Neilands, J.B. (1991) A brief history of iron metabolism. *Biol Met*, **4**, 1-6.

50. Donovan, A., Lima, C.A., Pinkus, J.L., Pinkus, G.S., Zon, L.I., Robine, S. and Andrews, N.C. (2005) The iron exporter ferroportin/Slc40a1 is essential for iron homeostasis. *Cell Metab*, **1**, 191-200.

51. Grass, G., Otto, M., Fricke, B., Haney, C.J., Rensing, C., Nies, D.H. and Munkelt, D. (2005) FieF (YiiP) from *Escherichia coli* mediates decreased cellular accumulation of iron and relieves iron stress. *Arch Microbiol*, **183**, 9-18.

52. Gupta, S., Chai, J., Cheng, J., D'Mello, R., Chance, M.R. and Fu, D. (2014) Visualizing the kinetic power stroke that drives proton-coupled zinc(II) transport. *Nature*, **512**, 101-104.

53. Lu, M. and Fu, D. (2007) Structure of the zinc transporter YiiP. *Science*, **317**, 1746-1748.

54. Nicolaou, S.A., Fast, A.G., Nakamaru-Ogiso, E. and Papoutsakis, E.T. (2013) Overexpression of *fetA* (*ybbL*) and *fetB* (*ybbM*), Encoding an Iron Exporter, Enhances Resistance to Oxidative Stress in *Escherichia coli*. *Appl Environ Microbiol*, **79**, 7210-7219.

55. Frawley, E.R., Crouch, M.L., Bingham-Ramos, L.K., Robbins, H.F., Wang, W., Wright, G.D. and Fang, F.C. (2013) Iron and citrate export by a major facilitator superfamily pump regulates metabolism and stress resistance in *Salmonella* Typhimurium. *Proc Natl Acad Sci U S A*, **110**, 12054-12059.

56. Frawley, E.R. and Fang, F.C. (2014) The ins and outs of bacterial iron metabolism. *Mol Microbiol*, **93**, 609-616.

57. Bhubhanil, S., Chamsing, J., Sittipo, P., Chaoprasid, P., Sukchawalit, R. and Mongkolsuk, S. (2014) Roles of *Agrobacterium tumefaciens* membrane-bound ferritin (MbfA) in iron transport and resistance to iron under acidic conditions. *Microbiology*, **160**, 863-871.

58. Sankari, S. and O'Brian, M.R. (2014) A bacterial iron exporter for maintenance of iron homeostasis. *J Biol Chem*, **289**, 16498-16507.

59. Mascher, T., Margulis, N.G., Wang, T., Ye, R.W. and Helmann, J.D. (2003) Cell wall stress responses in *Bacillus subtilis*: the regulatory network of the bacitracin stimulon. *Mol Microbiol*, **50**, 1591-1604.

60. Harwood, C.R., and Cutting, S. M. (1990) *Molecular Biological Methods for Bacillus*. Chichester: John Wiley and Sons, Ltd.

61. Quisel, J.D., Burkholder, W.F. and Grossman, A.D. (2001) *In vivo* effects of sporulation kinases on mutant Spo0A proteins in *Bacillus subtilis*. *J Bacteriol*, **183**, 6573-6578.

62. Mascher, T., Hachmann, A.B. and Helmann, J.D. (2007) Regulatory overlap and functional redundancy among *Bacillus subtilis* extracytoplasmic function sigma factors. *J Bacteriol*, **189**, 6919-6927.

63. Rensing, C., Fan, B., Sharma, R., Mitra, B. and Rosen, B.P. (2000) CopA: An *Escherichia coli* Cu(I)-translocating P-type ATPase. *Proc Natl Acad Sci U S A*, **97**, 652-656.

64. Sambrook, J., Fritsch, E. F., and Maniatis, T. (1990) *Molecular Cloning: A Laboratory Manual*. Cold Spring Harbor Press, Cold Spring Harbor, NY.

65. Rosadini, C.V., Gawronski, J.D., Raimunda, D., Arguello, J.M. and Akerley, B.J. (2011) A novel zinc binding system, ZevAB, is critical for survival of nontypeable *Haemophilus influenzae* in a murine lung infection model. *Infect Immun*, **79**, 3366-3376.

66. Bradford, M.M. (1976) A rapid and sensitive method for the quantitation of microgram quantities of protein utilizing the principle of protein-dye binding. *Anal Biochem*, **72**, 248-254.

67. Lanzetta, P.A., Alvarez, L.J., Reinach, P.S. and Candia, O.A. (1979) An improved assay for nanomole amounts of inorganic phosphate. *Anal Biochem*, **100**, 95-97.

68. Jolliffe, L.K., Doyle, R.J. and Streips, U.N. (1981) The energized membrane and cellular autolysis in *Bacillus subtilis*. *Cell*, **25**, 753-763.

Chapter 4

Bacillus subtilis Fur is a Transcriptional Activator for the PerR-Repressed *pfeT* Gene Encoding an Iron Efflux Pump[5]

> "*Looking more closely, we will see that knowing whole genome sequences opens up a new area of research, similar to the science of decoding texts written in unknown languages or cracking secret codes… we can only be amazed not to find it stated more often – that what counts in life is not objects themselves, but the relationships between them.*"
>
> *- Antoine Danchin, The Delphic Boat, 2002.*

4.1 Abstract

The physiological relevance of bacterial iron efflux has only recently been appreciated. The *Bacillus subtilis* P_{1B4}-type ATPase PfeT (peroxide-induced ferrous efflux transporter) was one of the first iron efflux pumps to be characterized, and cells lacking *pfeT* accumulate high levels of intracellular iron. The *pfeT* promoter region has binding sites for both PerR, a peroxide sensing Fur-family metalloregulator, and the ferric uptake repressor Fur. Both Fur and PerR bind DNA with Fe^{2+} as a cofactor. While reaction of PerR:Fe^{2+} with peroxide can account for the induction of *pfeT* under oxidative stress, binding of Fur:Fe^{2+} would be expected to lead to repression, which is inconsistent with the known role of PfeT as an iron efflux protein. Here, we show that expression of *pfeT* is repressed by PerR, as anticipated, and

[5] This chapter is adapted from Pinochet-Barros A. & Helmann J. D. Journal of Bacteriology 2020 Jan 27. doi: 10.1128/JB.00697-19

induced by Fur in response to Fe^{2+}. Activation by Fur is mediated by both antagonism of the PerR repressor, and by direct transcriptional activation as confirmed using *in vitro* transcription assays. A similar mechanism of regulation can explain the iron-induction of the *Listeria monocytogenes* PfeT ortholog and virulence factor, FrvA. Mutational studies support a model in which Fur activation involves regions both upstream and downstream of the *pfeT* promoter, and Fur and PerR have overlapping recognition of a shared regulatory element in this complex promoter region. This work demonstrates that *B. subtilis* Fur can function as an iron-dependent activator of transcription.

4.2 Significance statement

Iron homeostasis plays a key role at the host-pathogen interface during the process of infection. Bacterial growth restriction resulting from host imposed iron starvation (nutritional immunity) highlights the importance of iron import during pathogenesis. Conversely, bacterial iron efflux pumps function as virulence factors in several systems. The requirement for iron efflux in pathogens such as *Listeria monocytogenes*, *Streptococcus pyogenes*, and *Mycobacterium tuberculosis* suggests that both import and efflux are needed for cells to successfully navigate rapidly changing levels of iron availability in the host. Here, we provide insight into how iron efflux genes are controlled, an aspect of bacterial iron homeostasis relevant to infectious disease processes.

4.3 Introduction

Iron is an essential micronutrient across all domains of life, including bacteria. It is used as a cofactor by enzymes involved in a wide array of metabolic processes, including the TCA cycle, respiration, and DNA precursor (dNTP) synthesis (1). Although iron is abundant in nature, its bioavailability is limited in oxic environments because of its facile oxidation from its soluble Fe^{2+} (ferrous) form to the Fe^{3+} (ferric) form, which readily forms insoluble hydrates. As a result, microorganisms have evolved a variety of high affinity import mechanisms to acquire iron under iron-depleted conditions. The production of Fe^{3+}-binding siderophores is one of the most widespread adaptations to iron limitation in microorganisms, including Bacteria and many fungi (2).

Although the adaptive responses to iron limitation are widely appreciated, the role of iron efflux proteins has received comparatively little attention (3). Previously, we described the P_{1B4}-type ATPase PfeT (formerly ZosA) as an iron efflux pump in the model Gram-positive bacterium, *Bacillus subtilis* (4). PfeT is the first member of the P_{1B4}-type ATPases implicated in iron efflux, and amongst the first bacterial iron efflux systems to be discovered (4-8). Cells that lack *pfeT* accumulate high levels of intracellular iron and are therefore more sensitive to iron overload. Although the PfeT ATPase is specifically activated by ferrous iron it has a relatively low apparent binding affinity (520 ± 120 μM) *in vitro*, consistent with a function limited to relieving iron overload (4). Orthologs of PfeT have been identified in other Gram-

positive bacteria, many of which have been determined to act as virulence factors (9-12). These findings create a conundrum, since it is now clear that both iron deprivation and iron intoxication are physiologically relevant stresses that can limit the success of bacterial pathogens (3, 13). Presumably, these stresses occur at different stages or in different contexts during the infection process.

Oxidative stress and iron homeostasis are interlinked in light of the fact that ferrous iron acts as a catalyst for harmful Fenton reactions in which hydrogen peroxide (H_2O_2) is reduced with the generation of highly reactive hydroxyl radicals (14). To ameliorate the toxicity of H_2O_2, bacteria routinely deploy catalases and peroxidases to prevent endogenously produced intracellular H_2O_2 from accumulating. These enzymes work in concert with other proteins that can reduce the availability and reactivity of intracellular ferrous iron, often by sequestration. For example, in *B. subtilis* the Fur-family, peroxide-sensing metalloregulator PerR controls expression of two peroxide detoxification enzymes, catalase (KatA) and alkyl hydroperoxide reductase (AhpCF), as well as the Dps-like miniferritin MrgA that can sequester iron (15-18). The ferrous iron efflux pump PfeT is also regulated by PerR and is derepressed under conditions of oxidative stress (17, 19).

Prior studies of the PerR regulon in *Bacillus subtilis* have laid the groundwork for our understanding how bacteria respond to oxidative stress through PerR (17, 20). Genes under the control of this metalloregulator contain

one or more PerR operator sites defined by their characteristic consensus sequence (21). Upon exposure to H_2O_2, PerR:Fe^{2+} metal-catalyzed oxidation (MCO) of iron-coordinated histidines at the Fe^{2+}-binding site triggers a conformational change that causes PerR to become unbound from the DNA, thus derepressing transcription of the regulon (22, 23).

As a member of the PerR regulon, *pfeT* has a well conserved PerR operator site (here designated PerR I (PI)) within its promoter region (Fig. 4.1A & B). Through DNaseI footprinting assays and *in vivo* experiments it was shown that PerR binds to DNA regions overlapping the PI operator site (24). Although PfeT helps alleviate peroxide stress, it plays a secondary role compared to the enzymatic detoxification pathways, and likely works in concert with MrgA to help reduce the labile iron pool in the cell (4). PfeT plays a more prominent role in survival under conditions of iron overload. Although originally identified as under control of PerR (19), a reassessment of this promoter region revealed two additional regulator binding sites, shown to interact with Fur *in vitro* (24). One site is located upstream of the PI site (designated Fur II (FII)), and a second begins 65 bps downstream of the transcriptional start site (Fur III (FIII)) (Fig. 4.1A & B).

Here, we have investigated the interplay between the PerR and Fur metalloregulators in the regulation of the *pfeT* gene. Our genetic and biochemical results lead to a model in which PerR forms a repression complex that responds to elevated H_2O_2 to derepress *pfeT* expression. In parallel, Fur

senses elevated cytosolic iron, and both antagonizes PerR repression and directly activates *pfeT* transcription. These results reveal complexities of operator site overlap and regulator interaction in this complex control region.

4.4 Results

4.4.1 Molecular model for the regulation of *pfeT*

The *pfeT* regulatory region contains three operator sites defined by sequence similarity to the PerR and Fur consensus binding sites (Fig. 4.1A & B). The results presented here culminate in a model, presented at the outset for clarity, in which PerR forms a repression complex involving cooperative binding to both sites PI and FII (Fig. 4.1C), consistent with the extended region of PerR-binding noted in prior footprinting studies (24). When cytosolic iron levels are elevated, Fur replaces PerR at site FII, thereby disrupting the repression complex, and Fur protein bound to site FII and/or FIII contributes to activation of *pfeT* expression (Fig. 4.1C). This model results from a combination of *in vivo* and *in vitro* studies to explore the role of Fur and PerR in *pfeT* regulation.

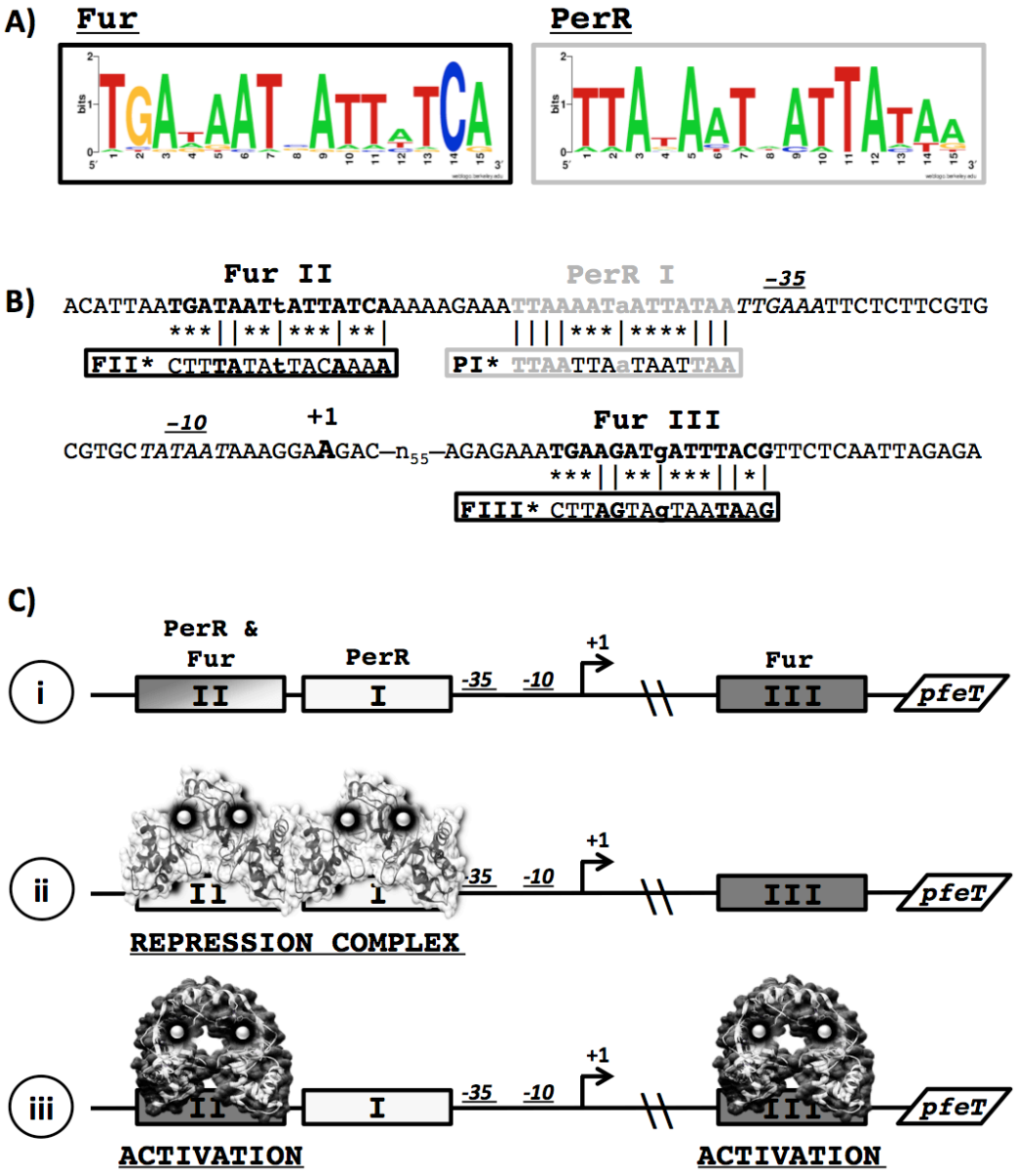

FIG. 4.1) Promoter region of *pfeT*.
(A) Sequence logo of the Fur and PerR consensus operator sites. A total of 23 Fur and 11 Per sites were used to generate the sequence logos with WEBLOGO. The list of sequences is found in Tables 4.1 and 4.2.
(B) Sequence of the *pfeT* promoter region contains one conserved PerR box (grey), named PerR I (PI), which is adjacent to the -35 region. Two Fur operator sites (bold), named Fur II (FII) and Fur III (FIII) are positioned both upstream and downstream of the Per site. FII is separated by 8 bps from the PerR box, whilst FIII is more than 55 bps downstream of the transcriptional start site. The transcriptional start site is denoted in bold. The -10 and -35 RNAP binding sites are in italics. Vertical lines (|) indicate conserved bases and asterisks (*) indicate mutated bases in those constructs containing operator site mutations.

(C) Model for (i) the *pfeT* control region, illustrating (ii) transcriptional repression by PerR (PDB code: 3F8N) binding at sites PI and FII, and (iii) induction by iron mediated by Fur (represented by the homolog ScZur: PDB code: 3MWM) binding at FII (to antagonize PerR repression and as a direct transcription activator) and/or FIII (as a transcription activator).

4.4.2 Expression of *pfeT* is induced in response to excess iron

To quantify the induction of *pfeT* in response to high iron levels, we fused the *pfeT* promoter region to a *lacZ* reporter. Cells grown in lysogeny broth (LB) medium showed a low basal level of expression of about 1-2 Miller units. When grown in LB medium amended with Fe^{2+}, *pfeT* was induced (Fig. 4.2A). This induction was not observed in LB amended with Zn, Mn or Co salts at concentrations known to induce genes responsive to these metals (25-27), indicating that *pfeT* induction is iron specific.

Cells grown over a range of iron concentrations in LB medium displayed an increase in *pfeT* induction as a function of added iron. We confirmed that this induction was dependent on the concentration of added $FeSO_4$ (dissolved in 0.1 N HCl), and was not observed in cells treated with 0.1 N HCl alone (Fig. 4.2B). Since cells lacking *pfeT* are unable to export iron, and have higher intracellular iron concentrations even with non-toxic amounts of added iron (4), we anticipated that induction of the *pfeT-lacZ* reporter would be more sensitive to Fe^{2+} in cells lacking PfeT. As expected, induction levels were increased in a *pfeT* null mutant when compared to WT (Fig. 4.2B). Thus, the

pfeT promoter region provides a sensitive bioreporter for sensing intracellular, bioavailable iron.

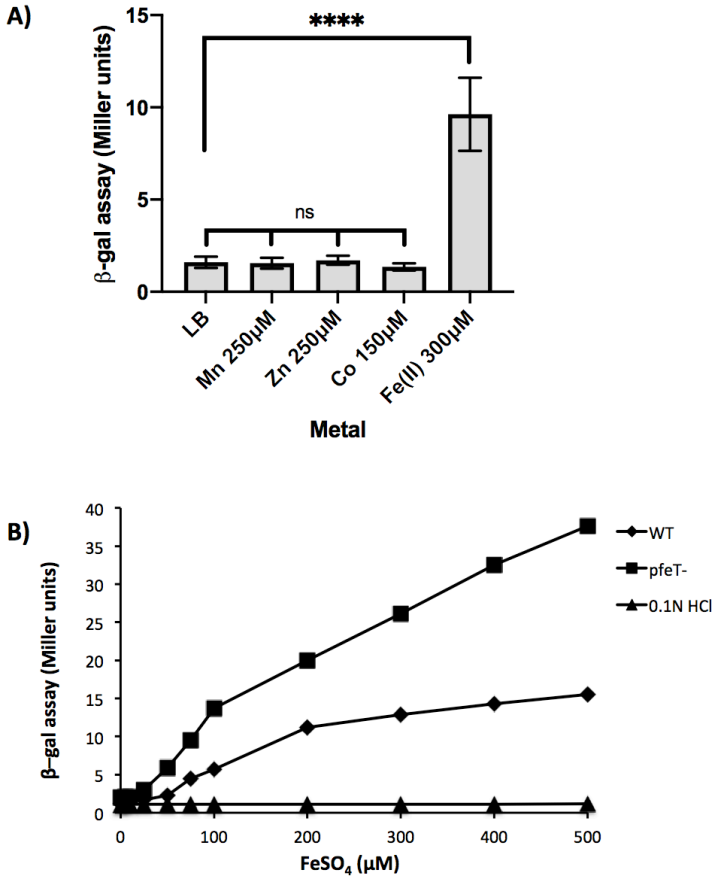

FIG. 4.2) Beta galactosidase assays showing induction of the *pfeT* gene is specific to iron.
(A) WT cells containing a *pfeT-lacZ* transcriptional fusion were grown in LB medium amended with different metals, each at specific concentrations, to an OD_{600} of 0.4. Beta galactosidase activity was measured. Data represent mean ± SD for three or more biological replicates. Multi-pronged significance bars indicate statistical significance for a given condition in reference to LB, and were calculated using a one-way ANOVA test (ns, no statistical significance). Significance between the iron and normal LB conditions was calculated using an unpaired student t-test, ****P<0.0001.
(B) Beta galactosidase assays to monitor *pfeT-lacZ* expression in LB amended with different concentrations of iron. WT cells (diamonds) show increasing levels of induction as a function of iron. Induction was even more sensitive to added iron when measured in *pfeT*::*kan* cells (squares). As a control, the strain was also grown in LB medium containing the equivalent volume of 0.1 N HCl for each particular iron concentration (triangles). Results shown are representative of three biological replicates.

4.4.3 Fur and PerR differentially contribute to *pfeT* expression *in vivo*

In order to understand how PerR and Fur contribute to the expression of *pfeT*, we measured expression levels in *perR*, *fur*, and *perR fur* null backgrounds in the presence or absence of added iron. As expected, in WT cells *pfeT* is iron-induced, whereas expression is constitutive in the *perR* null strain (Fig. 4.3). This confirms that PerR functions as a repressor (19). However, even in the *perR* null mutant, the addition of iron led to a modest, but reproducible, increase in *pfeT-lacZ* expression (Fig. 4.3). This suggests that gene induction in response to iron may be mediated by Fur. Consistent with this notion, transcription levels were somewhat lower, and no increase was observed upon iron addition, in a *perR fur* double mutant (Fig. 4.3). Studies of iron induction in the *perR* null mutant strain are challenging to interpret since this mutant is itself altered in iron homeostasis (28). Specifically, derepression of catalase and Fur in the *perR* null mutant combine to impose an iron restriction on growth (28).

Unlike the *perR* null strain, in the *fur* null mutant expression of *pfeT* is repressed and no longer iron-responsive (Fig. 4.3). We note that repression is not as strong as in WT cells. We suggest that this is due to an increased level of bioavailable iron in the *fur* mutant strain. The efficacy of PerR repression is known to be highly sensitive to the balance between Mn^{2+} and Fe^{2+} since PerR bound to Mn^{2+} as corepressor is less susceptible to oxidative inactivation

during aerobic growth (22, 29-31). Indeed, supplementation of LB medium with 25 mM Mn^{2+} reduces the expression of a *pfeT-lacZ* fusion in medium with 500 mM iron by several fold (from 17±2.3 to 3.6±0.6 Miller units). In this model, Fur activates *pfeT* expression, but the absence of Fur alters metal physiology to reduce the efficiency of PerR repression. Alternatively, these results are consistent with a model in which apo-Fur is a repressor of *pfeT*, and iron-binding leads to dissociation. While this alternative model can account for the modest derepression seen in the *fur* null mutant, it is inconsistent with the decrease in expression in the *perR fur* double mutant compared to the *perR* mutant (Fig. 4.3). To distinguish between these and other possible models**,** we next sought to define the role of each of the three protein binding sites in regulation.

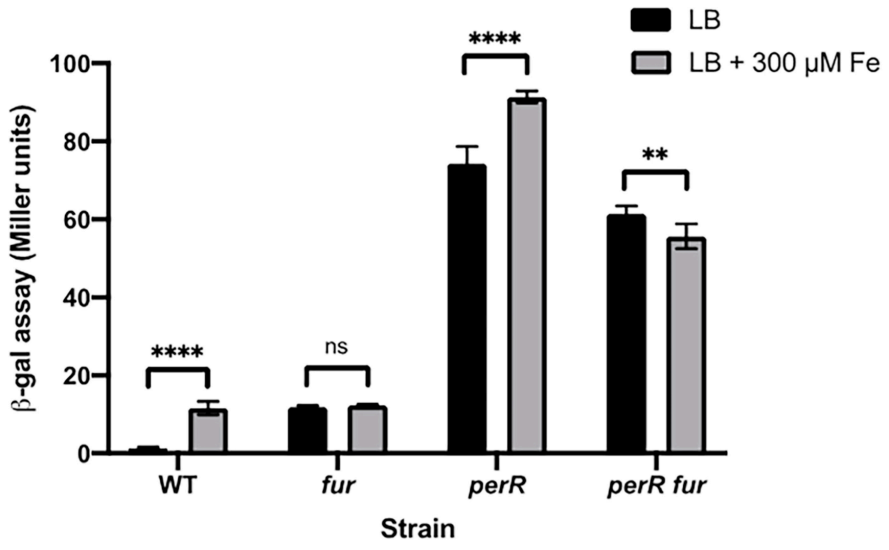

FIG. 4.3) Beta galactosidase assay of *pfeT* in different strain backgrounds. The *pfeT-lacZ* transcriptional fusion was monitored in WT, *fur*::*kan*, *perR*::*tet*, and *fur*::*kan perR*::*tet* strain backgrounds. Cells were grown in LB media containing either no added iron or 300μM iron (a concentration known to induce *pfeT*) to an OD_{600} of 0.4. Data represent mean ± SD for at least three biological replicates. **, P<0.01; ****, P<0.0001; ns, no statistical significance. Significance was calculated using a two-way ANOVA test with Šidák correction.

4.4.4 Functional analysis of the *pfeT* promoter region through operator site dissection *in vivo*

We made point mutations of each regulator binding site (Fig. 4.1B; PI*, FII*, FIII*) and used a *pfeT* promoter region-*lacZ* fusion to measure promoter activity in LB and LB amended with iron (Fig. 4.4A). Consistent with the reported role of PerR as a repressor, mutation of the PerR-binding site (PI*) led to derepression of *pfeT* (Fig. 4.4A). As we also observed in the strain lacking PerR (Fig. 4.3), we still noted an iron-dependent increase in *pfeT* expression in this strain.

Interpretation of the effects of mutations in the two Fur binding sites was not straightforward. For a simple activator protein binding site, one would expect a non-inducible phenotype as seen in a *fur* null (Fig. 4.3). However, the FII* mutation led to constitutive expression, similar to PI* (Fig. 4.4A and Fig. 4.3). We can rationalize this effect by proposing that PerR binds to FII, and this binding is important for formation of a PerR repression complex. In this model (Fig. 4.1C), binding of PerR is cooperative, and mutation of either FII (FII*) or PI (PI*) leads to derepression.

In both single FII* and FIII* mutant strains, there was still a statistically significant increase in expression in response to iron (~1.5 to 3.5-fold respectively) (Fig. 4.4A). In contrast, a strain with mutations in both Fur binding sites (FF**) no longer responds to iron. This supports the idea that Fur

is the physiologically relevant iron sensor, Fur is an activator of transcription, and Fur activation can occur with Fur bound at either FII or FIII (Fig. 4.1C).

In addition to its induction by high iron (Fig. 4.2), *pfeT* has previously been shown to be induced by H_2O_2 (17, 19). We decided to measure the contribution of each regulator binding site in the context of H_2O_2 induction by measuring *pfeT-lacZ* expression in a strain lacking the two major hydroperoxidases, KatA and AhpCF (Hpx^-). As observed also for comparable Hpx^- mutant strains in *E. coli* (32), the absence of H_2O_2 detoxification enzymes leads to an increase in endogenous levels of H_2O_2 sufficient to derepress the cognate stress response (Fig. 4.4B). In a strain with a mutation in the PerR binding site (PI*) *pfeT* is derepressed, and there is no further increase in the Hpx^- mutant background, consistent with the idea that PerR repression requires PI. In contrast, most strains with mutations in the Fur binding sites (FII* or FIII* or FF**), still display some increase in gene expression when transferred to the Hpx^- background, unless the PI box is also mutated (Fig. 4.4, strain 3*). The one exception is the FIII* PI* mutant, which still responds to elevated H_2O_2 in the absence of a PI site (Fig. 4.4B). This might reflect sensitivity of Fur bound at FII to H_2O_2 inactivation, or possibly an ability of PerR to bind to the FII region in this strain even in the absence of PI.

Together, the analysis of iron and H_2O_2 induction of strains bearing operator site mutations illustrates the complementary roles of the PerR and Fur regulatory proteins. When both Fur binding sites are mutated (FII* FIII*),

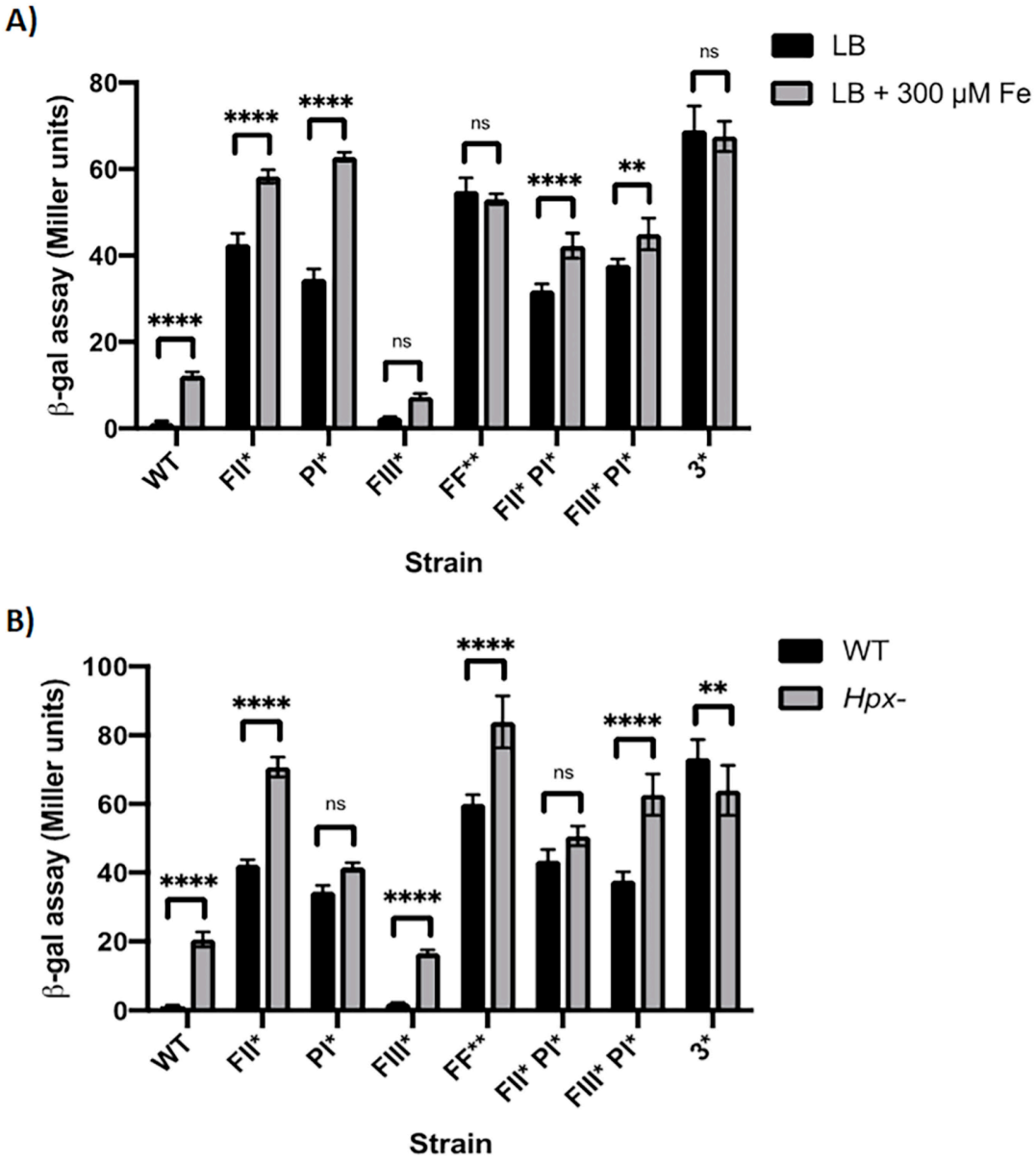

FIG. 4.4) Promoter dissection of *pfeT*.
(A) Beta galactosidase assay to monitor iron induction of *pfeT-lacZ* in cells grown in LB or in LB + 300 µM Fe. Data represent mean ± SD for at least three biological replicates. **, P<0.01; ****, P<0.0001; ns, no statistical significance. Significance was calculated using a two-way ANOVA test with Šidák correction.
(B) Comparison of beta galactosidase activities of the promoter constructs shown in (A) measured in WT and an Hpx- background grown in LB. Data represent mean ± SD for three or more biological replicates. **, P<0.01; ****, P<0.0001; ns, no statistical significance. Significance was calculated using a two-way ANOVA test with Šidák correction.

gene expression is elevated, but no iron induction is observed (Fig. 4.4A), whereas in an Hpx- background there is still a small but significant response to increased H_2O_2 (Fig. 4.4B). Conversely, the PI* mutation that disrupts the PerR repression complex leads to a loss of H_2O_2 responsiveness (Fig. 4.4B), but the cells retain iron induction (Fig. 4.4A).

4.4.5 Operator site specificity *in vitro*

To test the model for PerR repression and Fur activation that emerged from these gene expression studies (Fig. 4.1C), we measured the binding of PerR and Fur to the *pfeT* regulatory region using electrophoretic mobility shift assays (EMSAs). Both regulators were previously found to bind to this region (24), as confirmed here, and we have used our operator site mutations to test the role of each consensus site in complex formation. For these studies, both Fur and PerR were metallated with Mn^{2+}, known from prior studies to activate DNA-binding and to allow *in vitro* binding studies to be conducted aerobically (24, 33).

Fur binds to the WT promoter region (WT P_{pfeT}) with high affinity (dissociation constant [K_d] of ~20 nM) (Fig. 4.5A). Fur also bound with high affinity (K_d ~20 nM) with the PI^*_{pfeT} fragment. Given that the PI site is PerR-specific, according to the *in vivo* data (Fig. 4.4A & B) and prior results (19, 24), this was not surprising. Fur still bound with high affinity to promoter fragments retaining at least one Fur binding site (FII* P_{pfeT} and FIII* P_{pfeT}), but binding

was abolished when both were mutated (FF*, Fig. 4.5A). These data suggest that FII and FIII bind Fur independently and with high affinity, and either site can mediate iron-dependent activation (Fig. 4.4A and Fig. 4.5B). However, when both FII and FIII are inactivated (FF*), Fur no longer bound to the promoter region (Fig. 4.5B), and iron induction was no longer observed (Fig. 4.4A).

Next, we tested PerR binding to these same promoter region variants. The WT P_{pfeT} bound PerR with high affinity (K_d ~50 nM) (Fig. 4.6A). As expected, mutating the PI site compromised the ability of PerR to bind to DNA. Moreover, the FII* promoter variant also had a greatly reduced affinity for PerR (Fig. 4.6A & B). These results suggest that the PI and FII sites both interact with PerR, and that there is positive cooperativity in binding. This inference is consistent with prior results from DNase I footprinting that document that PerR binds to an extended region on the *pfeT* promoter spanning both the PI and FII sites (24). These results support a model in which PerR binding to PI and FII sites contributes to the formation of a stable repression complex (Fig. 4.1C).

Collectively, the Fur EMSA data (Fig. 4.5A & B) and the mutational results (Fig. 4.4A) suggest that the FII site is promiscuous. That is, although this site displays high similarity to the Fur operator consensus sequence (Fig. 4.1A), it seems to be able to bind both Fur and PerR *in vitro* (Fig. 4.5B & 4.6B), with a switch in operator occupancy accompanying the iron-dependent induction of *pfeT* (Fig. 4.1C).

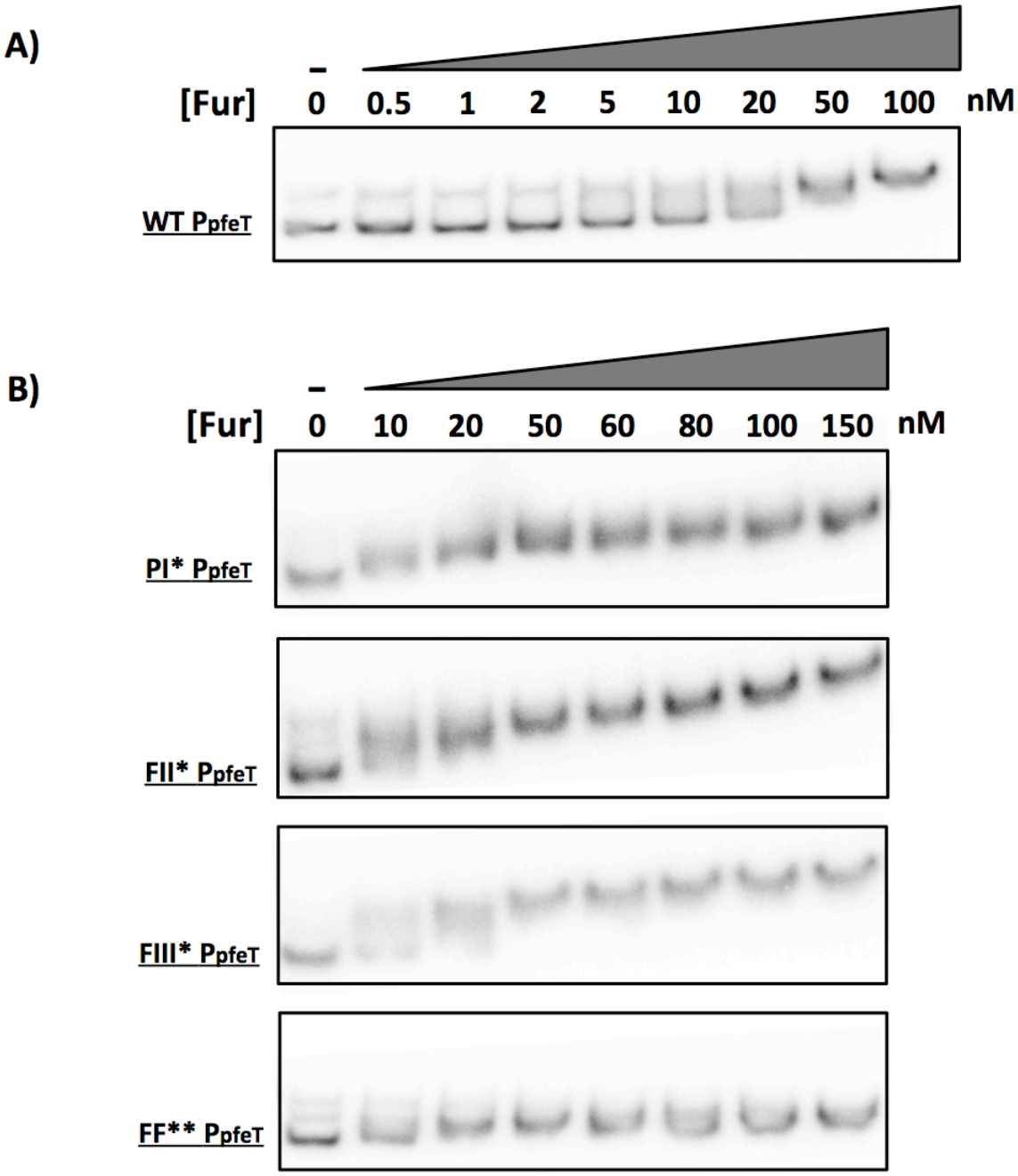

FIG. 4.5) Electrophoretic mobility shift assays (EMSA) of *pfeT* promoter region (268 bps) with Fur.
(A) EMSA of the WT *pfeT* promoter region showing Fur binding.
(B) EMSA of *pfeT* PI*, FII*, FIII*, and FF** promoter region mutants (Fig. 4.1B) showing the effect on Fur binding. All EMSAs were performed a total of three times with very similar results, and a representative result is shown.

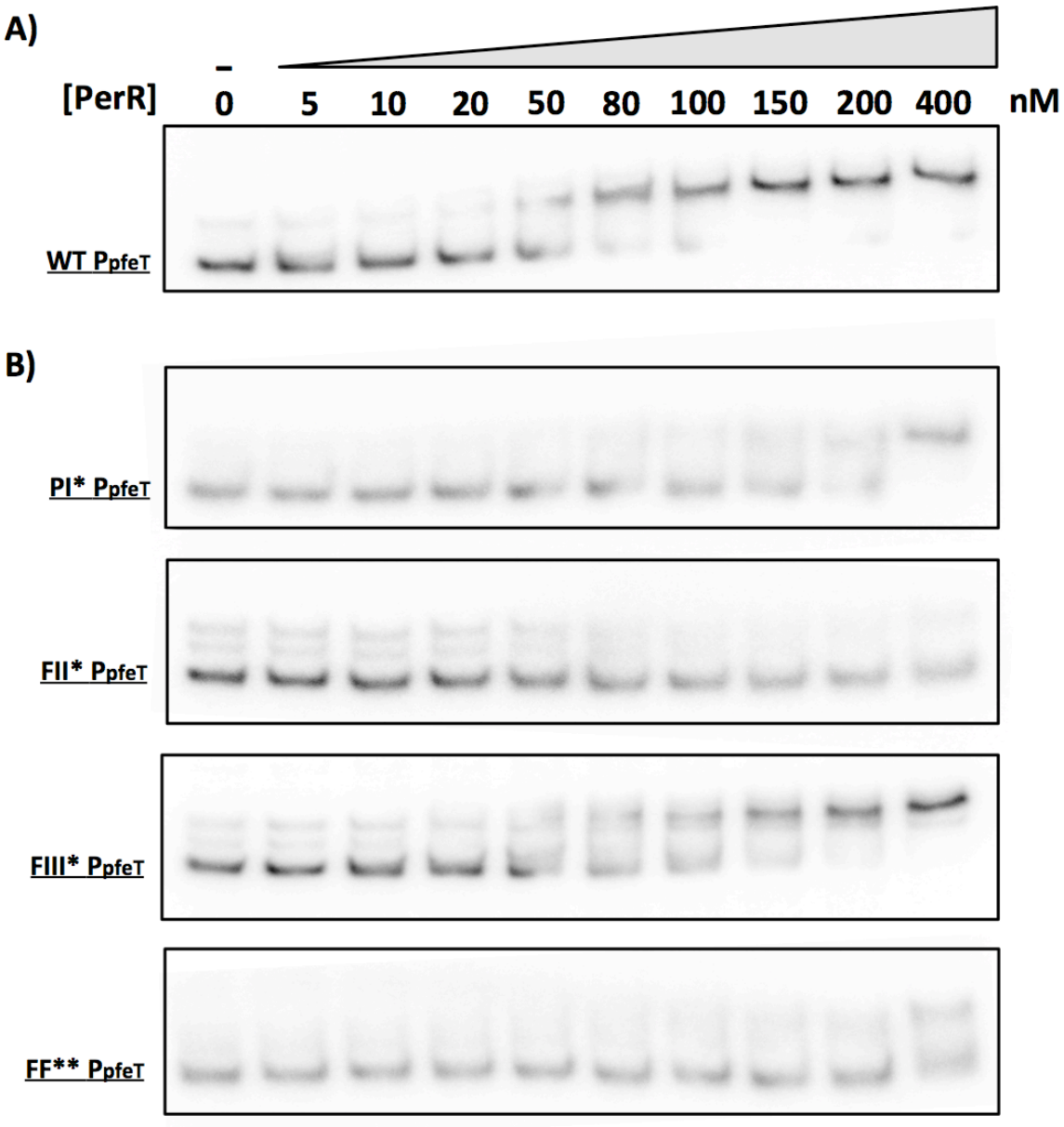

FIG. 4.6) Electrophoretic mobility shift assays (EMSA) of *pfeT* promoter region (268 bps) with PerR.
(A) EMSA of the WT *pfeT* promoter region showing PerR binding.
(B) EMSA of *pfeT* PI*, FII*, FIII*, and FF** promoter region mutants (Fig 4.1B) showing the effect on PerR binding. All EMSAs were performed a total of three times with very similar results, and a representative result is shown.

4.4.6 Fur is a direct activator of *pfeT in vitro*

The emerging model for *pfeT* regulation postulates the Fur can function both to disrupt the PerR repression complex (by competition for FII), and also as a direct activator of transcription (Fig. 4.1C). We therefore performed *in vitro* transcription assays to test this model. In the absence of both regulators, *pfeT* is transcribed at a basal level (Fig. 4.7A – lane 1), consistent with the high expression noted in the *perR fur* null mutant (Fig. 4.3). Upon addition of PerR, *pfeT* transcription was almost completely abolished (Fig. 4.7A – lane 2), consistent with the role of PerR as a repressor. Conversely, when Fur was added, transcription was activated beyond the level obtained with RNAP alone (Fig. 4.7A – lane 3 vs. 1), consistent with Fur as an activator of transcription.

To test the hypothesis that Fur may act to antagonize the PerR repression complex, we explored the effect of order of addition of PerR and Fur. When Fur was incubated with the DNA for 5 min. prior to the addition of PerR (lane 3), transcript levels were 3-fold higher than with RNAP alone (lane 1). When PerR was added first followed by Fur (lane 5), transcription was elevated compared to the PerR repressed state (lane 2), but not as high as when Fur was added first. Thus, with only 5 min. allowed for regulator competition the system has not reached equilibrium. This is consistent with the expected slow off rate for dissociation of PerR:Mn^{2+} from FII, which may be prerequisite for Fur binding at this site to preclude formation of the PerR repression complex.

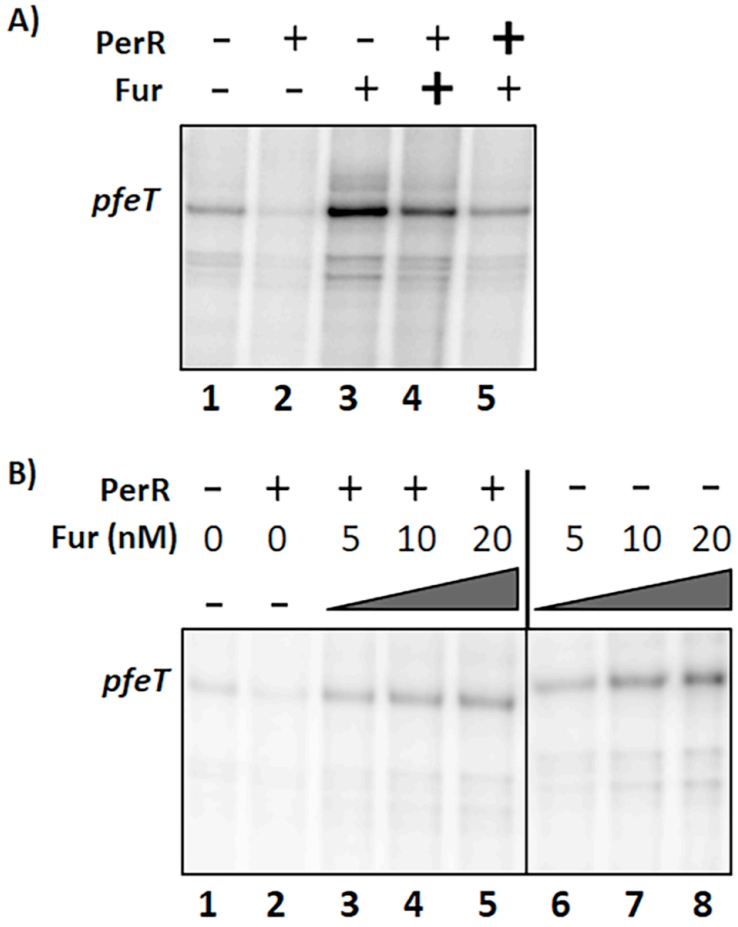

FIG. 4.7) *In vitro* transcription (IVT) of *pfeT*.
(A) Polyacrylamide gel electrophoresis (PAGE) was used to visualize radiolabeled RNA (run-off transcripts) from the *pfeT* promoter region. The *pfeT* transcript is labeled by the arrow and is 171 bps long. Manganese was present in the reaction at 10 µM and RNAP holoenzyme was present at 100 nM. PerR and Fur regulators were both added to a final concentration of 50 nM each. Crosses (+) indicate presence of a component, dashes (-) indicate absence, and bold crosses (**+**) indicate that this regulator was added 5 min prior to the second regulator, with an additional 5 min equilibration prior to initiation of the reaction. Band quantification values were determined using ImageJ. Values for lanes 1 through 5 normalized to lane 1 (set to 100) are 27, 294, 191, and 110 respectively.
(B) PAGE analysis of run-off transcripts illustrating activation by Fur in the presence or absence of PerR. Manganese was present in the reaction at 10 µM and RNAP holoenzyme was present at 100 nM. PerR regulator was added to a final concentration of 30 nM to each reaction. Fur was added at the indicated concentrations to each reaction. The black vertical line distinguishes the two sets of reactions, one where PerR was added (after Fur) and one where PerR was not added. Band quantification values were determined using ImageJ. Values for lanes 1 through 8 are 100, 52, 179, 217, 290, 230, 370, and 439 respectively, and are normalized with respect to lane 1.

To further assess the effects of Fur on *pfeT* activation, we carried out a Fur titration in the presence or absence of PerR (Fig. 4.7B). As expected, *pfeT* was expressed at a low level in the absence of both metalloregulators and highly repressed when only PerR was added to the reaction (Fig. 4.7B - lane 1&2). We confirmed that *pfeT* expression increases as a function of Fur concentration with and without PerR. Transcript bands were stronger in the Fur only reactions even at 20 nM (Fig. 4.7B – lane 8), compared to the reactions containing PerR. This is indicative of the fact that Fur can act as an anti-repressor in the presence of PerR, as well as a direct activator (Fig. 4.7A). This is in alignment with our *in vivo* data wherein we also see PerR-dependent repression and Fur activation (Fig. 4.3).

4.4.7 Fur activation of *pfeT* orthologs

A homolog of PfeT, the Fur-regulated virulence protein FrvA, has been previously identified in *Listeria monocytogenes* (9). These two efflux pumps share 54% protein identity (Fig. 4.9), although FrvA displays a greater affinity for Fe^{2+} as judged by the amount required for activation of ATPase activity (9). The similarity between these two efflux pumps extends to the architecture of their promoter regions (Fig. 4.11 and Fig. 4.8). They both possess a PerR box and multiple Fur binding sites across the promoter region. In fact, *frvA* also has a predicted Fur box adjacent to a PerR binding site (which itself overlaps with the -10 region) and another Fur binding site beyond the transcriptional

start site (Fig. 4.10A and Fig. 4.8B). Previous studies support the idea that Fur is a transcriptional activator of FrvA (9, 34), although other studies suggested that it might function as a repressor (10, 35).

Here, we used *in vitro* transcription assays to test the effects of PerR and Fur on transcription of the *L. monocytogenes frvA* gene. Since the *B. subtilis* and *L. monocytogenes* regulators and RNAP are highly similar in sequence, we used purified *B. subtilis* proteins in this study. In the absence of Fur and PerR, basal levels of *frvA* transcription were observed (Fig. 4.10B – lane 1). Upon addition of PerR to the reaction, this basal level of transcription was completely abolished (lane 2). Addition of Fur to the reaction increased transcript levels in a protein concentration dependent manner (Fig. 4.10B – lane 3-6), as observed for *pfeT* (Fig. 4.7B).

FIG. 4.8) Full promoter sequences of *pfeT* and *frvA*.
(A) Sequence of the *B. subtilis pfeT* promoter showing the designated Fur and PerR boxes in bold and grey, respectively. Operator sites are aligned with the conserved 7- 1-7 operator sites for these regulators. Fur boxes show the full, classical 19 bp sequence both in the sequence and for the conserved alignment sequence. The -35 and -10 regions are in italics and underlined. The transcriptional start site is in bold black.
(B) Complete sequence of the *L. monocytogenes frvA* promoter showing the designated Fur and PerR boxes boxes in bold and grey, respectively. Fur boxes show the full, classical 19 bp sequence both in the sequence and for the consensus. The -35 and -10 regions are in italics and underlined. The transcriptional start site is in bold.

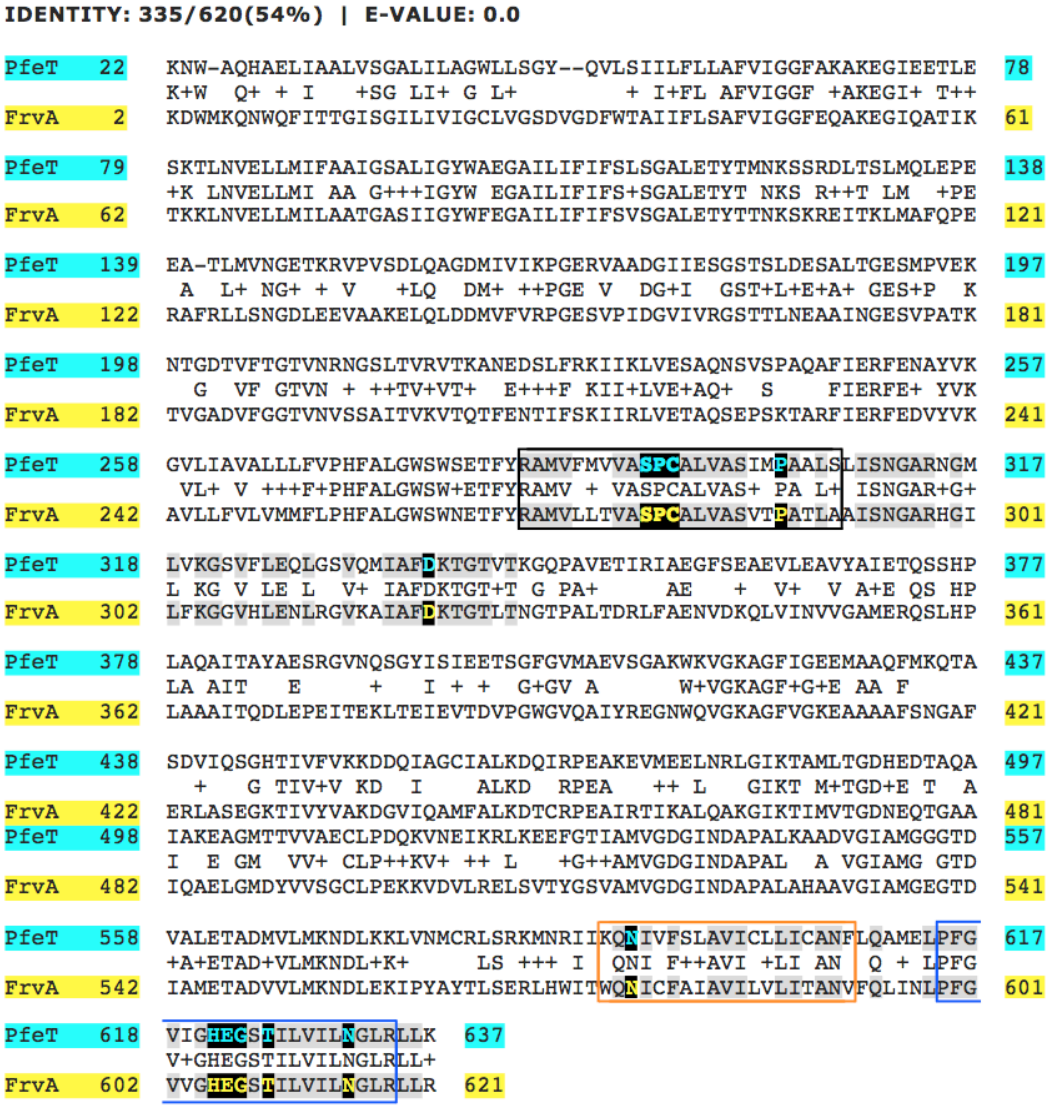

FIG. 4.9) Protein sequence identity between PfeT and FrvA.
BLAST alignment was used to illustrate protein sequence identity between *B. subtilis* PfeT and *L. monocytogenes* FrvA. H6, H7 and H8 conserved transmembrane segments characteristic of P_{1B4}-ATPases are highlighted by black, orange and blue boxes, respectively.

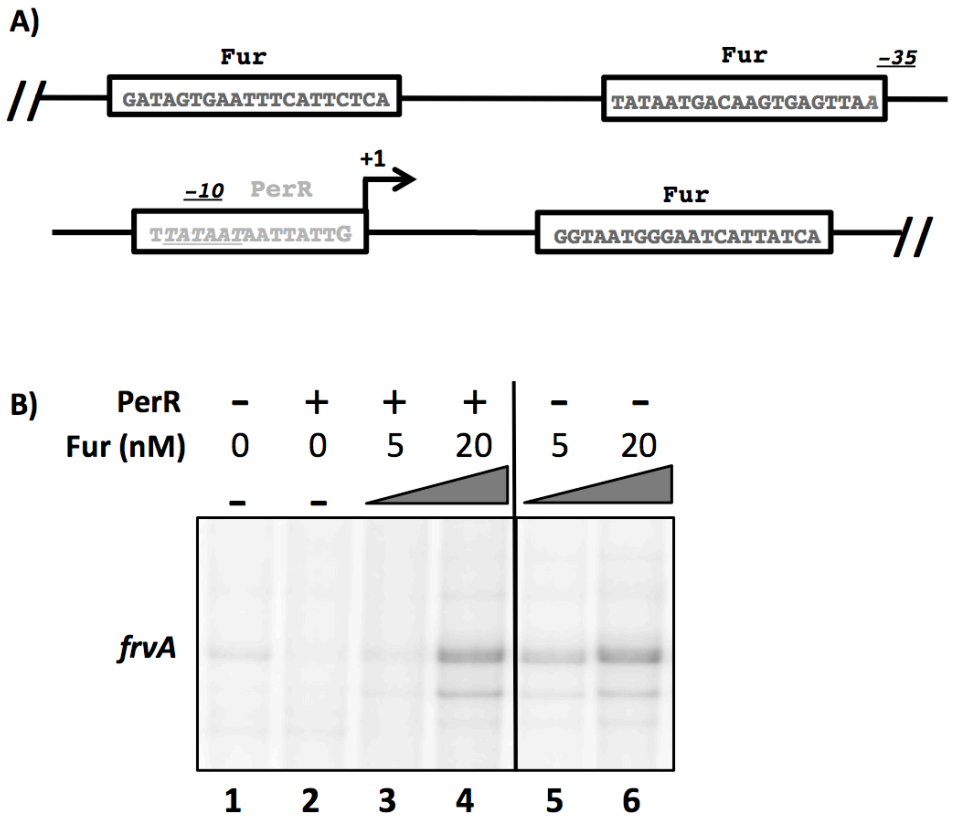

Figure 4.10) Promoter analysis of the *Listeria monocytogenes* ortholog, *frvA*.
(A) Promoter region of *frvA* reveals a similar structure to that seen for *pfeT*. A conserved PerR box (light grey) overlaps with the -10 region (italics) of the RNAP binding site. Like *pfeT*, *frvA* has two Fur operator sites. One is located upstream of the PerR box and is adjacent to the -35 region, and the other is downstream of the transcriptional start site (in bold black). All lanes were from a single PAGE experiment, with the black line indicating the deletion from the image of intervening lanes for clarity.
(B) PAGE of run-off RNA transcripts showing PerR repression and Fur activation of *frvA*. The *frvA* transcript is 182 bps long. Manganese was present in the reaction at 10 µM and RNAP holoenzyme was present at 100 nM. *B. subtilis* PerR was added to a final concentration of 30 nM to each reaction. *B. subtilis* Fur was added at the indicated concentrations to each reaction. The black vertical line distinguishes the two sets of reactions, one where PerR was added (after 5 min Fur incubation) and one where PerR was not added. Band quantification values were determined using ImageJ. Values for lanes 1 through 6 are 100, 25, 49, 498, 291, and 500 respectively, and are normalized with respect to lane 1. All lanes were from a single PAGE experiment, with the black line indicating the deletion from the image of intervening lanes for clarity.

4.5 Discussion

Bacterial iron homeostasis has been an active area of research for many years (2). In many environments, iron is a limiting nutrient and bacteria devote considerable resources to obtaining iron. Given this focus on iron import, a role for iron efflux was initially dismissed as unlikely to be physiologically important (36). PfeT was the first P_{1B4}-type ATPase to be characterized as an Fe^{2+} efflux pump (3, 4). Homologous proteins that also serve as Fe^{2+} efflux systems play important roles in pathogenesis (9-12) (Fig. 4.11). However, the mechanisms by which these transporters are transcriptionally regulated are still poorly understood and seem to vary across bacterial types as is evident by the differences in their promoter architecture (24, 35, 37, 38).

Bacterial Fur proteins function as Fe^{2+}-dependent repressors to control genes required during iron depletion (39). Previous work in *B. subtilis* has mapped the Fur regulon, which includes ~60 genes that are repressed under iron replete conditions (40, 41). In addition, Fur indirectly activates the expression of some genes in response to Fe^{2+} as mediated by the Fur-repressed small RNA, FsrA (42-44). Our work here has shown that Fur also functions as a direct transcription activator of *pfeT* under high iron conditions (Fig. 4.7A), and that this mode of regulation is conserved for the *L. monocytogenes* ortholog *frvA* (Fig. 4.10B). Fur has been previously shown to function as an activator for selected genes in Gram-negative bacteria like *Escherichia coli* (45), *Salmonella enterica* (46), and *Neisseria meningitidis*

(47). Past studies in Gram-Positive bacteria like *Staphylococcus aureus* (48) and *L. monocytogenes* (9, 34) have suggested Fur might also function as a transcriptional activator in these systems, but have never shown it directly.

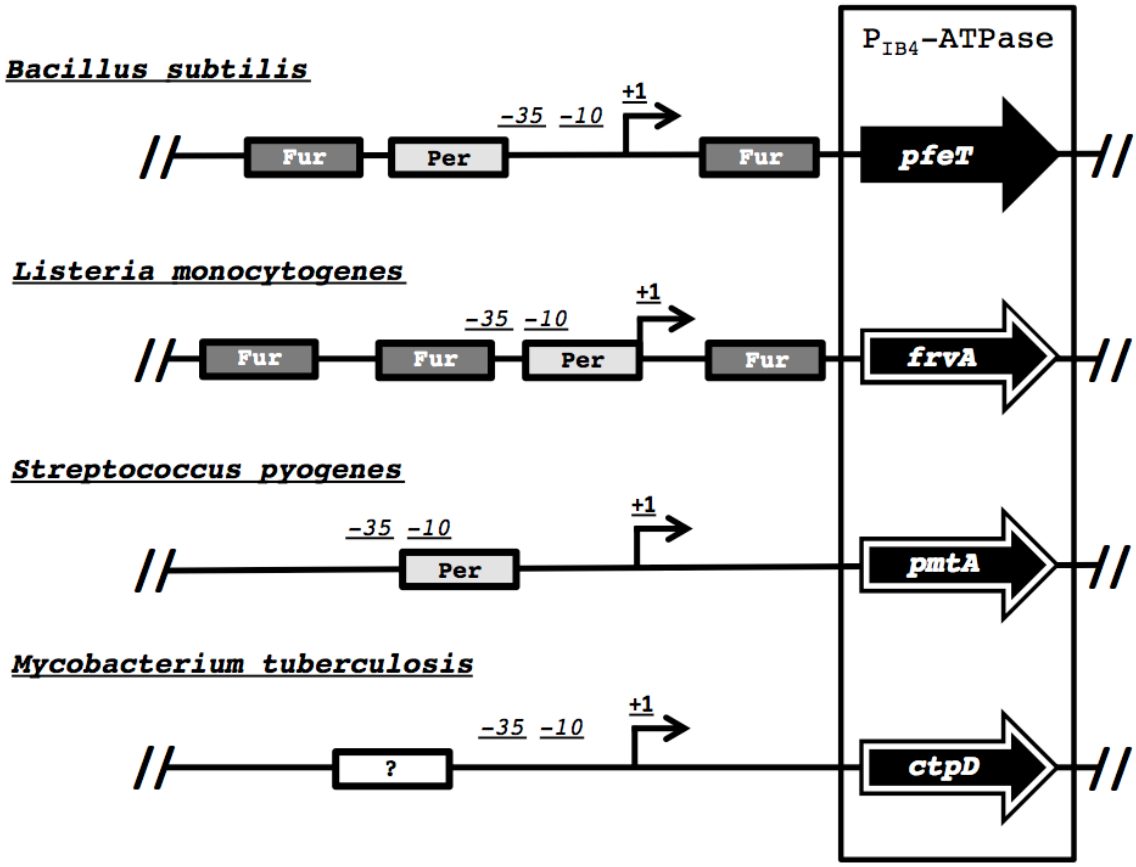

FIG. 4.11) Promoter structure of *pfeT* orthologs.
Schematic showing the different regulatory regions controlling *pfeT* orthologs in *L. monocytogenes* (*frvA*), *Streptococcus pyogenes* (*pmtA*), and *Mycobacterium tuberculosis* (*ctpD*). Genes highlighted with white-outline are virulence factors.

Our new understanding of *pfeT* and *frvA* transcription will provide insight into how and when iron efflux is activated during infection. Host-imposed iron limitation, by sequestration and through efflux pumps that deplete the phagocytic vacuole of iron, are countered by the induction of high

affinity bacterial iron uptake systems (49-51). Transient iron overload, due to the expression of high affinity iron uptake systems and the transition to a comparatively iron-replete environment, may need to be counterbalanced by efflux pumps that serve as a “relief valve” to help adjust cytosolic iron levels. When this occurs during infection is not well understood, but we have previously suggested that it might be correlated with escape of *L. monocytogenes* from the phagocytic vacuole into the host cytosol (9).

The precise way in which Fur activates gene transcription remains unclear and will require further attention. Our mutational analysis of the different operator sites of the *pfeT* promoter region suggests that either FII or FIII can support gene induction (Fig. 4.4A, Fig. 4.5A & B). Inactivation of both of these sites prevents Fur binding and therefore gene activation. Multiple Fur binding sites are also present in the *frvA* promoter region (Fig. 4.8B). In *B. subtilis*, MntR-mediated activation of the genes encoding the manganese efflux pumps MneP and MneS also involves multiple operator sites upstream of the transcriptional start site. In this case, these multiple sites appear to all be required for activation (25). Operator sites located downstream of the transcriptional start site are typically involved in gene repression. However, in some cases downstream sites may play a positive role in gene expression. For example, for *E. coli* virulence regulator Rns, as well as related AraC family members, can activate gene expression from downstream sites (52).

Our results here provide an example of operator site promiscuity in which a single site can interact with either PerR or Fur. Previous work has defined the binding specificity of Fur family proteins (Fur, PerR, and Zur) at their cognate operator sites (24, 39). In this prior work, it was shown that introduction of two point mutations into the *mrgA* PerR box to match the Fur consensus site resulted in a promoter region ($mrgA_{Fur}$) that was bound by both Fur and PerR *in vitro*. Moreover, high level expression of an $mrgA_{Fur}$-*lacZ* fusion was observed in a double *fur perR* mutant, but not in the single mutants (24). The FII site here matches the operator site introduced in the $mrgA_{Fur}$ construct, and appears to represent the first naturally occurring example of a site recognized by both regulators.

Our work shows that the PerR and Fur regulons are interlinked. Formation of a PerR repression complex involves cooperative binding of PerR to both the PI and FII sites. This extended DNA binding behavior is reminiscent of what has been previously observed for *E. coli* Fur (53, 54). Activation is mediated by Fur binding to either FII or FIII (Fig. 4.1C). These results extend our understanding of the regulation of iron efflux genes, and thereby set the stage for a new understanding of host-pathogen interactions.

4.6 Methods

Bacterial strains, phage, plasmids, and growth conditions

Bacillus subtilis strains derived from CU1065 (WT) were grown on lysogeny

broth (LB) medium (10 g/L casein digest peptone, 5 g/L yeast extract, 5 g/L NaCl) at 37^{O}C with vigorous shaking. Ferrous iron ($FeSO_4 \cdot 7H_2O$) was titrated into the media as indicated from a freshly made 100mM iron stock solution dissolved in 0.1 N HCl. Ampicillin (*amp*; 100 μg ml^{-1}) was used to select *E. coli* transformants. Erythromycin (*ery*; 1 μg ml^{-1}) and lincomycin (*linc*; 25 μg ml^{-1}; for testing macrolide-lincosamide-streptogramin B [MLS] resistance), spectinomycin (spec; 100 μg ml^{-1}), kanamycin (*kan*; 10 μg ml^{-1}), and neomycin (*neo*; 10 μg ml^{-1}) were used for the selection of various *B. subtilis* strains.

Mutant strain construction

Null mutant strains were obtained from the BKE collection (a *B. subtilis* 168 gene knockout library) available from the Bacillus Genetic Stock Center (BGSC). Each BKE strain contains an erythromycin-resistance cassette inserted into the gene in the *B. subtilis* 168 genome. Mutations were transformed into CU1065 for this study. The pDR244 plasmid (from BGSC) was used to excise the BKE erythromycin cassette to generate a markerless deletion of the target gene (55). Isolation of *B. subtilis* chromosomal DNA, transformation and specialized SPβ transduction were performed as described (56). Strains were confirmed by PCR.

Reporter strain construction

For monitoring gene expression, we generated promoter region-*cat-lacZ*

operon fusions integrated into the SPβ prophage as previously described (57). Promoter regions were cloned into pJPM122 which integrates in single copy into the chromosome of strain ZB307A. This strain (SPβ*c2*Δ*2*::Tn*917*::pBSK10Δ6) carries a plasmid (pPSK10Δ6) with a promoterless *lacZ* gene inserted into a Tn917 transposon inside a temperature-sensitive derivative of the SPβ prophage designated SPβ*c*2Δ2 (57). Integration of pJPM122 derivatives into strain ZB307A generates promoter region-*cat-lacZ* operon fusions that can be mobilized by specialized transduction after induction of phage by temperature shift to 50^{O}C for 15 min. The *cat-lacZ* operon fusions generated in strain ZB307A were moved to different backgrounds by SPβ transduction and selection for MLS and neomycin resistance. All strains were confirmed by PCR. The SPβ prophage containing the reporter fusions were all stable under the experimental conditions tested (including high iron and elevated peroxide production in Hpx^{-} cells) as judged by a lack of visible cell lysis and by phage titers. In contrast, heat stress leads to cell lysis and SPβ phage induction.

Site directed mutagenesis of the *pfeT* promoter

PCR primers containing the desired changes within the PI, FII, and FIII boxes were used to amplify the *pfeT* promoter region from CU1065 WT chromosomal DNA. Final fragments were restriction digested with High Fidelity HindIII and BamHI enzymes (NEB) and cloned into the pJPM122 vector (57). Plasmids

containing the desired fragments were transformed into competent DH5α *E. coli* and selected with ampicillin. All constructs were verified by DNA sequencing prior to transfer into strain ZB307A.

β-galactosidase assays

Cells containing the *pfeT* promoter *lacZ* fusions were grown in LB amended with different concentrations of $FeSO_4 \cdot 7H_2O$ to an OD_{600} of ~0.4. Cells were then harvested and β-galactosidase assays were performed as described previously in (58), except that cells were lysed with 0.1 mg ml^{-1} lysozyme for 30 min at $37^{O}C$ instead of chloroform.

Electrophoretic mobility shift assays (EMSA)

PCR fragments (268 bps) containing the wild-type and mutant promoter regions of *pfeT* (WT, PI*, FII*, FIII*, and FF**) were purified (PCR purification kit, Qiagen) and labeled with [γ-^{32}P]-ATP using T4 polynucleotide kinase. After labeling, a G10 column (NucAwayTM spin columns, Invitrogen) was used to remove the unincorporated [γ-^{32}P]-ATP and radioactivity of each probe was quantified by a scintillation counter. The γ-^{32}P-labelled promoter fragments were incubated with either Fur or PerR in 1x binding buffer at room temperature for 15min. The 1x binding buffer used for Fur reactions contained 10 mM Tris-HCl (pH 8.0), 50 mM NaCl, 5% glycerol, 1 mM DTT, 50 μg/mL BSA, 10 μM $MnCl_2$, and 2 μg/mL salmon testes DNA. The 1x binding buffer

used for PerR binding reactions was as previously described in (22). Fur and PerR proteins were purified as previously described (31, 33). Samples were loaded on a 5% polyacrylamide gel and run in 40 mM Tris-acetate buffer (no EDTA, pH 8.0). The gel was dried and exposed to a phosphorimager screen overnight and scanned using a Typhoon FLA 7000 system.

Multiple round *in vitro* transcription

In vitro transcription was performed as previously described (59). Briefly, σ^A-saturated RNAP holoenzyme was reconstituted by mixing purified RNAP with purified σ^A (1:5 molar ratio) in transcription buffer (10 mM Tris (pH 8.0), 10 mM $MgCl_2$, 1 mM DTT, 10 mM potassium glutamate, 10 μg ml^{-1} acetylated BSA) and incubated on ice for 15 min. Ten nanomolar of promoter DNA fragment and 50 nM PerR and/or Fur in transcription buffer were mixed and incubated for 10 min at room temperature. Both PerR and Fur were incubated with Mn^{2+} on ice for 15 min to ensure full metallation before adding to the reaction. For the transcription reaction, a ~400 bp PCR product was amplified from CU1065 *B. subtilis* chromosomal DNA to give a DNA fragment that yields a 171 nt transcript. For the *L. monocytogenes* ortholog, a 478 bp PCR fragment was amplified from WT *L. monocytogenes* chromosomal DNA to give a DNA fragment that yields a 182 nt transcript. Next, RNAP was added and the reactions were incubated for 10 min at 37^OC. Transcription was initiated by adding 0.5 mM of each GTP, CTP and ATP, 0.1 mM of UTP and 2.5 mCi of [α-

^{32}P]-UTP. After 10 min incubation, the reaction products were ethanol precipitated in the presence of 0.3 M sodium acetate (pH 5.2) and 1 mL of GlycoBlue (15 mg ml^{-1}, Ambion). The RNA pellet was washed with 70% cold ethanol, dried and dissolved in formamide loading dye and separated on a 6% denaturing polyacrylamide sequencing gel (UreaGEL^{TM}). A single stranded DNA ladder was made by generating [γ-^{32}P]-ATP labelled PCR fragments of 100 bps, 200 bps, and 300 bps in size from a pET17b plasmid. The fragments were pooled, dissolved in formamide loading dye, and boiled for 5 min at 90^{O}C. The gel was dried and exposed to a phosphorimager screen overnight and scanned by Typhoon FLA 7000 system. These experiments were repeated at least twice. Band quantification and normalization was performed using ImageJ.

Table 4.1) List of Fur operator sites used to generate logo sequences

Fur regulated genes	OPERATOR SEQUENCE
dhbA	T**GA**TAATCATTA**TC**A
ykuN1	T**GA**AAATCATTA**TC**A
ykuN2	T**GA**AAATCATTA**TC**A
yuiI (*besA*)	T**GA**AAATCATTA**TC**A
feuABCybbA	T**GA**TAATAGTTA**TC**A
yxeB	T**GA**TAATGATAA**TC**A
ydbN	T**GA**TTATCAATA**TC**G
yfiY	T**GA**TAATGAATT**TC**A
ybbB (*btr*)	T**GA**AAATGATTA**TC**A
fhuB/D	A**GA**GAATCATTA**TC**A
ywjA	T**GA**GAAATATTA**TC**A
yhfQ	T**GA**TAATGATTC**TC**A

yoaJ	T**GA**TAATGATTC**TC**A
ywbL (*efeU*)	T**GA**TAATCATTT**TC**A
yfmC (*fecC*)	T**GA**TAATGATTC**TC**A
yfkM	TT**A**GGCTAAGTA**TC**A
yclN (*fpbN*)	T**GA**TAATGATAA**TC**A
yfiZ	T**GA**GAATAATCC**TC**A
yusV1	T**GA**AAATGATTT**TC**A
yusV2	TCGGAATCATTTG**C**A
yfhC	T**GA**TAATCATTT**TC**A
pfeT1	T**GA**TAATTATTA**TC**A
pfeT2	T**GA**AGATGATTTA**C**G

23 Fur operator sites from Fur-regulated genes (numbers indicate the presence of multiple sites in a single regulatory region) were used to generate the sequence logo. The letters in bold represent the conserved signature bases that distinguish Fur operator sites from those regulated by PerR and Zur.

Table 4.2) List of PerR operator sites used to generate logo sequences

PerR regulated genes	OPERATOR SEQUENCE
mrgA	T**TA**TAATTATTA**TA**A
ahpC1	T**TA**GAATTATTA**T**TG
ahpC2	TA**A**TAATTCATA**TA**T
ahpC3	A**TA**TATTAATTAATA
katA	T**TA**TAATAATTA**TA**A
fur	T**TA**TAATAATTA**TA**G
perR1	T**TA**CACTAATTA**TA**A
perR2	T**TA**TAAACATTAC**A**A
hemAXCDBL1	T**TA**TAATTATTA**TA**A
hemAXCDBL2	T**TA**GAATGATTA**TA**A
pfeT	T**TA**AAATAATTA**TA**A

11 PerR operator sites from PerR-regulated genes (numbers indicate the presence of multiple sites in a single regulatory region) were used to generate the sequence logo. The letters in bold represent the conserved signature bases that distinguish PerR operator sites from those regulated by Fur and Zur.

Table 4.3) Strains and plasmids used in this study

STRAIN	GENOTYPE	REFERENCE
B. subtilis		
CU1065	W168 *attSP*β *trpC2*	Laboratory stock
ZB307A	W168 SPβ *c2*Δ*2*::Tn*917*::pSK10Δ6	Laboratory stock
HB18022	CU1065 SPβ *c2*Δ*2*::Tn*917*::φ(*pfeT-cat-lacZ*)	This work
HB2118	CU1065 *perR*::*kan* SPβ *c2*Δ*2*::Tn*917*::φ(*pfeT-cat-lacZ*)	(Fuangthong et al. 2002)
HB2111	CU1065 *fur*::*kan* SPβ *c2*Δ*2*::Tn*917*::φ(*pfeT-cat-lacZ*)	(Fuangthong et al. 2002)
HB2139	CU1065 *perR*::*spc fur*::*kan* SPβ *c2*Δ*2*::Tn*917*::φ(*pfeT-cat-lacZ*)	(Fuangthong & Helmann 2003)
HB8116	CU1065 *pfeT*::*kan* SPβ *c2*Δ*2*::Tn*917*::φ(*pfeT-cat-lacZ*)	Laboratory stock
HB18068	CU1065 SPβ *c2*Δ*2*::Tn*917*::φ(PI**pfeT-cat-lacZ*)	This work
HB18075	CU1065 SPβ *c2*Δ*2*::Tn*917*::φ(FII**pfeT-cat-lacZ*)	This work
HB18076	CU1065 SPβ *c2*Δ*2*::Tn*917*::φ(FIII**pfeT-cat-lacZ*)	This work
HB18074	CU1065 SPβ *c2*Δ*2*::Tn*917*::φ(FF***pfeT-cat-lacZ*)	This work
HB18127	CU1065 SPβ *c2*Δ*2*::Tn*917*::φ(FII*PI**pfeT-cat-lacZ*)	This work
HB18125	CU1065 SPβ *c2*Δ*2*::Tn*917*::φ(FIII*PI**pfeT-cat-lacZ*)	This work
HB18126	CU1065 SPβ *c2*Δ*2*::Tn*917*::φ(3**pfeT-cat-lacZ*)	This work
HB18228	CU1065 Δ*katA*, *ahpCF*::*kan*	This work
HB18220	CU1065 Δ*katA*, *ahpCF*::*kan* SPβ *c2*Δ*2*::Tn*917*::φ(*pfeT-cat-lacZ*)	This work
HB18221	CU1065 Δ*katA*, *ahpCF*::*kan* SPβ *c2*Δ*2*::Tn*917*::φ(PI**pfeT-cat-lacZ*)	This work
HB18222	CU1065 Δ*katA*, *ahpCF*::*kan* SPβ *c2*Δ*2*::Tn*917*::φ(FII**pfeT-cat-lacZ*)	This work
HB18223	CU1065 Δ*katA*, *ahpCF*::*kan* SPβ *c2*Δ*2*::Tn*917*::φ(FIII**pfeT-cat-lacZ*)	This work
HB18224	CU1065 Δ*katA*, *ahpCF*::*kan* SPβ *c2*Δ*2*::Tn*917*::φ(FF***pfeT-cat-lacZ*)	This work
HB18225	CU1065 Δ*katA*, *ahpCF*::*kan* SPβ *c2*Δ*2*::Tn*917*::φ(FII*PI**pfeT-cat-lacZ*)	This work
HB18226	CU1065 Δ*katA*, *ahpCF*::*kan* SPβ *c2*Δ*2*::Tn*917*::φ(FIII*PI**pfeT-cat-lacZ*)	This work
HB18227	CU1065 Δ*katA*, *ahpCF*::*kan* SPβ *c2*Δ*2*::Tn*917*::φ(3**pfeT-cat-lacZ*)	This work
E. coli		
DH5α	φ80*lacZ*ΔM15 *recA1 endA1 gyrA96 thi-1 hsdR17*(rK-mK+)*supE44 relA1 deoR* Δ(*lacZYA-argF*)U169	Laboratory stock
PLASMID	**DESCRIPTION**	**REFERENCE**
pJPM122	*cat-lacZ* operon fusion vector for SPβ.	(Slack et al. 1993)
pDR244	For removal of the erythromycin resistance cassette to	(Koo et al.

	generate in-frame deletions.	2017)
pET17b	Used as template for the IVT ladder.	Laboratory stock

Table 4.4) Oligonucleotides used in this study

NUMBER	NAME	SEQUENCE
6927	IVT pfeT-F	GCAAACAAGCTGACGTTTCCGATTGTCCTT
6928	IVT pfeT-R	TTTCCCTCTTGTCTGTTTTCAATGGCTCATG
7115	IVT frvA-F	CAGTGGTTGGTACAATGAATCCAGGAAGAA
7116	IVT frvA-R	CAACATCACTACCGACCAAACAGCCAAT
9052	IVT ladder F1	GCCGCAGTGTTATCACTCATGGT
9053	IVT ladder R1	TGGTTGAGTACTCACCAGTCACAGAA
9054	IVT ladder R2	AGCACTTTTAAAGTTCTGCTATGTGGCG
9055	IVT ladder R3	TGCTGAAGATCAGTTGGGTGCAC
7277	bgal-pfeT-F	GCCAAGCTTCCCAACATCATTTTTGCTGAAT
7278	bgal-pfeT-R	GCGGATCCGGGTCGCGTTGAACGATAA
9002	EMSA pfeT-F	GCTGAGAGCATAGACTCTCAGCTTT
7032	pointPI-F	TGATAATTATTATCAAAAAGAAATTAATTAATAATTAATT GAAATTCTCTTCGT
7174	pointPI-R	TTAATTATTAATTAATTTCTTTTTGATAATAATTATCATTA ATGTTTATTCACTTC
7352	pointFIII-F	GTTTTTATAAGAGAAACTTAGTAGTAATAAGTTCTCAAT TAGAGA
7353	pointFIII-R	CTTATTACTACTAAGTTTCTCTTATAAAAAC
7440	pointFII-F	GAAGAAGTGAATAAACATTAACTTTATATTACAAAAAAA AGAAA
7351	pointFII-R	TTTTGTAATATAAAGTTAATGTTTATTCACTTCTTC
9094	katA check-F	CACTTACTCTGCTTGTTTCGCAA
9093	katA check-R	GAACACCGAAGGCTCTTATCGTT
6326	BKE MLS check R	TTTTCTCGTTCATAGTAGTTCCTCC
535a	pJPM122 check F	GTACATATTGTCGTTAGAACGCGGC
366	pJPM122 check R	ACTCTCCGTCGCTATTGTAACCAG

4.7 References

1. Andrews SC, Robinson AK, Rodríguez-Quiñones, F. 2003. Bacterial iron homeostasis. FEMS Microbiol Rev 27:215-37.

2. Cornelis P, Andrews SC (ed). 2010. Iron Uptake and Homeostasis in Microorganisms. Caister Academic Press.

3. Pi H, Helmann JD. 2017. Ferrous iron efflux systems in bacteria. Metallomics 9:840-851.

4. Guan G, Pinochet-Barros A, Gaballa A, Patel SJ, Argüello JM, Helmann JD. 2015. PfeT, a P_{1B4} -type ATPase, effluxes ferrous iron and protects *Bacillus subtilis* against iron intoxication. Mol Microbiol 98:787-803.

5. Bhubhanil S, Chamsing J, Sittipo P, Chaoprasid P, Sukchawalit R, Mongkolsuk S. 2014. Roles of *Agrobacterium tumefaciens* membrane-bound ferritin (MbfA) in iron transport and resistance to iron under acidic conditions. Microbiology 160:863-71.

6. Sankari S, O'Brian MR. 2014. A bacterial iron exporter for maintenance of iron homeostasis. J Biol Chem 289:16498-507.

7. Frawley ER, Crouch ML, Bingham-Ramos LK, Robbins HF, Wang W, Wright GD, Fang FC. 2013. Iron and citrate export by a major facilitator superfamily pump regulates metabolism and stress resistance in *Salmonella Typhimurium*. Proc Natl Acad Sci U S A 110:12054-9.

8. Frawley ER, Fang FC. 2014. The ins and outs of bacterial iron metabolism. Mol Microbiol 93:609-16.

9. Pi H, Patel SJ, Argüello JM, Helmann JD. 2016. The *Listeria monocytogenes* Fur-regulated virulence protein FrvA is an Fe(II) efflux P_{1B4}-type ATPase. Mol Microbiol 100:1066-79.

10. McLaughlin HP, Xiao Q, Rea RB, Pi H, Casey PG, Darby T, Charbit A, Sleator RD, Joyce SA, Cowart RE, Hill C, Klebba PE, Gahan CG. 2012. A putative P-type ATPase required for virulence and resistance to haem toxicity in *Listeria monocytogenes*. PLoS One 7:e30928.

11. Patel SJ, Lewis BE, Long JE, Nambi S, Sassetti CM, Stemmler TL, Arguello JM. 2016. Fine-tuning of Substrate Affinity Leads to Alternative Roles of *Mycobacterium tuberculosis* Fe^{2+}-ATPases. J Biol Chem 291:11529-39.

12. VanderWal AR, Makthal N, Pinochet-Barros A, Helmann JD, Olsen RJ, Kumaraswami M. 2017. Iron Efflux by PmtA Is Critical for Oxidative Stress Resistance and Contributes Significantly to Group A *Streptococcus* Virulence. Infect Immun 85. pii: e00091-17.

13. Silva-Gomes S, Vale-Costa S, Appelberg R, Gomes MS. 2013. Iron in intracellular infection: to provide or to deprive? Front Cell Infect Microbiol 3:96.

14. Imlay JA. 2013. The molecular mechanisms and physiological consequences of oxidative stress: lessons from a model bacterium. Nat Rev Microbiol 11:443-54.

15. Chen L, Keramati L, Helmann JD. 1995. Coordinate regulation of *Bacillus subtilis* peroxide stress genes by hydrogen peroxide and metal ions. Proc Natl Acad Sci U S A 92:8190-4.

16. Faulkner MJ, Helmann JD. 2011. Peroxide stress elicits adaptive changes in bacterial metal ion homeostasis. Antioxid Redox Signal 15:175-89.

17. Helmann JD, Wu MF, Gaballa A, Kobel PA, Morshedi MM, Fawcett P, Paddon C. 2003. The global transcriptional response of *Bacillus subtilis* to peroxide stress is coordinated by three transcription factors. J Bacteriol 185:243-53.

18. Chen L, Helmann JD. 1995. *Bacillus subtilis* MrgA is a Dps(PexB) homologue: evidence for metalloregulation of an oxidative-stress gene. Mol Microbiol 18:295-300.

19. Gaballa A, Helmann JD. 2002. A peroxide-induced zinc uptake system plays an important role in protection against oxidative stress in *Bacillus subtilis*. Mol Microbiol 45:997-1005.

20. Helmann JD. 2014. Specificity of metal sensing: iron and manganese homeostasis in *Bacillus subtilis*. J Biol Chem 289:28112-20.

21. Herbig AF, Helmann JD. 2001. Roles of metal ions and hydrogen peroxide in modulating the interaction of the *Bacillus subtilis* PerR peroxide regulon repressor with operator DNA. Mol Microbiol 41:849-59.

22. Lee JW, Helmann JD. 2006. The PerR transcription factor senses H_2O_2 by metal-catalysed histidine oxidation. Nature 440:363-7.

23. Jacquamet L, Traore DA, Ferrer JL, Proux O, Testemale D, Hazemann JL, Nazarenko E, El Ghazouani A, Caux-Thang C, Duarte V, Latour JM. 2009. Structural characterization of the active form of PerR: insights into the metal-induced activation of PerR and Fur proteins for DNA binding. Mol Microbiol 73:20-31.

24. Fuangthong M, Helmann JD. 2003. Recognition of DNA by three ferric uptake regulator (Fur) homologs in *Bacillus subtilis*. J Bacteriol 185:6348-57.

25. Huang X, Shin JH, Pinochet-Barros A, Su TT, Helmann JD. 2017. *Bacillus subtilis* MntR coordinates the transcriptional regulation of manganese uptake and efflux systems. Mol Microbiol 103:253-268.

26. Ma Z, Chandrangsu P, Helmann TC, Romsang A, Gaballa A, Helmann JD. 2014. Bacillithiol is a major buffer of the labile zinc pool in *Bacillus subtilis*. Mol Microbiol 94:756-70.

27. Moore CM, Gaballa A, Hui M, Ye RW, Helmann JD. 2005. Genetic and physiological responses of *Bacillus subtilis* to metal ion stress. Mol Microbiol 57:27-40.

28. Faulkner MJ, Ma Z, Fuangthong M, Helmann JD. 2012. Derepression of the *Bacillus subtilis* PerR peroxide stress response leads to iron deficiency. J Bacteriol 194:1226-35.

29. Fuangthong M, Herbig AF, Bsat N, Helmann JD. 2002. Regulation of the B*acillus subtilis fur* and *perR* genes by PerR: not all members of the PerR regulon are peroxide inducible. J Bacteriol 184:3276-86.

30. Ji CJ, Kim JH, Won YB, Lee YE, Choi TW, Ju SY, Youn H, Helmann JD, Lee JW. 2015. *Staphylococcus aureus* PerR Is a Hypersensitive Hydrogen Peroxide Sensor using Iron-mediated Histidine Oxidation. J Biol Chem 290:20374-86.

31. Ma Z, Lee JW, Helmann JD. 2011. Identification of altered function alleles that affect *Bacillus subtilis* PerR metal ion selectivity. Nucleic Acids Res 39:5036-44.

32. Park S, You X, Imlay JA. 2005. Substantial DNA damage from submicromolar intracellular hydrogen peroxide detected in Hpx- mutants of *Escherichia coli*. Proc Natl Acad Sci U S A 102:9317-22.

33. Ma Z, Faulkner MJ, Helmann JD. 2012. Origins of specificity and cross-talk in metal ion sensing by *Bacillus subtilis* Fur. Mol Microbiol 86:1144-55.

34. Ledala N, Sengupta M, Muthaiyan A, Wilkinson BJ, Jayaswal RK. 2010. Transcriptomic response of *Listeria monocytogenes* to iron limitation and Fur mutation. Appl Environ Microbiol 76:406-16.

35. Rea R, Hill C, Gahan CG. 2005. *Listeria monocytogenes* PerR mutants display a small-colony phenotype, increased sensitivity to hydrogen

peroxide, and significantly reduced murine virulence. Appl Environ Microbiol 71:8314-22.

36. Neilands JB. 1991. A brief history of iron metabolism. Biol Met 4:1-6.

37. Brenot A, King KY, Caparon MG. 2005. The PerR regulon in peroxide resistance and virulence of *Streptococcus pyogenes.* Mol Microbiol 55:221-34.

38. Raimunda D, Long JE, Padilla-Benavides T, Sassetti CM, Argüello JM. 2014. Differential roles for the Co^{2+}/Ni^{2+} transporting ATPases, CtpD and CtpJ, in *Mycobacterium tuberculosis* virulence. Mol Microbiol 91:185-97.

39. Lee JW, Helmann JD. 2007. Functional specialization within the Fur family of metalloregulators. Biometals 20:485-99.

40. Baichoo N, Wang T, Ye R, Helmann JD. 2002. Global analysis of the *Bacillus subtilis* Fur regulon and the iron starvation stimulon. Mol Microbiol 45:1613-29.

41. Pi H, Helmann JD. 2018. Genome-Wide Characterization of the Fur Regulatory Network Reveals a Link between Catechol Degradation and Bacillibactin Metabolism in *Bacillus subtilis*. MBio 9. pii: e01451-18.

42. Gaballa A, Antelmann H, Aguilar C, Khakh SK, Song KB, Smaldone GT, Helmann JD. 2008. The *Bacillus subtilis* iron-sparing response is mediated by a Fur-regulated small RNA and three small, basic proteins. Proc Natl Acad Sci U S A 105:11927-32.

43. Smaldone GT, Antelmann H, Gaballa A, Helmann JD. 2012. The FsrA sRNA and FbpB protein mediate the iron-dependent induction of the *Bacillus subtilis lutABC* iron-sulfur-containing oxidases. J Bacteriol 194:2586-93.

44. Smaldone GT, Revelles O, Gaballa A, Sauer U, Antelmann H, Helmann JD. 2012. A global investigation of the *Bacillus subtilis* iron-sparing response identifies major changes in metabolism. J Bacteriol 194:2594-605.

45. Seo SW, Kim D, Latif H, O'Brien EJ, Szubin R, Palsson BO. 2014. Deciphering Fur transcriptional regulatory network highlights its complex role beyond iron metabolism in *Escherichia coli*. Nat Commun 5:4910.

46. Teixidó L, Carrasco B, Alonso JC, Barbé J, Campoy S. 2011. Fur activates the expression of *Salmonella enterica* pathogenicity island 1 by directly interacting with the *hilD* operator *in vivo* and *in vitro*. PLoS One 6:e19711.

47. Delany I, Rappuoli R, Scarlato V. 2004. Fur functions as an activator and as a repressor of putative virulence genes in *Neisseria meningitidis*. Mol Microbiol 52:1081-90.

48. Horsburgh MJ, Ingham E, Foster SJ. 2001. In *Staphylococcus aureus*, Fur is an interactive regulator with PerR, contributes to virulence, and is

necessary for oxidative stress resistance through positive regulation of catalase and iron homeostasis. J Bacteriol 183:468-75.

49. Gunshin H, Mackenzie B, Berger UV, Gunshin Y, Romero MF, Boron WF, Nussberger S, Gollan JL, Hediger MA. 1997. Cloning and characterization of a mammalian proton-coupled metal-ion transporter. Nature 388:482-8.

50. Knutson MD, Oukka M, Koss LM, Aydemir F, Wessling-Resnick M. 2005. Iron release from macrophages after erythrophagocytosis is up-regulated by ferroportin 1 overexpression and down-regulated by hepcidin. Proc Natl Acad Sci U S A 102:1324-8.

51. Palmer LD, Skaar EP. 2016. Transition Metals and Virulence in Bacteria. Annu Rev Genet 50:67-91.

52. Munson GP, Holcomb LG, Scott JR. 2001. Novel group of virulence activators within the AraC family that are not restricted to upstream binding sites. Infect Immun 69:186-93.

53. Escolar L, Pérez-Martín J, de Lorenzo V. 1998. Binding of the Fur (ferric uptake regulator) repressor of *Escherichia coli* to arrays of the GATAAT sequence. J Mol Biol 283:537-47.

54. Escolar L, Pérez-Martín J, de Lorenzo V. 1999. Opening the iron box: transcriptional metalloregulation by the Fur protein. J Bacteriol 181:6223-9.

55. Koo BM, Kritikos G, Farelli JD, Todor H, Tong K, Kimsey H, Wapinski I, Galardini M, Cabal A, Peters JM, Hachmann AB, Rudner DZ, Allen KN, Typas A, Gross CA. 2017. Construction and Analysis of Two Genome-Scale Deletion Libraries for *Bacillus subtilis*. Cell Syst 4:291-305 e7.

56. Harwood CR, Cutting SM. 1990. Molecular biological methods for *Bacillus*. Wiley, Chichester.

57. Slack FJ, Mueller JP, Sonenshein AL. 1993. Mutations that relieve nutritional repression of the *Bacillus subtilis* dipeptide permease operon. J Bacteriol 175:4605-14.

58. Miller JH. 1972. Experiments in molecular genetics. Cold Spring Harbor Laboratory, Cold Spring Harbor, N.Y.

59. Gaballa A, MacLellan S, Helmann JD. 2012. Transcription activation by the siderophore sensor Btr is mediated by ligand-dependent stimulation of promoter clearance. Nucleic Acids Res 40:3585-95.

Chapter 5

The MntR Regulon Impacts Iron Homeostasis and Oxidative Stress in *Bacillus subtilis*

> "*There was a definite pattern there somewhere, but he just couldn't quite grasp it… Momentarily overcome by exhaustion, Mendeleyev leaned forward, resting his shaggy head on his arms. Almost immediately he fell asleep, and had a dream.*"
>
> *- Paul Strathern, Mendeleyev's Dream, 2019.*

5.1 Abstract

Homeostasis of the essential element manganese (Mn^{2+}) is maintained in *Bacillus subtilis* by the MntR metalloregulator. This Mn^{2+}-sensing, DNA-binding bi-functional regulator represses expression of Mn^{2+} import and directly activates transcription of two cation diffusion facilitator (CDF) Mn^{2+} efflux pumps, MneP and MneS. An *mntR* null mutant is highly sensitive to Mn^{2+}, resulting from derepression of import and an inability to express efflux genes. Ferrous iron (Fe^{2+}) efflux in *B. subtilis* occurs through PfeT, which is under transcriptional control of two Fur family metalloregulators: Fur (ferric uptake regulator) and PerR (peroxide stress regulator). A *pfeT* null strain is very Fe^{2+} sensitive and previous studies show that high iron media amended with Mn^{2+} helps alleviate this toxicity. Unexpectedly, in an *mntR* null mutant we see iron sensitivity caused by drastic iron accumulation, which is exacerbated in an *mntR pfeT* double null mutant. Moreover, we see Mn^{2+}-dependent peroxide

(H_2O_2) sensitivity and an *mntR* null mutant is more sensitive to H_2O_2 than an *mntR pfeT* double null strain. We propose that these effects on Fe^{2+} and H_2O_2 sensitivity arise from dysregulation of the MntR regulon that impacts iron homeostasis and the PerR regulon. We show that MneP and MneS act as iron as well as manganese efflux pumps, and that derepression of Mn^{2+} import favors PerR:Mn^{2+} metallation, which increases repression of *katA, ahpCF*, and *mrgA*.

5.2 Introduction

Homeostasis of the essential transition element iron (Fe^{2+}) in *Bacillus subtilis* is maintained by Fur family metalloregulators Fur and PerR (1,2). The ferric uptake repressor Fur is the primary iron sensing metalloregulator that represses transcription of genes encoding iron acquisition proteins under iron replete conditions (3-5). Under these same conditions, Fur indirectly activates expression of abundant iron-sulfur containing enzymes like LutABC through repression of the translational repressor small RNA FsrA (6). Moreover, under iron overload conditions, Fur is a direct transcriptional activator of the P_{1B4}-type ATPase iron efflux pump PfeT (see Chapter 4).

In *B. subtilis,* the adaptive response to hydrogen peroxide (H_2O_2) stress is coordinated by PerR. Similarly to Fur, PerR binds Fe^{2+} (and Mn^{2+}) at its metal-sensing site to repress gene expression (7,8). The PerR oxidative stress response is comprised of genes that directly detoxify H_2O_2 (like catalase KatA,

and alkyl hydroperoxide reductase AhpCF) and those that alleviate toxicity by impacting iron levels (1,9). The latter include MrgA (a dodecameric mini-ferritin that sequesters iron from the cytosol in the presence of oxidant) (10), the heme biosynthetic pathway HemAXCDBL (which is an iron utilizing cofactor required for KatA catalytic function), the iron metalloregulator Fur, and the iron efflux pump PfeT (11).

Manganese (Mn^{2+}) is commonly considered as an antioxidant that can help rescue cells undergoing oxidative stress (12). This is likely attributed to the fact that Mn^{2+} is not redox active under typical cytosolic conditions and can thereby serve as an alternative cofactor for some iron-mononuclear enzymes that have been oxidized (13,14). Additionally, Mn^{2+} is important for activity of Mn^{2+}-utilizing superoxide dismutase (15). In the iron-centric bacterium *E. coli*, Mn^{2+} uptake takes place through the proton-coupled importer of the NRAMP family, MntH, which is controlled by the main oxidative stress regulator OxyR (12,16,17). This provides an easy route for Mn^{2+} acquisition and maintenance of cellular enzymatic function.

Unlike *E. coli*, Mn^{2+} is an essential micronutrient in *B. subtilis* required for many important cellular processes including DNA synthesis and replication as well as central carbon metabolism (18). Mn^{2+} homeostasis in *B. subtilis* is controlled by MntR, a DtxR family regulator (19). MntR is a homodimeric protein with an N-terminal DNA binding domain and a C-terminal domain involved in the dimerization of the two monomers (20). Each subunit binds to

two Mn^{2+} ions at the metal sensing sites known as sites A and C. Classical DtxR regulators are involved in iron sensing (21). Homologue comparative studies have pinpointed two residue differences at the metal sensing sites in MntR that determine metal selectivity, namely D8 and E99. Mutational experiments reverting these residues to the equivalent DtxR amino acids in *Corynebacterium diphtheriae* allow MntR to be iron responsive *in vivo* (22).

A role for *B. subtilis* MntR in Mn^{2+} homeostasis was first proposed when *mntR* null strains were shown to be highly sensitive to Mn^{2+} compared to wild-type (WT) cells (19). Later work showed that this high sensitivity is partly due to derepression of Mn^{2+} import as Mn^{2+}-bound MntR represses expression of MntH and an ABC transporter (MntABC) (19,23). However, further transcriptomic analysis of the Mn^{2+} stimulon in *mntR* null and WT cells, as well as an inability to restore Mn^{2+} resistance in an *mntR mntH mntA* triple mutant, indicated that there are additional genes under MntR control (24). This led to the discovery of two cation diffusion facilitator (CDF) Mn^{2+} efflux pumps, MneP and MneS, which are transcriptionally activated directly by Mn^{2+}-bound MntR. Although both efflux pumps are required for survival under Mn^{2+} overload conditions, MneP acts as the primary efflux pump, whilst MneS plays a secondary role (24).

In past work, PfeT was identified as a major iron efflux pump in *B. subtilis* (11). Mutants lacking PfeT are very sensitive under iron overload conditions and amending the media with micromolar levels of Mn^{2+} helps

restore resistance (11). Unexpectedly, when we tested iron sensitivity in an *mntR* null mutant, cells were very sensitive and in an *mntR pfeT* double mutant this effect was additive. Moreover, *mntR* null mutants also appear to be highly sensitive to H_2O_2. Accumulation of Mn^{2+} has been previously observed to potentiate this sensitivity in *B. subtilis* (19,25) and recently in *S. aureus* (26). However, the reason for this remains unclear.

Here we propose a model in which dysregulation of the MntR regulon both impacts iron homeostasis and sensitizes the cell to oxidative stress. We show that iron sensitivity is due to the ability of MneP and particularly MneS to act as iron efflux pumps. However, H_2O_2 sensitivity is primarily due to derepression of Mn^{2+} import and not the inability to efflux iron through MneP and MneS. We provide a mechanism of mangano-oxidative stress toxicity wherein Mn^{2+} accumulation causes shutdown of the PerR regulon due to tight repression by a now predominantly Mn^{2+}-metallated and redox unresponsive PerR.

5.3 Results

5.3.1 An *mntR* mutation strain is very iron sensitive

A *B. subtilis pfeT* mutant strain is sensitive to iron overload as monitored by the zone of growth inhibition in a disk diffusion assay (11). As previously observed, iron sensitivity in a *pfeT* mutant is characterized by an increase in the inner zone of growth inhibition compared to wild-type (WT), as

well as a large zone of lower density (ZOLD) which is absent in WT cells (Fig. 5.1A & B). These zones were also quantified using Image J as a function of pixel density (Fig. 5.1C).

Prior work showed that micromolar levels of Mn^{2+} help restore resistance in iron sensitive cells. We therefore tested iron sensitivity in *mntR* mutant strains as they accumulate intracellular Mn^{2+}. Surprisingly, cells lacking MntR have an even larger inner zone of inhibition than *pfeT* mutants (Fig. 5.1A). Iron sensitivity in a *pfeT mntR* double mutant is additive for not only is the inner zone of inhibition comparable to that of an *mntR* mutant, but there is also an even more pronounced ZOLD (Fig. 5.1A-C).

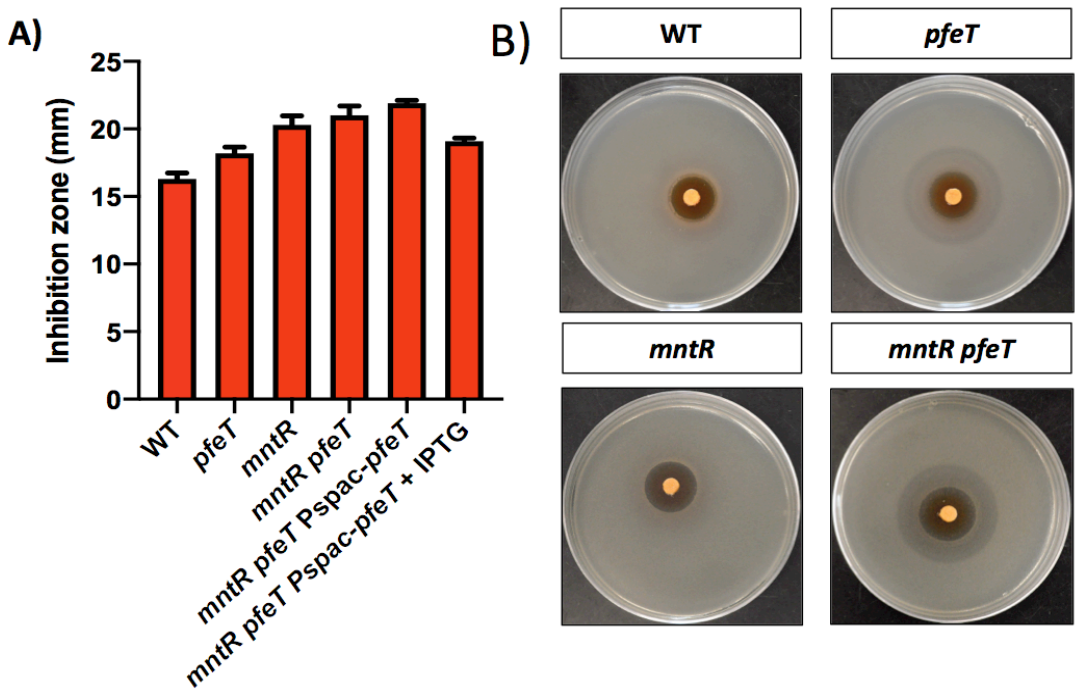

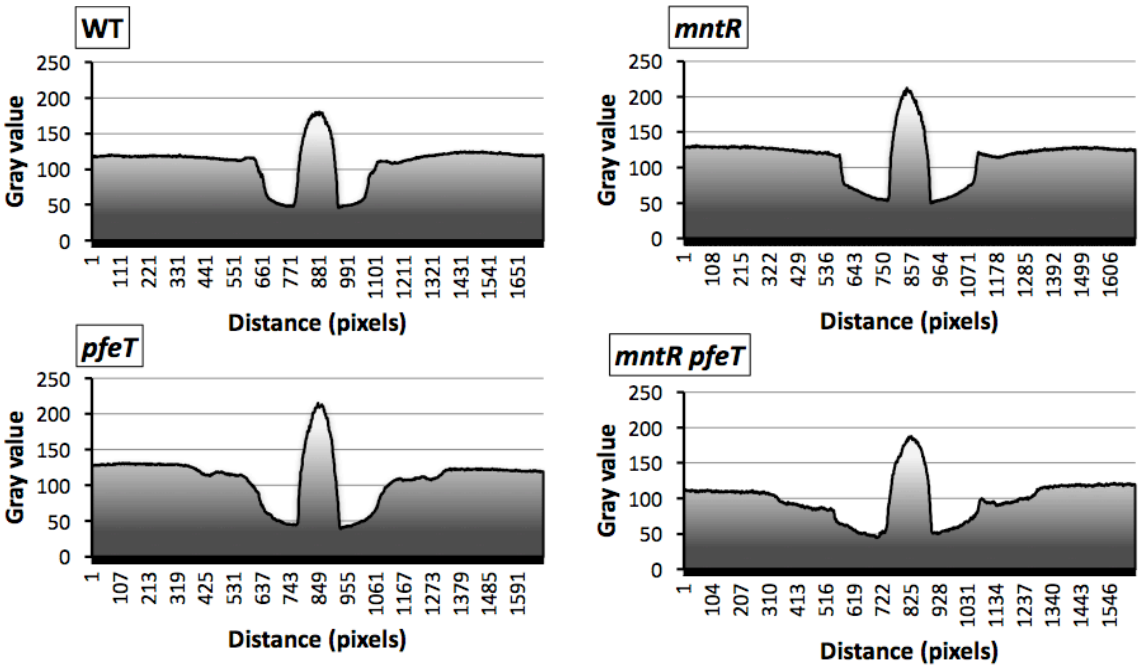

FIG. 5.1) *mntR* and *mntR pfeT* mutants are sensitive to iron.
A) Sensitivity of WT, *pfeT, mntR,* and *pfeT mntR* mutant to Fe^{2+} as monitored using a disk diffusion (zone of inhibition) assay. The results are expressed as the diameter of the inhibition zone (mm) and were repeated more than three times.
B) Representative images of the zone of inhibition plates showing the inner zone of sensitivity and the ZOLD for each strain.
C) Histogram showing pixel density (as grey value) across zone of inhibition plates containing respective strains. Pixel density represents cell density, highlighting the variations in ZOLD, as well as the inner zones of growth inhibition.

5.3.2 Iron sensitivity in an *mntR* mutant is not due to deprepression of manganese import

In an *mntR* mutant, manganese import genes *mntH* and *mntA* are derepressed. In *B. subtilis*, these are primarily involved in Mn^{2+} uptake, but orthologs in other organisms have been shown to also import Fe^{2+} (27-32). We therefore tested *mntH* and *mntA* mutants in strains lacking MntR to see if resistance would be restored under high iron conditions. Both *mntR mntH* and

mntR mntA strains are just as iron sensitive as an *mntR* mutant (Fig. 5.2). In addition to this, an *mntH* mutant was also tested in iron sensitive *pfeT* and *mntR pfeT* mutant backgrounds. In both cases, cells remained equally iron sensitive (Fig. 5.2).

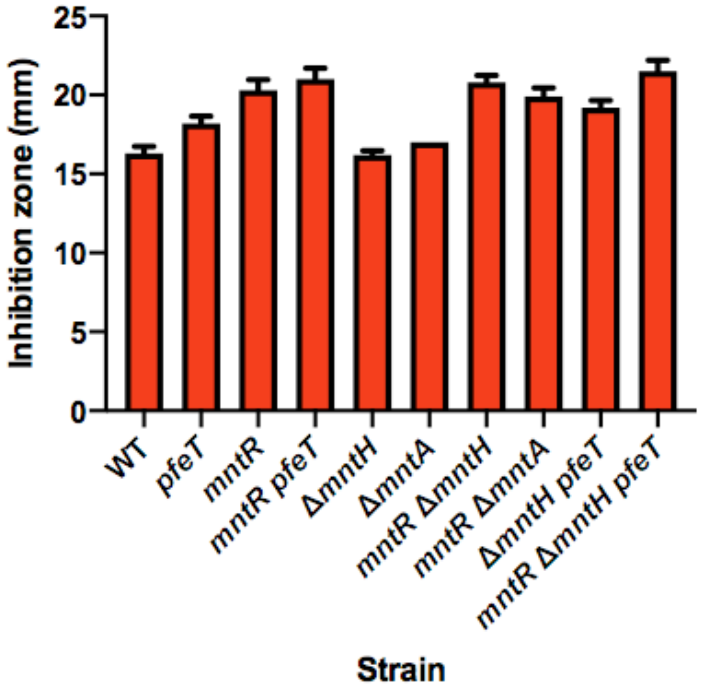

FIG. 5.2) Manganese importers do not contribute to iron sensitivity.
Iron zone of inhibition assays were carried out on strains mutated for manganese import systems. Data is representative of more than three biological replicates.

5.3.3 Mutants lacking manganese efflux genes are iron sensitive

Having ruled out MntH and MntA as a possible source of iron uptake that would lead to iron sensitivity in *mntR* mutant strains, we tested the effect of CDF Mn^{2+} efflux pumps MneP and MneS. If either of these pumps is involved in iron efflux, null strains should be more iron sensitive due to the

intracellular accumulation of the metal ion. This level of iron accumulation might be enough to cause iron sensitivity even in the presence of PfeT, since the affinity of the P_{1B4}-type ATPase is relatively low, with a $K_{1/2}$ of 520 ± 120 μM (11).

Previously in Huang et al. 2017, iron sensitivity was detected in an *mneP mneS* double null strain. Here we confirmed this phenotype and note that iron sensitivity as measured by the inner zone of growth inhibition is comparable to that of a *pfeT* mutant. However, when we tested *mneP* and *mneS* single mutants to determine if the sensitivity could be attributed to one of these CDF exporters, iron sensitivity was the same as in WT cells (Fig. 5.3A). Furthermore, neither *mneP* or *mneS* is induced by iron (Fig. 5.3D). An *mntR mneP mneS* triple mutant phenocopies an *mntR* mutant, suggesting that iron sensitivity in cells lacking MntR is due to an inability to activate expression of *mneP* and *mneS* (24). Indeed, ectopic expression of either *mneP* or *mneS* lowered iron sensitivity almost back to WT levels (Fig. 5.3B), although only *mneS* expression abolishes the *mntR pfeT* ZOLD (Fig. 5.3C). Finally, iron sensitivity in strains lacking all three efflux pumps (a *pfeT mneP mneS* triple mutant) is additive and phenocopies an *mntR pfeT* strain (Fig. 5.3A).

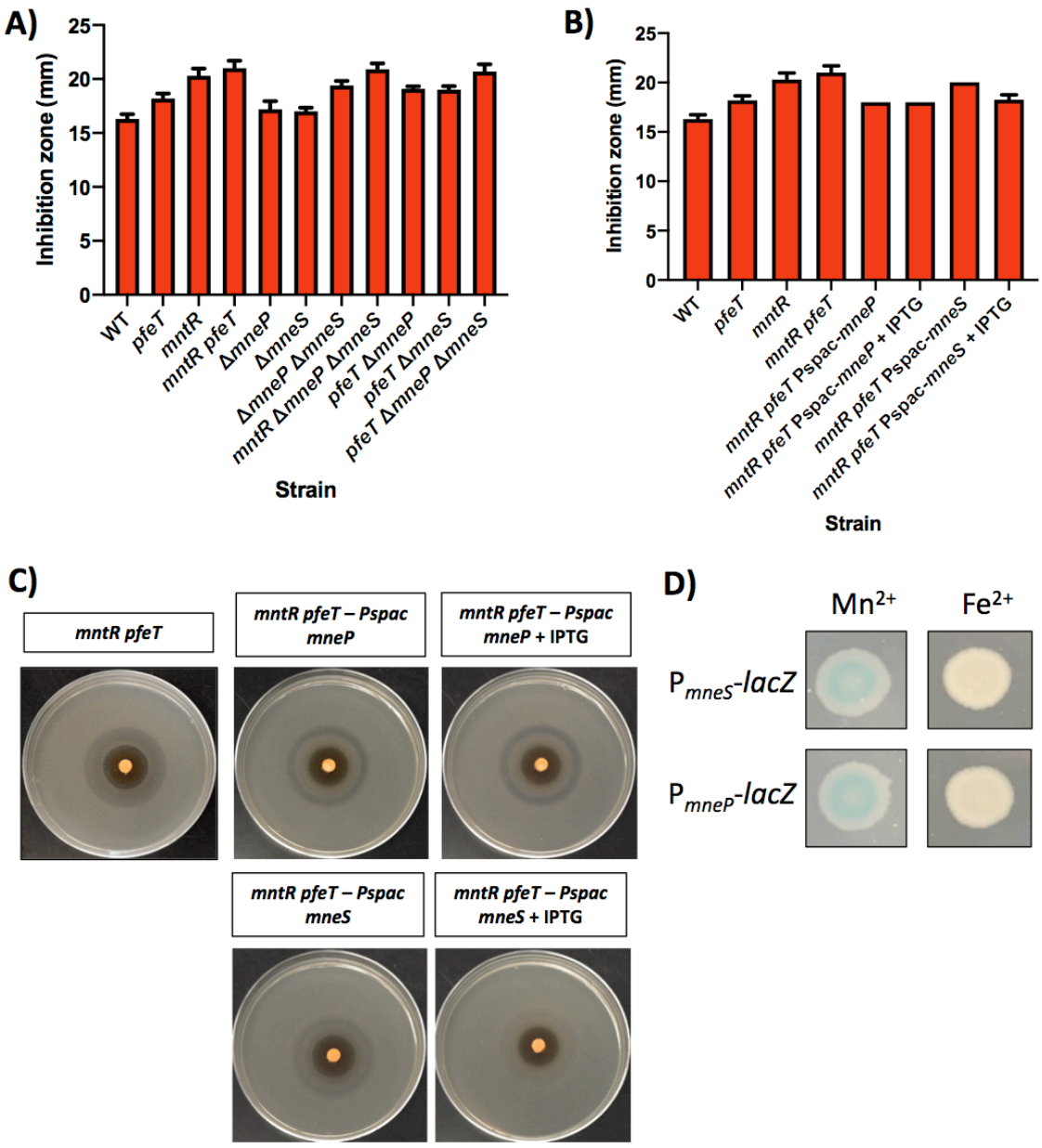

FIG. 5.3) MneP and MneS contribute to iron resistance.
A) Iron zone of inhibition assays were performed on a combination of strains lacking MneP and MneS.
B) Ectopic expression of *mneP* and *mneS* in an *mntR pfeT* mutant background show increased iron resistance as per the zone of inhibition assay.
C) Representative images of plates used in (B).
D) Spot plating of WT cells containing transcriptional *lacZ* fusions of *mneP* and *mneS* onto LB plates containing X-Gal and either 250 µM $MnCl_2$ or 300 µM $FeSO_4$.
Data is representative of more than three biological replicates.

5.3.4 Iron sensitivity in an *mntR* mutant is due to intracellular iron accumulation

Previously we constructed a transcriptional *pfeT-lacZ* fusion that acts as a bioreporter for sensing increasing intracellular iron levels (Chapter 4). We transduced this bioreporter into an *mntR* mutant and *mntR pfeT* double mutant background to compare it against a WT and *pfeT* mutant strain. As expected, promoter activity increases as a function of iron concentration in a WT background and this induction curve shifts to the left in a *pfeT* mutant (Fig. 5.4A). In *mntR* mutant cells, *pfeT* induction is slightly higher than in a *pfeT* mutant, which can be explained by an inability to efflux iron through MneP and MneS, both of which are expressed at a low basal level in the absence of MntR. An *mntR pfeT* double mutant shows an even steeper curve of induction. This and the high iron sensitivity seen in an *mntR pfeT* and a *pfeT mneP mneS* strain (Fig. 5.4A), support a model of two different pathways of iron export.

We further assessed intracellular iron accumulation by measuring streptonigrin (SN) sensitivity. SN is a quinone antibiotic whose bactericidal activity is correlated with intracellular iron availability (33). A *pfeT* mutant is more sensitive to SN when grown in LB amended with 100 μM Fe^{2+} compared to WT (Fig. 5.4C). An *mntR* mutant is also SN sensitive, even in conditions where iron was not added to the media (Fig.5.4B & C). It's possible that an *mntR* mutant shows higher SN sensitivity and slightly higher level of *pfeT*

induction compared to a *pfeT* mutant because of *mntH* and *mntA* derepression. Influx of Mn^{2+} could lead to partial repression of the PerR regulon, including *pfeT* (34), inadvertently causing a slightly higher increase in Fe^{2+} accumulation, which is even higher in the absence of PfeT in the *mntR* mutant background (Fig.5.4B & C).

The high SN sensitivity in *mntR pfeT* mutant cells grown in LB + 100 µM Fe^{2+} is lowered when iron efflux pump *pfeT* is ectopically expressed (Fig.5.4B & C). If MneP and MneS also function as iron efflux pumps they should show a similar phenotype. In both cases, ectopic expression partially recovers SN resistance in the presence of Fe^{2+} (Fig. 5.4D & E).

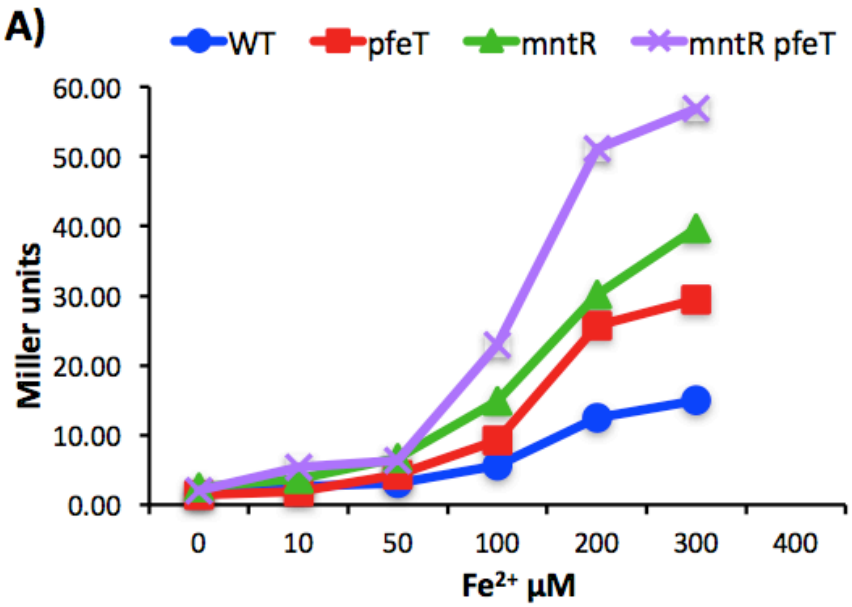

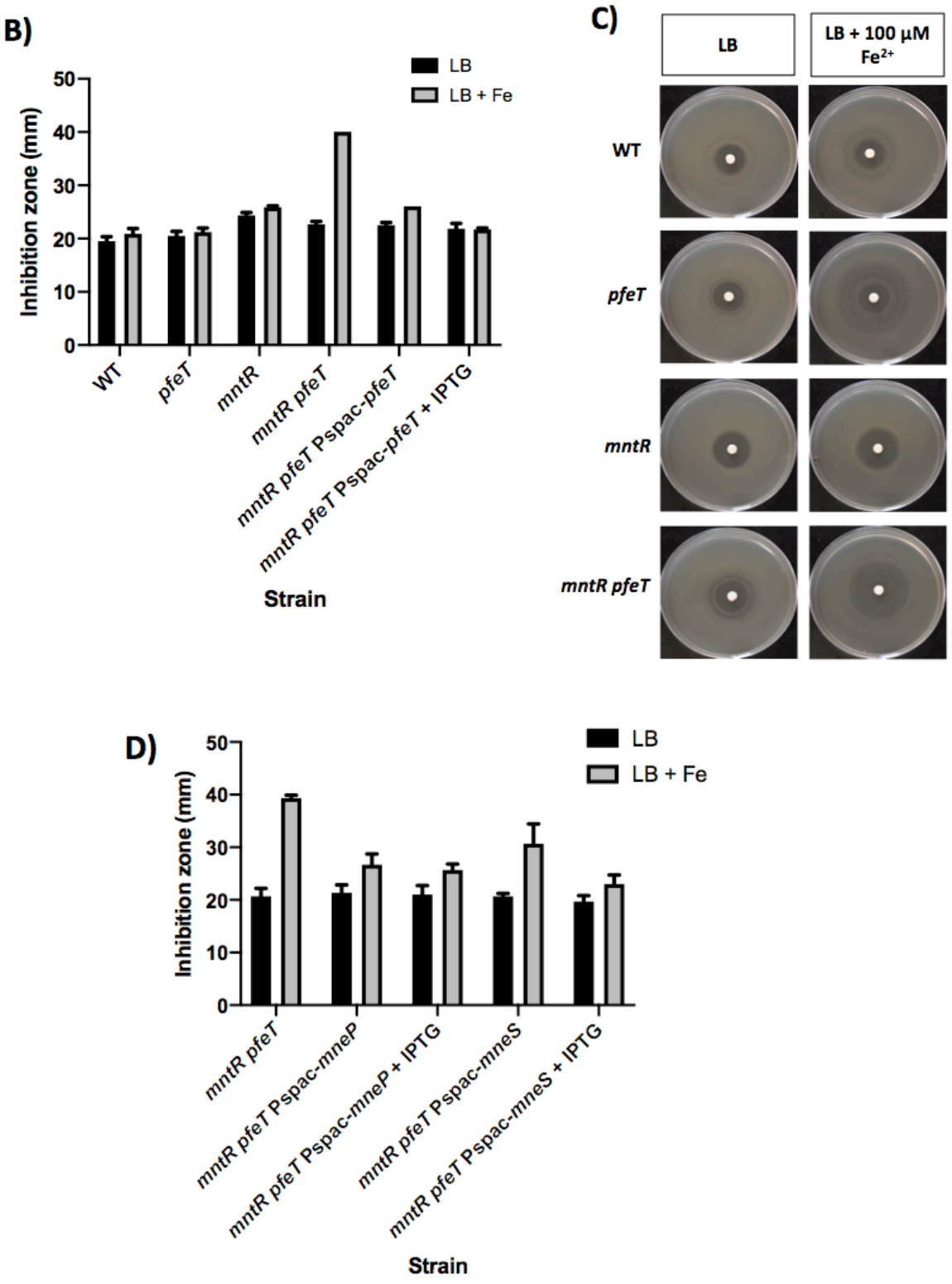
B)
LB
LB + Fe
Inhibition zone (mm)
50
40
30
20
10
0
WT
pfeT
mntR
mntR pfeT
mntR pfeT Pspac-pfeT
mntR pfeT Pspac-pfeT + IPTG
Strain
C)
LB
LB + 100 µM Fe2+
WT
pfeT
mntR
mntR pfeT
D)
LB
LB + Fe
Inhibition zone (mm)
50
40
30
20
10
0
mntR pfeT
mntR pfeT Pspac-mneP
mntR pfeT Pspac-mneP + IPTG
mntR pfeT Pspac-mneS
mntR pfeT Pspac-mneS + IPTG
Strain

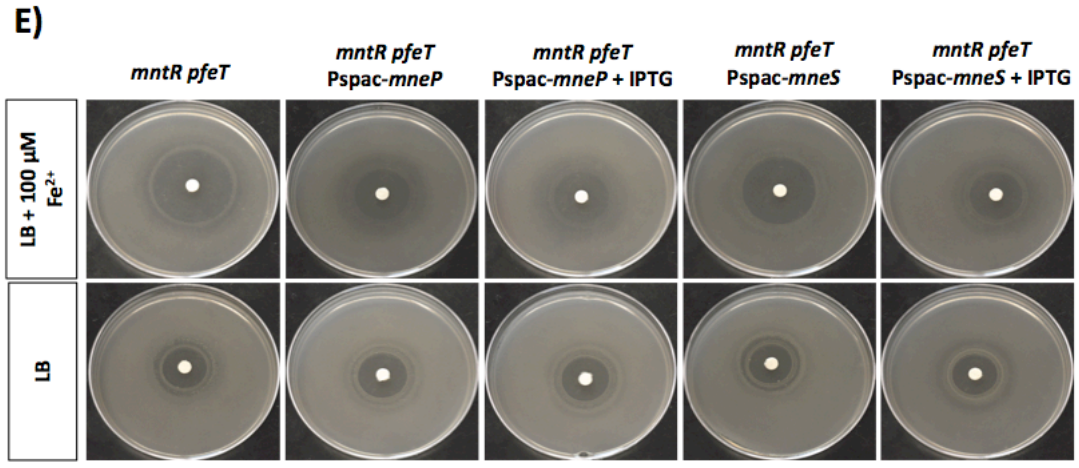

FIG. 5.4) *mntR* and *mntR pfeT* mutants accumulate intracellular iron.
A) Beta galactosidase assays to monitor *pfeT-lacZ* expression in WT, *pfeT, mntR*, and *mntR pfeT* mutant backgrounds grown in LB amended with different concentrations of iron.
B) & **C)** Streptonigrin (SN) zone of inhibition assay in LB media with and without 100 µM Fe^{2+} performed on the labeled strains and their respective plate images.
D) & **E)** Streptonigrin (SN) zone of inhibition assay in LB media with and without 100 µM Fe^{2+} performed on strains expressing *mneP* and *mneS* through an IPTG inducible promoter and their respective plate images.
Data is representative of more than three biological replicates.

5.3.5 H_2O_2 sensitivity does not correlate with iron accumulation and is linked to the MntR regulon

Iron homeostasis and oxidative stress are linked through the production of reactive oxygen species (ROS) via Fenton reactions. Cells that accumulate high levels of iron should be more susceptible to hydrogen peroxide (H_2O_2) stress. However, *pfeT* mutant cells are not more sensitive to H_2O_2 than WT (Fig. 5.5), which is in line with past work showing this same phenotype (11). What was even more surprising was that although iron also accumulates in *mntR* mutant cells, these are more H_2O_2 sensitive than a *pfeT* mutant. Further,

an *mntR pfeT* double mutant, which shows the highest level of iron accumulation (Fig. 5.4), was less H_2O_2 sensitive than an *mntR* mutant strain (Fig. 5.5). In fact, ectopic expression of *pfeT* in an *mntR pfeT* mutant background, which helps restore iron resistance, seemed to exacerbate H_2O_2 sensitivity (Fig. 5.5).

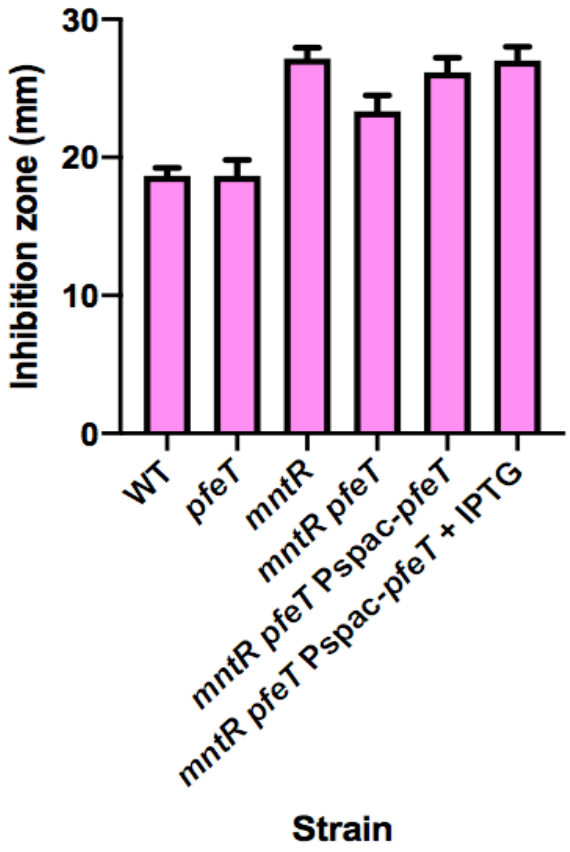

FIG. 5.5) An *mntR* mutant is highly sensitive to H_2O_2.
Peroxide zone of inhibition assays were performed in the labeled strains.
Data is representative of more than three biological replicates.

Analysis of H_2O_2 sensitivity in *pfeT* mutant cells across the MntR regulon showed that iron efflux helps maintain H_2O_2 resistance even in a *pfeT*

mneS mneP triple mutant strain (Fig. 5.6A). Sensitivity is only apparent in strains lacking MntR, which are even more sensitive in the absence of MneP and MneS. It is possible that somehow, derepression of Mn^{2+} import might enhance peroxide toxicity since an *mntR* mutant is more resistant when either Mn^{2+} importer is absent, particularly MntA (Fig. 5.6A). Indeed, when *mntH* is ectopically expressed in an *mntR* and *mntR pfeT* mutant background, H_2O_2 sensitivity increases (Fig. 5.6B & C) and expression of *mneP* and *mneS* helps restore resistance.

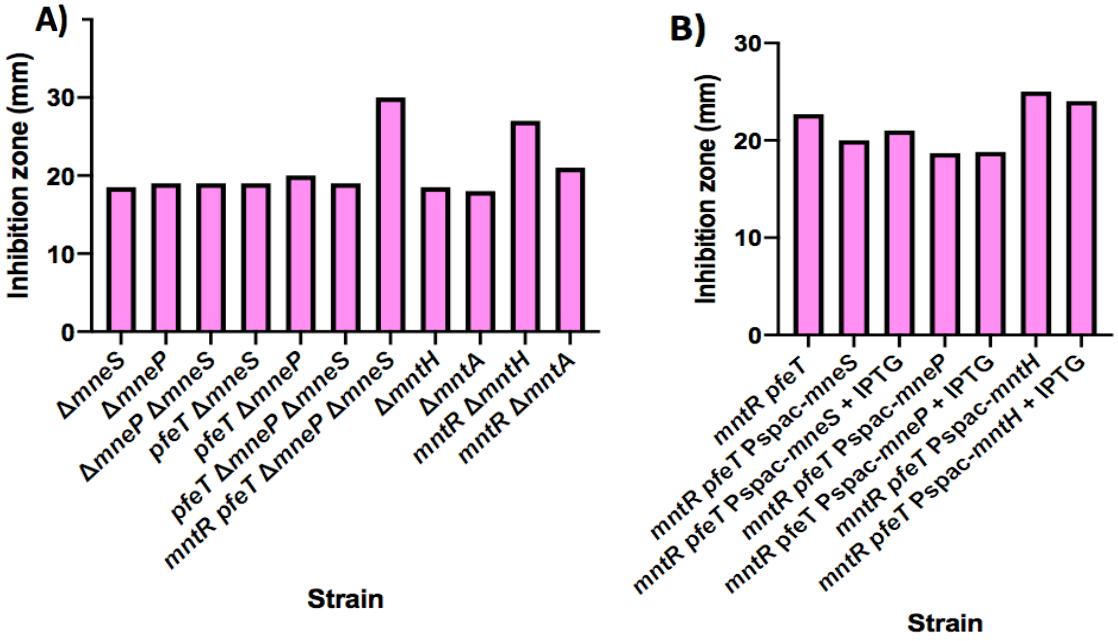

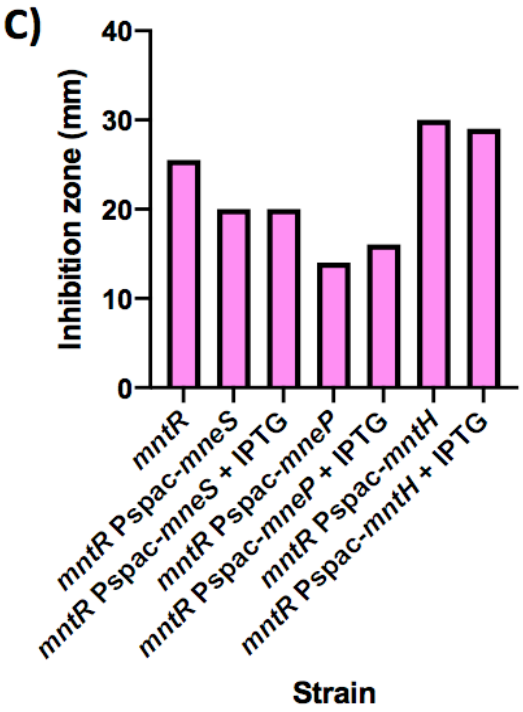

FIG. 5.6) H_2O_2 sensitivity is enhanced by Mn^{2+} import.
A) Peroxide zone of inhibition assays were performed in strains spanning the MntR regulon.
B) & **C)** *mntR pfeT* and *mntR* mutant strains containing IPTG inducible copies of MneS, MneP, and MntH were tested for peroxide sensitivity as per the zone of inhibition assay.
This set of experiments has been done once and requires more replicates.

5.3.6 Manganese enhanced sensitivity to H_2O_2 is caused by PerR:Mn

An *mntR* mutant is very sensitive to H_2O_2 and mutating *pfeT* in this background helps restore some resistance (Fig. 5.5). Genetically we have shown that Mn^{2+} import enhances H_2O_2 toxicity (Fig. 5.6). Chemical supplementation of Mn^{2+} in a H_2O_2 zone of inhibition assay supports this as all strains tested, in particular *mntR* and *mntR pfeT* mutants that naturally accumulate Mn^{2+}, are more susceptible to oxidative stress (Fig. 5.7).

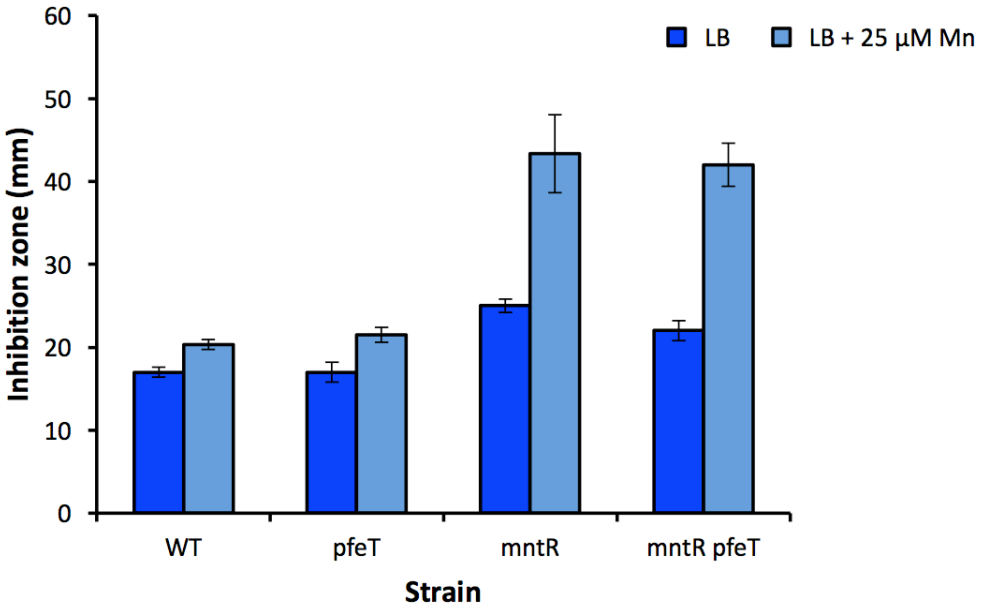

FIG. 5.7) Mn^{2+} exacerbates peroxide sensitivity.
Peroxide zone of inhibition assays in LB plates containing 25 µM $MnCl_2$. Data is representative of more than three biological replicates.

It is surprising that Mn^{2+}, a micronutrient normally used to suppress the effects of oxidative stress, enhances H_2O_2 toxicity (Fig. 5.7) whereas Fe^{2+} helps alleviate this sensitivity (Fig. 5.5). The metalloregulator PerR controls expression of genes encoding enzymes that alleviate H_2O_2 toxicity like *katA* (catalase), *ahpCF* (alkyl hydroperoxide reductase), and *mrgA* (a mini-ferritin) (1,7). PerR binds to Fe^{2+} or Mn^{2+} at its metal sensing site to effect repression. Upon H_2O_2 exposure, only PerR:Fe responds through a metal catalyzed oxidation (MCO) event that triggers a DNA-unbinding conformational change, effectively derepressing gene expression (8). Even in the presence of H_2O_2, PerR:Mn remains an active repressor (8).

We measured *katA*, *ahpCF*, and *mrgA* expression levels in WT, *pfeT*, *mntR*, and *mntR pfeT* mutant backgrounds to see how changes in Fe^{2+} and Mn^{2+} in these strains affect PerR regulon expression. Cells lacking PfeT show higher mRNA levels of these genes, particularly *katA*, whereas tight gene repression is observed in an *mntR* mutant (Fig. 5.8A). Relative mRNA levels of these genes in an *mntR pfeT* mutant were somewhat comparable to those seen in a *pfeT* mutant, except *katA* expression was not as high (Fig. 5.8A). This, along with previous Mn^{2+} transcriptomic data (Fig. 5.8B) (23) suggests that the mechanism of Mn^{2+} enhanced H_2O_2 toxicity is through the predominant Mn^{2+} metallation of PerR. This is even more striking in an *mntR* mutant which derepresses Mn^{2+} uptake genes.

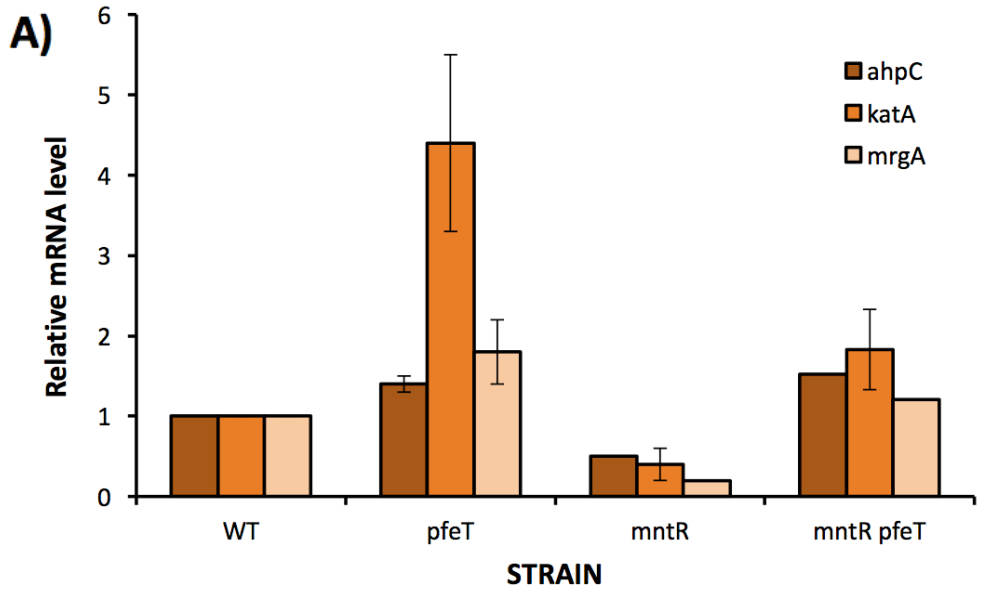

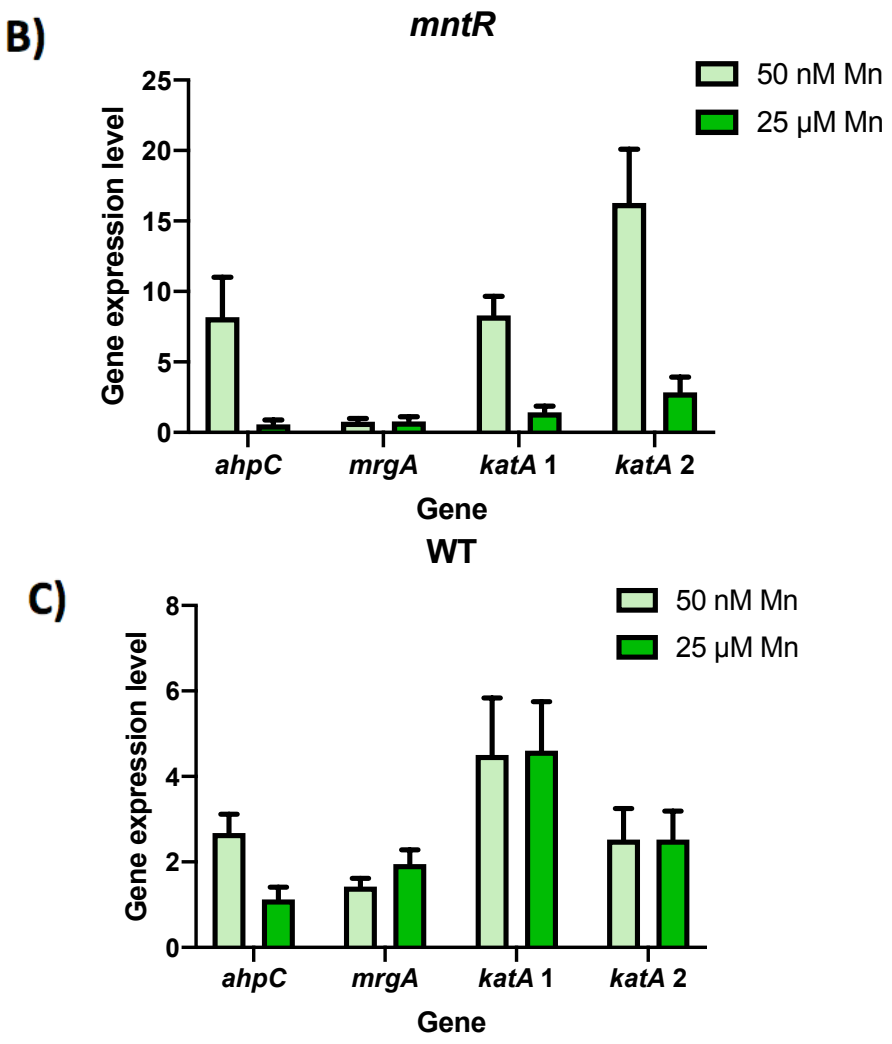

FIG. 5.8) PerR regulon repression in *mntR* mutant strains.
A) qRT-PCR data showing relative mRNA levels for *ahpC*, *katA*, and *mrgA* genes measured in the respective strain backgrounds. Data obtained in mutant strains was normalized with respect to WT. Experiments were performed twice.
B) & **C)** Microarray data modified from Guedon et al. 2003 showing differential expression of the PerR regulon in WT and an *mntR* mutants grown in minimal media amended with either 50 nM or 25 μM $MnCl_2$.

5.4 Discussion and future directions

Cation diffusion facilitator (CDF) transporters are ubiquitous, dimeric transporters that harness energy from proton motif force for metal cation

transport. Each monomer contains an N-terminal six transmembrane domain (TMD) and a variable C-terminal cytoplasmic domain (CTD) (35,36). Structural studies of the *Escherichia coli* Fe^{2+} and Zn^{2+} CDF efflux pump FieF (YiiP) have provided insight into how metal export occurs in these transporters (37,38). Each monomer has four metal binding sites (A, B, C1, and C2) and it has been proposed that metal selectivity occurs at conserved motfis in binding site A (37-39). Primary sequence analysis of site A in the Zn^{2+} efflux CDF transporter (CzcD) and the Mn^{2+} efflux CDF pump in *Streptococcus pneumoniae* suggests that HD-DD and ND-DD motifs respectively determine cation discrimination (39).

In *Bacillus subtilis*, the two CDF Mn^{2+} efflux pumps are the primary and secondary MntR controlled MneP and MneS (respectively) (24). MneS has the conserved, Mn^{2+} efflux associated ND-DD motif, MneP has the HD-DD motif, previously associated with Zn^{2+} efflux. No Zn^{2+} export function has been detected in MneP. Our data herein provide evidence that MneP and MneS also involved function as Fe^{2+} efflux pumps. The only other CDF transporter identified as being able to efflux Fe^{2+} and Mn^{2+} is EmfA in *Rhizobium etli*. They show high Mn^{2+} sensitivity in *emfA* mutant cells, as well as Mn^{2+} dependent induction (40). However, iron sensitivity was only observed in experiments carried out in *E. coli* and although Fe^{2+} dependent induction was detected, fold induction was considerably higher in the presence of Zn^{2+} (40). Bioinformatic analysis of the EmfA A site reveal an EN-HD motif, which varies from that of

iron and manganese CDF exporters like FieF and MntE, as well as Mn^{2+}/Fe^{2+} efflux pumps MneP and MneS. How metal selectivity is determined in these transporters therefore demands further study.

The only previously characterized Fe^{2+} efflux pump in *B. subtilis* is the PerR and Fur controlled P_{1B4}-type ATPase, PfeT (11). Cells that lack PfeT accumulate intracellular iron and become sensitive. Biochemical experiments have shown PfeT's high affinity for iron, with a $K_{1/2}$ of 520 ± 120μM. This would allow activation of iron export to take place only under conditions of iron overload. Here we show that *mneP mneS* double null cells are iron sensitive and that MneS seems to play a primary role in Fe^{2+} efflux compared to MneP. Neither of these CDF pumps is induced by iron. Although transcriptional activation is dependent on MntR under high intracellular Mn^{2+}, basal levels of expression have been detected under regular growth conditions (24). We suggest a model of *B. subtilis* iron efflux where MneP and MneS act as a "release valve" for low level iron fluctuations until a drastic increase in iron levels activates PfeT iron efflux.

Manganese is commonly referred to as an antioxidant as it helps alleviate oxidative stress through metallation of Mn^{2+}-utilizing superoxide dismutase (SOD) and oxidized iron mono-nuclear enzymes (12-14). On the other hand, iron is known to be detrimental to cells under conditions of oxidative stress through the generation of ROS via Fenton reactions. In this study we have seen an apparent reversal of these roles, wherein Mn^{2+}

sensitizes *B. subtilis* to H_2O_2 toxicity and Fe^{2+} alleviates it. Similar results have been observed in *Staphylococcus aureus*, where CDF Mn^{2+} exporter and virulence factor MntE is required for oxidative stress resistance (26). However, no mechanism of toxicity is provided. In our work we show that H_2O_2 sensitivity in an *mntR* mutant is due to derepression of Mn^{2+} importers MntH and MntA. The dysregulation of the MntR regulon leads to sufficient Mn^{2+} accumulation to repress the PerR regulon by favoring PerR:Mn over PerR:Fe metallation.

Future directions for this work include completing peroxide sensitivity assays for some of the efflux pump mutants and complementation strains. We will perform inductively coupled plasma mass spectroscopy (ICP-MS) measurements to quantify iron accumulation in *mntR* mutant and *mneP mneS* null cells. Catalase assays in *mntR* mutants versus WT, *pfeT*, and *mntR pfeT* mutant strains will be performed to further confirm this PerR:Mn regulon repression. Finally, β-Galactosidase assays will be performed in *mneP mneS* null and *mneP mneS pfeT* mutant backgrounds to measure *pfeT-lacZ* induction response to iron.

5.5 Methods

Bacterial strains, phage, plasmids, and growth conditions

Bacillus subtilis strains derived from CU1065 (WT) were grown on lysogeny broth (LB) medium (10 g/L casein digest peptone, 5 g/L yeast extract, 5 g/L NaCl) at $37^{O}C$ with vigorous shaking. Ferrous iron ($FeSO_4 \cdot 7H_2O$) was titrated

into the media as indicated from a freshly made 100mM iron stock solution dissolved in 0.1 N HCl. SPβ phage are derivatives of SPβ*c2*Δ2 (41,42) and were constructed by integration of a promoter region-*cat-lacZ* operon fusion constructed in pJPM122 into strain ZB307A as described previously (43). Ampicillin (amp; 100 μg ml^{-1}) was used to select *E. coli* transformants. Erythromycin (ery; 1 μg ml^{-1}) and lincomycin (linc; 25 μg ml^{-1}; for testing macrolide-lincosamide-streptogramin B [MLS] resistance), spectinomycin (spec; 100 μg ml^{-1}), kanamycin (kan; 10 μg ml^{-1}), and neomycin (neo; 10 μg ml^{-1}) were used for the selection of various *B. subtilis* strains.

Overexpression strain construction

For complementation, PCR products were amplified from genomic DNA, digested with HindIII and BglII, and cloned into pPL82 (44). The resulting constructs, which allow IPTG-inducible expression of genes, were linearized with PstI and integrated into the *B. subtilis* chromosome at the *amyE* locus

Reporter strain construction

The *cat-lacZ* operon fusions generated in strain ZB307A (45) were moved to different backgrounds by SPβ transduction and selected for by MLS and neomycin resistance. Specifically, SPβ phage from the starting strains containing the *pfeT* promoter region were transduced into the CU1065 *mntR*::*tet* and *mntR*::*kan pfeT*::*spc* backgrounds. Strains were confirmed by

PCR.

Zone of inhibition (ZoI) assays

Disk diffusion assays were performed as described (46). Briefly, strains were grown to an OD_{600} of 0.4. A 100 µl aliquot of these cultures was mixed with 4 ml of 0.75% LB soft agar (kept at 50°C) and directly poured onto LB plates (containing 15 ml of 1.5% LB agar). The plates were dried for 10 min in a laminar airflow hood. Filter paper disks containing 10 µl of the chemicals to be tested were placed on the top of the agar, and the plates were incubated at 37°C overnight. The overall diameter of the inhibition zones was measured along two orthogonal lines. For IPTG-treated cells, IPTG was added to both the soft agar and the plates to a concentration of 0.1 mM. For media containing additional $MnCl_2$ or $FeSO_4$, it was added to both the soft agar and the plates to a final concentration of 25 µM and 100 µM respectively. Unless otherwise noted, 10 µl of the following chemicals was used in the disk diffusion assays: 1 M $FeSO_4$, 0.88 M H_2O_2. For SN sensitivity tests, $FeSO_4$ was added to both the soft agar and the plates to a concentration of 0.1 mM, 5 mg ml^{-1} SN solution in dimethyl sulfoxide (DMSO) was added to the filter paper disks.

ImageJ zone of lower density analysis

Briefly, bird's eye view photogrpaphs of the zone of inhibition plates were taken with a Nikon D5000 camera and converted to black and white images.

These were run through Image J where the software generates a pixel density histogram across a highlighted zone.

β-Galactosidase assays

Cells containing the *pfeT* promoter *lacZ* fusions were grown in LB amended with different concentrations of $FeSO_4 \cdot 7H_2O$ to an OD_{600} of ~0.4. Cells were then harvested and β-galactosidase assays were performed as described previously in (42), except that cells were lysed with 0.1 mg ml^{-1} lysozyme for 30 min at 37°C instead of chloroform.

qRT-PCR

Strains of interest were grown to an OD_{600} of ~0.5. 1.5 mL of culture was used for RNA extraction. RNA isolation (Qiagen, USA) and cDNA preparation (Thermofisher, USA) was carried out as suggested by the manufacturer. qRT-PCR was carried out using a Bio-Rad iTaq universal SYBR green super mix. 23S rRNA was used to normalize the cycle threshold (Ct) value.

Table 5.1) Strains and plasmids used in this study

STRAIN	GENOTYPE	REFERENCE
CU1065	W168 *attSP*β *trpC2*	Laboratory stock
ZB307A	W168 SPβ *c2*Δ*2*::Tn*917*::pSK10Δ6	Laboratory stock
HB18022	CU1065 SPβ *c2*Δ*2*::Tn*917*::ϕ(*pfeT-cat-lacZ*)	(Pinochet-Barros & Helmann 2020)
HB8116	CU1065 *pfeT*::*kan* SPβ *c2*Δ*2*::Tn*917*::ϕ(*pfeT-cat-lacZ*)	Laboratory stock
HB17802	CU1065 *pfeT*::*spc*	(Guan et al. 2015)
HB2621	CU1065 *mntR*::*kan*	(Guedon et al.

		2003)
HB17806	CU1065 *mntR*::*kan pfeT*::*spc*	(Guan et al. 2015)
HB18190	CU1065 *mntR*::*kan pfeT*::*spc amyE*::Pspac-*pfeT* (cat)	This work
HB17767	CU1065 Δ*mntA*	(Huang et al. 2017)
HB17768	CU1065 Δ*mntH*	(Huang et al. 2017)
HB17780	CU1065 *mntR*::*tet* Δ*mntH*	(Huang et al. 2017)
HB17779	CU1065 *mntR*::*tet* Δ*mntA*	(Huang et al. 2017)
HB17827	CU1065 *pfeT*::*spc* *mntH*::*mls*	(Guan et al. 2015)
HB17828	CU1065 *mntR*::*kan pfeT*::*spc* *mntH*::*mls*	(Guan et al. 2015)
HB17773	CU1065 Δ*mneP*	(Huang et al. 2017)
HB17769	CU1065 Δ*mneS*	(Huang et al. 2017)
HB17784	CU1065 Δ*mneP* Δ*mneS*	(Huang et al. 2017)
HB17795	CU1065 *mntR*::*tet* Δ*mneP* Δ*mneS*	(Huang et al. 2017)
HB17796	CU1065 *thrC*::P_{mneS}-*lacZ* (mls)	(Huang et al. 2017)
HB17797	CU1065 *thrC*::P_{mneP}-*lacZ* (mls)	(Huang et al. 2017)
HB18195	CU1065 *pfeT*::*spc* Δ*mneP*	This work
HB18194	CU1065 *pfeT*::*spc* Δ*mneS*	This work
HB19554	CU1065 *pfeT*::*spc* Δ*mneP* Δ*mneS*	(Huang et al. 2017)
HB18196	CU1065 Δ*mneP* Δ*mneS* *pfeT*::*spc* *mntR*::*kan*	This work
HB18056	CU1065 *mntR*::*tet* SPβ *c2*Δ*2*::Tn*917*::φ(*pfeT-cat-lacZ*)	This work
HB18197	CU1065 *mntR*::*kan pfeT*::*spc* SPβ *c2*Δ*2*::Tn*917*::φ(*pfeT-cat-lacZ*)	This work
HB18198	CU1065 Pspac-*mneP* (cat)	This work
HB18199	CU1065 Pspac-*mneS* (cat)	This work
HB18202	CU1065 *pfeT*::*spc* Pspac-*mneP* (cat)	This work
HB18203	CU1065 *pfeT*::*spc* Pspac-*mneS* (cat)	This work
HB18210	CU1065 *mntR*::*kan* Pspac-*mneP* (cat)	This work
HB18211	CU1065 *mntR*::*kan* Pspac-*mneS* (cat)	This work
HB18200	CU1065 *mntR*::*kan pfeT*::*spc* Pspac-*mneP* (cat)	This work
HB18201	CU1065 *mntR*::*kan pfeT*::*spc* Pspac-*mneS* (cat)	This work
HB18204	CU1065 Pspac-*mntH* (cat)	This work
HB18205	CU1065 *pfeT*::*spc* Pspac-*mntH* (cat)	This work
HB18206	CU1065 *mntR*::*kan* Pspac-*mntH* (cat)	This work
HB18207	CU1065 *mntR*::*kan pfeT*::*spc* Pspac-*mntH* (cat)	This work
HB18217	CU1065 Δ*mneP* Δ*mneS* SPβ *c2*Δ*2*::Tn*917*::φ(*pfeT-cat-lacZ*)	This work
HB18218	CU1065 *pfeT*::*spc* Δ*mneP* Δ*mneS* SPβ *c2*Δ*2*::Tn*917*::φ(*pfeT-cat-lacZ*)	This work
PLASMID	**DESCRIPTION**	**REFERENCE**
pJPM122	*cat-lacZ* operon fusion vector for SPβ.	(Slack et al. 1993)
pPL82	Expression of gene under P_{spac} promoter.	(Quisel et al. 2001)

Table 5.2) Oligonucleotides used in this study

NUMBER	NAME	SEQUENCE
7750	qPCR mrgA-F	GCTCCACCGTTTCCATTGGTATGTGAA

7751	qPCR mrgA-R	CGTCTGTGATAGATGCATGCTCAGTGTA
8541	qPCR katA-F	CCTGCGACACTTCGCCACAT
8542	qPCR katA-R	GGTAATCAGGGTTTTCACCGGCAA
8543	qPCR ahpC-F	CCCAACTGAGCTTGAAGATCTTCAAGAACAA
8544	qPCR ahpC-R	CGTCAAGAACATCGAAGTTGCGAGAGAT
7277	bgal-pfeT-F	GCCAAGCTTCCCAACATCATTTTTGCTGAAT
7278	bgal-pfeT-R	GCGGATCCGGGTCGCGTTGAACGATAA
6416	mneS up F	CCTACAAATAGGCCGGCTCC
6417	mneS down R	TGGCGATGTCTCGTTTTCCA
6427	mneP up F	TCGCTGATCTTTCCGACCAA
6428	mneP down R	GCGTCGGGAGATCTTTCGTT
6420	mntH up F	CCGGCTTTGCTATTTTCCCG
6421	mntH down R	AGAACCGACCAAGAAGGTGC
8537	mneP-F	GGAACAGCAAAGCGATTATAGCGATTGCGTA
8538	mneP-R	GCACATCAACAGACGGCCTGATTA
8539	mneS-F	CCTGATGCTGATCGTTTACCGGTACAAT
8540	mneS-R	CGATCACAAACGCAGTGACCGTATCAAT
8533	mntH-F	GGCACCGACAGTGTGCTTCTT
8534	mntH-R	GCATTAATAGCCCCTGCAATCAGCAT
535a	pJPM122 check F	GTACATATTGTCGTTAGAACGCGGC
366	pJPM122 check R	ACTCTCCGTCGCTATTGTAACCAG
1293	cat-fwd	CGGCAATAGTTACCCTTATTATCAAG
1294	cat-rev	CCAGCGTGGACCGGCGAGGCTAGTTACCC

5.6 References

1. Faulkner, M.J. and Helmann, J.D. (2011) Peroxide stress elicits adaptive changes in bacterial metal ion homeostasis. *Antioxid Redox Signal*, **15**, 175-189.
2. Pinochet-Barros, A. and Helmann, J.D. (2018) Redox Sensing by Fe^{2+} in Bacterial Fur Family Metalloregulators. *Antioxid Redox Signal*, **29**, 1858-1871.

3. Bsat, N., Herbig, A., Casillas-Martinez, L., Setlow, P. and Helmann, J.D. (1998) *Bacillus subtilis* contains multiple Fur homologues: identification of the iron uptake (Fur) and peroxide regulon (PerR) repressors. *Mol Microbiol*, **29**, 189-198.

4. Ollinger, J., Song, K.B., Antelmann, H., Hecker, M. and Helmann, J.D. (2006) Role of the Fur regulon in iron transport in *Bacillus subtilis*. *J Bacteriol*, **188**, 3664-3673.

5. Pi, H. and Helmann, J.D. (2017) Sequential induction of Fur-regulated genes in response to iron limitation in *Bacillus subtilis*. *Proc Natl Acad Sci U S A*, **114**, 12785-12790.

6. Smaldone, G.T., Antelmann, H., Gaballa, A. and Helmann, J.D. (2012) The FsrA sRNA and FbpB protein mediate the iron-dependent induction of the *Bacillus subtilis lutABC* iron-sulfur-containing oxidases. *J Bacteriol*, **194**, 2586-2593.

7. Herbig, A.F. and Helmann, J.D. (2001) Roles of metal ions and hydrogen peroxide in modulating the interaction of the *Bacillus subtilis* PerR peroxide regulon repressor with operator DNA. *Mol Microbiol*, **41**, 849-859.

8. Lee, J.W. and Helmann, J.D. (2006) The PerR transcription factor senses H_2O_2 by metal-catalysed histidine oxidation. *Nature*, **440**, 363-367.

9. Faulkner, M.J., Ma, Z., Fuangthong, M. and Helmann, J.D. (2012) Derepression of the *Bacillus subtilis* PerR peroxide stress response leads to iron deficiency. *J Bacteriol*, **194**, 1226-1235.

10. Chen, L. and Helmann, J.D. (1995) *Bacillus subtilis* MrgA is a Dps(PexB) homologue: evidence for metalloregulation of an oxidative-stress gene. *Mol Microbiol*, **18**, 295-300.

11. Guan, G., Pinochet-Barros, A., Gaballa, A., Patel, S.J., Arguello, J.M. and Helmann, J.D. (2015) PfeT, a P_{1B4}-type ATPase, effluxes ferrous iron and protects *Bacillus subtilis* against iron intoxication. *Mol Microbiol*, **98**, 787-803.

12. Imlay, J.A. (2013) The molecular mechanisms and physiological consequences of oxidative stress: lessons from a model bacterium. *Nat Rev Microbiol*, **11**, 443-454.

13. Anjem, A. and Imlay, J.A. (2012) Mononuclear iron enzymes are primary targets of hydrogen peroxide stress. *J Biol Chem*, **287**, 15544-15556.

14. Sobota, J.M., Gu, M. and Imlay, J.A. (2014) Intracellular hydrogen peroxide and superoxide poison 3-deoxy-D-arabinoheptulosonate 7-phosphate synthase, the first committed enzyme in the aromatic biosynthetic pathway of *Escherichia coli*. *J Bacteriol*, **196**, 1980-1991.

15. Merchant, S.S. and Helmann, J.D. (2012) Elemental economy: microbial strategies for optimizing growth in the face of nutrient limitation. *Adv Microb Physiol*, **60**, 91-210.

16. Anjem, A., Varghese, S. and Imlay, J.A. (2009) Manganese import is a key element of the OxyR response to hydrogen peroxide in *Escherichia coli*. *Mol Microbiol*, **72**, 844-858.

17. Kehres, D.G., Janakiraman, A., Slauch, J.M. and Maguire, M.E. (2002) Regulation of *Salmonella enterica* serovar Typhimurium *mntH* transcription by H_2O_2, Fe^{2+}, and Mn^{2+}. *J Bacteriol*, **184**, 3151-3158.

18. Jakubovics, N.S. and Jenkinson, H.F. (2001) Out of the iron age: new insights into the critical role of manganese homeostasis in bacteria. *Microbiology*, **147**, 1709-1718.

19. Que, Q. and Helmann, J.D. (2000) Manganese homeostasis in *Bacillus subtilis* is regulated by MntR, a bifunctional regulator related to the diphtheria toxin repressor family of proteins. *Mol Microbiol*, **35**, 1454-1468.

20. McGuire, A.M., Cuthbert, B.J., Ma, Z., Grauer-Gray, K.D., Brunjes Brophy, M., Spear, K.A., Soonsanga, S., Kliegman, J.I., Griner, S.L., Helmann, J.D. *et al.* (2013) Roles of the A and C sites in the manganese-specific activation of MntR. *Biochemistry*, **52**, 701-713.

21. Boyd, J., Oza, M.N. and Murphy, J.R. (1990) Molecular cloning and DNA sequence analysis of a diphtheria tox iron-dependent regulatory

element (*dtxR*) from *Corynebacterium diphtheriae*. *Proc Natl Acad Sci U S A*, **87**, 5968-5972.

22. Guedon, E. and Helmann, J.D. (2003) Origins of metal ion selectivity in the DtxR/MntR family of metalloregulators. *Mol Microbiol*, **48**, 495-506.

23. Guedon, E., Moore, C.M., Que, Q., Wang, T., Ye, R.W. and Helmann, J.D. (2003) The global transcriptional response of *Bacillus subtilis* to manganese involves the MntR, Fur, TnrA and sigmaB regulons. *Mol Microbiol*, **49**, 1477-1491.

24. Huang, X., Shin, J.H., Pinochet-Barros, A., Su, T.T. and Helmann, J.D. (2017) *Bacillus subtilis* MntR coordinates the transcriptional regulation of manganese uptake and efflux systems. *Mol Microbiol*, **103**, 253-268.

25. Chen, L., Keramati, L. and Helmann, J.D. (1995) Coordinate regulation of *Bacillus subtilis* peroxide stress genes by hydrogen peroxide and metal ions. *Proc Natl Acad Sci U S A*, **92**, 8190-8194.

26. Grunenwald, C.M., Choby, J.E., Juttukonda, L.J., Beavers, W.N., Weiss, A., Torres, V.J. and Skaar, E.P. (2019) Manganese Detoxification by MntE Is Critical for Resistance to Oxidative Stress and Virulence of *Staphylococcus aureus*. *MBio*, **10**.

27. Davies, B.W. and Walker, G.C. (2007) Disruption of *sitA* compromises *Sinorhizobium meliloti* for manganese uptake required for protection against oxidative stress. *J Bacteriol*, **189**, 2101-2109.

28. Fleming, M.D., Trenor, C.C., 3rd, Su, M.A., Foernzler, D., Beier, D.R., Dietrich, W.F. and Andrews, N.C. (1997) Microcytic anaemia mice have a mutation in Nramp2, a candidate iron transporter gene. *Nat Genet*, **16**, 383-386.

29. Gunshin, H., Mackenzie, B., Berger, U.V., Gunshin, Y., Romero, M.F., Boron, W.F., Nussberger, S., Gollan, J.L. and Hediger, M.A. (1997) Cloning and characterization of a mammalian proton-coupled metal-ion transporter. *Nature*, **388**, 482-488.

30. Kitphati, W., Ngok-Ngam, P., Suwanmaneerat, S., Sukchawalit, R. and Mongkolsuk, S. (2007) *Agrobacterium tumefaciens fur* has important physiological roles in iron and manganese homeostasis, the oxidative stress response, and full virulence. *Appl Environ Microbiol*, **73**, 4760-4768.

31. Runyen-Janecky, L., Dazenski, E., Hawkins, S. and Warner, L. (2006) Role and regulation of the *Shigella flexneri* Sit and MntH systems. *Infect Immun*, **74**, 4666-4672.

32. Sabri, M., Leveille, S. and Dozois, C.M. (2006) A SitABCD homologue from an avian pathogenic *Escherichia coli* strain mediates transport of iron and manganese and resistance to hydrogen peroxide. *Microbiology*, **152**, 745-758.

33. Yeowell, H.N. and White, J.R. (1982) Iron requirement in the bactericidal mechanism of streptonigrin. *Antimicrob Agents Chemother*, **22**, 961-968.

34. Fuangthong, M., Herbig, A.F., Bsat, N. and Helmann, J.D. (2002) Regulation of the *Bacillus subtilis fur* and *perR* genes by PerR: not all members of the PerR regulon are peroxide inducible. *J Bacteriol*, **184**, 3276-3286.

35. Kolaj-Robin, O., Russell, D., Hayes, K.A., Pembroke, J.T. and Soulimane, T. (2015) Cation Diffusion Facilitator family: Structure and function. *FEBS Lett*, **589**, 1283-1295.

36. Montanini, B., Blaudez, D., Jeandroz, S., Sanders, D. and Chalot, M. (2007) Phylogenetic and functional analysis of the Cation Diffusion Facilitator (CDF) family: improved signature and prediction of substrate specificity. *BMC Genomics*, **8**, 107.

37. Lu, M., Chai, J. and Fu, D. (2009) Structural basis for autoregulation of the zinc transporter YiiP. *Nat Struct Mol Biol*, **16**, 1063-1067.

38. Lu, M. and Fu, D. (2007) Structure of the zinc transporter YiiP. *Science*, **317**, 1746-1748.

39. Martin, J.E. and Giedroc, D.P. (2016) Functional Determinants of Metal Ion Transport and Selectivity in Paralogous Cation Diffusion Facilitator Transporters CzcD and MntE in *Streptococcus pneumoniae*. *J Bacteriol*, **198**, 1066-1076.

40. Cubillas, C., Vinuesa, P., Tabche, M.L., Davalos, A., Vazquez, A., Hernandez-Lucas, I., Romero, D. and Garcia-de los Santos, A. (2014) The cation diffusion facilitator protein EmfA of *Rhizobium etli* belongs to a novel subfamily of Mn^{2+}/Fe^{2+} transporters conserved in alpha-proteobacteria. *Metallomics*, **6**, 1808-1815.

41. Miller, J.H. (1972) *Experiments in molecular genetics*. Cold Spring Harbor Laboratory, Cold Spring Harbor, N.Y.

42. Miller, J.H. (1972) *Experiments in molecular genetics*. Cold Spring Harbor Laboratory, Cold Spring Harbor, N.Y.

43. Liu, H., Haga, K., Yasumoto, K., Ohashi, Y., Yoshikawa, H. and Takahashi, H. (1997) Sequence and analysis of a 31 kb segment of the *Bacillus subtilis* chromosome in the area of the *rrnH* and *rrnG* operons. *Microbiology*, **143 (Pt 8)**, 2763-2767.

44. Quisel, J.D., Burkholder, W.F. and Grossman, A.D. (2001) *In vivo* effects of sporulation kinases on mutant Spo0A proteins in *Bacillus subtilis*. *J Bacteriol*, **183**, 6573-6578.

45. Slack, F.J., Mueller, J.P. and Sonenshein, A.L. (1993) Mutations that relieve nutritional repression of the *Bacillus subtilis* dipeptide permease operon. *J Bacteriol*, **175**, 4605-4614.

46. Mascher, T., Hachmann, A.B. and Helmann, J.D. (2007) Regulatory overlap and functional redundancy among *Bacillus subtilis* extracytoplasmic function sigma factors. *J Bacteriol*, **189**, 6919-6927.

Whose woods these are I think I know.
His house is in the village though;
He will not see me stopping here
To watch his woods fill up with snow.

My little horse must think it queer
To stop without a farmhouse near
Between the woods and frozen lake
The darkest evening of the year.

He gives his harness bells a shake
To ask if there is some mistake.
The only other sound's the sweep
Of easy wind and downy flake.

The woods are lovely, dark and deep,
But I have promises to keep,
And miles to go before I sleep,
And miles to go before I sleep.

- Robert Frost
(*Stopping by Woods on a Snowy Evening - 1923*)

APPENDIX I

Generation of H_2O_2 Resistant Suppressors Across the MntR Regulon

A1.1 Abstract

The oxidative stress response in *Bacillus subtilis* is under control of the Fur family metalloregulator PerR. This homodimeric protein binds to either manganese (Mn^{2+}) or iron (Fe^{2+}) to repress gene expression by binding to specific PerR DNA operator sites. Exposure of PerR:Fe to hydrogen peroxide (H_2O_2) leads to a reaction that oxidizes two histidine residues at the metal sensing site, thereby causing derepression of the regulon. When PerR is metallated with less redox sensitive Mn^{2+} however, protein oxidation does not occur and gene repression remains. An *mntR* mutant strain sees derepression of Mn^{2+} uptake systems (MntH and MntA) as well as an inability to activate expression of CDF efflux pumps MneP and MneS. This leads to the accumulation of intracellular Mn^{2+} which in turn favors the metallation of PerR:Mn, effectively repressing the regulon even under conditions of oxidative stress. Here we lay out a group of suppressor hits generated from MntR regulon mutant strains exposed to H_2O_2.

A1.2 Introduction

Manganese (Mn^{2+}) is an essential micronutrient across all domains of life. The metal is used as an enzymatic cofactor across many cellular processes including the detoxification of reactive oxygen species (ROS), dNTP synthesis required for DNA replication, and central carbon metabolism (1,2). Whilst some bacteria, like *Escherichia coli*, have a more iron-centric physiology wherein they only import Mn^{2+} under oxidative stress (4), *Bacillus subtilis* depends on Mn^{2+} for growth (5).

In *B. subtilis*, Mn^{2+} homeostasis is controlled by the DtxR family dual regulator MntR. The sensitivity of an *mntR* mutant to Mn^{2+} is in part attributed to the derepression of Mn^{2+} import systems MntH and MntA, which it normally represses (6,7). Later studies showed that MntR directly activates transcription of cation diffusion facilitator (CDF) Mn^{2+} efflux pumps MneP and MneS (8). Recent work has shown that *mntR* mutant cells are very peroxide (H_2O_2) sensitive, as the accumulation of Mn^{2+} through derepression of *mntH* and *mntA* favours metallation of the peroxide response regulator PerR with Mn^{2+} instead of Fe^{2+}. This leads to repression of the PerR regulon, preventing transcription of ROS detoxifying enzyme genes (see Chapter 5).

Here, we have isolated spontaneous suppressors from H_2O_2 zone of inhibition assays in *mntR* regulon mutants. Preliminary results suggest that these suppressors are more H_2O_2 resistant than their mother strains. Whole genome sequencing results point to specific mutations that may have

conferred this resistance. Further experiments need to be done to understand these hits and their role in H_2O_2 resistance.

A1.3 Results

A1.3.1 Suppressor whole genome sequencing results

Spontaneous suppressors were streak isolated and tested again for H_2O_2 resistance by zone of inhibition assay (Fig. A1.1). Strains that showed lower sensitivity with respect to their mother strain were sent for whole genome sequencing. The data showed mutation hits in genes encoding enzymes like ribonucleotide reductase (*nrdF*), phosphoglycerate mutase (*pgm*), and *mntH*, amongst others (Table 6.1, Fig. A1.2, and Fig. A1.3).

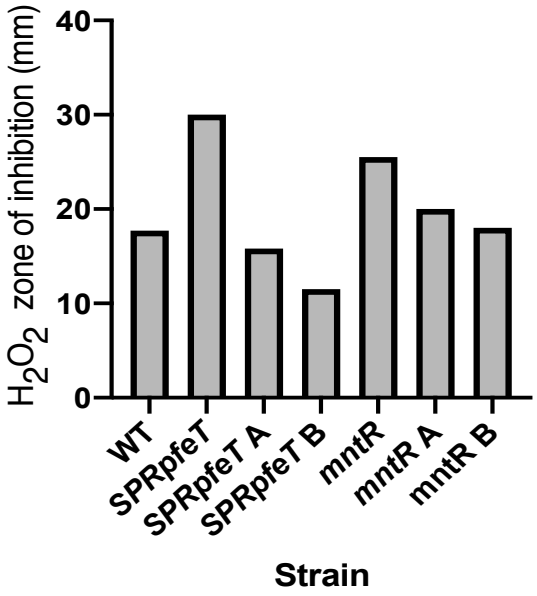

FIG. A1.1) Peroxide zone of inhibition assay of suppressors
Suppressors that were streak isolated were tested once for H_2O_2 sensitivity in comparison to their original mother strains and WT. This does not include sequenced suppressor *SPRpfeT* A', which came from a later round of ZoI collected suppressors.

STRAIN	Reference Position	Type	Overlapping annotations	Nucleotide change	Amino acid change	Gene function
***mntR* A**	2161581	SNV	CDS: nrdF, Gene: nrdF	NP_389886.2:c.198T>G	NP_389886.2:p.Asp66Glu	Ribonucleoside-diphosphate reductase (beta subunit). Synthesis of deoxyribonucleoside triphosphates
***mntR* B**	491283	SNV	CDS: mntH, Gene: mntH	NP_389690.1:c.48C>T	NP_388317.1:p.Pro381Gln	Mn importer
***SPRpfeT* A**	490009	IN	CDS: ydaP, Gene: ydaP	NP_388315.1:c.1179_1180insA	NP_388315.1:p.Met395fs	Putative pyruvate oxidase
	88678	SNV	between yacF and lysS			YacF → putative tRNA-dihydrouridine synthase B. tRNA maturation. LysS→ lysyl-tRNA synthetase
	492927	SNV	between ydaS and ydaT			YdaS→ Unkown. General stress response. SigB regulated. YdaT → Unkown. General stress protein, survival of ethanol stress and low temperatures. SigB regulated.
	1285193	SNV	CDS: yjgB, Gene: yjgB	NP_389097.1:c.253G>T	NP_389097.1:p.Gly85Trp	Ethanol stress survival. SigB regulated.
***SPRpfeT* B**	944429	SNV	between ygaF and perR			YgaF → Unknown. Similar to thioredoxin-dependent hydroperoxide peroxidase. PerR → oxidative stress metalloregulator.
***SPRpfeT* A'**	491209	SNV	Gene: mntH, CDS: mntH		Trp406Arg	Mn importer
	3478224	SNV	Gene: pgm, CDS: pgm		Leu397Ile	2,3-bisphosphoglycerate-independent phosphoglycerate mutase. Enzyme in glycolysis / gluconeogenesis.
	2480667	SNV	between zwf and gndA			Zwf→ Initiation of the pentose phosphate pathway. Glucose 6-phosphate dehydrogenase. gndA → Pentose phosphate pathway. NADP-dependent phosphogluconate dehydrogenase.

Table 6.1) Suppressor whole genome sequencing hits.
List of mutation hits obtained for each strain tested.

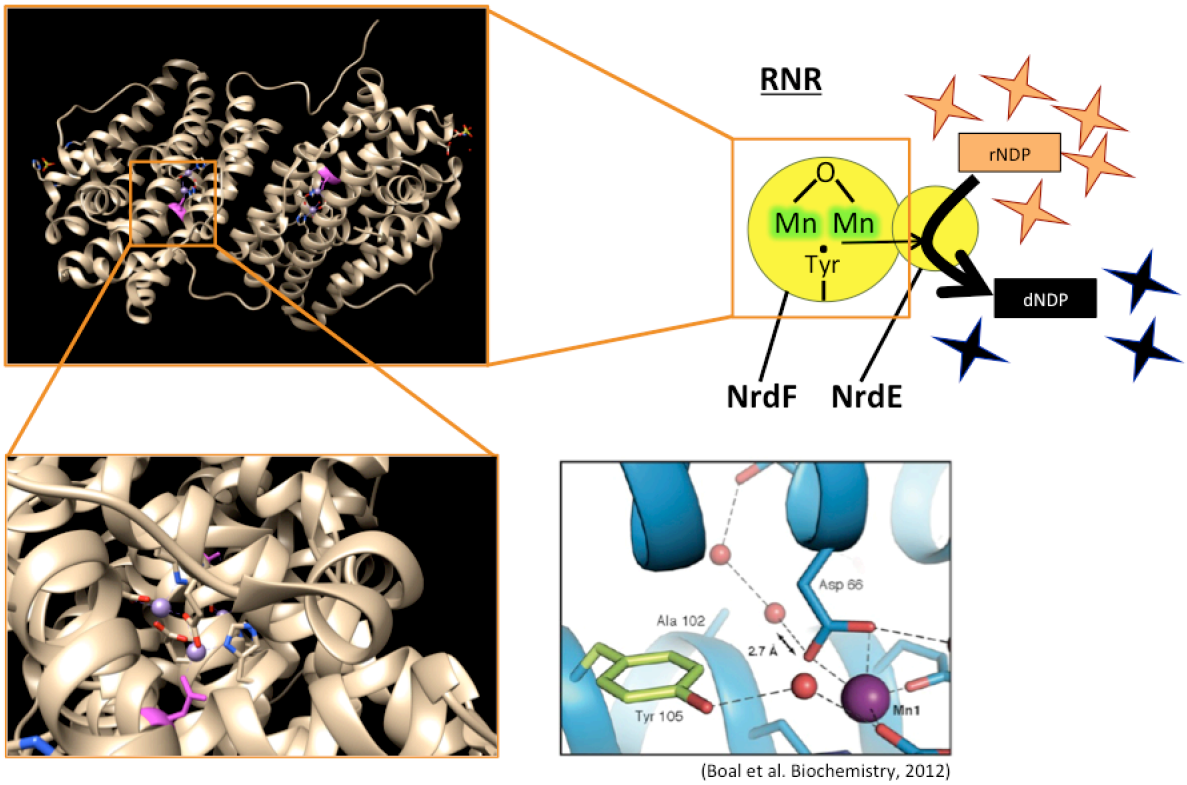

FIG. A1.2) NrdF Asp66Glu mutation.
Sequence analysis from suppressor *mntR* A revealed a mutation in the metal containing unit NrdF of the class Ib ribonucleotide reductase. A general depiction of the NrdEF complex is provided on the top right. The conversion of Asp66 to Glu localizes in the conserved metal coordinating pocket and is highlighted in pink. The *Bacillus subtilis* NrdF structure used to visualize the mutation is derived from PDB code 4DR0. Comparison of the structure model to previous analysis of the metal binding pocket by Boal et al. 2012 (3) is provided .

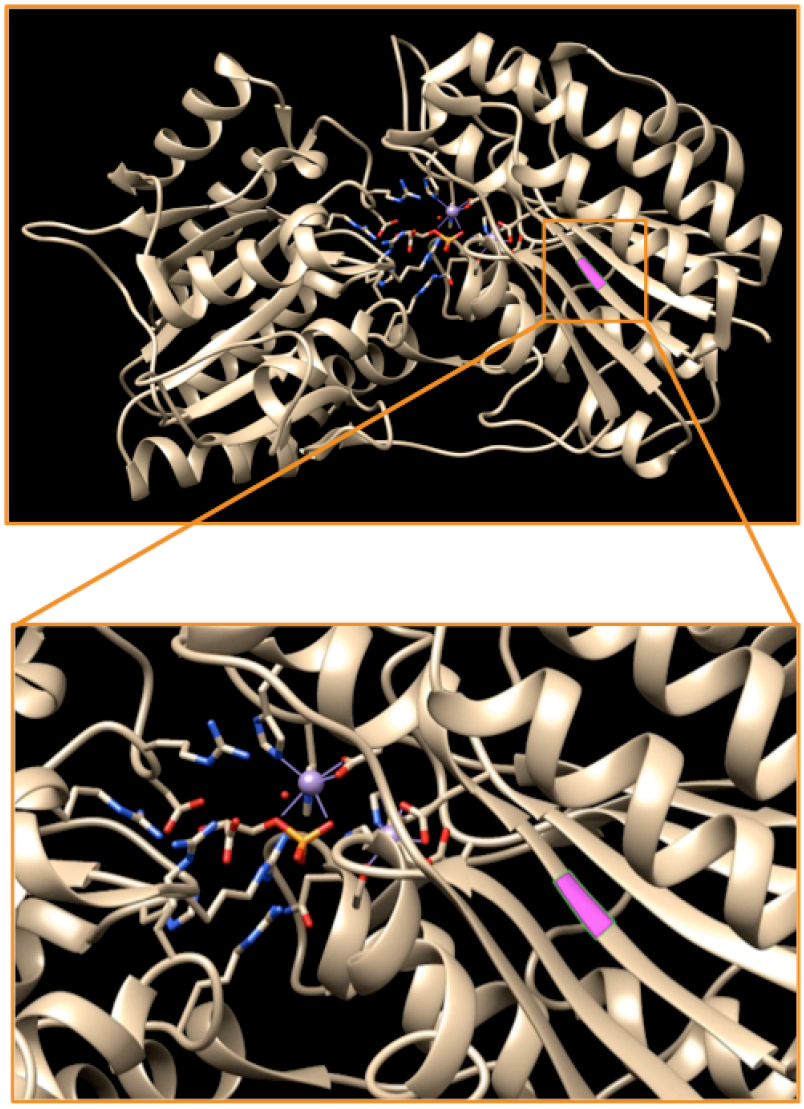

FIG. A1.3) Pgm Leu397Ile mutation.
Sequence analysis from suppressor *SPRpfeT* A' revealed a Leu397Ile point mutation in phosphoglycerate mutase. Structure analysis of *Geobacillus stearothermophilus* Pgm (PDB code 1EJJ) shows the location of the mutated residue, highlighted in pink.

A1.4 Discussion and future directions

In Chapter 5 we have shown that *mntR* mutant strains accumulate Mn^{2+} and Fe^{2+} because they cannot repress Mn^{2+} uptake systems and their inability to activate transcription of Fe^{2+}/Mn^{2+} CDF exporters MneP and MneS. The high Mn^{2+} accumulation leads to the predominant metallation of PerR:Mn which tightly represses regulon expression, thus sensitizing the cells to oxidative stress.

In *E. coli*, ROS toxicity is caused by the oxidation of iron mono-nuclear enzymes (9,10). In this case, Mn^{2+} import provides these enzymes with an alternative cofactor that allows enzymatic function to continue under these conditions. ROS also generates a variety of DNA lesions that are detrimental to the cell (11-13). Aside from activation of the OxyR regulon during oxidative stress, expression of the Mn^{2+}-utilizing ribonucleotide reductase (RNR) *nrdEF* is also upregulated (14).

RNR enzymes are essential, as they synthesize dNTPs needed for DNA replication. There are three main RNR classes (I, II, III), of which class I is comprised of three subclasses. Each class and subclass uses a different metal cofactor (15). It is not uncommon for bacteria to have more than one class RNR, as this ensures dNTP synthesis under shifting nutritional conditions. This is the case of *E. coli* which has two class I RNRs, the housekeeping Fe^{2+}-utilizing class Ia NrdAB and the class Ib NrdEF, which is used under conditions of iron starvation (16).

In *B. subtilis* there are no alternative RNRs such that the cell is fully dependent on the class Ib NrdEF (17). There is currently no evidence to suggest that oxidative stress induces expression of the *nrdIEF* operon in *B. subtils.* Moreover, biochemical studies have shown NrdEF catalytic activity to be Mn^{2+}-dependent, although Fe^{2+} can also maintain function albeit at a lower rate (18). The NrdF Asp66Glu mutation localizes at a conserved region that coordinates the di-manganese cofactor (3). It is unclear how this mutation might confer resistance to H_2O_2. One possible explanation might be that since both Fe^{2+} and Mn^{2+} levels rise in an *mntR* mutant, the chances of NrdF being metallated by Fe^{2+} increase. In the presence of H_2O_2, this might make the enzyme more susceptible to oxidation and inactivation. Hence, this point mutation might help prevent access by the oxidant, which would be beneficial if the cell is accumulating high iron levels. However, further work needs to be done to help elucidate this.

Another enzyme that came up in the suppressor list is phosphoglycerate mutase, Pgm. This glycolytic/gluconeogenic protein is conditionally essential (19) and requires Mn^{2+} for function (20,21). In this case, the Leu397Ile point mutation does not localize to the active site so how this might benefit the cell during oxidative stress remains unknown and needs further attention (Fig. A1.3).

Mutations were found twice in MntH, which suggest that Mn^{2+} import might be targeted for inactivation to help alleviate H_2O_2 sensitivity. A mutation

between *ygaF* and *perR* localizes approximately within the promoter region of the latter. It is possible that this is a promoter mutation that inactivates *perR* expression, thus priming the cell to deal with oxidative stress. Other unknown SigB regulated proteins might also make cells more H_2O_2 resistant (Table 6.1).

Future work will involve repeating conditions for suppressor generation in order to see the frequency of these hits. Transposon mutagenesis using Mariner in these background strains would also be useful. In the meantime, linkage and further characterization of these suppressors needs to be done.

A1.5 Methods

Zone of inhibition (ZoI) assays

Disk diffusion assays were performed as described (22). Briefly, strains were grown to an OD_{600} of 0.4. A 100 µl aliquot of these cultures was mixed with 4 ml of 0.75% LB soft agar (kept at 50°C) and directly poured onto LB plates (containing 15 ml of 1.5% LB agar). The plates were dried for 10 min in a laminar airflow hood. Filter paper disks containing 10 µl of the chemicals to be tested were placed on the top of the agar, and the plates were incubated at 37°C overnight. The overall diameter of the inhibition zones was measured along two orthogonal lines. Ten microliters of 0.88 M H_2O_2 added to the filter paper disks.

Spontaneous suppressor analysis

Spontaneous suppressors of *mntR*::*kan* and Δ*mneP* Δ*mneS pfeT*::*spc* *mntR*::*kan* (*SPRpfeT*) were picked from the clear zone of H_2O_2 zone of inhibition assay after overnight incubation at 37°C. Chromosomal DNA extracted from these suppressors was sequenced using an Illumina machine. The sequencing data were analyzed using CLC genomics workbench.

A1.6 References

1. Jakubovics, N.S. and Jenkinson, H.F. (2001) Out of the iron age: new insights into the critical role of manganese homeostasis in bacteria. *Microbiology*, **147**, 1709-1718.
2. Kehres, D.G., Janakiraman, A., Slauch, J.M. and Maguire, M.E. (2002) Regulation of *Salmonella enterica* serovar Typhimurium *mntH* transcription by H_2O_2, Fe^{2+}, and Mn^{2+}. *J Bacteriol*, **184**, 3151-3158.
3. Boal, A.K., Cotruvo, J.A., Jr., Stubbe, J. and Rosenzweig, A.C. (2012) The dimanganese(II) site of *Bacillus subtilis* class Ib ribonucleotide reductase. *Biochemistry*, **51**, 3861-3871.
4. Anjem, A., Varghese, S. and Imlay, J.A. (2009) Manganese import is a key element of the OxyR response to hydrogen peroxide in *Escherichia coli*. *Mol Microbiol*, **72**, 844-858.
5. Helmann, J.D. (2014) Specificity of metal sensing: iron and manganese homeostasis in *Bacillus subtilis*. *J Biol Chem*, **289**, 28112-28120.

6. Guedon, E., Moore, C.M., Que, Q., Wang, T., Ye, R.W. and Helmann, J.D. (2003) The global transcriptional response of *Bacillus subtilis* to manganese involves the MntR, Fur, TnrA and sigmaB regulons. *Mol Microbiol*, **49**, 1477-1491.

7. Que, Q. and Helmann, J.D. (2000) Manganese homeostasis in *Bacillus subtilis* is regulated by MntR, a bifunctional regulator related to the diphtheria toxin repressor family of proteins. *Mol Microbiol*, **35**, 1454-1468.

8. Huang, X., Shin, J.H., Pinochet-Barros, A., Su, T.T. and Helmann, J.D. (2017) *Bacillus subtilis* MntR coordinates the transcriptional regulation of manganese uptake and efflux systems. *Mol Microbiol*, **103**, 253-268.

9. Anjem, A. and Imlay, J.A. (2012) Mononuclear iron enzymes are primary targets of hydrogen peroxide stress. *J Biol Chem*, **287**, 15544-15556.

10. Sobota, J.M., Gu, M. and Imlay, J.A. (2014) Intracellular hydrogen peroxide and superoxide poison 3-deoxy-D-arabinoheptulosonate 7-phosphate synthase, the first committed enzyme in the aromatic biosynthetic pathway of *Escherichia coli*. *J Bacteriol*, **196**, 1980-1991.

11. Dizdaroglu, M., Nackerdien, Z., Chao, B.C., Gajewski, E. and Rao, G. (1991) Chemical nature of *in vivo* DNA base damage in hydrogen peroxide-treated mammalian cells. *Arch Biochem Biophys*, **285**, 388-390.

12. Imlay, J.A. (2003) Pathways of oxidative damage. *Annu Rev Microbiol*, **57**, 395-418.

13. Park, S., You, X. and Imlay, J.A. (2005) Substantial DNA damage from submicromolar intracellular hydrogen peroxide detected in Hpx- mutants of *Escherichia coli*. *Proc Natl Acad Sci U S A*, **102**, 9317-9322.

14. Monje-Casas, F., Jurado, J., Prieto-Alamo, M.J., Holmgren, A. and Pueyo, C. (2001) Expression analysis of the *nrdHIEF* operon from *Escherichia coli*. Conditions that trigger the transcript level in vivo. *J Biol Chem*, **276**, 18031-18037.

15. Torrents, E. (2014) Ribonucleotide reductases: essential enzymes for bacterial life. *Front Cell Infect Microbiol*, **4**, 52.

16. Martin, J.E. and Imlay, J.A. (2011) The alternative aerobic ribonucleotide reductase of *Escherichia coli*, NrdEF, is a manganese-dependent enzyme that enables cell replication during periods of iron starvation. *Mol Microbiol*, **80**, 319-334.

17. Huang, M., Parker, M.J. and Stubbe, J. (2014) Choosing the right metal: case studies of class I ribonucleotide reductases. *J Biol Chem*, **289**, 28104-28111.

18. Zhang, Y. and Stubbe, J. (2011) *Bacillus subtilis* class Ib ribonucleotide reductase is a dimanganese(III)-tyrosyl radical enzyme. *Biochemistry*, **50**, 5615-5623.

19. Commichau, F.M., Pietack, N. and Stulke, J. (2013) Essential genes in *Bacillus subtilis*: a re-evaluation after ten years. *Mol Biosyst*, **9**, 1068-1075.

20. Chander, M., Setlow, B. and Setlow, P. (1998) The enzymatic activity of phosphoglycerate mutase from gram-positive endospore-forming bacteria requires Mn^{2+} and is pH sensitive. *Can J Microbiol*, **44**, 759-767.

21. Watabe, K. and Freese, E. (1979) Purification and properties of the manganese-dependent phosphoglycerate mutase of *Bacillus subtilis*. *J Bacteriol*, **137**, 773-778.

22. Mascher, T., Hachmann, A.B. and Helmann, J.D. (2007) Regulatory overlap and functional redundancy among *Bacillus subtilis* extracytoplasmic function sigma factors. *J Bacteriol*, **189**, 6919-6927.

APPENDIX II

Mechanisms of Zinc Intoxication in *Bacillus subtilis* Hpx- Mutants[6]

A2.1 Abstract

Reactive oxygen species (ROS) target redox sensitive metalloenzymes for inactivation. In order to overcome this, bacteria have evolved ways to sense peroxide levels and affect expression of genes encoding proteins that either directly detoxify H_2O_2 or prevent the exacerbation of these effects. In the case of the model Gram-positive bacterium *Bacillus subtilis*, the main peroxide sensing protein is the Fur-family metalloregulator PerR, which controls expression of the two main peroxide detoxifying enzymes catalase (KatA) and alkyl hydroperoxide reductase (AhpCF), amongst other genes. A strain lacking both KatA and AhpCF is referred to as a hydroperoxidase minus (Hpx-) strain and shows a growth defect under normal growth conditions. This growth defect is suppressed by amending the media with manganese (Mn). Upon deletion of the main Mn importer MntH in an Hpx- background there was no additive effect with respect to growth defects, however this strain displayed an unexpectedly high sensitivity to zinc (Zn). Our studies suggest that ROS accumulation in an Hpx- strain targets redox sensitive metalloenzymes that

[6] This work was done with the help of (at the time) rotation students Bixi He, Caroline Steingard, and Lisette Payero. They helped push this study along through strain construction and preliminary zone of inhibition assays.

can either be re-metallated by Mn to help maintain catalytic activity or by Zn to cause enzyme inactivation. Current work is focused on teasing apart the genetics of this relation between oxidative stress, manganese, and zinc homeostasis and its apparent impact on cell physiology.

A2.2 Introduction

Growing in an oxic environment inevitably leads to the generation of reactive oxygen species (ROS) like hydrogen peroxide (H_2O_2) and superoxide (O_2^-) which are toxic to the cell. In order to deal with this, cells employ ROS detoxifying enzymes like superoxide dismutase (SOD), catalase, and alkyl hydroperoxide reductase. *Escherichia coli* hydroperoxidase minus (Hpx-) mutants accumulate endogenous ROS as they lack their main peroxide detoxifying enzymes and are growth defective. This toxicity has been shown to be caused by ROS targeting iron mono-nuclear enzymes like deoxy-D-arabinoheptulosonate 7-phosphate synthase (DAHP synthase), ribulose-5-phosphate 3-epimerase (Rpe), and peptide deformilase (PDF) (1-3). For example, DAHP synthase inactivation by ROS mediated Zn^{2+}-mismetallation leads to aromatic amino acid auxotrophy which can be alleviated by amending the growth media with Tyr, Phe, and Trp (2).

The mechanism of toxicity relies on the fact that the reaction of ROS with these iron centers oxidizes ferrous iron (Fe^{2+}) cofactor into ferric iron (Fe^{3+}), which yields apo-protein. This allows other metals like zinc (Zn^{2+}) to

bind tightly to the protein and either lower or abolish catalytic activity (4). This is, in part, why Mn^{2+} rescues growth under these conditions as it acts as a functional alternative cofactor that is less redox-sensitive, thus sustaining enzymatic activity.

In *Bacillus subtilis*, Hpx- strains are also growth defective and although no known targets have been identified, our preliminary data suggests that iron-utilizing enzymes might also be targeted by ROS and, consequently, be subject to mismetallation. Although no auxotrophies have been identified, media supplementation with low micromolar levels of Mn^{2+} restores growth. Moreover, in Hpx- cells that are Mn^{2+} limited through the deletion of *mntH* are increasingly Zn^{2+} sensitive. Here we propose a similar model of ROS mediated mismetallation as in *E. coli*, however, specific targets have yet to be identified.

A2.3 Results

A2.3.1 Mn^{2+} restores growth defect in Hpx- mutants

WT and *Hpx*- strains streaked on regular LB show different growth phenotypes. Whilst WT cells grow well, *Hpx*- mutants show a growth defect phenotype under aerobic conditions. This growth sensitivity is alleviated when the LB media is amended with low micromolar levels of Mn. This suggests that Hpx- cells are undergoing peroxide toxicity that inhibits growth, but Mn somehow restores resistance back to WT levels (Fig. A2.1).

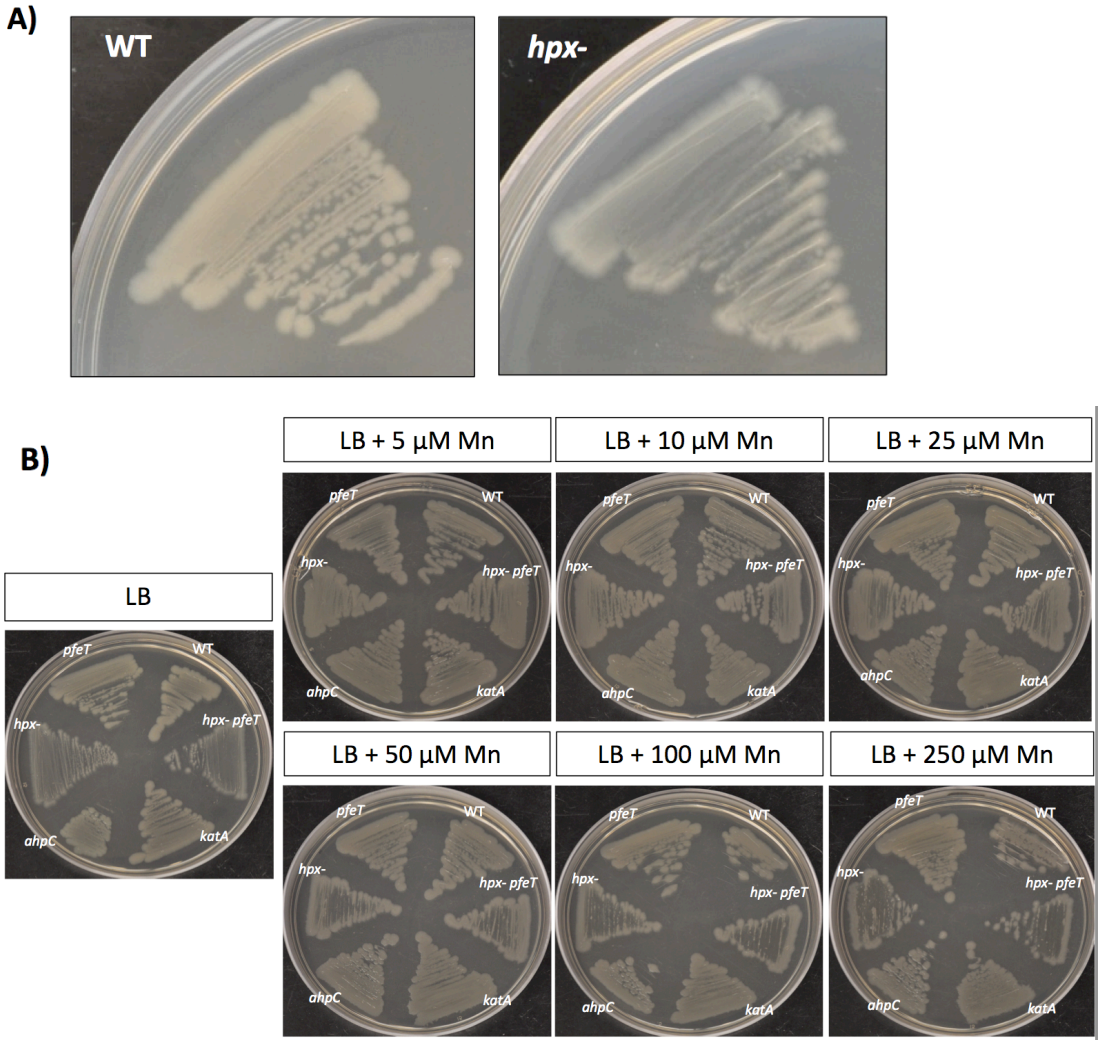

FIG. A2.1) *Hpx*- mutants are sensitive to aerobic growth under normal conditions and this growth defect is suppressed by Mn^{2+}.
(A) Streak assay of WT and Hpx- mutants on LB medium. Hpx- mutants exhibit a growth defect.
(B) Streak assay was performed in LB medium containing a range of Mn concentrations on WT, *Hpx*-, *katA*, *ahpC*, and *Hpx- pfeT* mutants. Growth defect is suppressed by amending the media with 5-25 µM $MnCl_2$.

A2.3.2 *Hpx*- mutants are Zn^{2+} sensitive in the absence of MntH

Given the method of peroxide induced protein mismetallation seen in *E. coli* (2), we performed zinc disk diffusion sensitivity assays to see if increased exposure to this cation would make cells more sensitive. Only when *mntH* is

knocked out do we see a drastic increase in zinc sensitivity (Fig. A2.2). *B. subtilis* is a manganese-centric organism and restriction of manganese through deletion of MntH could prevent alternate metallation of peroxide targeted iron-utilizing enzymes that would otherwise be mismetallated by zinc. Complementation of *mntH* restores zinc sensitivity (Fig. A2.2B). This zinc sensitivity phenotype is exacerbated in minimal media growth conditions (Fig. A2.4).

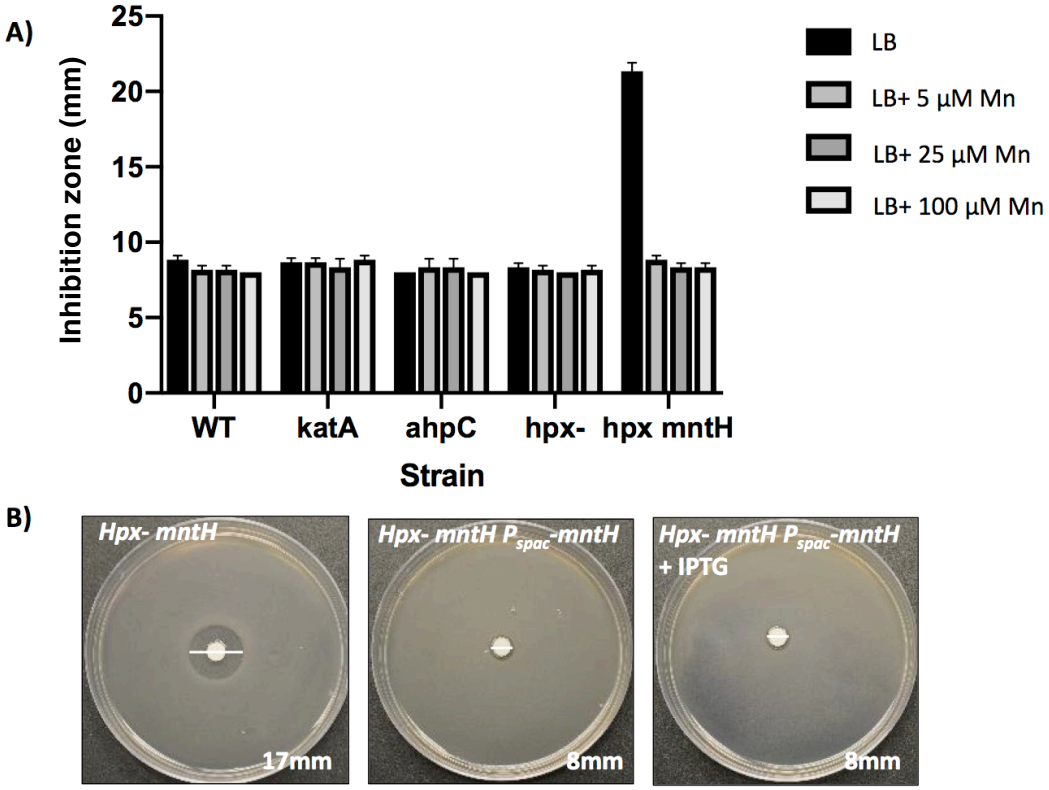

FIG. A2.2) *Hpx- mntH* mutants are highly sensitive to Zn, and this sensitivity is suppressed by Mn.
(A) Sensitivity of WT, *katA, ahpC, Hpx-* and *Hpx- mntH* mutants to zinc was measured with a zinc disk diffusion assay. The measured zone of growth inhibition is defined as the diameter of the growth if inhibition zone. Sensitivity was monitored in LB medium amended with increasing concentrations of $MnCl_2$. Experiments were done a total of three times.
(B) IPTG inducible complementation of *mntH* restores zinc resistance in an *Hpx- mntH* background. Experiment only performed once.

It is curious that we did not see zinc sensitivity in an *Hpx- mntA* strain, suggesting that only MntH can alleviate this toxicity (Fig. A2.3). MntA in other organisms has been shown to be targeted by zinc to shut down function. Deletion of either *mneP* or *mneS* helped restore resistance, on account of their Mn^{2+} efflux activity and deletion of the major zinc importer ZnuA restored resistance back to WT levels (Fig. A2.3).

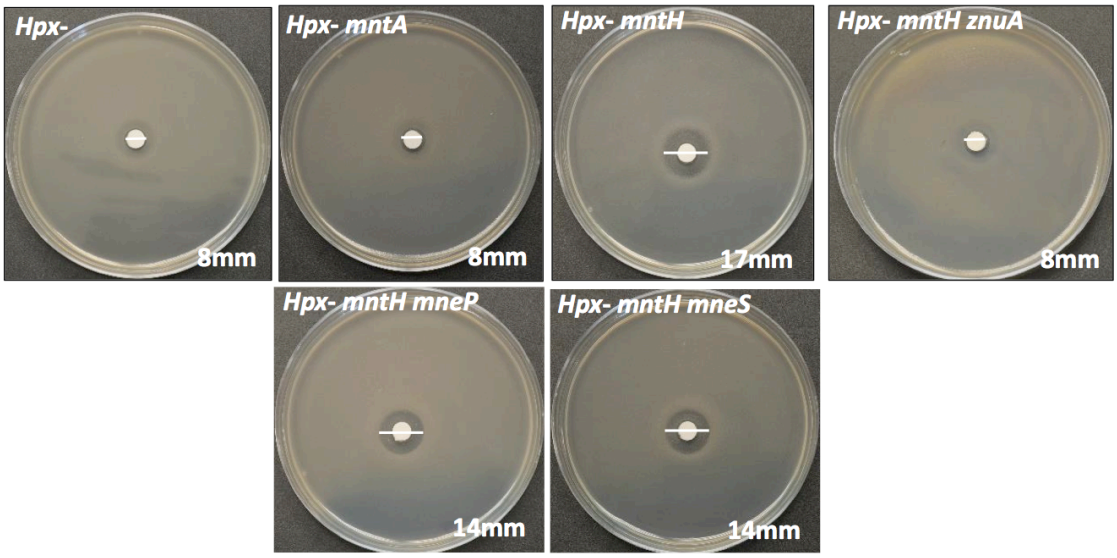

FIG. A2.3) Zinc sensitivity in different *Hpx-* backgrounds
Zinc disk diffusion assay was performed once in *Hpx- mntA* as well as *Hpx mntH in mneP, mneS or znuA* mutant backgrounds.

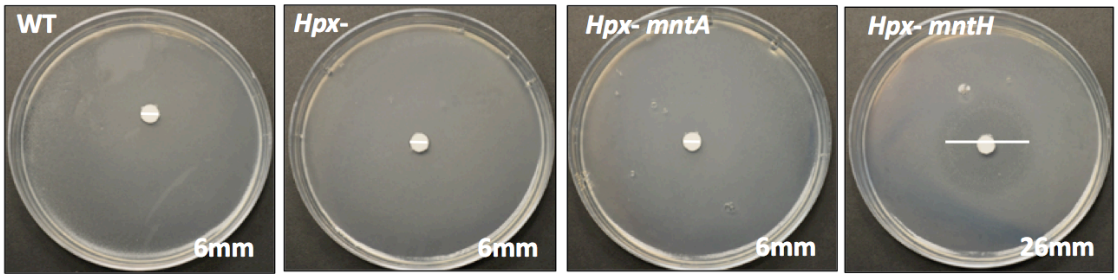

FIG. A2.4) Sensitivity to zinc is exacerbated *Hpx- mntH* grown in minimal media
Zinc zone of inhibition assays were performed once in minimal media plates. Strains tested include WT, *Hpx-*, *Hpx- mntH,* and *Hpx- mntA.*

A2.3.3 Zn^{2+} resistant suppressors

During our zinc sensitivity experiments, spontaneous suppressors were generated in the zone of inhibition. These were streak isolated and tested for zinc resistance. All of the isolated suppressors saw an almost complete restoration of zinc resistance almost back to WT levels (Fig. A2.5). Possible targets might include inactivation of ZnuA, given that an *Hpx- mntH znuA* strain is highly zinc resistant.

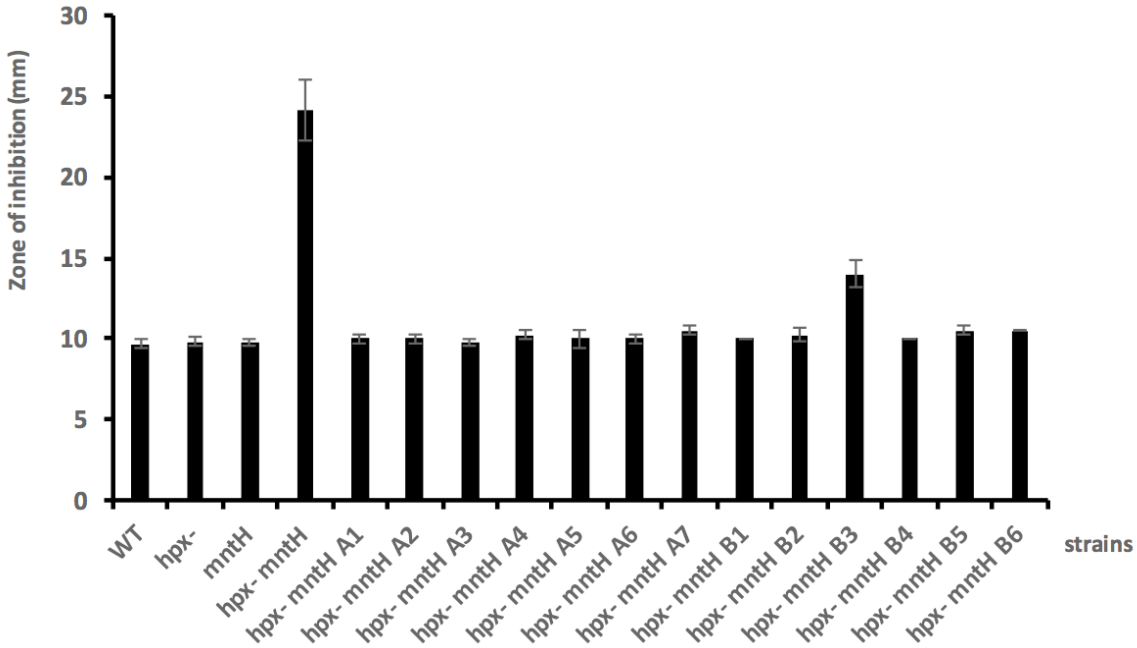

FIG. A2.5) Spontaneous *Hpx- mntH* suppressors show zinc resistance Spontaneous suppressors from previous *Hpx- mntH* zinc zone of inhibition assays were isolated and tested for resistance using the same assay. Experiments were repeated three times.

A2.4 Discussion and future directions

The data herein is supportive of a model where redox sensitive enzymes, such as iron mono-nuclear enzymes might be targeted by peroxide and be

subsequently mismetallated by Zn. Further genetic work needs to be done to tease apart how metal ion homeostasis in *B. subtilis* contributes to zinc toxicity under oxidative stress and the role that Mn plays in alleviating this sensitivity.

In the future we will send the resistant suppressors for whole genome sequencing to see which mutated genes are responsible for conferring this level of resistance. In addition to this, microscopy would be helpful in detecting the morphological effects of *Hpx*- sensitive mutants. Finally, testing for auxotrophies will also provide insight into which pathways might be inactivated by zinc.

A2.5 Methods

Mutant strain construction

Null mutant strains are from the BKE collection (a *B. subtilis* 168 gene knockout library) available from the Bacillus Genetic Stock Center (BGSC). Each BKE strain contains an erythromycin-resistance cassette inserted into the gene in the *B. subtilis* 168 genome. Mutations were transformed into CU1065 for this study. The pDR244 plasmid (from BGSC) was used to excise the BKE erythromycin cassette to generate a markerless deletion of the target gene (5). Isolation of *B. subtilis* chromosomal DNA, transformation and specialized SPβ transduction were performed as described (6). Strains were confirmed by PCR.

Streak assays

Strains were streaked from frozen stocks onto LB plates containing either $ZnCl_2$ or $MnCl_2$ at the indicated concentrations. Plates were incubated at 37°C overnight, after which streak growth was examined.

Zone of inhibition (ZoI) assays

Disk diffusion assays were performed as described (7). Briefly, strains were grown to an OD_{600} of 0.4. A 100 µl aliquot of these cultures was mixed with 4 ml of 0.75% LB soft agar (kept at 50°C) and directly poured onto LB plates (containing 15 ml of 1.5% LB agar). The same setup was carried out in minimal media (MM) plates. The plates were dried for 10 min in a laminar airflow hood. Filter paper disks containing 10 µl of the chemicals to be tested were placed on the top of the agar, and the plates were incubated at 37°C overnight. The overall diameter of the inhibition zones was measured along two orthogonal lines. For IPTG-treated cells, IPTG was added to both the soft agar and the plates to a concentration of 0.1 mM. For media containing additional $MnCl_2$, it was added to both the soft agar and the plates to the specified final concentrations. Unless otherwise noted, 10 µl of the following chemicals was used in the disk diffusion assays: 50 mM $ZnCl_2$, 0.88 M H_2O_2.

A2.6 References

1. Anjem, A. and Imlay, J.A. (2012) Mononuclear iron enzymes are primary targets of hydrogen peroxide stress. *J Biol Chem*, **287**, 15544-15556.
2. Sobota, J.M., Gu, M. and Imlay, J.A. (2014) Intracellular hydrogen peroxide and superoxide poison 3-deoxy-D-arabinoheptulosonate 7-phosphate synthase, the first committed enzyme in the aromatic biosynthetic pathway of *Escherichia coli*. *J Bacteriol*, **196**, 1980-1991.
3. Sobota, J.M. and Imlay, J.A. (2011) Iron enzyme ribulose-5-phosphate 3-epimerase in *Escherichia coli* is rapidly damaged by hydrogen peroxide but can be protected by manganese. *Proc Natl Acad Sci U S A*, **108**, 5402-5407.
4. Imlay, J.A. (2014) The mismetallation of enzymes during oxidative stress. *J Biol Chem*, **289**, 28121-28128.
5. Koo, B.M., Kritikos, G., Farelli, J.D., Todor, H., Tong, K., Kimsey, H., Wapinski, I., Galardini, M., Cabal, A., Peters, J.M. *et al.* (2017) Construction and Analysis of Two Genome-Scale Deletion Libraries for *Bacillus subtilis*. *Cell Syst*, **4**, 291-305 e297.
6. Harwood, C.R. and Cutting, S.M. (1990) *Molecular biological methods for Bacillus*. Wiley, Chichester.

7. Mascher, T., Hachmann, A.B. and Helmann, J.D. (2007) Regulatory overlap and functional redundancy among *Bacillus subtilis* extracytoplasmic function sigma factors. *J Bacteriol*, **189**, 6919-6927.